THESIS
3
2001

This is to certify that the

dissertation entitled

Aqueous-Phase Hydrogenation of Biomass Derived
Lactic Acid to Propylene Glycol

presented by

Zhigang Zhang

has been accepted towards fulfillment
of the requirements for

Ph.D. degree in Chemical Engineering

Dennis J. Miller
Major professor

Date 8/7/00

MSU is an Affirmative Action/Equal Opportunity Institution O-12771

LIBRARY
Michigan State
University

PLACE IN RETURN BOX to remove this checkout from your record.
TO AVOID FINES return on or before date due.
MAY BE RECALLED with earlier due date if requested.

DATE DUE	DATE DUE	DATE DUE
APR 2 5 2002		
JUL 2 0 2007		
JUL 1 1 2009		
AUG 1 1 2009		

11/00 c/CIRC/DateDue.p65-p.14

AQUEOUS-PHASE HYDROGENATION OF BIOMASS DERIVED LACTIC ACID TO PROPYLENE GLYCOL

By

Zhigang Zhang

A DISSERTATION

Submitted to
Michigan State University
in partial fulfillment of the requirements for the degree of

DOCTOR OF PHILOSOPHY

Department of Chemical Engineering
College of Engineering

July 19, 2000

A

and

over

and

the

with

used

been

and

ABSTRACT

AQUEOUS-PHASE HYDROGENATION OF BIOMASS DERIVED LACTIC ACID TO PROPYLENE GLYCOL

BY ZHIGANG ZHANG

Aqueous phase hydrogenation of biomass-derived lactic acid (L+ 2-hydroxy-propionic acid) to propylene glycol (PG) has been performed using a stirred batch reactor and a continuous trickle bed reactor. In the optimal reaction conditions and catalysts, over 90% PG selectivity with 95% lactic acid conversion can be achieved in both batch and trickle bed reactors. The major side reactions are the formation hydrocarbon (methane, ethane, and propane). When reaction temperature is lower than 170°C, PG is the only liquid product, which makes the product separation very simple. The best active metal is ruthenium and the best catalyst supports are selected activated carbons. In the stirred batch reactor, optimal selectivity and high reaction rate are reached at a temperature of 150°C and high pressure of hydrogen (1500~2000psi). In the trickle bed reactor, the reaction temperature can be as low as 80°C with a pressure as low as 800psi without significant sacrifice of PG selectivity. The reaction temperature and pressure used in this process are very mild compared to carboxylic acid hydrogenation reported in literature.

In the stirred batch reactor, the measured gas-liquid mass transfer coefficient and theoretical mass transfer analysis have shown that gas-liquid, liquid-solid, and intra-particle mass transfer are negligible at our reaction conditions. The intrinsic kinetics have been analyzed and the activation energy for lactic acid hydrogenation is 96kJ/mole. Lactic acid consumption rate is sensitive to reaction temperature and catalyst loading but

insensitive to hydrogen pressure. The performance of laboratory prepared carbon-supported ruthenium catalysts are as good as commercial catalysts in the batch reactor.

Granular carbon supported ruthenium catalysts were prepared and used in the trickle bed reactor to continuously hydrogenate lactic acid to PG. Experiments and calculation have verified that gas-liquid, liquid-solid and intra-particle mass transfers and surface chemical reaction together control the lactic acid hydrogenation reaction in the trickle bed reactor. Gas-liquid mass transfer is the major resistance. Lactic acid conversion increases with temperature at the same pressure and fixed hydrogen to lactic acid molar ratio. Like the reaction in the batch reactor, propylene glycol selectivity increases with hydrogen pressure. The overall activation energy in the trickle bed reactor is only 48kJ/mole, which indicates that mass transfer controls this hydrogenation reaction.

Hydrogen solubility at high pressure and trickle bed dynamic liquid holdup, which are two key parameters in the trickle bed reactor modeling, were measured in the trickle bed reactor. A one-dimensional trickle bed reactor model was derived. This model consists of two differential and two algebraic equations and forms a typical two-point boundary value problem mathematically. With simplification, the model was solved in Mathematica. Liquid phase hydrogen and lactic acid concentration and catalyst surface hydrogen and lactic acid concentration profiles were plotted. The results give us more information about the role of gas-liquid and liquid-solid mass transfer.

I
and Dr.
Berglun
of my d

Dushya
collabo

Cargill
suppor

ACKNOWLEDGEMENTS

I am very grateful for the suggestions and express guidance of Dr. Dennis J Miller and Dr. James Jackson throughout the development of this work. Thanks to Dr. Kris Berglund, Dr. Ramani Narayan and Dr. Smith, Milton R III for their Service as members of my doctoral committee.

Thanks to Bryan P Hogle for performing catalyst characterization. Thanks to Dushyant Shekhawat, Frank Jere, and Shubham Chopade for excellent suggestions and collaboration.

Thanks to the Chemical Engineering Department at Michigan State University, Cargill Corporation and the consortium plant Biotechnology Research for their financial support of this work.

Dedicated to people who help me in the past and the future! These people include:

養育我的父親安和母親，沒有他們的含辛茹苦，也沒有我的今天！我的妻子李榮林，她給我帶來了無數的歡樂和一雙可愛的兒女！中國科學院山西煤炭化學研究所人事教育處的楊常理老師！沒有他親自去長城化工廠，我不可能離開那個偏遠的小型化工廠。當然沒有今天這本博士論文！中國科學院山西煤炭化學研究所氣化研究室的王洋老師！我給他添了無數的麻煩。他給了我無數的幫助。沒有他的幫忙，我不可來到美國。當然沒有今天這本博士論文！密歇根州立大學化工系的米勒博士，沒有他在學習和生活上的幫忙，也沒有今天這本博士論文！最後是我自己，沒有我五年的苦工，當然也沒有這本博士論文！

本人簡歷：三十多年前出身于中國河北省張家口蔚縣城東關。先畢業于河北化工學院，然後長城化工廠工作三年。於是到中國科學院山西煤炭化學研究所氣化研究室王洋老師手下讀工程碩士凡三年！而後在那裡工作又四年。然後到密歇根州立大學化工系米勒博士手下讀化工博士。六年中完成化工和電機工程兩個碩士外加這個博士。

LIST O
LIST C
ABBR
NOTA
CHAP
1.1.
1.1
1
1.
1.2.
1.2
1.2
1.2
1.2
1.3.
1.3

TABLE OF CONTENTS

LIST OF TABLES xiv

LIST OF FIGURES xvii

ABBRIVIATIONS xxi

NOTATION xxiii

CHAPTER 1. BACKGROUND 1

1.1. LITERATURE REVIEW 2

1.1.1. Lactic acid 4

1.1.1.1. History of discovery 4

1.1.1.2. Production of lactic acid 5

1.1.1.3. Synthetic technology 7

1.1.1.4. The production of lactic acid from fermentation 9

1.1.1.5. Lactic acid market 10

1.1.2. Propylene glycol 12

1.2. LACTIC ACID REACTIONS 13

1.2.1. Lactic acid reduction 14

1.2.2. Polymerization 17

1.2.3. Dehydration 17

1.2.4. Condensation to 2,3-pentanedione 18

1.3. HYDROGENATING CARBOXYLIC ACIDS WITH MOLECULAR HYDROGEN 19

1.3.1. Heterogeneous catalysts 23

1.3.2.
1.3.3.
1.3.4.
1.3.5.
1.4. TR
1.5. RA
CHAPTE
2.1. RE
2.2. CA
2.2.1
2.2.2
2.2
2.2
2.2
2.2.3
2.2.4
2.3. B
2.3.
2.3.
2.4. C
2.4.
2.4.

1.3.2. Homogeneous hydrogenation catalysts.. 24

1.3.3. Hydrogenation of carboxylic acid salts.. 26

1.3.4. Hydrogen solubility 27

1.3.5. Hydrogenation mechanism 27

1.4. TRICKLE BED REACTOR (TBR) AND MODELING.. 28

1.5. RATIONALE OF THIS RESEARCH 31

CHAPTER 2. EQUIPMENT AND EXPERIMENTAL METHODS 33

2.1. REAGENTS.. 33

2.2. CATALYSTS.. 34

2.2.1. Commercial catalyst samples 34

2.2.2. Catalyst preparation... 35

2.2.2.1. Impregnation 35

2.2.2.2. Drying... 36

2.2.2.3. Reduction 36

2.2.3. Powder catalyst.. 37

2.2.4. Granular catalyst.. 38

2.3. BATCH REACTOR (AUTOCLAVE) 38

2.3.1. Reactor system... 39

2.3.2. Operating procedure for the batch rector... 40

2.4. CONTINUOUS TRICKLE BED REACTION SYSTEM.. 42

2.4.1. Specifications of the trickle bed system 43

2.4.2. Operating procedure for the trickle bed reactor... 43

2.5. PR
2.5.1.
2.5
2.5
2.5.2.
2.5
2.5
2.5.3
CHAPT
3.1. C
3.1.1
3.1.2
3.1.
3.1.
3.1.
3.1.
3.2. L
3.3. L
3.3
3.3.
3.4. C
3.5. C

2.5. PRODUCTS ANALYSIS 45

2.5.1. Mass spectrometer 45

2.5.1.1. Gas phase by-products identification 46

2.5.1.2. Quantitative analysis 51

2.5.2. High performance liquid chromatography (HPLC) 53

2.5.2.1. Calibration of HPLC 55

2.5.2.2. Liquid compound peak assignment 57

2.5.3. Catalyst characterization 59

CHAPTER 3. LACTIC ACID HYDROGENATION IN AUTOCLAVE 61

3.1. COMMERCIAL CATALYST TESTING 61

3.1.1. Catalyst screening 61

3.1.2. Temperature and pressure optimization (Matrix –1) 63

3.1.3. Catalyst loading effects (Matrices 2 and 3) 66

3.1.4. Catalyst pre-reduction effect 69

3.1.5. Lactic acid concentration effects 70

3.1.6. Gas product evolution 71

3.2. LACTIC ACID CONVERSION OVER LABORATORY PREPARED CATALYSTS 74

3.3. LACTATE SALT HYDROGENATION 77

3.3.1. Potassium lactate hydrogenation 78

3.3.2. Calcium ion 80

3.4. CARBON BALANCE 82

3.5. CONCLUSION 84

CHAPTE

TRICKLI

4.1. Co

4.1.1

4.

4.

4

4

4.1

4

4

4.2.

4.

4

4

4

4

4

4

4

4.3

CHAPTER 4. CONVERSION OF LACTIC ACID TO PROPYLENE GLYCOL IN A TRICKLE BED REACTOR 86

4.1. CONTROL PARAMETERS AND CATALYSTS IN TRICKLE BED REACTOR 86

4.1.1. Control parameters 87

4.1.1.1. Liquid superficial velocity 87

4.1.1.2. Gas superficial velocity 87

4.1.1.3. Flash vaporization 88

4.1.1.4. Conditions of operation 89

4.1.2. Catalysts 89

4.1.2.1. Catalyst characterization 89

4.1.2.2. Initial autoclave test of granular catalysts 91

4.2. TRICKLE BED REACTION (RACEMIC LACTIC ACID) 92

4.2.1. Results 93

4.2.1.1. Charges 1 and 2 93

4.2.1.2. Charge 3 94

4.2.2. Temperature effect 95

4.2.3. Pressure effect (Charge 3, fully filled CG6M) 97

4.2.4. Hydrogen/lactic acid molar ratio 99

4.2.5. The effect of changing liquid flow-rate 100

4.2.6. Long time and low concentration lactic acid hydrogenation 102

4.2.7. High lactic acid concentration feed 102

4.2.8. Addition of sulfur to lactic acid feed 104

4.3. CONVERSION OF UNREFINED LACTIC ACID TO PG IN TRICKLE BED REACTOR 106

4.3.1. Reaction conditions 107

4.3.2. Results and discussion 107

4.3.2.1. Hydrogenation at different Pressure and Temperature 107

4.3.2.2. Catalyst deactivation from impurities in Cargill lactic acid 109

4.3.2.3. The effect of lactic acid sources 111

4.3.3. Summary 113

4.4. CONCLUSION 113

CHAPTER 5. MASS TRANSFER, KINETICS AND MODELING 115

5.1. H_2 SOLUBILITY MEASUREMENT 115

5.1.1. Apparatus 116

5.1.2. Experimental steps 116

5.1.3. Calculation and results 117

5.1.4. Solubility of hydrogen in 10% lactic acid 118

5.2. CHARACTERIZATION OF MASS TRANSFER IN THE BATCH REACTOR (AUTOCLAVE). 119

5.2.1. Suspension of catalyst 119

5.2.2. Maximum reaction rate and pseudo first order rate constant in batch reactor120

5.2.3. Gas-liquid mass transfer 121

5.2.3.1. Principle and procedure 122

5.2.3.2. Data analysis 122

5.2.3.3. Results and comparison with literature 123

5.2.3.4. Comparing G-L mass transfer with reaction rate 125

5.2.3.5. Comparing with literature correlation 126

5

5.2

5.2

5.2

5.

5.

5.3

5

5

5

5

5

5

5.

5.2.3.6. Verification by investigating the stirring speed effect 127
5.2.4. Liquid-solid mass transfer 128
5.2.5. Intra-particle mass transfer 130
5.2.6. Summary of mass transfer in the batch reactor 131
5.2.7. Batch reactor macro kinetics 131
5.2.7.1. Initial reaction rate 132
5.2.7.2. Activation energy 134
5.2.8. Kinetics model 136
5.2.8.1. Model derivation 136
5.2.8.2. Fitting the data of the reactions at 130°C 138
5.3. CONTINUOUS REACTOR (TRICKLE BED) 140
5.3.1. Dynamic Liquid holdup 140
5.3.2. Residence time distribution (species adsorption on catalyst) 142
5.3.3. Reaction rate and pseudo first order constant in the trickle bed 145
5.3.4. Mass transfer coefficients in the trickle bed 147
5.3.5. Intra-particle mass transfer in the trickle bed 151
5.3.6. Trickle bed kinetics 152
5.3.6.1. Macro kinetics in trickle bed 152
5.3.6.2. The limiting reactant in liquid phase 154
5.4. TRICKLE BED MODELING 155
5.4.1. Model equations and boundary conditions 155
5.4.2. Analysis of the model 157
5.4.3. Modeling of trickle bed 159

5.4.
5.4
5.5. S
CHAPT
6.1. (
6.1
6.
6.
6.
6.2.
6
6
6
6.3
6
CH

5.4.4. Model parameters 160

5.4.5. Simulation results at 100°C 161

5.5. SUMMARY 163

CHAPTER 6. MECHANISTIC INSIGHT 165

6.1. CONTROL EXPERIMENTS FOR MECHANISM ELUCIDATION 165

6.1.1. PG hydrogenation (M47, M48) 166

6.1.2. Ethanol and methanol hydrogenation on Ru/C catalyst (M49) 168

6.1.3. Propanoic acid hydrogenation 170

6.1.4. Adding PG in lactic acid hydrogenation 171

6.2. GAS BY-PRODUCT INFORMATION AT DIFFERENT REACTION CONDITIONS 173

6.2.1. Gas composition for low pressure hydrogenation (330psi) 175

6.2.2. Gas product distribution in trickle bed reactor 175

6.2.3. Catalyst deactivation by unrefined Cargill lactic acid samples 177

6.3. RATIONALIZATION OF THE REACTION PATHS 177

6.3.1. Side reaction 1(methane formation) 181

6.3.2. Side reaction 2 (propanol formation) 182

6.3.3. Side reaction 3 (propane formation) 183

6.3.4. Side reaction 4 (ethane formation) 183

6.4. SUMMARY 184

CHAPTER 7. SUMMARY AND RECOMMENDATIONS 185

7.1. SUMMARY 185

7.1.1. Hydrogenation of lactic acid in autoclave 185

7.1.2. H

7.1.3. C

7.1.4.

7.1.5.

7.2. RECO

7.2.1. S

7.2.2. S

7.2.3. Pr

APPENDIX

A.1. LACT

A.2. BUL

A.3. EXT

A.4. INT

A.5. D

A.6. B

A.6

A

A

A.6.

A.6.3

REFEREN

7.1.2. Hydrogenation reaction in trickle bed reactor 187

7.1.3. Catalyst characterization and deactivation 187

7.1.4. Kinetic parameter measurement and trickle bed modeling 188

7.1.5. Reaction pathway 188

7.2. RECOMMENDATIONS 189

7.2.1. Surface reaction pathway investigation 189

7.2.2. Selective deactivation of the catalyst and yield enhancement 190

7.2.3. Production of optically active propylene glycol 190

APPENDIX A. PARAMETERS CALCULATION AND PHYSICAL DATA 191

A.1. LACTIC ACID CONSUMPTION RATE AND HYDROGEN CONSUMPTION RATE 191

A.2. BULK DENSITY OF CATALYST 191

A.3. EXTERNAL POROSITY 192

A.4. INTERNAL POROSITY AND CATALYST DENSITY 192

A.5. DIFFUSION COEFFICIENTS 192

A.6. BASIC PHYSICAL DATA USED IN KINETIC CALCULATION 193

A.6.1. Lactic acid 193

A.6.1.1. Density of aqueous solution of lactic acid 193

A.6.1.2. Viscosity of aqueous solution of lactic acid 194

A.6.2. Saturation pressures of lactic acid and propylene glycol 195

A.6.3. Equilibrium of lactic acid hydrogenation to PG 195

REFERENCE 197

TA

TA

TA

TA

TA

TA

TAB

TAB

TAB

TAB

TAB

TAB

TAB

TAB

TAB

TAB

TAB

TAB

TAB

TAB

TAB

TAB

LIST OF TABLES

Table 1-1. Propylene glycol production 12

Table 1-2. Important lactic acid reactions 14

Table 1-3. Lactic hydrogenation results from patent US5731479 15

Table 1-4. Typical results of carboxylic acid hydrogenation 21

Table 1-5. Broadbent's carboxylic acid hydrogenation results 21

Table 1-6. Propionate hydrogenation (50) 27

Table 1-7. Solubility (ml/mlH_2O) of hydrogen in water [0] 27

Table 2-1. Reagents used in the hydrogention of lactic acid 34

Table 2-2. Commercial catalysts 35

Table 2-3. Results of incipient wetness testing 35

Table 2-4. Details of MSU Ru/C powder catalysts 38

Table 2-5. Experimental parameters 42

Table 2-6. HPLC operation parameters 54

Table 2-7. Real peak position and menu value 59

Table 2-8. Peak assignment 59

Table 3-1. Optimization Matrix-1 63

Table 3-2. Experiment numbers for Matrices 2 and 3 65

Table 3-3. Details of MSU ruthenium catalysts and test conditions 74

Table 3-4. Conversion and selectivity 75

Table 3-5. Summary of all experiments for lactate salt hydrogenation 78

Table 3-6. Summary of carbon balance 83

Table 4-1. Gas superficial velocity at 1200psi and 100°C 88

TABLE
TABLE
TABLE
TABL
TABL
TABL
TABL
TABL
TABL
TABL
TAB
TAB
TAB
TAB
TAB
TAB
TAB
TAB
TA
TA
TA
TA
TA

TABLE 4-2. CATALYST SUPPORTS SPECIFICATION 90

TABLE 4-4. CATALYST PROPERTIES 90

TABLE 4-5. THREE CATALYST CHARGES USED IN TRICKLE BED 92

TABLE 4-6. TRICKLE BED REACTION SUMMARY (CHARGE 1 AND CHARGE 2) 94

TABLE 4-7. RESULTS OF TRICKLE BED WITH 48GRAM CATALYST (CHARGE 3) 95

TABLE 4-8. RESULTS OF 17.2% LACTIC ACID FEEDING 103

TABLE 4-9. RESULTS OF ADDING SULFUR 104

TABLE 4-10. CALCULATION SHOWS THE DEACTIVATION IS FAST 105

TABLE 5-1. SOLUBILITY IN HPLC WATER (ML (STP)/G) 117

TABLE 5-2. SOLUBILITY OF HYDROGEN IN 10% LACTIC ACID (ML(STP)/G) 119

TABLE 5-3. REACTION RATE FOR THREE CATALYSTS LOADING AT 150°C AND 2000PSI.. 121

TABLE 5-4. PSEUDO FIRST ORDER CONSTANT 121

TABLE 5-5. SUMMARY OF MASS TRANSFER COEFFICIENT 124

TABLE 5-6. STIRRING SPEED EFFECTS 128

TABLE 5-7. REGRESSION RESULTS 135

TABLE 5-8. REGRESSION RESULTS FOR 130°C IN AUTOCLAVE 138

TABLE 5-9. RESIDUAL SPECIES AFTER SWITCHING TO WATER 145

TABLE 5-10. BALANCE OF DESORPTION AND ADSORPTION 145

TABLE 5-11. PSEUDO FIRST ORDER REACTION CONSTANTS IN TRICKLE BED 146

TABLE 5-12. COMPARISONS OF H_2 MASS TRANSFER AND OBSERVED REACTION RATE 150

TABLE 5-13. PSEUDO FIRST ORDER CONSTANT AT DIFFERENT TEMPERATURE 153

TABLE 5-14. MODEL EQUATIONS AND BOUNDARY CONDITIONS FOR TRICKLE BED 157

TABLE 5-15. MODEL PARAMETERS AT 100°C 160

TABLE
TABLE
TABLE
TABLE
TABLE
TABLE
TABLE
TABLE
TABLE
TABLE
TABLE

TABLE 5-16. L-S MASS TRANSFER COEFFICIENTS FOR HYDROGEN AND LACTIC ACID...... 161

TABLE 5-17. SIMULATION RESULTS FOR K_1 161

TABLE 6-1. PRODUCT DISTRIBUTION FOR PG HYDROGENATION AT 170°C.......... 167

TABLE 6-2. AVERAGE BOND ENERGY 178

TABLE 6-3. AB INITIO ENERGY (KCAL/MOLE) FOR DIFFERENT STRUCTURES (*) 179

TABLE 6-4. AB INITIO ENERGY CHANGE DURING REACTION.......... 180

TABLE A-1. CATALYST DENSITY AND POROSITY 192

TABLE A-2. DIFFUSIVITY (CM^2/SEC).......... 193

TABLE A-3. THERMODYNAMIC PROPERTIES FOR LA AND PG 193

TABLE A-4. DENSITIES OF AQUEOUS SOLUTIONS OF LACTIC ACID.......... 194

TABLE A-5. VISCOSITIES AS A FUNCTION OF CONCENTRATION AND TEMPERATURE (CP) 194

FIGU
FIGU
FIGU
FIGU
FIGU
FIGU
FIGU
FIGU
FIGU
FIGU
FIGU
FIGU
FIGU
FIGU
FIGU
FIGU
FIGU
FIGU
FIGU
FIGU
FIGU
FIGU

LIST OF FIGURES

FIGURE 1-1. ANNUAL LACTIC ACID PRODUCTION 7

FIGURE 1-2. CHEMICAL SYNTHESIS OF LACTIC ACID 8

FIGURE 1-3. PROPYLENE GLYCOL USE DISTRIBUTION ^{0} 12

FIGURE 1-4. EE EFFICIENCY VS. TEMPERATURE IN L (+) LACTIC ACID HYDROGENATION .. 16

FIGURE 2-1. HYDROGEN CHLORINE EVOLUTION PROFILE DURING REDUCTION 37

FIGURE 2-2. BATCH REACTOR AND CONTROLLER 39

FIGURE 2-3. BATCH REACTION SYSTEM 40

FIGURE 2-4. TRICKLE BED REACTOR SYSTEM 43

FIGURE 2-5. MASS SPECTROMETER SYSTEM 45

FIGURE 2-6. FINAL GAS PHASE ANALYSIS FROM MASS SPECTROMETER (AUTOCLAVE) 46

FIGURE 2-7. GAS PHASE ANALYSIS FROM MASS SPECTROMETER (TRICKLE BED REACTOR) 47

FIGURE 2-8. STANDARD MASS SPECTRUMS FOR METHANE 47

FIGURE 2-9. STANDARD MASS SPECTRUMS FOR ETHANE 48

FIGURE 2-10. STANDARD MASS SPECTRUMS FOR ETHENE 48

FIGURE 2-11. STANDARD MASS SPECTRUMS FOR PROPANE 49

FIGURE 2-12. STANDARD MASS SPECTRUMS FOR PROPENE 49

FIGURE 2-13. BACKGROUND OF PURE HYDROGEN 50

FIGURE 2-14. CALIBRATION OF CH_4, CO AND CO_2 51

FIGURE 2-15. TYPICAL CHROMATOGRAPH FOR LIQUID ANALYSIS 53

FIGURE 2-16. SCHEMATIC OF HPLC SYSTEM 54

FIGURE 2-17. RESPONSE OF LACTIC ACID ANALYSIS IS A CONSTANT 56

FIGURE 2-18. RESPONSE OF PROPYLENE GLYCOL ANALYSIS IS A CONSTANT 57

FIGUR
FIGUR
FIGUR
FIGUR
FIGUR
FIGUR
FIGUR
FIGUR
FIGUR
FIGUR
FIGUR
FIGUR
FIGUR
FIGUR
FIGURE
FIGURE
FIGURE
FIGURE
FIGURE
FIGURE
FIGURE
FIGURE
FIGURE

Figure 2-19. Typical HPLC chromatograph of liquid products 58

Figure 3-1. Five-hour conversion (temperature and pressure in parentheses). 62

Figure 3-2. Lactic acid conversion vs. pressure & temperature after 5 hours 64

Figure 3-3. Liquid by-products distribution after 3 hours 65

Figure 3-4. Catalyst loading effect at low temperature and pressure 67

Figure 3-5. Catalyst loading effect at high temperature and pressure............ 67

Figure 3-6. Selectivity changes with catalyst loading at 150°C......................... 68

Figure 3-7. Selectivity change with catalyst loading at 130°C 69

Figure 3-8. Pre-reduction effect 70

Figure 3-9. Reactions at different lactic acid concentration 71

Figure 3-10. Gas product evolution for Ru/C (PMC)... 73

Figure 3-11. Gas product evolution for Ru/Alumina (Degussa).......................... 73

Figure 3-12. Five-hour conversion and selectivity for MSU catalysts 76

Figure 3-13. Gas by-product distribution after five-hour reaction................... 77

Figure 3-14. K^+ ion effect on lactic acid hydrogenation at 170°C...................... 79

Figure 3-15. Adding potassium sulfate to lactic acid at 150°C 79

Figure 3-16. Calcium ion effect at 150°C 81

Figure 3-17. Catalyst loading effect on the gas products at1500psi and 150°C84

Figure 4-1. Flash vaporization and steam saturation pressure.......................... 88

Figure 4-2. Hydrogen desorption profile during dispersion measurement........ 90

Figure 4-3. Granular catalysts performance in batch reactor.......................... 91

Figure 4-4. Lactic acid conversion vs. reaction temperature 96

Figure 4-5. PG selectivity vs. reaction temperature 96

FIGURE 4-6. CONVERSION PROFILE VS. TEMPERATURE AND PRESSURE.............................. 97

FIGURE 4-7. SELECTIVITY PROFILE VS. TEMPERATURE AND PRESSURE 98

FIGURE 4-8. EFFECT OF MOLAR RATIO ON CONVERSION 99

FIGURE 4-9. EFFECT OF MOLAR RATIO ON SELECTIVITY... 100

FIGURE 4-10. CONVERSION AND SELECTIVITY VS. WEIGHT HOUR SPACE VELOCITY........ 101

FIGURE 4-11. EFFECT OF WEIGHT HOUR SPACE VELOCITY 101

FIGURE 4-12. CONVERSION AND SELECTIVITY OF EXTENDED TIME REACTION 102

FIGURE 4-13. SELECTIVITY AND CONVERSIONS FOR TWO CONCENTRATIONS.................. 103

FIGURE 4-14. CONVERSION AND SELECTIVITY CHANGE WITH ADDITION OF SULFUR 106

FIGURE 4-15. CONVERSION PROFILE COMPARISON OF CARGILL AND PURE LACTIC ACID 108

FIGURE 4-16. SELECTIVITY PROFILE OF CARGILL AND REGULAR LACTIC ACID................ 108

FIGURE 4-17. CATALYST DEACTIVATION (SWITCH FROM CARGILL TO PURE LACTIC ACID110

FIGURE 4-18. CONVERSION, SELECTIVITY AND YIELD OF THREE LACTIC ACIDS 111

FIGURE 4-19. GAS PHASE COMPOSITION CHANGES WITH REACTION TIME AND FEED....... 112

FIGURE 5-1. APPARATUS FOR SOLUBILITY MEASUREMENT 116

FIGURE 5-2. COMPARISON OF MEASURED SOLUBILITY AND LITERATURE DATA 118

FIGURE 5-3. MINIMUM STIRRING SPEED FOR CATALYST SUSPENSION............................. 120

FIGURE 5-4. HYDROGEN–WATER MASS TRANSFER COEFFICIENT IN THE AUTOCLAVE...... 125

FIGURE 5-5. COMPARISON OF BERN'S CORRELATION AND MEASUREMENT..................... 127

FIGURE 5-6. L-S MASS TRANSFER COEFFICIENT FROM SANO'S CORRELATION 129

FIGURE 5-7. MASS TRANSFER COEFFICIENT FROM BOON-LONG'S EQUATION.................. 130

FIGURE 5-8. OBSERVABLE MODULUS CHANGES WITH CATALYST DIAMETER 131

FIGURE 5-9. FIT CONCENTRATION CURVE TO 4TH ORDER POLYNOMIAL.......................... 132

FIGUR
FIGUR
FIGUR
FIGUR
FIGURE
FIGURE
FIGURE
FIGURE
FIGURE
FIGURE
FIGURE
FIGURE 5
FIGURE 5
FIGURE 5
FIGURE 5
FIGURE 6-
FIGURE 6-
FIGURE 6-
FIGURE 6-
FIGURE 6-5
FIGURE 6-6
FIGURE 6-7
FIGURE 6-8

FIGURE 5-10. GET INITIAL REACTION RATE FROM EXTRAPOLATING THE RATE CURVE 133

FIGURE 5-11. INITIAL REACTION RATES WITH CATALYST LOADING.................................. 133

FIGURE 5-12. COMPARISON OF EXPERIMENT AND PREDICTED RATES.............................. 135

FIGURE 5-13. COMPARISON OF MODEL PREDICTION (130°C)... 139

FIGURE 5-14. LIQUID HOLDUP AT DIFFERENT LIQUID FLOW RATES................................. 141

FIGURE 5-15. LIQUID RESIDENCE TIME IN THE TRICKLE BED 141

FIGURE 5-16. OUTLET CONCENTRATION CHANGE WITH TIME AFTR SWITCH TO SOLUTION143

FIGURE 5-17. OUTLET CONCENTRATION CHANGE WITH TIME AFTER SWITCHING 143

FIGURE 5-18. G-L MASS TRANSFER COEFFICIENT VS. FLOW RATE.................................. 148

FIGURE 5-19. L-S MASS TRANSFER COEFFICIENT VS. LIQUID FLOW RATE........................ 150

FIGURE 5-20. OBSERVABLE MODULUS IN TRICKLE BED (100°C AND 1200PSI) 151

FIGURE 5-21. ARRHENIUS PLOT FOR PSEUDO FIRST ORDER REACTION 153

FIGURE 5-22. H_2 IN BULK LIQUID WITH CONSTANT LIQUID REACTANT CONCENTRATION. 159

FIGURE 5-23. SIMULATION RESULTS AT 100°C AND 400~1200PSI 162

FIGURE 5-24. COMPARISON OF BULK LIQUID AND SURFACE CONCENTRATION 162

FIGURE 6-1. GAS PRODUCTS FROM PROPYLENE GLYCOL HYDROGENATION 167

FIGURE 6-2. LIQUID PRODUCTS FROM PG HYDROGENATION AT 170°C 168

FIGURE 6-3. CONVERSION OF METHANOL AND ETHANOL HYDROGENATION AT 150°C ... 169

FIGURE 6-4. GAS PHASE ANALYSIS OF METHANOL AND ETHANOL HYDROGENATION 169

FIGURE 6-5. COMPARISON OF LACTIC ACID AND PROPANOIC ACID HYDROGENATION 171

FIGURE 6-6. CONVERSION PROFILES FOR ADDING DIFFERENT PG CONCENTRATION........ 172

FIGURE 6-7. PG ADDITION EFFECT LACTIC ACID HYDROGENATION AT 150°C................ 173

FIGURE 6-8. GAS PRODUCT COMPOSITION CHANGE WITH CATALYST LOADING 174

FIGURE 6
FIGURE 6
FIGURE 6
FIGURE 6
FIGURE 6
FIGURE 6
FIGURE 6
FIGURE 6
FIGURE 6
FIGURE 6
FIGURE 6
FIGURE 6
FIGURE A
FIGURE A

FIGURE 6-9. GAS PRODUCT COMPOSITION CHANGE WITH CATALYST LOADING 174

FIGURE 6-10. GAS PRODUCT COMPOSITION CHANGE WITH CATALYST LOADING 174

FIGURE 6-11. GAS PRODUCT COMPOSITION CHANGE WITH CATALYST LOADING 174

FIGURE 6-12. GAS PHASE SPECTRUM AFTER 12 HOURS AT 330PSI AND 150°C................ 175

FIGURE 6-13. GAS PHASE ANALYSIS FOR CG6M CATALYST IN TRICKLE BED.................. 176

FIGURE 6-14. GAS PHASE ANALYSIS FOR CG5P CATALYST IN TRICKLE BED 177

FIGURE 6-15. H_2 ADSORPTION AND DESORPTION CHANGE AFTER DEACTIVATION 178

FIGURE 6-16. PG FORMATION PATH 181

FIGURE 6-17. SCHEME OF PG HYDROLYSIS 182

FIGURE 6-18. PROPANOL FORMATION SCHEME 182

FIGURE 6-19. PROPANE FORMATION SCHEME 183

FIGURE 6-20. ETHANE FORMATION SCHEME 183

FIGURE A-1. SATURATION PRESSURES OF LACTIC ACID AND PROPYLENE GLYCOL 195

FIGURE A-2. LA EQUILIBRIUM CONVERSION 196

LA

BET

C2

C3

CG6M

CG5M

G-L

GC

HPLC

WHS

H-W

L-S

Mass

MSU

PG

PMC

Rpm

RdC

T

W

PT

PD

ABBREVIATIONS

LA	Lactic acid (water solution)
BET	Surafce are measured by BET method
C2	Hydrocarbon contained two carbon atoms
C3	Hydrocarbon contained three carbon atoms
CG6M	Active carbon support and the catalyst based on this support
CG5M	Active carbon support and the catalyst based on this support
G-L	Gas-liquid
GC	Gas chromatography
HPLC	High performance liquid chromatography
WHSV	Weight hour space velocity
H-W	Hougen-Watson model
L-S	Liquid-solid (catalyst surface)
Mass	The m/e in mass spectrum
MSU	Michigan State University
PG	Propylene glycol (water solution)
PMC	Pressure Chemical Corporation
Rpm	Round per minutes
Ru/C	Ruthenium on carbon support
T	Temperature (°C)
W%	Weight percentage
PT	Propane-1,1,2-triol
PD	2-Hydroxy-propionaldehyde

NOTATION

a	Gas liquid interfacial area per unit volume of catalyst (cm^2/cm^3)
a_P	Gas liquid interfacial area per unit volume of reactor (cm^2/cm^3)
A_L	Hydrogen concentration in bulk liquid ($mole/cm^3$)
A_{Li}	Hydrogen concentration in liquid in inlet (at $x=0$) ($mole/cm^3$)
A_S	Hydrogen surface concentration ($mole/cm^3$)
A^*	Saturation concentration (hydrogen solubility) ($mole/cm^3$)
B_L	Lactic acid concentration in bulk liquid ($mole/cm^3$)
B_{Li}	Lactic acid concentration in liquid in inlet (at $x=0$) ($mole/cm^3$)
B_S	Liquid concentration on catalyst surface ($mole/cm^3$)
C_{LA}	Lactic acid concentration (mole/ml) (autoclave)
C^0_{LA}	Lactic acid concentration at start (mole/ml) (autoclave)
D_A	Hydrogen diffusivity (cm^2/s)
D_B	Lactic acid diffusivity (cm^2/s)
De	Effective diffusivity (cm^2/s)
F_L	Liquid feed flow rate (ml/min)
K_L	Gas to liquid mass-transfer coefficient (m/s)
k_S	Liquid to solid mass-transfer coefficient (m/s)
h_d	Dynamic liquid holdup {ml(liquid)/ml(catalyst)}
LHSV	Liquid hourly space velocity (hr^{-1})
z	Dimensionless distance

C_L

C_S

C_{bl}

a_{GL}

a_{LS}

a_p

V_R

η_c

u_L

μ

m, n

ρ

ρ_B

ρ_L

$Pe_A =$

$Pe_B =$

R_A, r_A

r_{obs}

C_L	Dimensionless concentration of hydrogen
C_S	Dimensionless surface concentration of hydrogen
C_{LI}	Dimensionless inlet concentration of hydrogen
α_{GL}	Dimensionless gas –liquid mass transfer coefficient
α_{LS}	Dimensionless liquid solid mass transfer coefficient
α_R	Dimensionless reaction rate constant
V_R	Catalyst volume in trickle bed (ml)
η_C	Catalytic effectiveness factor
u_L	Liquid flow velocity (m/s)
μ	Liquid viscosity (g/cm.sec)
m, n	Reaction order respecting to A and B
ρ	Catalyst density (0.84 g/mL)
ρ_B	Catalyst bulk density 0.44
ρ_L	Liquid density g/mL (1.1 for 10% lactic acid solution)
$Pe_A = \frac{u_L L}{D_A}$	Peclet number for H_2
$Pe_B = \frac{u_L L}{D_B}$	Peclet number for lactic acid
R_G, r_A	Reaction rate (mole/gcat.min)
r_{obs}	Observed reaction rate (mole/gcat.min)

Chapter 1. Background

The current chemical production technology is deeply rooted in petroleum as the carbonaceous resource, for which the storage is limited and will be depleted in the near future. So, alternative carbon sources should be found to replace it. Of course, the best way is to find a renewable carbon resource. On our earth, it seems that plants (biomass) are the only renewable carbon resource. Biomass offers potential for producing a wide variety of chemical species, either as unique new products or as competitive alternatives to traditionally petroleum-derived species. Biomass-based feedstocks (organic acids, etc...) are attractive in making chemicals because they have the potential to be converted to a series of useful chemicals. Also, they can be produced via highly selective fermentation pathways and have high hydrogen to carbon ratio, and have low concentrations of undesirable impurities such as ash, trace metals, sulfur and phosphorus.

It is well known that sulfur and phosphorus are deadly poisons for many catalysts and the purification processes (removing S and P) are very costly.

Lactic acid will be used as a starting point for further utilizing biomass carbon resource, because it can be used as a precursor to synthesize many valuable chemicals and is readily available and very cheap in the future. Worldwide production of lactic acid (2-hydroxy-propionic acid) has dramatically increased since the early 1990s. The viability of making an inexpensive biodegradable polymer (poly-lactic acid) from lactic acid has sparked extensive interest and research in the area of producing and recovering relatively pure lactic acid from fermentation of corn starch. Recent advancements in fermentation technologies for lactic acid production will make it even more inexpensive.

The primary focus of this work is on the formation of propylene glycol from lactic acid by aqueous phase hydrogenation over supported metal catalysts in mild reaction conditions.

1.1. Literature Review

The possible carbon resources in the future are coal and renewable biomass. The coal resource is very large compared to petroleum, but the impurities (especially, sulfur and phosphorus) in coal make its utilization very difficult and costly, and also it could run out some day. The CO_2 in atmosphere could be used as a carbon resource, but from the present techniques and energy sources, it is not practical to get carbon directly from air. We have to use plant as a media, which can adsorb CO_2 directly from air and store it in the form of biomass. So, renewable biomass seems to be the final choice for mankind as a carbon resource. Also, some chemicals cannot be synthesized with present techniques or the procedures are too complicated and the cost is too high for chemical synthesis, and the only way is to use biomass fermentation (for example, most of the anti-bacteria drugs). With technical progress in fermentation and separation, it is also possible to produce chemicals as competitive alternatives to traditional petroleum-derived chemicals. The process of using biomass as a feedstock will produce less toxic waste and less pollution to the environment. This is another advantage compared to petroleum-based technology.

Biomass consists of collectible plant derived materials that are abundant in nature, inexpensive, and potentially convertible to feedstocks in chemical production by fermentation processes. Currently, biomass used for fermentation mainly comes from agriculture, such as starch (corn, wheat, potato, and sago palm), because these are mass-produced, uniform in quality and oversupplied in some countries and the U.S. However, lignocellulose (wood, agricultural residue, grass) should be the major source of biomass in the future since it is both available in large quantities and has no competing use as food. From fermentation by using bacteria, fungi or yeast under mostly anaerobic conditions, various organic acids can be yielded. However, the fermentation process always produces some by-products other than the main compound, and the process economics are decided mostly by product separations. The separations will take most of the production cost.

Propylene glycol (PG) is a valuable and mass produced chemical and has many uses in food and chemical industries. The trickle bed reactor (TBR) is a concurrent downflow packed column. It provides a good means of carrying out a reaction in which gaseous and liquid reactants are to be contacted with catalyst particles. TBR is a relatively new type of reactor, so some review will be given here.

1.1

eth

mil

(cu

Cal

and

and

acid

part

and

1.1.1

there

rotati

well a

and ch

the mo

referen

sour m

Henn. E

1.1.1. Lactic acid

$CH_3CHOHCO_2H$, is a colorless liquid organic acid. It is miscible with water or ethanol. Lactic acid is a fermentation product of lactose (milk sugar); it is present in sour milk, koumiss, leban, yogurt, and cottage cheese. The protein in milk is coagulated (curdled) by lactic acid. Lactic acid is produced in the muscles during intense activity. Calcium lactate, a soluble lactic acid salt, is used as a source of calcium in the diet. Lactic acid is produced commercially for use in pharmaceuticals and foods, in leather tanning and textile dyeing, and in making plastics, solvents, inks, and lacquers. Chemically, lactic acid occurs as two optical isomers, a dextro and a levo form; only the levo form takes part in animal metabolism. Currently, commercial synthetic lactic acid is racemic mixture and currently, all most all fermentation lactic acid is an optically active L (+) form.

1.1.1.1. History of discovery

Lactic acid is the simplest hydroxyl acid having an asymmetric carbon atom and it therefore exists in a racemic form and in two optically active forms with opposite rotations of polarized light. Lactic acid occurs widely in nature as the racemic form as well as the optically active acid. The story of lactic acid is the history of modern biology and chemistry; the development of the industrial making of lactic acid is the history of the modern chemical industry (Benninga (1)). The following story is also from this reference.

In 1780, famous Swedish chemist Carl Wilhelm Scheele (2) found a new acid from sour milk, and named it after its origin Mjölksyra (acid of milk). In 1813, French chemist Henri Braconnot (1781-1855) found "another organic acid" (he called nanceic acid) from

rice w
thoug
Germ
scienti

regard
two ac
the sal
were d
as sarc
acid di
on the p
identica
chemist
activity
almost t
molecula

1.1.1.2. P

Th
Avery was
built in 18
production
per year! I

rice water, beet juice, boiled beans and peas, and soured suspensions of baker's yeast. He thought it was different from the acid discovered by Scheele in the sour milk. Although German chemist Vogel proved the identity of lactic and nanceic acid later, many scientists believed that the lactic acid was no more than impure acetic acid in that time.

Originally the lactic acid from fermentation and that found in muscle tissue were regarded as identical. In 1847, Liebig re-examined meat extract and suspected that the two acids might not be same. Engelhardt found that the crystallization and solubility of the salts of the two lactic acids were different, and thus he concluded that these two acids were different. Heintz examined the two acids further and named the muscle lactic acid as sarco-lactic acid. The confusing properties of fermentation lactic acid and meat lactic acid did not get solved until the discovery of chemical's optical activity. A lengthy paper on the properties of sarco-lactic acid in 1873 explained that the two lactic acids have identical chemical structure, nevertheless differ in optical activity. Finally in 1874, Dutch chemist Van't Hoff proposed a geometrical model to explain the phenomenon of optical activity; in the same year French scientist Le Bel (1847-1930) independently arrived at almost the same explanation of the optical rotation and connected the optical rotation to molecular asymmetry.

1.1.1.2. Production of lactic acid

The principle source of lactic acid is fermentation, even today. Charles Ellery Avery was the first lactic acid manufacturer in the US (1). The US $100,000 plant was built in 1882 in Littleton, Boston and the production began around 1883. Although the production capacity is unclear, the annual coal consumption was high, up to 22000 tons per year! In 1893, Merck began the production of lactic acid in Germany, and from then

Germany was the major lactic acid maker in the world for a long time. Its lactic acid was exported to many industrialized countries such as England, France, Japan and US. For a fairly long time (until WWII), German export of lactic acid was over 2000 tons (pure) per year.

The first preparation of synthetic lactic acid was performed by Strecker in 1850 by the reaction of alanine, 2-aminopropionic acid, with nitrous acid. A more suitable synthesis was found by Wislicenus (1) in 1863 by reacting acetaldehyde with hydrogen cyanide to from lactonitrile, which can be hydrolyzed to lactic acid in the presence of hydrochloric acid. Although the study of synthetic lactic acid started in the same time as the discovery of lactic acid, fermentation was the only method to produce lactic acid until 1960s.

Monsanto's 4500 t/a synthetic lactic acid plant was built in 1962 in Texas City and doubled in its capacity in 1969. Du Pont closed the old lactic acid plant at Gray's Ferry in 1963. America Maize finished its lactic acid operation at 1964. Clinton, the largest manufacturer at that time, kept lactic acid production until 1982, but never made a sizable investment again. It looked like the synthetic route would replace fermentation for lactic acid production in no time. But the invention of producing enantiomerically pure L (+) lactic acid from fermentation in HVA laboratory (around 1967) saved the fermentation lactic acid production because the major uses of lactic acid are the food industry.

L (+) isomer occurs normally in human metabolism, but the D (-) isomer is a foreign substance that metabolized differently. L (+) lactic acid will be converted to glycogen and D (-) lactic acid is oxidized or excreted in the urine, so L (+) lactic acid is natural for humans and D (-) is not. Only L (+) lactic acid is natural to humans and does not have any side effects, so it can be used in food safely.

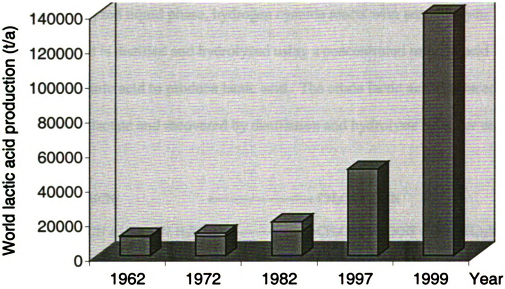

Figure 1-1. Annual lactic acid production

Worldwide lactic acid production is shown Figure 1-1. The top parts in 1962~ 1982 are synthetic production, but none of these data are available for 1997 and 1999, as most is from fermentation according to the sources. This figure is compiled with data from Bennina (1) and Chemical Market Report (3).

1.1.1.3. Synthetic technology

The currently used chemical synthetic method was first found by German chemist Wislicenus in 1863, and the first patent was requested by a German company in 1930. Du Pont was granted another patent (1984415) in 1933 for preparation of lactonitrile. In 1949, Musashino Chemical Laboratory Ltd. of Tokyo, Japan realized Wislicenus's idea in pilot scale plant with output of 330 tons per year. Because synthetic lactic acid is a racemic mixture of two enantiomers, it is not good for food industry. The largest synthetic plant (Monsanto) is based on a byproduct from acrylonitrile synthesis, so no other competitor appears except the only pilot plant in Japan.

In base-catalyzed liquid phase, hydrogen cyanide reacts with acetaldehyde. The lactonitrile produced is distilled and hydrolyzed using a concentrated mineral acid like hydrochloric or sulfuric acid to produce lactic acid. The crude lactic acid produced is esterified to methyl lactate and recovered by distillation and hydrolysis by water under acid catalysts (4).

$$CH_3CHO + HCN \longleftrightarrow CH_3CHO\ HCN$$

$$CH_3CHO\ HCN + H_2O + 1/2\ H_2SO_4 \longleftrightarrow CH_3CHOHCOOH + 1/2\ (NH_4)_2SO_4$$

$$CH_3CHOH\ COOH + CH_3OH \longleftrightarrow CH_3CHOH\ COOCH_3 + H_2O$$

$$CH_3CHOHCOOCH_3 + H_2O \longleftrightarrow CH_3CHOH\ COOH + CH_3OH$$

Figure 1-2. Chemical synthesis of lactic acid

A heavily researched and even piloted process is the oxidation of propylene with nitrogen peroxide. This process is based on the discovery of Levy and Scaife (5) in 1944. French's Rhône-Poulenc and German's BASF filed patents in 1966 and 1965 for this process and even the Russian scientists worked on its reaction mechanism (1). In this process, propylene gas mixed with oxygen is passed at a temperature near the freezing point through a solution of about 16% nitrogen peroxide in concentrated nitric acid (70%). Propylene gas is absorbed quantitatively and the oxygen immediately oxidizes low nitrogen oxides formed in reaction back to nitrogen peroxide at same time. Finally, this process was given up, the possible reason is the unstable by-products, which may decompose uncontrollably and even explode (6). In addition, the major market is the food industry and only pure L (+) lactic acid is preferable. Another not commercialized synthetic

α-chlorop

1.1.1.4. T

O

mixture.

acid meta

L (+) lact

fermented

productio

bacteria

syrup, and

product in

immediat

purpose.

sulfuric ac

water (8 v

prevent fo

maintain p

calcium la

production

Re

to the use o

column, an

synthetic routes include direct oxidation of ethanol or propylene glycol and hydrolysis of α-chloropropionic acid (7).

1.1.1.4. The production of lactic acid from fermentation

Originally, the lactic acid produced from natural fermentation was a racemic mixture. With the pressure from synthetic lactic acid and the knowledge of racemic lactic acid metabolism, HVA laboratory at Schiedam began to work on the production of pure L (+) lactic acid from fermentation. With their successful work, at the end of 1967, the fermented 90% L (+) lactic acid was on the market (1). Currently, most commercial production of lactic acid via carbohydrate fermentation uses *lactobacillus delbreuckii* bacteria (8) to make pure L (+) lactic acid. Many carbohydrates, including whey, corn syrup, and cane, can be sources for the fermentation. Because lactic acid is an end product inhibitor, it must be converted to salt or extracted from the fermentation broth immediately as it is produced. Traditionally, calcium hydroxide has been used for this purpose. The recovered calcium lactate is then purified by evaporation and acidified with sulfuric acid to give lactic acid (9). However, since calcium lactate has a low solubility in water (8 wt %), only low concentration of lactate can be produced from fermentation to prevent formation of a large fraction of solid hydrated calcium lactate in solution and maintain product flow throughout the process. The cost of purifying dilute solution of calcium lactate and disposal of large amount of $CaSO_4$ has always been a drawback in the production of lactic acid via fermentation.

Recent developments in simultaneous or coupled extractive technology have led to the use of nano-filtration membranes (10), anion-exchange resin (11) activated carbon column, and solvent extraction (12) for recovering lactic acid from fermentation broth.

Ele

salt

And

Bec

bro

Am

pres

amr

amr

ferm

from

pres

rege

acids

subs

cons

prod

1.1.1

acidi

Proce

agent

Electrodialysis also is a possible way for recovering highly purified lactic acid from its salt form (12). These new innovations will lower the production cost of lactic acid. Another technique is to use ammonia as a pH control instead of calcium hydroxide (13). Because ammonium lactate is highly soluble in water, the concentration of lactate in broth can be up to 30% before activity of the fermentation organism is impaired. Ammonium lactate can subsequently be converted to lactate esters and ammonia in the presence of gaseous CO_2 and alcohol at around 160°C and moderate pressure (14). The ammonia is then recycled back to the fermentation broth. These advantages have made ammonia very attractive as a replacement for calcium hydroxide.

Another very interesting process for producing and separating lactic acid from fermentation was invented by Cargill (15). In this process, the lactate solution obtained from a fermentation broth is extracted by a water immiscible trialkyl amine in the presence of carbon dioxide. Lactic acid is recovered from the resulting organic phase, and regenerated extractant is recycled for reuse in the extraction. So, the consumption of acids and bases are avoided and the generation of waste salts and other by-production are substantially reduced, if not eliminated. Theoretically, CO_2 is the only material for consumption. If such a advanced technique can be commercialized, the lactic acid production cost will be even lower.

1.1.1.5. Lactic acid market

The primary user of L (+) lactic acid is the food industry. It is used as a food acidulant/flavoring/pH-buffering agent or as an inhibitor of bacterial spoilage in several processed foods like soups, candy, bread, etc. Another application is as an emulsifying agent in foods such as bakery goods. Another major use is the leather tanning.

Pharmaceutical and cosmetic applications include use in topical ointments, lotions, and biodegradable polymers for medical applications. The use of lactic acid and other 2-hydroxycarboxylic acids have been shown to alleviate or improve signs of skin, nail, and hair changes associated with intrinsic or extrinsic aging. The only known manufacturer of D (-) lactic acid is Rhône-Poulenc, which built a fermentation plant at Melle to produce exclusive D (-) lactic acid as a building block for stereo-isomeric herbicides (1, p448).

Since the early 1990s, worldwide production of lactic acid has dramatically increased and is currently estimated to be over 130000 tons/year (3) (Figure 1-1), of which most is produced by fermentation. The possibility of making an inexpensive biodegradable polymer (poly lactic acid) from lactic acid has further stimulated the interest in investment and research in the area of producing pure lactic acid from fermentation of carbohydrates. For enlarging the lactic acid production ability, the major corporations including ADM, Cargrill, Purac, and A. E. Staley have ventured into the manufacture of lactic acid (16). The availability of a high volume of inexpensive lactic acid has also inspired the research of using lactic acid as an alternative feedstock for the production of many special and commercial chemicals such as acrylic acid (17), propionic acid, 2,3-pentanedione, pyruvic acid, and propylene glycol (18).

The current market price of lactic acid ranges between $0.70/lb to $0.85/lb depending on its purity (19). In 1997, US consumes over 9000 tons of lactic acid annually, of which 85% is used in food-related applications to improve meat shelf-life and flavors, pH buffering agent, acidulant, and the production of emulsifying agents.

1.1.2. Propylene glycol

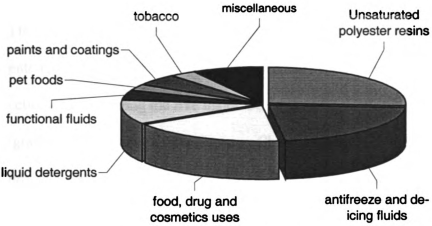

Figure 1-3. Propylene glycol use distribution (20)

Propylene glycol is a nontoxic chemical and has many industrial applications. The use distribution is shown in Figure 1-3. UPR (unsaturated polyester resin), antifreeze/coolants and deicing fluids and food products are the major consumption. Tobacco, paints, synthetic marbles, propylene glycol ether (PGEs), high-performance industrial solvents for paints and coatings, cleaners, inks, and a variety of other pharmaceuticals consume the other part.

Propylene glycol is a mass produced commercial chemical (450000 tons /year, 1998). The production capacity profiles are given in Table 1-1 (20).

Table 1-1. Propylene glycol production

PRODUCER	CAPACITY (Million lb/year)
Arco, Bayport, Tex.	565
Dow, Freeport, Tex.	250
Dow, Plaquemine, La.	230
Eastman, South Charleston, W. Va.	72
Huntsman, Port Neches, Tex.	120
Olin, Brandenburg, Ky	75
Total (per year)	1312 Million lb
	600000 ton

Currently, all commercial production of PG is from the hydration of propylene oxide. Di- and tri-propylene glycols, as well as small quantities of higher glycols, are also produced in the same plant. Propylene glycol (PG) capacities at some locations can be supplemented by shifting hydration equipment normally used for ethylene glycol (EG) to the production of PG. Among the five major US producers of PG, only Arco and Dow are back integrated into propylene oxide. Eastman Chemical acquired its South Charleston, W. Va., propylene glycol plant from Arco Chemical in 1991, and Huntsman purchased the Port Neches glycol plant from Texaco in 1994.

The market demand for propylene glycol 460000 tons in 1997 and 476300 tons in 1998. The predicted demand in 2002 is 570000 tons. The production has grown at about 3~4% per year since 1988. The market price is high, up to 0.68$/lb in 1997 and the current price is 0.6$/lb USP grade and $0.47/lb industry grade (21). Lancaster Synthesis Ltd. (UK) produces optical active propylene glycol, but the market demand is unclear.

1.2. Lactic acid reactions

Lactic acid ($C_3H_6O_3$) and starch ($C_6H_{10}O_5$+H_2O) have same C, H, O ratio, therefore, starch can be converted to lactic acid at very high yield in fermentation process. In addition, the price of starch from corn is only $0.07~$0.10/lb. With the progress of fermentation technology, it is possible to produce lactic acid at a price lower than 20 cent/lb. This potential further simulates the research about lactic acid derivatives.

Lactic acid is a simple compound containing both hydroxyl and carboxylic acid groups, which permit it to participate in many interesting and valuable chemical reactions. Among the known reactions of lactic acid (Table 1-2), the dehydration to acryli

conde

1.2.1. L

rhenium

from rhe

acid to c

per mole

3800 psi.

dilactide.

Broadber

temperatu

high from

only one c

Re

alcohols b

ruthenium

reduced wi

presence of

acrylic acid, the polymerization to poly (lactic acid) and the newly discovered condensation to 2,3-pentanedione (22) are potentially the most profitable pathways.

Table 1-2. Important lactic acid reactions

Reaction	Product
Dehydration	Acrylic acid
Condensation	2,3-pentanedione
Reduction	Propylene glycol
Polymerization	Poly lactic acid

1.2.1. Lactic acid reduction

Broadbent *et al* (23) began the catalytic hydrogen reduction of lactic acid by using rhenium black as catalyst. Their work was about high activity rhenium powder prepared from rhenium heptoxide. They could hydrogenate many organic acids including lactic acid to corresponding alcohols. For lactic acid hydrogenation, they used 1 g ruthenium per mole lactic acid with no solvent. The total reaction time was 8 hours at 150°C and 3800 psi. The final products are 84% propylene glycol and 16% of lactic acid and dilactide. They did not give any information about the purity of lactic acid used. Because Broadbent *et al* used *in situ* reduced high active rhenium black, they could use mild temperature to achieve high conversion. However, the pressure he used was still quite high from the viewpoint of process equipment requirements. In addition, lactic acid is only one of many acids used to test their catalyst, so no more details are given.

Recently, Antons (24) patented a process for the preparation of optically active alcohols by reducing optically active carboxylic acids with hydrogen in the presence of ruthenium catalysts. In this patent, carboxylic acids with an alpha or beta branch are reduced with hydrogen at temperatures below 160°C and pressures below 3000 psi in the presence of ruthenium contained catalysts. For hydrogenating lactic acid, 4g of Ru black and 89g of L- (+)-lactic acid were placed in 700g of water in a 1.3 L stainless steel autoclave. After flushing with nitrogen, the apparatus was closed and brought to a hydrogen pressure of 100bar. Over 2 hours the temperature was raised to 80°C and the hydrogen pressure to 200bar. The mixture was stirred at 80°C and 200bar until the uptake of hydrogen had ended. It was then cooled to room temperature, the catalyst was filtered off, and the water was distilled off. The residue obtained was distilled under nitrogen at 16 mbar to give 64g of L-(+)-propane-1,2-diol (b.p.= 74° C.; $[\alpha]_d^{20}$ +16.2°; ee>97%). Other examples of lactic acid hydrogenation are summarized in Table 1-3.

Table 1-3. Lactic hydrogenation results from patent US5731479

Catalyst	Amount	Yield	ee %
Ru black	4	85	>97
10% by weight Ru-on-carbon	20	74	>97
RuO_2 reduced at 150° C	2	88	>97
5% by weight Ru-on-Al_2O_3	20	68	>97
RuO_2 reduced at 150°C	10	86	97
5% by weight Ru-on-carbon	10	35	>97
5% by weight Ru-on-carbon	20	64	>97

To maintain optical activity, Antons used very low temperature and high pressure. Although he did not give the reaction time, the reaction should very long due to the low temperature used. This patent shows the ee efficiency of lactic acid hydrogenation is only sensitive to the reaction temperature (Figure 1-4). The catalyst state (metal, supported metal or oxide) and catalyst support type (carbon or Al_2O_3) and catalyst loading do not affect the ee efficiency of formed L (+) propane 1,2-diol. The patent did not give the pressure effect on the ee efficiency.

very hi

product

acid at

optical

reaction

reductio

pressure

E

to propa

be unim

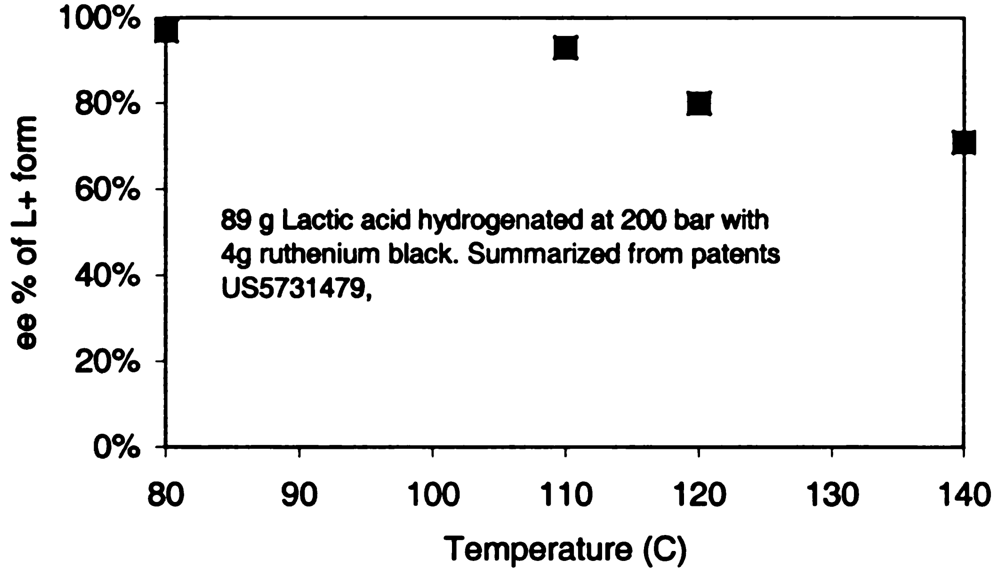

Figure 1-4. ee efficiency vs. temperature in L (+) lactic acid hydrogenation

For the above two published lactic acid hydrogenation studies, the first one used very high pressure, and the catalyst had to be prepared *in situ*. They did not mention by-products and corrosion in their paper, which are obvious problems for concentrated lactic acid at high temperature and pressure. The purpose of patent US5731479 is to produce an optically actively alcohol; to avoid racemization, a very low temperature was used, so the reaction time is possibly too long to be practical in industry. In summary, lactic acid reduction is not an easy task as highly active catalyst and elevated temperature and pressure are needed.

Beside hydrogenation to propylene glycol, lactic acid also can be directly reduced to propanoic acid by bacteria in fermentation process. However, this reduction path may be unimportant in industry, so only a few papers mention it (25).

1.2.2. Polymerization

Because lactic acid contains both the hydroxyl and carboxylic acid groups, it can undergo self-esterification to form either dilactide or lactoyllactic acid (26). Similar to all esterifications, the latter reaction is acid-catalyzed. The production of dilactide is catalyzed by primarily weak base (27). Continued esterification of lactoyllactic acid gives poly lactic acid, but the produced polymer usually has low average molecular weight because of the equilibrium constraint imposed by water concentration. The commercialized route patented by Du-Pont for the production of high molecular weight biodegradable poly(lactic acid) from lactic acid involves two catalytic steps. After the formation of lactide, water is removed by distillation and then a simple catalytic ring-opening polymerization of the purified lactide produces polylactide. Currently, poly (lactic acid) is estimated to cost in the range of $1.00-$1.50/lb. Co-polymerization of lactic acid and diisocyanate has also been examined in the production of poly (ester-urethane) (28). Because the poly lactic acid is a biodegradable polymer, the market prospect is very good due to the ever tighter environmental regulation. The numerous patents (29) about polylactic acid show the demand for cheap biodegradable polymer.

1.2.3. Dehydration

The dehydration of lactic acid to acrylic acid has been the focus of many studies in the past due to the demand for acrylate-based polymers. In 1956, a patent by Holmen claims the invention of a process in which 68% acrylic acid yields are obtained at around 400°C using sulfate and phosphate catalysts. It has been known that phosphate salts are commonly used in catalytic dehydration, but no complete mechanistic explanation has been proposed. Monobasic sodium phosphate catalyst buffered with sodium bicarbonate has also been used to obtain 58% acrylic acid yield from lactic acid (30). Recently, Mok published an in-depth study of lactic acid reactions in supercritical water (31). A mechanism for the dehydration of lactic acid to acrylic acid without catalyst was proposed which involved the leaving of the α-hydroxyl group and the carboxyl hydrogen instead of hydrogen from the methyl group, forming a lactone as an intermediate. They had also identified the decarbonylation of lactic acid to acetaldehyde as the major competing reactions since both go through similar transition states. Further studies on lactic acid conversion in supercritical water using phosphate catalysts resulted in a 58% acrylic acid yield (32). Extensive conversion studies of lactic acid to acrylic acid over various sodium salts and supports have been performed by Gunter and Langford (33). It was found that sodium metasilicate and bromate exhibit the highest selectivity toward the formation of acrylic acid.

1.2.4. Condensation to 2,3-pentanedione

The condensation of lactic acid to 2,3-pentanedione over basic sodium salt catalysts was discovered by Gunter et al (34), and extensively investigated by Man (22). Their research shows lactic acid obtained from fermentation can be converted to 2,3-pentanedione with acetaldehyde, acrylic acid, and propionic acid as lower value by-products in a fixed-bed, down-flow reactor. Formation of acrylic acid from lactic acid is relatively low at 23% yield over NaOH at 350°C because of the competing decarboxylation reaction to acetaldehyde at high temperature. However, 2,3-pentanedione can be produced in high yield over alkali metal catalysts at temperatures between 280-300°C with yield increasing in the order of Na < K < Cs. 2,3-Pentanedione yield as high as 60% theoretical with a 80% selectivity is obtained over a 2 mmol

CsOH/g silica catalyst at 280°C. Catalyst loading also increases the yield to 2,3-pentanedione proportionally up to a saturation limit of 2 mmol of metal per gram of support. Post reaction FTIR spectra of these alkali metal catalysts after exposure to lactic acid vapor indicate the formation of alkali lactate as the dominant species on the surface at 260-320°C. He concluded that the anions of initial sodium salts used do not participate in the condensation to 2,3-pentanedione, and the formation of 2,3-pentanedione involves presence of both lactic acid and alkali lactate. Conversion of the alkali salt to lactate is found to be the greatest when a low melting point salt with a volatile conjugate acid is used. The decarbonylation of lactic acid to acetaldehyde can be greatly reduced by using a silica support with low surface acidity.

1.3. Hydrogenating carboxylic acids with molecular hydrogen

Because molecular hydrogen is not reactive chemically at low temperature and its solubility in aqueous phase is very low at low pressure (35), almost all hydrogenation reactions need catalysts and high temperature and pressure. The carboxylic group is very stable to molecular hydrogen even with catalyst at strenuous conditions. The corresponding ester is much easier to hydrogenate to alcohol at relative mild reaction conditions. Therefore, some researchers hydrogenate the ester instead of free carboxylic acid to prepare corresponding alcohols. Before 1960s, hydrogenation catalysts were largely confined to heterogeneous systems involving metals, metal oxides and some salts. Since the development of transition metal complexes, which replicate the catalytic properties of the metals, and are effective in homogeneous reaction systems, homogeneous catalysts also attract the attention of many researchers (F. J. Mcquillin (36)).

The earliest works of ester hydrogenation date back to the publications of Brown & Adkins (37) in 1934. In their work, copper-chromium oxide and nickel catalyst were used to hydrogenate optically active esters and ketones to optically active alcohols at temperature of ~250°C and pressure of 150-200atm. Most esters could maintain their optical activity during the hydrogenation, except for butyl lactate that lost it optical activity after 2 hours hydrogenation at 225°C and 200atm. The paper of Adkins *et al* (38) in 1947 was about hydrogenation of esters to alcohols over Raney nickel. By using very large catalyst loading, they could hydrogenate esters of alpha amino acids to corresponding amino acohols at 50°C and 150~200atm. The extremely low temperature is advantageous in save the amino group and avoiding racemization.

In early 1930s, catalytic hydrogenation of carboxylic acids to the corresponding alcohols were accomplished with copper catalysts at temperatures above 300°C, with promoted copper catalysts at temperatures above 240°C, or with cobalt catalysts at temperatures above 220°C and at pressure above 200atm (39). The high temperature lead to very poor alcohol yields. Around 1952, Ford (40) and Carnahan *at al* (39) used ruthenium based catalysts to directly hydrogenate carboxylic acids at much low temperature, but they had to use pressure in excess of 500atm for best results. Their typical results are shown in Table 1-4. According to their investigation, the chief side reaction appeared to be further hydrogenation of the formed alcohol. They found byproduct ethanol during the hydrogenation of oxalic acid, and methane and ethane were detected when they hydrogenated hydroxyl acetic acid at 250°C. At some conditions, ester also formed and slowed the reaction. The problems with all of these studies are that the pressure is too high to be practical and/or the yield is very poor.

Table 1-4. Typical results of Carnahan *et al* (39) carboxylic acid hydrogenation

Substrate	T (° C)	t (hr)	P (atm)	Catalyst	Yield %
Acetic acid	147-170	10	700-950	RuO_2	88
Oxalic acid	94-170	10.5	630-990	RuO_2	47
Adipic acid	150-175	0.5	520-700	RuO_2	48
Succinic acid	152-192	4-5	720-950	RuO_2	59
Hydroxyacetic acid	145-149	0.16	700-710	Ru/C	83

In Broadbent's paper (23), *in situ* preparation of high activity rhenium powder catalyst could reduce formic, acetic, propionic, butyric, capric, lauric, stearic, lactic, maleic, succinic and glutaric acids to corresponding alcohols at 137~286 °C and 150-325atm. But the highly branched trimethylacetic (pivalic) acid could not be reduced to any recognizable product even at 264°C. Their carboxyl acid results are summarized in Table 1-5. Compared to Carnahan's works, Broadbent lowered the reaction pressure with good yield. The *in situ* catalyst preparation is a disadvantage. The strenuous reaction conditions used by Broadbent , Ford and Carnahan show that directly catalytic hydrogenation of carboxyl acids is very difficult even with highly active catalyst.

Table 1-5. Broadbent's carboxylic acid hydrogenation results

Acid	T (° C)	P atm)	t (hr)	Yield % and products
Formic	240	238	12	CO2, methane
Acetic acid	150	168	10	100 Ethanol
Trifluoroacetic	270	300	18.5	100 Trifluoroethanol
Propionic	165	252	1.5	92 Propyl alcohol
Butyric	150	178	11	89 butyl alcohol
Isobutyric	165	156	4	75 Isobutyl alcohol
Caprylic	200	188	2	93 n-Hexyl alcohol
Capric	137	173	3.5	100 n-decyl alcohol
Lauric	160	186	10	100 n-Dodecyl alcohol
Stearic	265	245	23.5	43 n-Octadecyl alcohol
Lactic	150	258	8	84 propylene glycol
Maleic acid	196	286	12	91 succinic acid
Succinic acid	210	245	4	94 (1,4-diol)
Glutaric	250	179	50	1001,5-Pentanediaol

carbo
patent
α or β
hydro
carbo
are w
cond
bar. T
wise.
active
cost a

benze
with
phase
meta
batch
hydro
inter

at the
the c

Special neighbor atom (or group) can activate the carboxylate group, so the carboxylic acid can be hydrogenated with catalyst in relatively mild conditions. In the patent of Antons (24) (1998), the carboxylic acids have to have a neighboring group at the α or β position. This group could be linear or branched C1 -C4 -alkyl, benzyl, and hydroxyl. The reduction is carried out in the presence of a solvent for optically active carboxylic acids and the product is optically active alcohol. Examples of suitable solvents are water, water-miscible organic solvents and mixtures of the two. Suitable reaction conditions are temperatures in the range 50 to 150°C. and pressure in the range 5 to 250 bar. The process according to this invention can be carried out continuously or batch wise. The surprising advantages of the process are that it provides access to optically active alcohols in a simple manner, at relatively low temperatures and pressures, at low cost and with a high selectivity (enantiomeric excess, ee, usually over 90%).

Miroslav's patent (1981) (41) shows that fluorine-containing alkyl, cycloalkyl, and benzene carboxylic acids could be hydrogenated to the corresponding primary alcohols with heterogeneous catalysts. The hydrogenation can be carried out in the liquid or vapor phase in the presence of a solid rhodium or iridium catalyst employed as the metal, metallic oxide, or mixture. In the liquid phase, the hydrogenation can be carried out in batch reactor at 50-150°C and 5-15 atmospheres. The main purpose of this invention is to hydrogenate trifluoroacetic acid in the liquid phase to 2,2,2-trifluoroethanol, which is an intermediate in the synthesis of the anesthetic, isoflurane, $CF_3CHClOCHF_2$.

Some catalysts can hydrolyze α-hydroxyl group while saving the carboxyl group at the same time. A 1987 patent granted to Velenyi *et al.* describes a catalytic process for the conversion of α-hydroxyl carboxylic acid to aliphatic carboxylic acid and aldehyde

[45]. The

impregna

of the co

the silica

nitrogen

Velenyi

350°C an

acid from

showed a

suppress t

1.3.1. Het

Th

metal oxid

active cata

synthetic s

acid hydro

hydrogenat

of acid will

effective ca

carbon are e

alcohol or g

(130-225°C

(42). The catalysts used have the formula $M_aM'_bO_x$. The catalyst is prepared by impregnation of 30 % metal oxides onto 70 % silica (or silica-alumina support). Because of the complexity of the catalyst system, the exact structures of these oxide complexes on the silica support are not known. The feed (~26 wt % of lactic acid) is carried by nitrogen through a down flow, fixed bed reactor. Using $Mo_5Cu_4SnO_x$ on silica-alumina, Velenyi was able to obtain a 64% propionic acid yield with a total conversion of 99% at 350°C and atmospheric pressure. Man (22) also investigated the formation of propionic acid from lactic acid over molybdenum and other mixed transition metal catalysts, and showed a 28% yield at 350°C and 5 second residence time. But, his purpose was to suppress this reaction to achieve high yield of 2,3-pentanedione.

1.3.1. Heterogeneous catalysts

The most commonly used catalysts in organic acid hydrogenation are metals and metal oxides in solid state. Generally, organic acid hydrogenation is not easy, even with active catalysts, and vigorous conditions are still needed for successful reduction on a synthetic scale. At 150 °C and 2000 psig, Rh_2O_3 become a useful catalyst for carboxylic acid hydrogenation (43). Ruthenium is well known for its ability to promote the hydrogenation of aromatic rings without hydrolysis of hydroxyl groups, and the presence of acid will completely deactivate its ability to hydrogenate C=C bonds. It is also a very effective catalyst for organic acid hydrogenation. Ruthenium dioxide and ruthenium on carbon are effective catalysts for hydrogenation of mono and di-carboxylic acids to alcohol or glycol. High-pressure (5000-10000 psi) and elevated temperatures (130~225°C) have been used in prior research (43). Yields of alcohol tend to be less than perf

obta

temp

also

gave

prom

temp

arom

on su

obtain

cataly

1.3.2.

industr

will be

1938. I

in 1939

tempera

has led

reported

effective

aqueous

perfect because of esterification of the alcohol. Near quantitative yields of alcohol can be obtained by mixing ruthenium and copper chromite catalysts to reduce the esters.

Hydrocarbon by-products increase if the catalyst is reused or with increased temperature, but decrease with increased pressure. Rhodium or palladium with rhenium also shows synergistic effects (44). Catalysts made from Re_2O_7 and Pd $(NO_3)_2$ on carbon gave a 97% yield of 1,6-hexanediol from adipic acid. Copper chromite and barium-promoted copper chromite have been used for organic acid reductions but very high temperature (300 °C) are needed (43). Rhenium oxides are also useful in reduction of aromatic acids to alcohols without ring saturation. Strongly synergistic effects were found on substituting half of the Re_2O_7 with ruthenium on carbon, and excellent results can be obtained at part attributable to competition of substrate, hydrogen, and solvent for catalyst sites (43).

1.3.2. Homogeneous hydrogenation catalysts

While heterogeneous catalysts still dominate the hydrogenation practice in industry, an increasing number of studies and patents indicate that homogeneous catalysts will become increasingly important. Calvin (45) reported the first homogeneous catalyst in 1938. Iguchi (46) found the activation of molecular hydrogen by rhodium (III) complexes in 1939. The finding of adsorption of hydrogen by cobalt cyanide solution at room temperature in an amount corresponding to almost one hydrogen atom per cobalt atom has led to the widely study of homogeneous hydrogenation catalysts. In 1961, Halpern (47) reported that under mild conditions, aqueous solutions of chlororuthenate(II) were effective catalysts for the hydrogenation of olefins. In 1966, Halpern (48) found that aqueous hydrochloric acid solutions containing chlororuthenate(II) complexes (thought to be $RuCl_4^{2-}$) hydrogenate maleic to succinic acids at 65 to 90 °C and up to 1 atm hydrogen pressure. The initial blue solutions, produced by titanous reduction of ruthenium (III, IV) solutions, rapidly turned yellow in the presence of unsaturated organic acids and the rate of hydrogen adsorption was proportional to H_2 pressure and Ru^{II} concentration. Ando (49) also found the homogeneous catalysts can hydrogenate organic acids and anhydrides, but not esters. Mcquillin (36) summarized the homogeneous hydrogenation development in "Homogeneous hydrogenation in organic chemistry" (1976)

Currently, the available homogeneous catalyst hydrogenations are to a considerable extent complementary to heterogeneous counterparts. Compared to heterogeneous catalysts, most homogeneous catalytic systems still stay in the scientist's lab. Homogeneous catalysts are inherently simple chemically and kinetically, much more amenable to detailed study, need even milder reaction conditions than heterogeneous catalysts, and give high selectivity in the hydrogenation of double bonds while saving hydroxyl groups (For example, hydrogenating maleic acid to succinic acid (48)). The mild reaction condition and specially designed homogeneous catalysts have the ability to maintain optical activity during the hydrogenation. There is, however, the practical disadvantage that recovery of hydrogenation products may commonly require chromatography, which makes its industrial utilization very difficult and costly. In addition, the catalytic complex may consequently be effectively lost during the products separation, even though it is likely that this disadvantage may be overcome by introduction of supported homogeneous catalyst.

13.3

form

Ada

this

wor

salt

form

g c

for

mo

of

Th

Th

sh

pr

to

m

pr

hy

1.3.3. Hydrogenation of carboxylic acid salts

Hydrogenating carboxylic acid salts is difficult in aqueous phase because the formed base (hydroxyl) will change the solution's pH quickly and resists further reaction. Adam *et al* (50) (1952) tried to directly hydrogenate Cd-Ni propionate. The key point for this reaction is removing water, and not all salt can be hydrogenated to alcohol. In their work, 1.44g of sodium propionate was treated with cation exchange resin to convert the salt to the free acid, then 1.7g cadmium chloride and 0.24g nickel nitrate was added. The formed precipitate was carefully dried in an air stream. The reactor vessel containing 1.5 g copper chromite catalyst was evacuated and maintained at a pressure of 50-micron Hg for 4-8 hours to remove final traces of water. It was observed that the presence of moisture at this point markedly reduced yield. The reactor vessel was filled to a pressure of 235 atm with electrolytic hydrogen and heated to 240°C with shaking for nine hours. The product is 74% propanol in water (94% yield). More data are shown in Table 1-6. The other salt hydrogenation related works are fatty acid salts. Richardson and Taylor (51) showed at 133 atm and 340°C for 3 hours, Cd-Ni oleate can be hydrogenated to propyl propionate. That means that the C=C bond is broken. To continue the reduction of ester to the alcohol in one step process, copper chromite catalyst was added to the reaction mixture but the product consisted chiefly of a low boiling hydrocarbon, presumably propane or propylene. These are the only works to investigate carboxylate salt hydrogenation.

Table 1-6. Propionate hydrogenation (50)

H_2 Pressure atm	Temperature (°C)	Reaction time (hour)	Products	
			Propane	Propanol
133	340	0.5	12	60
133	340	3	68	15
150	320	1	17	57
150	280	9	2	47
200	270	9	59	30
200	240	9	2	74
235	240	9	<1	92

1.3.4. Hydrogen solubility

Because the dissociation of gaseous hydrogen into atoms is endothermic ($\Delta H=104$ Kcal/mole), its reactivity is very low. The solubility of hydrogen in aqueous phase is very low and not even measurable at higher temperature and atmospheric pressure (see Table 1-7). High pressure favors the dissolution of hydrogen, so high pressures will indubitably increase the reaction rate.

Table 1-7. Solubility (ml/mlH_2O) of hydrogen in water (52)

T(°C)	Solubility (1 atm)	T (°C)	Solubility	P (atm)20 °C	Solubility
0	0.0214	60	0.0129	10	0.19
10	0.0193	80	0.0085	20	0.38
20	0.0178	100	0.0000	30	0.57
30	0.0163			40	0.76
40	0.0153			50	0.95

1.3.5. Hydrogenation mechanism

Investigation of the reaction mechanism of carboxylic acid hydrogenation in condensed phase with heterogeneous catalysts is rarely found in the literature. In homogeneous catalytic hydrogenation of fumaric acid and maleic acid to succinic acid (hydrogenate C=C bond, not carboxyl), Halpern (48) used isotopic tracers to investigate the hydrogenation mechanism. He found that the hydrogenation of fumaric or maleic acid w

s

w

In

ol

th

nc

di

se

ad

pa

1.4

rea

coo

ope

in i

non

appl

syn

hydr

with D_2 in H_2O solution yielded un-deuterated succinic acid, while H_2 (or D_2) in D_2O solutions yielded 2,3-dideutero-succinic acid. They concluded that the hydrogen atoms, which added to the double bond, originate from the solvent rather than the hydrogen gas. In addition, at the reaction condition, no isotopic exchange between D_2 and H_2O was observed, i.e., there was no appearance of HD or H_2 in the gas phase. This implies that the uptake of hydrogen by this catalyst system, at least beyond the disassociate stage, is not reversible.

There are two possible paths for the carboxylic acid hydrogenation. One is to directly hydrogenate free acid, and another is to hydrogenate the corresponding ester. The second path probably is easier than the first one. Adam (50)'s work shows that without adding copper chromite, the hydrogenation will stop at ester stage. These possible pathways make the hydrogenation kinetic investigation more complicated.

1.4. Trickle bed reactor (TBR) and modeling

Trickle-bed reactors are packed beds of catalyst over which liquid and gas reactants flow cocurrently downward. One of the first practical applications of a cocurrent trickle bed reactor was the synthesis of butynediol (53). Due to the wide range of operating conditions that they can accommodate, trickle-bed reactors are used extensively in industrial practice, both at high pressures (e.g., hydro-processing, etc.) and at the normal pressures (e.g., bio-processing, etc.)(54). Currently, some of the well-known applications in chemical processing are hydrodesulfurization of petroleum fractions, synthesis of 2-butyne-1, 4, -diol from acetylene and formaldehyde, and selective hydrogenation of acetylene (Henry and Gilbert (55)).

How
packe
conta
supe
plant
supe
react
vario
packi
pulsi
liqui

uncer
effici
exter
over
only i
liquid
hydro
reduce
decrea
reacta

Trickle bed reactor is physically similar to the packed bed adsorption column. However, they are different in gas and liquid velocities and in the role of solid phase. In a packed bed, the packing is an inert that has the main purpose of improving the gas-liquid contact, while in the trickle bed, the packing is a porous active catalyst. The range of superficial liquid velocity encountered in trickle beds is from 0.01 to 0.3 cm/s in a pilot plant trickle-bed reactor and from 0.1 to 2 cm/s in commercial reactors. Similarly, the superficial gas velocity based on operating pressure can be from 2 to 45 cm/s in pilot reactors and from 15 to 3000 cm/s in commercial reactors. Sato et al (56) observed the various flow regimes in cocurrent downflow in packed beds using glass spheres as packing. They classified these into three distinct flow pattern: trickling at low liquid rate, pulsing flow at higher gas and/ or liquid rates, and dispersed bubble flow at very high liquid rate and low gas rate.

For laboratory scale trickle bed-reactors, catalyst partial wetting is a very uncertainly and yet important parameter. The accurate estimation of catalyst wetting efficiency is essential to determine trickle bed performance (54). The reaction rate over externally incompletely wetted catalyst can be greater or smaller than the rate observed over completely wetted catalyst. This depends on whether the limiting reactant is present only in the liquid phase or in both gas and liquid phases. For instance, if the reaction is liquid limited and the limiting reactant is nonvolatile, such as occurs in many hydrogenation processes, then a decrease in the catalyst-liquid contacting efficiency reduces the surface available for mass transfer between the liquid and catalyst, causing a decrease in the observed reaction rate. However, if the reaction is gas limited, the gaseous reactant can easily access the catalyst pores from externally dry areas, and consequently a higher reaction rate is observed with a decreased level of external catalyst wetting. Of course, the above analysis is based on the assumption that particles in trickle beds are always internally wetted. Kim *et al* (57) (1981) present criteria that allow one to estimate when internal pore dry-out can occur. Actually, internal wetting occurs in almost all trickle bed reactors.

Compared to three-phase slurry reactors, trickle-bed reactors do not need special equipment for the separation of deactivated powder catalyst, so the initial investment of equipment and operation cost is low. In addition, its flow pattern is close to the plug flow (if the bed diameter is not too large), which is very convenient if high conversion is required. The low effectiveness factor of catalyst pellets in TRB reactor results from their large size, and the requirement for high mechanical strength of the pellets to avoid erosion by the liquid reaction mixture, are the two major disadvantages of trickle bed reactors.

Modeling of trickle beds always is a frustrating task due to the lack of reliable mass transfer data, although many researchers put many efforts on this issue. Because mass transfer controls the trickle bed reaction in most cases, modeling the trickle bed actually equates to modeling the mass transfer. The complicated three-phase fluid dynamics in a trickle bed makes parameter measurement and estimation very difficult. Since catalyst wetting, liquid holdup, gas-liquid liquid-solid and pore diffusion all depend on the special system and catalyst used, it is very difficult to find generalized correlations to calculate the parameters.

Goto and Smith (58) gave a systematical investigation of a trickle bed reactor. For the first time, they used a true trickle bed system to measure liquid hold up, gas-liquid mass transfer and liquid-solid mass transfer coefficient. Based on their parameter measurements, a one-dimension trickle bed model was derived and used for trickle bed oxidation of formic acid [(59)]. Recently the residence time distribution was measured and modeled by Stegeman *et al* [(60)]. They concluded that the residence time of liquid phase could be well correlated to the Reynolds and modified Galileo numbers. Wammes investigated the hydrodynamics in trickle beds at elevated pressure [(61)]. Their results show that the hydrodynamic states are the same at equal gas densities.

In summary, compared to fixed bed reactors, the knowledge of the trickle bed still is in the early stage. Its mathematical modeling and scaling up still are still far from real use. However, its inherent advantage and wide use in industrial practices show that it is a good choice for our aqueous phase hydrogenation investigation. Specially, it is well fitted to our requirements for hydrogenation of organic acids.

1.5. Rationale of this research

This research has both scientific and economic significance. The aqueous phase catalytic conversion of biomass-derived lactic acid to propylene glycol is part of the worldwide effort of utilizing renewable carbon resource. This project could provide carbon resource for mankind after the depletion of petroleum and other fossil carbons. Comparing to petroleum pathway of production of propylene glycol, the proposed techniques will produce less toxic waste and be less polluting to the environment.

The even more important part of this research lies on its potential industrial value. Even though the market price of lactic acid is 0.7~0.8$/lb (88% food grade) [(21)], the purification process occupies over 70% of the total production cost. With the use of new fermentation technology, the unrefined lactic acid could only cost about $0.15~0.20/lb.

The market price of 1,2 propylene glycol from petroleum synthesis is $0.6/lb (21). Apparently, if we can use unpurified lactic acid to produce 1,2 propylene glycol, there is a large margin between feedstock and product. It is apparent that this margin is large enough for commercialization.

Chapter 2. Equipment and experimental methods

The hydrogenation reactions were conducted in a batch reactor (autoclave) and a trickle bed (continuous) reactor. The liquid phase products are analyzed by high performance liquid chromatography (HPLC) and gas phase by mass spectrometer. A Micromeretics Chemisorb 2700 was used to characterize the surface properties of catalysts.

2.1. Reagents

The main reactants were lactic acid and hydrogen. For catalyst screening and reaction condition optimization, 85% racemic lactic acid (J. T. Baker) and L (+) lactic acid (Purac) at 88% (weight) water solution were used. Unrefined L (+) lactic acid samples provided by Cargill were used to test catalyst deactivation. Compressed hydrogen gas with 99.999% purity was a product of AGA. All reagents are listed in Table 2-1.

Re
Li-
Lac
Li-
Lac
Pro
HP
Hy
H-
Et
Me
Ac
Pro
1-p
2-p
CG
CG
RuC
Ru-

2.2. Ca

catalys

suppor

2.2.1. (

were ei

2-2).

Table 2-1. Reagents used in the hydrogention of lactic acid

Regent	Purity %	Use	Source
L(+) lactic acid	88	Reaction	Purac
Lactic acid	85	Reaction	J. T. Baker
L(+) lactic acid	50	Reaction, catalyst deactivation	Cargill
Lactic acid	85	Calibration	Aldrich
Propylene glycol	99.9	Calibration, reaction	Aldrich
HPLC water	N/A	Solution for reaction	J. T. Baker
Hydrogen	99.999	Reaction	AGA
H_2+CO+CO_2	N/A	Mass spectrometer calibration	AGA
Ethanol	99.9	By-products identification	Sigma
Methanol	99.9	By-products identification	J. T. Baker
Acrylic acid	99	By-products identification	Aldrich
Propionic acid	99.9	By-products identification	Sigma
1-propanol	99.9	By-products identification	Aldrich
2-propanol	99.9	By-products identification	Aldrich
CG6M	N/A	Active carbon, catalyst support	Yakima
CG5P	N/A	Active carbon, catalyst support	Yakima
$RuCl_3$ hydrate	~49% Ru	Preparing catalyst	Aldrich
Ru-nitrosyl nitrate	1.5% Ru	Preparing catalyst	Alfa

2.2. Catalysts

The catalysts included commercial materials, our laboratory prepared powder catalyst, and granular carbon supported catalysts. All catalysts are metal, metal oxide, or supported metals.

2.2.1. Commercial catalyst samples

Commercial catalysts were used in the initial stage of this project. These catalysts were either samples of commercial catalysts or recently developed new catalysts (Table 2-2).

Table 2-2. Commercial catalysts

No	Catalyst	Active metal	Support	Manufacturer
1	Pd/C	Palladium	Carbon	England Corporation
2	Ru on alumina	Ruthenium	Alumina	Degussa Corporation
3	Ru/1940C	Ruthenium	Carbon	Precision Metal Incorporation
4	Ru/C-new	Ruthenium	Carbon	Precision metal Incorporation
5	Ru on Titania	Ruthenium	Titania	Degussa Corporation
6	Nickel/Alumina	Nickel	Alumina	Pressure Chemical Corporation
7	CuCr-99B-13	Copper & Chromium	None	United Catalysts Inc
8	A-7063 (Ni)	Nickel	None	Activated Metals & Chemicals
9	Ru/CP	Ruthenium	Carbon	Calgon carbon Corporation
10	Ru/RB carbon	Ruthenium	Carbon	Calgon carbon corporation
11	Ru/C	Ruthenium	Carbon	England Corporation

2.2.2. Catalyst preparation

The preparation of supported metal catalysts consisted of impregnating, drying and reduction. For powder catalyst preparation, granular active support was ground into powder in a food blender and a 100~200-mesh fraction was collected as catalyst support.

2.2.2.1. Impregnation

To control the metal loading in supported catalysts, the incipient wetness of support has to be measured before impregnation. First, the support was dried for 5 hours at 100°C and 30 in of Hg of vacuum. Then, HPLC water was added to about 5-gram dried support until the appearance of liquid phase. From the maximum water addition just before the appearance of liquid, incipient wetness could be calculated. The incipient wetness values for the three granular active carbon supports used are shown in Table 2-3.

Table 2-3. Results of incipient wetness testing

Support	Support weight(g)	HLLC water (g)	Incipient wetness
CG5P	4.4	5.0	1.14 g water/ g support
CG6M	6.3	9.7	1.54 g water/ g support
Nuchar	3.5	6.3	1.80 g water/ g support

Precursor solution was prepared by dissolving ruthenium salt into HPLC water. The weight of salt was calculated from the metal loading requirement and the water requirement was computed from incipient wetness. Then the weighed support was added all at once to the precursor solution in a beaker and the mixture was stirred for 5 minutes to ensure the salt solution was well distributed in the catalyst support.

2.2.2.2. Drying

For preparing powder catalysts, the mixture was placed on the rotating evaporator and the heat and vacuum were slowly increased to 80°C and 25 in of Hg. The total drying time was 2 hours. Then the mixture was cooled in room temperature for 5~10 hours. After that, the mixture was transferred to quartz tube reactor for reduction.

For granular catalysts preparation, the mixture was dried on a metal sheet in ambient conditions for 24 hours and then placed in quartz reactor under 30 in Hg of vacuum at room temperature for additional 4 hours. After that, the temperature was slowly increased to 50°C in 2 hours and held for 5 hours to complete the drying. The mixture was left in reactor and cooled to room temperature for reduction

2.2.2.3. Reduction

The same quartz tube used in granular catalyst drying was the reactor for catalyst reduction. First, the reactor was briefly purged with argon at room temperature. Hydrogen was then passed over the catalyst at 30 ml/min, and the temperature was ramped at 2°C/min to 400°C and held there for 16 hours. Finally, the catalyst was cooled under a helium (or argon) flow to room temperature and passivated by helium with 2% oxygen for 1 hour.

During the reduction, effluent gas was monitored by a mass spectrometer. For CG5P catalyst, the formed hydrogen chloride change with temperature is shown in Figure 2-1. The reduction began at about 200°C, and reached to a maximum at 280°C. The high background at 400°C came from the condensed yellow liquid (HCl+H_2O) in the outlet of the quartz reactor.

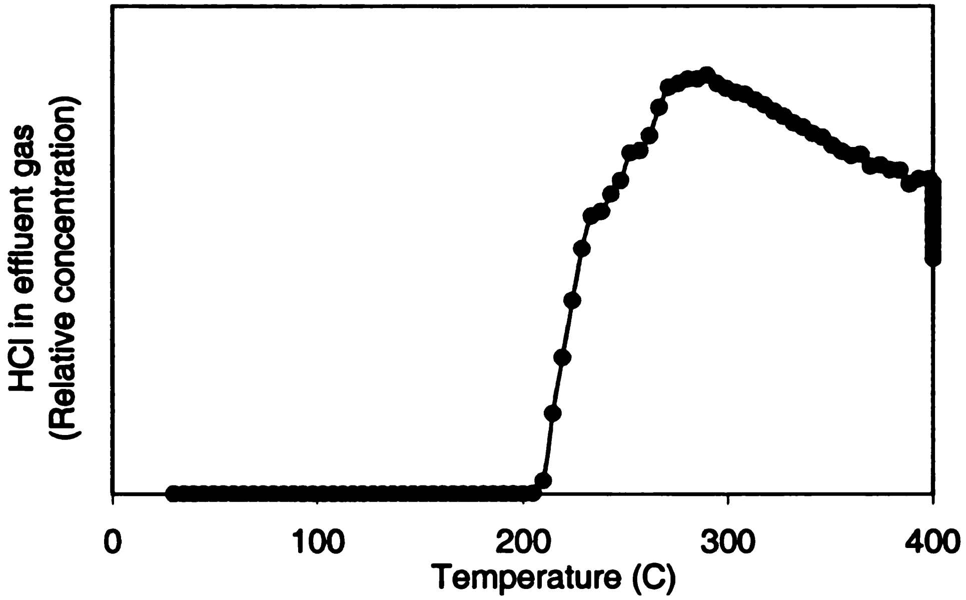

Figure 2-1. Hydrogen chlorine evolution profile during reduction

2.2.3. Powder catalyst

Powder Ru/carbon catalysts were prepared by Paul Fanson in our laboratory. The detailed parameters are given in Table 2-4.

Table 2-4. Details of MSU Ru/C powder catalysts

Catalyst	Precursor	Support:		Dispersion	Loading
		Name	BET m^2/g		
CG5P - G	Aldrich ruthenium (III) chloride hydrate (aq)	Cameron - Yakima INC. CG5P-200 Mesh	648	6 %	5.0%
CG6M - F		Cameron - Yakima macroporous-100 +200	728	13%	5 %
SA135-C		Aldrich Silica-alumina, grade 135, -100 mesh	440	14%	5.0%
SG6 – D		Cameron - Yakima INC. micro-porous 100 mesh	777	10%	4.4%
CG5P - A		Cameron – Yakima INC. CG5P(20*50 Mesh)	648	10%	5.4%
AL100 - B		Aldrich alpha aluminum oxide (-100 + 200 Mesh)	0.24	0%	5%
ALg – E		Alfa gamma alumina Size:+100 mesh	45	13.5%	4.7%
TiP25-C19 - J		Degussa P25 Titania-200 Mesh	49	N/A	5.0%
CG5P - H	Aldrich ruthenium(III) chloride hydrate (EtOH)	Cameron - Yakima INC. CG5P-200 Mesh	648	3 %	5.0%
CG5P-NO1-I	Alfa ruthenium nitrosyl nitrate hydrate (aq)	Cameron - Yakima INC. CG5P-200 Mesh	648	38%	5.0%

2.2.4. Granular catalyst

Granular catalysts were prepared for trickle bed reactor. Three active carbon supports were used in the first batch of catalyst preparation. After three catalysts were tested in autoclave, the catalyst prepared from WV-B (Nuchar) was discarded because its activity was too low. After trickle bed evaluation of CG5P and CG6M, CG5P was discarded because CG6M is apparently superior to CG5P. Therefore, only CG6M support was used in the second batch preparation.

2.3. Batch reactor (autoclave)

Batch reactor was extensively used in this research for catalyst selection and optimization of reaction conditions.

2.3.1. Reactor system

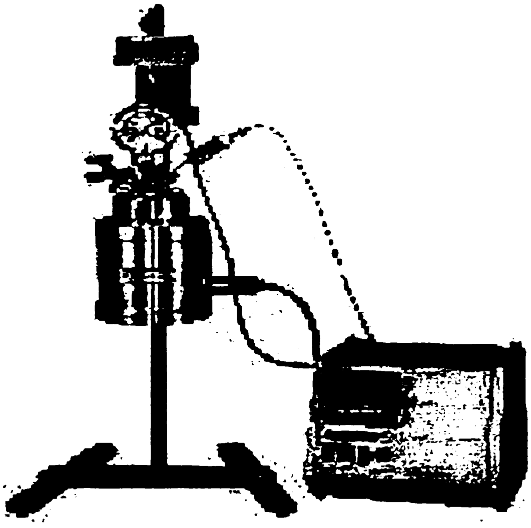

Figure 2-2. Batch reactor and controller

The batch reactor used in this project was purchased from Parr Instrument Company. It is a 300-ml mini stirred tank reactor (Model 4561) shown in Figure 2-2. The internal diameter is 3-in and height is 4-in; the total volume (excluding the cooling loop and stirrer) is 300 ml. It is mounted in a bench top stand designed for conducting liquid-gas reactions. The maximum temperature is 350°C and maximum pressure is 3000 psi. The whole reactor is made of T316 stainless steel. A quartz liner also is used for further protection from corrosion at elevated temperature. This reactor is equipped with a gas inlet valve for continuously charging gas into the reactor, and a gas release valve for releasing pressure and gas sampling. A dip tube connected to a liquid sampling valve is used for withdrawing liquid sample from the reactor under pressure without interrupting the reaction. A safety rupture disk provides over pressure protection. A thermocouple is located in the vessel for temperature measurement and control. A stirring shaft with attached impellers (or gas entrainer) is used to suspend catalyst and entrain gas into the liquid phase. A stirrer driving system with a packless magnetic drive and a self-sealing packing gland maintains a gas-tight seal around the rotating shaft. This reactor is controlled by a Model 4852 controller (also from Parr Instrument Company), which provides adjustable stirring speeds and automatic temperature control via electrical control of the heating mantle and the air-cooling loop inside the reactor. The whole reactor system consists of liquid feeding, gas feeding, reactor, controller and sampling tank (Figure 2-3).

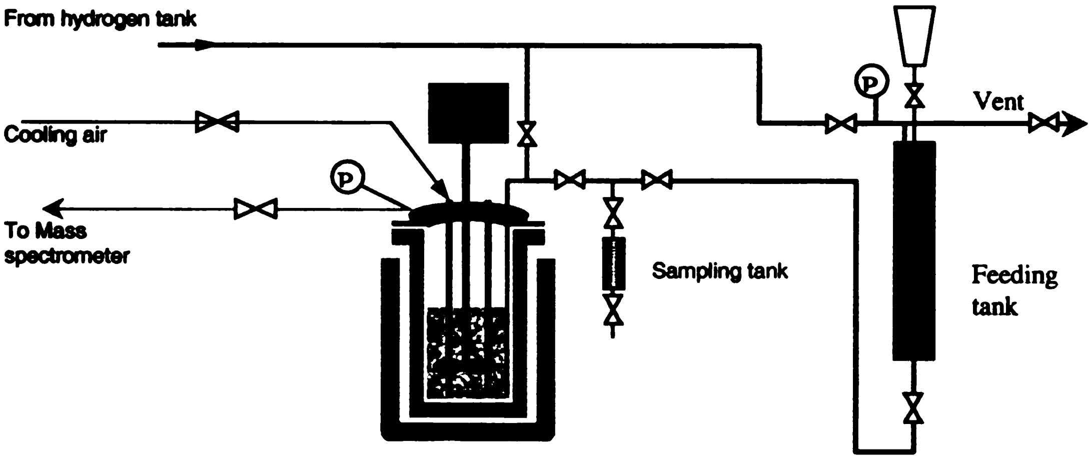

Figure 2-3. Batch reaction system

2.3.2. Operating procedure for the batch rector

Operation of batch reactor included reactor setup, steady state reaction and final liquid & gas volume measurements and analysis. First, weighed catalyst was loaded into quartz liner to avoid direct contact of lactic acid with the steel vessel. A stainless steel screen was put into the inlet of dip tube to act as a filter to keep the powder catalyst in the reactor during the liquid sampling. The reactor then was sealed. After reactor was installed on the stand, gas-lines and stirrer motor were hooked up. Then the reactor was purged by inert and hydrogen.

For the safety of operation, the sealed reactor was first purged with inert gas (helium or argon reason), which was slowly filled into the reactor to 500psi. Then the reactor was slowly depressurized to atmosphere. In this stage, the oxygen concentration in the reactor should be less than 0.6 % (volume) if the inert gas was completely mixed with the air in sealed reactor. It should be safe to fill hydrogen into the reactor. However, for safety considerations, the reactor was filled with inert gas one more time and depressurized to atmosphere to make the theoretical oxygen concentration inside the reactor less than 0.02 %. After that, hydrogen was used to replace inert gas to purge the reactor twice to make the inert concentration in reaction less than 0.1 %.

The next step was to reduce the catalyst. The role of this pre-reduction was to reduce the metal possibly oxidized during the catalyst transfer. The catalyst pre-reduction was done at stirring speed of 20~50rpm, temperature of 150°C, and hydrogen pressure of 500psi. The temperature stabilization needed about 10 minutes and additional 0.5~12 hours was used to complete catalyst reduction.

After the pre-reduction, the reactor was depressurized again to atmospheric pressure. The reactant solution was filled into the feeding tank, and then the feeding tank was pressurized to 500psi. With the opening of liquid inlet valve, the solution was transferred to reactor by pressure. Then, the reactor was depressurized again. After about 10 minutes, the reactor was heated to desired temperature. When the temperature was stabilized, reactor was charged with hydrogen to desired pressure. Then the stirring speed was increased to 1000~1200 rpm, which is the time zero for this reaction.

One (or half) hour later, the first sample was taken from the sampling loop. Before sampling, the sampling tank and sampling loop (a piece of tubing) was purged by high-pressure hydrogen to clean the residual liquid there. Normally, the sampling valve had to opened three times to collect 1~2ml liquid sample. The liquid sample was then filtered by micro filter and mixed with reference solution for HPLC analysis. Gas samples were taken out the reactor from a needle valve on the top of reactor and continuously fed into the mass spectrometer at rate of 5 ml/min.

After 5 (or more) hours reaction, all valves were closed and electrical power was turned off after the last liquid sample was taken. Then the reactor was left in air for cooling. When the reactor temperature was decreased below 40°C, the final gas phase volume was measured by water replacement (if necessary) while reactor was depressurized. After that, the rector was de-assembled and liquid volume was measured.

Table 2-5. Experimental parameters

Parameter	Range	Typical
Reactant volume	100~150g	120g
Temperature	100 to 170°C	150°C
Pressure	500 to 2000-psi	1500psi
Reactant concentration	5~30%	5%, 10%
Catalyst (g)/100g solution	1~4g	1~2g
Pre-reduction (temperature)	100~200°C	150°C
Pre-reduction (time)	0.5~12 hours	1 hour
Reaction time	2 to 10 hour	5 hours

2.4. Continuous trickle bed reaction system

A trickle bed reactor system was constructed in our lab for related hydrogenation studies. A gas liquid separator was added to continuously analyze the effluent gas composition.

2.4.1. Specifications of the trickle bed system

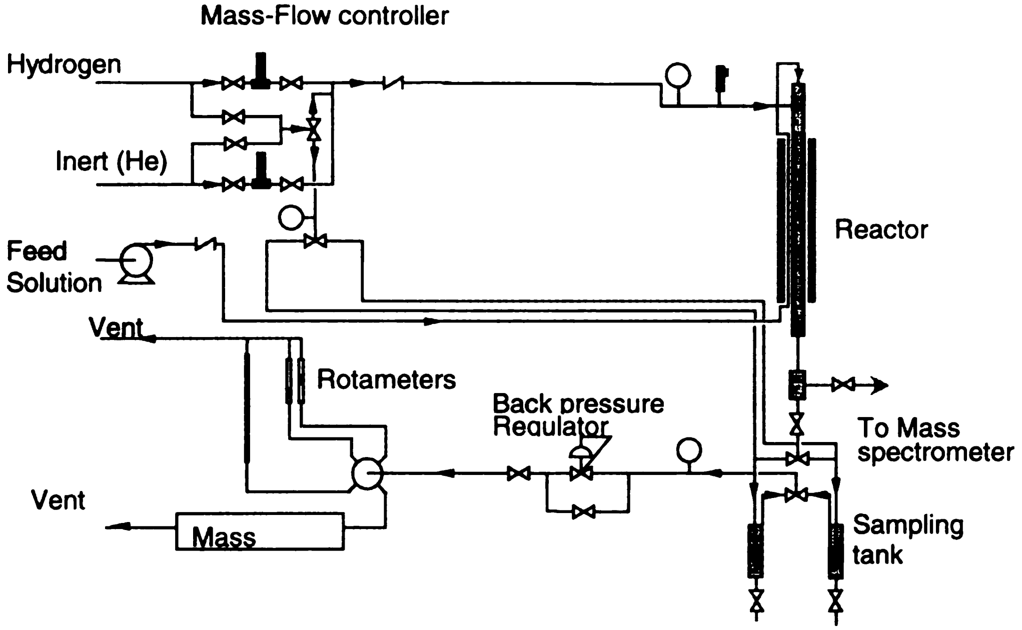
Mass-Flow controller
Hydrogen
Inert (He)
Feed Solution
Vent
Reactor
Rotameters
Back pressure Regulator
To Mass spectrometer
Vent
Mass
Sampling tank

Figure 2-4. Trickle bed reactor system

The reactor tube was 1.57cm ID and 61cm length 316 Stainless Steel tube. Its total volume was 118 ml. Gas flow rate (controlled by mass flow controller) could be 25~500 ml/min (STD) and liquid flow rate (depend on high-pressure liquid pump) could be 0.1 to 10 ml/min. The maximum temperature was 350°C, and the maximum pressure (limited by mass flow controller and pressure gauge) was 1280psi. The liquid distributor was 10cm height and packed with 2mm (diameter) glass beads.

2.4.2. Operating procedure for the trickle bed reactor

The first thing was to prepare catalyst column. Stainless Steel screens were used to support the catalyst on the bottom and separate liquid distributor (glass beads) and catalyst at the top of reactor tube. A thermocouple was placed into the catalyst bed to measure and control the reactor temperature. Then the top and bottom of reactor were connected to the tube to complete the preparation of catalyst column. Then, the column was hooked up to the trickle bed system, and all power cords and thermocouple lines were connected. Helium was charged into trickle bed system from bypass valve to 1000psi for leaking testing. Soap solution was used to test the all connecting-points. When pressure could hold for one-half hour (pressure drop less than 10psi), the leaking test was done and reactor was depressurized for catalyst reduction.

During the catalyst reduction, reactor pressure was controlled at 800psi by the back pressure regulator. Then, the reactor was heated to 150°C and held for 2~8 hours to complete the *in situ* pre-reduction. This reduction was done for new catalyst and after 20 hours reaction. After reduction, HPLC water was pumped into trickle bed at 1ml/min and temperature and pressure were controlled at desired values. When the trickle bed was fully stabilized, liquid feed was switched from water to lactic acid solution and the gas-sampling valve was opened to monitor the gas composition by mass spectrometer. It typically took 90-120 minutes for steady state product compositions to be achieved at most of reaction conditions, so several different reaction conditions could be evaluated over the course of a day. After about 2 hours reaction, the system was fully stabilized, liquid sample was taken from the sampling tank, filtered with a 0.2 micro syringe filter, mixed with internal reference solution and analyzed by HPLC. After finishing all desired experiments, the system needed to be shut down. In shutdown operation, liquid feed was switched from lactic acid solution to pure water for 1~2 hours to purge lactic acid out of the reactor, then all gas valves were closed and all power was turned off.

2.5. Products analysis

The gas phase was mainly analyzed by a Quadrupole mass spectrometer. Gas chromatography (GC) was used only for verification. High performance liquid chromatography (HPLC), manufactured by Thermo Separation Products, was used for liquid phase analysis.

2.5.1. Mass spectrometer

An Ametek Dycor M100M Quadrupole Mass mounted on a vacuum chamber that is capable of achieving a pressure down to 10^{-8}torr, is equipped with an electron multiplier for analysis of species concentrations down to 100ppm, and is interfaced with a personal computer for data collection and manipulation. Product gases from both reactors as well as calibration gases pass by one end of a one-meter long quartz fine capillary tube which continuously draws sample gases to the vacuum chamber, and achieves the final pressure reduction to 10^{-4}–10^{-5}torr. A system sketch is given in Figure 2-5. The mass spectrum can be displayed on the screen of the controller or interfaced by another computer to collect data and save to files for further analysis.

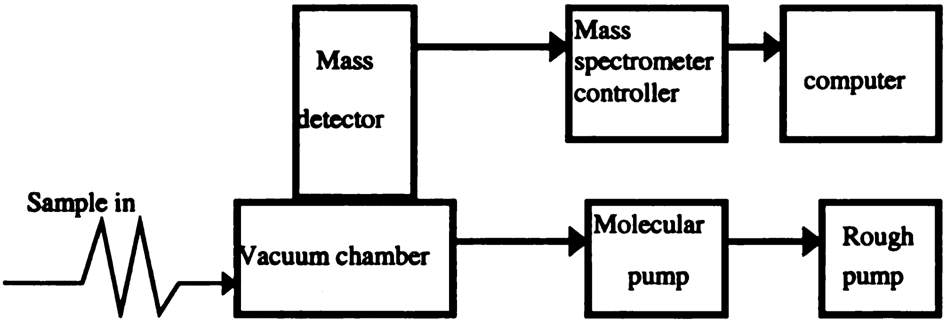

Figure 2-5. Mass spectrometer system

2.5.1.1. Gas phase by-products identification

Figure 2-6 and Figure 2-7 are typical gas phase mass spectrums in the final stage of reaction in batch reactor and trickle bed reactor. Compared to the standard mass spectrum (*) of methane (Figure 2-8), it can be seen that methane is one of the major gas products (characteristic peaks are Mass15 & Mass16, and Mass16>Mass15). The big Mass 28 peak could be either ethane or ethene. From the relative height of Mass 28 and the small peaks (Mass 26, Mass 27 and Mass 30) (Figure 2-6 and Figure 2-9), we can conclude that the major C2 gas by-product is ethane, but we cannot exclude a trace amount of ethene forming. For C3 gas product, the major component should be propane because the big Mass 29 peak (Figure 2-6 and Figure 2-11) and the small peak around Mass 39~Mass 44. However, we cannot exclude the trace amount of propene because of the peaks at Mass 39~Mass 43 (Figure 2-12).

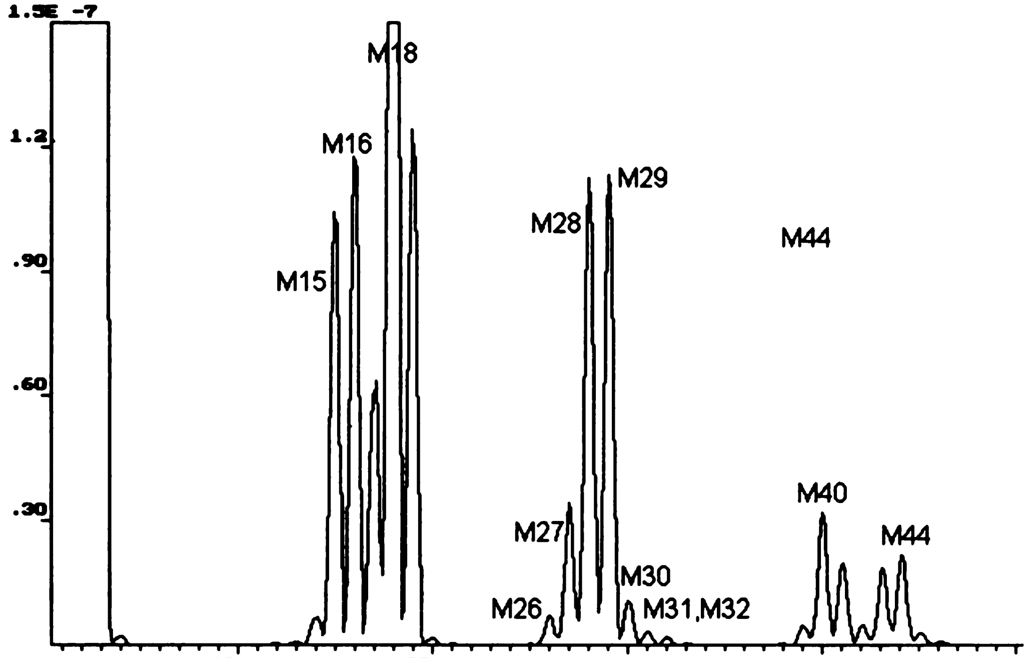

Figure 2-6. Final gas phase analysis from mass spectrometer (autoclave)

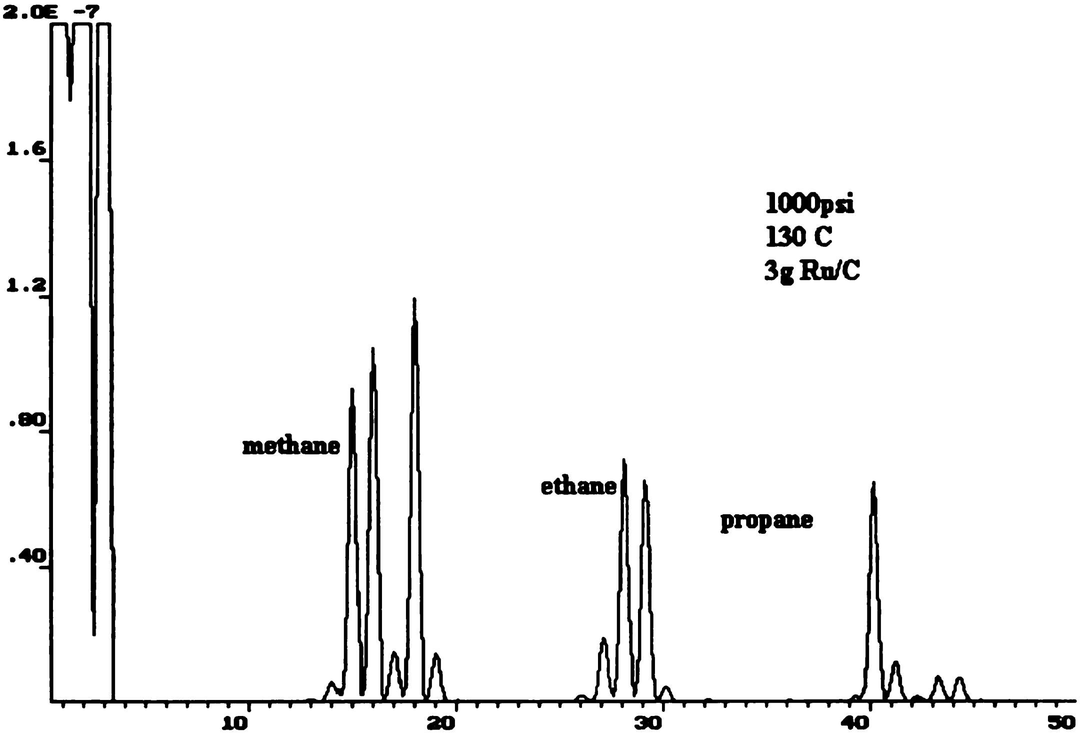

Figure 2-7. Gas phase analysis from mass spectrometer (trickle bed reactor)

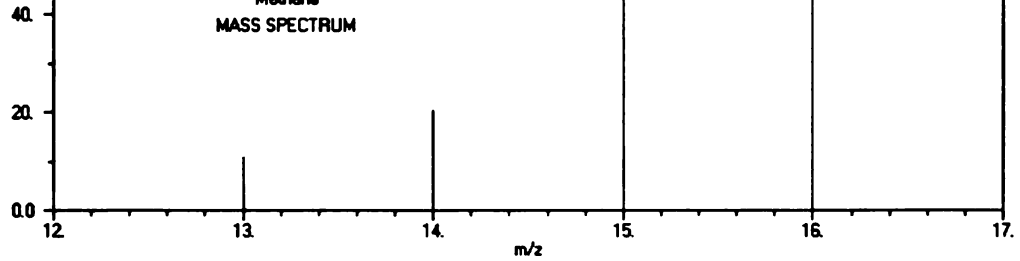

Figure 2-8. Standard mass spectrums for methane

---

* http://webbook.nist.gov/

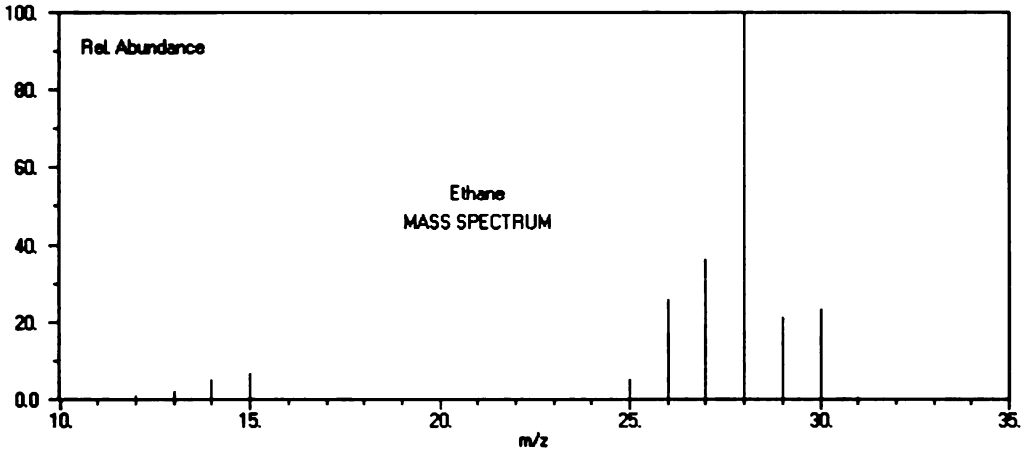

Figure 2-9. Standard mass spectrums for ethane

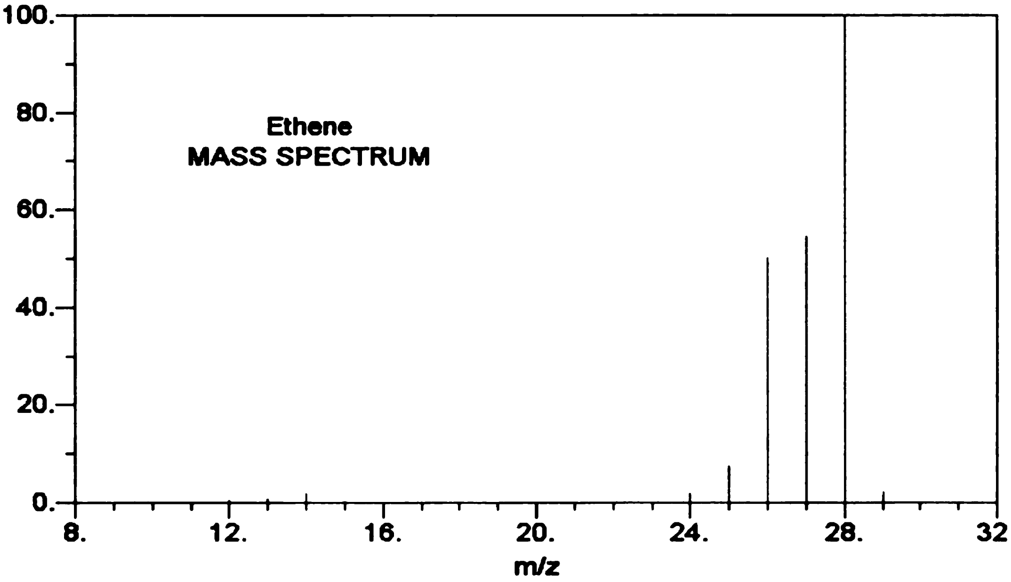

Figure 2-10. Standard mass spectrums for ethene

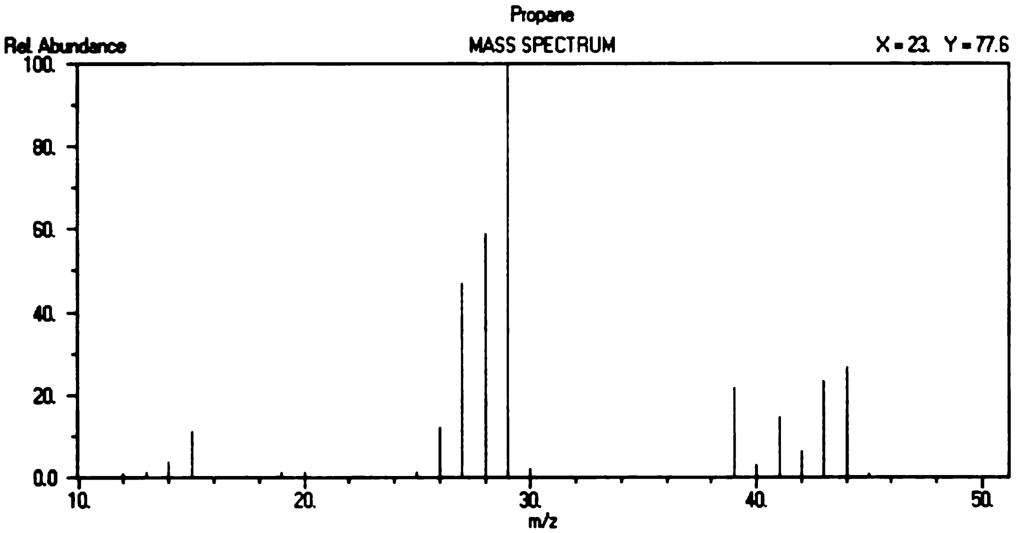

Figure 2-11. Standard mass spectrums for propane

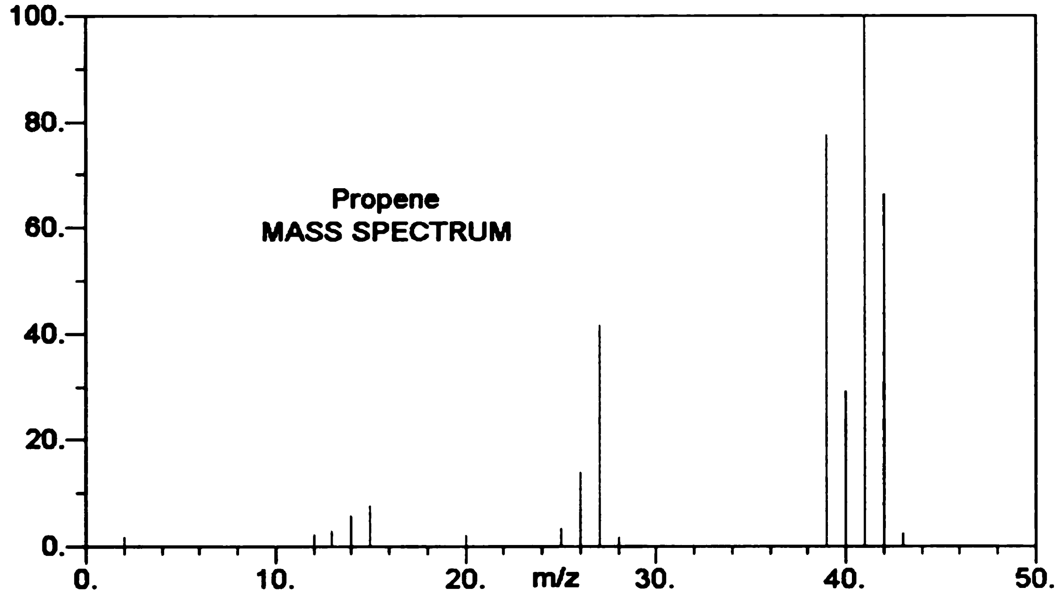

Figure 2-12. Standard mass spectrums for propene

In summary, the major by-products in gas phase consist of methane, ethane and propane and may contain traces amount of ethene and propene. The composition highly depends on the catalyst, reaction conditions, and the type of reactor. In Figure 2-6, the C1, C2 and C3 are almost in the same level; for Figure 2-7 methane peak is higher than that of ethane and propane. In addition, the backgrounds of carrier gas (pure H_2) are much less than the peak height of gas sample (Figure 2-13). For Mass 16 (Methane), the background is only 1% of that in most gas samples; for Mass 28, the background is less than 3% of that in gas samples. Therefore, the gas analysis is reliable. Figure 2-14 shows the calibration spectrum and the response of CH_4, CO and CO_2 is very close.

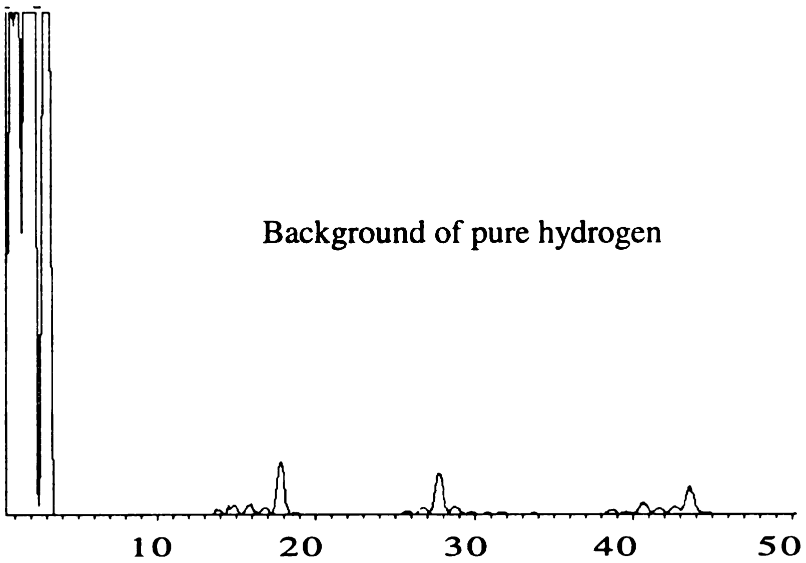

Figure 2-13. Background of pure hydrogen

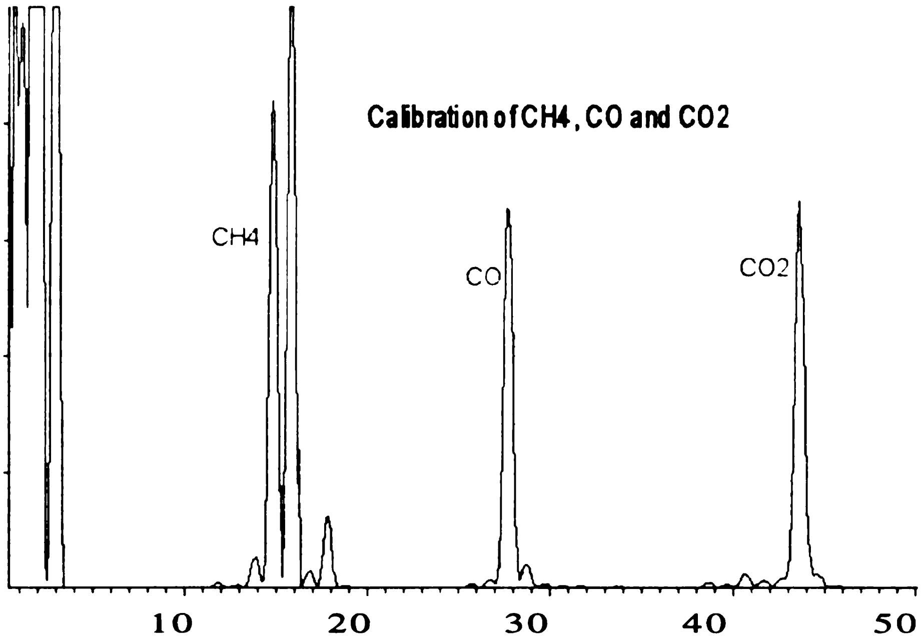

Figure 2-14. Calibration of CH_4, CO and CO_2

2.5.1.2. Quantitative analysis

Calibration of the mass spectrometer was performed by scanning a blend of AGA certified standard multicomponent gas mixture, which contains 2.05% CO, 2.03% CO_2, 2.01% CH_4, and balance hydrogen. Five scans of pure hydrogen (containing no essential species of interest) were taken to obtain background levels, averaged, and then subtracted from the average of five scans of calibration gases or samples to obtain actual peak values. The mole fractions of key species in the calibration gas were then divided by the corrected mass spectrometer peak values to obtain actual responses (R_i). Then the gas phase sample was continuously passed for at least 5 minutes to stabilize the mass spectrometer to measure or continuously monitor the gas compositions. For the batch reactor, a flow rate of 5-ml per minute was used to minimize the disturbance in the reaction.

For a

volume V_T

displaceme

by

R_i

C_i

m

R:

I:

H

H.

m

E

meter. B

The tota

m_r

fm

T

the stabi

that the

2%, whic

For autoclave reactor, final gas composition was analyzed and the total gas volume V_T (produced and un-reacted hydrogen) in reactor was measured by water displacement. From these data, we could calculate the quantity of gas by-product moles by

$$R_i = C_i/(H_{Ci} - H_{0i})$$

$$C_i = R_i * (H_{si} - H_{0i})$$

$$m_i = C_i * V_T / 22.4$$

R: Response factor

I: Methane, ethane and propane.

H_C Calibration peak height

H_0 Background peak height

m_i Gas moles for species i.

Effluent gas flow rate vt in the trickle bed (ml/min) was measured by soap bubble meter. By-product flow rate fm_i (mole/min) is calculated by

$$fm_i = vt_i * C_i / 22400$$

The total carbon in the gas phase equals

$m_{methane}/3 + 2*m_{ethane}/3 + m_{propane}$ moles lactic acid equivalent for batch

$fm_{methane}/3 + 2*fm_{ethane}/3 + fm_{propane}$ mole/minute for trickle bed reactor

The analytical errors for gas analysis depend on the gas volume measurement and the stability of the mass spectrometer. For spectrometer, repeated experiments showed that the maximum error was less than 2%. The gas volume error in batch was less than 2%, which was introduced by the temperature uncertainty during the volume measurem

depends o

2.5.2. Hig

Th

Thermo S

and RI d

exchang

was cont

The liqu

mobile p

paramet

Figure 2

measurement. The error of gas flow rate in trickle bed was less than 3%, which mainly depends on the stability of the trickle bed system.

2.5.2. High performance liquid chromatography (HPLC)

The liquid phase was analyzed by a Spectra Tech P1000 HPLC manufactured by Thermo Separation Products. It consists of an HPLC (mobile phase) pump, UV detector, and RI detector (Figure 2-16). The separation column was an Aminex HPX 87H H^+ ion exchange type, which was a product of BIO-RAD Company. The column temperature was controlled to 50°C by a heating tape for better resolution and lower pressure drop. The liquid sample was filtered before injecting to HPLC to protect the column. The mobile phase was 5 mmole H_2SO_4 in HPLC grade water and the other operation parameters are shown in Table 2-6. Typical reaction progress chromatograph is shown in Figure 2-15.

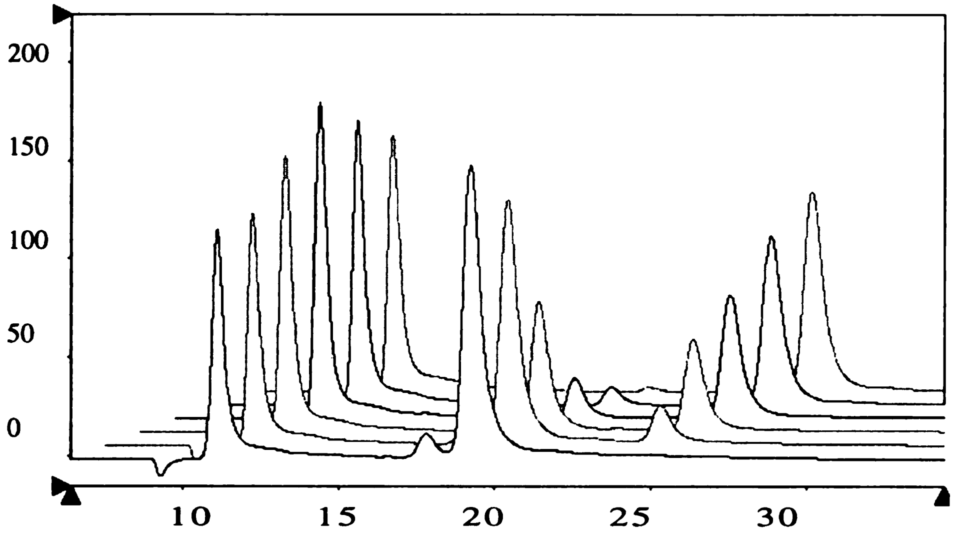

Figure 2-15. Typical chromatograph for liquid analysis

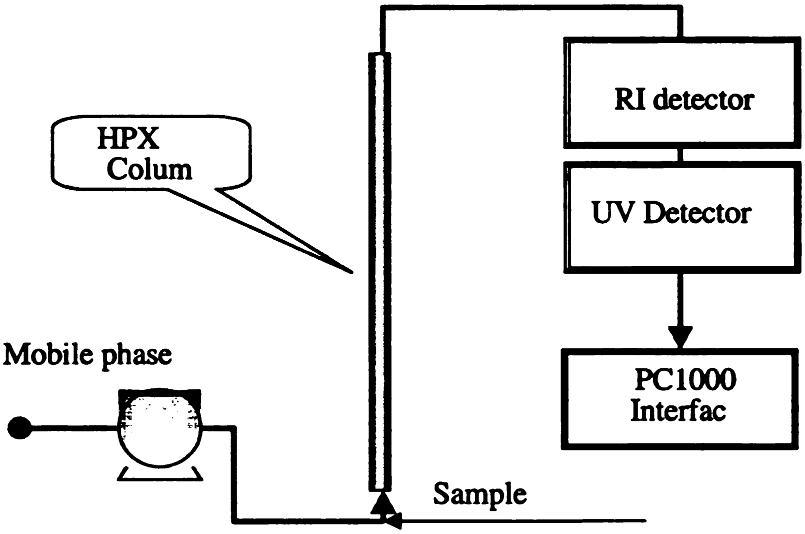
RI detector
UV Detector
HPX
Colum
Mobile phase
PC1000
Interfac
Sample

Figure 2-16. Schematic of HPLC system

Table 2-6. HPLC operation parameters

Column	Aminex HPX 87H
Mobile phase	5mmH_2SO_4 in HPLC water
Column Temperature	50 °C
Mobil phase flow rate ml/min	0.6
Lactic acid peak time (min)	20
Propylene glycol peak time (min)	26
Sucrose	12
Ethanol	26

2.5.2.1. Calibration of HPLC

An internal reference was used in HPLC analysis. Sugar (sucrose) peak appeared in the beginning of chromatograph, but its peak could split into two peaks in some column and conditions. Ethanol peak is located after lactic acid and propylene glycol, but its position overlapped with some liquid by-products. So, each reference was used at certain conditions. If no liquid byproduct was ascertained, ethanol was used. Otherwise, sugar was used as internal reference.

For calibration, W_{SC} gram standard solution (about 3% lactic acid C_{LAC} and 3% propylene glycol C_{PGC} in water) was mixed with reference solution (W_{RC} gram) to get the calibration chromatography. The peak area was obtained for lactic acid (A_{LAC}), propylene glycol (A_{PGC}) and reference peak (A_{RC}). From the concentrations and corresponding peak areas, we could calculate the response factors for lactic acid (R_{LA}) and propylene glycol (R_{PG}).

$$R_{LA} = \frac{C_{LAC} \times W_{SC} \times A_{RC}}{W_R * A_{LAC}}$$

$$R_{PG} = \frac{C_{PG} \times W_{SC} \times A_{RC}}{W_R * A_{PGC}}$$

The exact concentration of reference was not required, but same reference solution should be used for both calibration and actual analysis. The concentration of lactic acid and propylene glycol in real sample could be calculated by

$$C_{LA} = R_{LA}\frac{W_R \times A_{LA}}{W_S * A_R} \qquad \text{and } C_{PG} = R_{PG}\frac{W_R \times A_{PG}}{W_S * A_R}.$$

The reliability of HPLC analysis was confirmed by analyzing lactic acid and propylene glycol solution with known concentration. When $W_R \times A_{LA} / W_S * A_R$ vs. C_{LA}

was plotted for different lactic acid concentration, all data were located on a straight line, which shows the response factor R_{LA} was a constant over lactic acid concentration range. The average error was less than 2.6% (see Figure 2-17) for lactic acid analysis. In the same way, we could verify the reliability of propylene glycol analysis, which is shown in Figure 2-18. The average analysis error was 1.8% for propylene glycol. This error was smaller than that of lactic acid because lactic acid has two peaks at high concentration (dilactate).

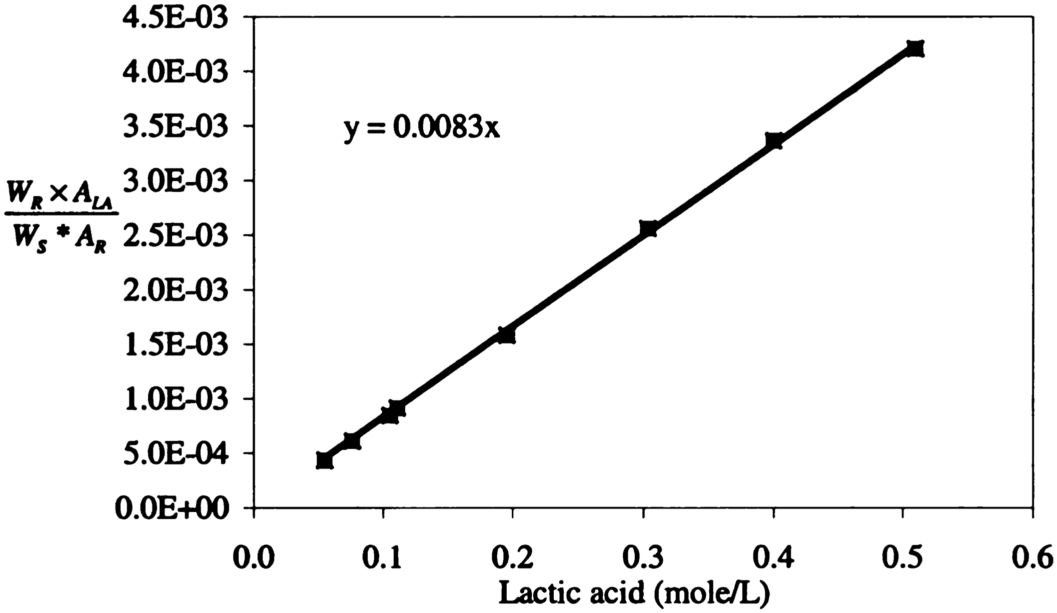

Figure 2-17. Response of lactic acid analysis is a constant

$$\frac{W_R \times A}{W_S *}$$

2.5.2.2.

F

referenc

small pe

peaks ar

and prop

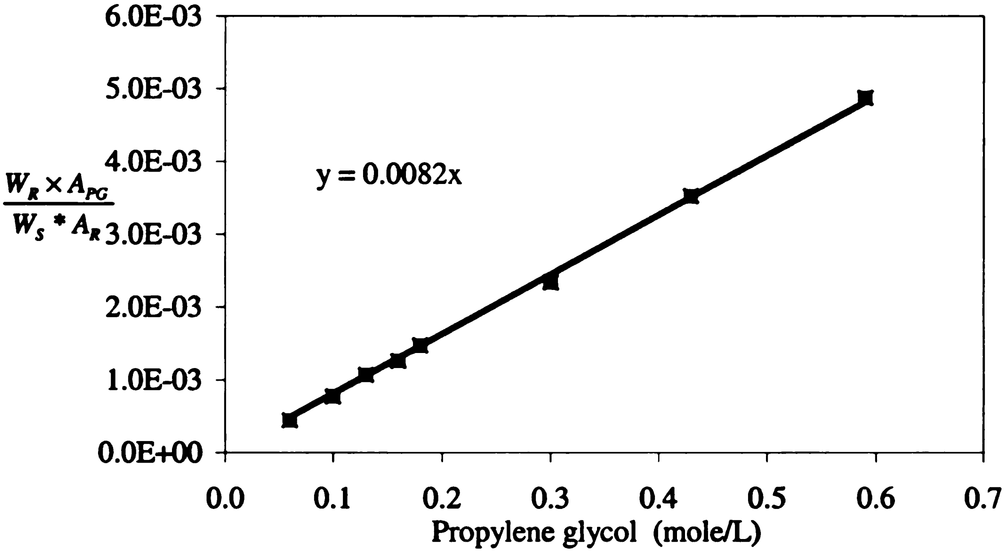

Figure 2-18. Response of propylene glycol analysis is a constant

2.5.2.2. Liquid compound peak assignment

Figure 2-19 is a typical calibration chromatograph with sugar as internal reference. The reference peak is far from lactic acid and propylene glycol, even though a small peak always following the main peak for unknown reason. Lactic acid and products peaks are well separated from each other. The peak assignments for reference, lactic acid and propylene glycol were done by injecting pure compounds.

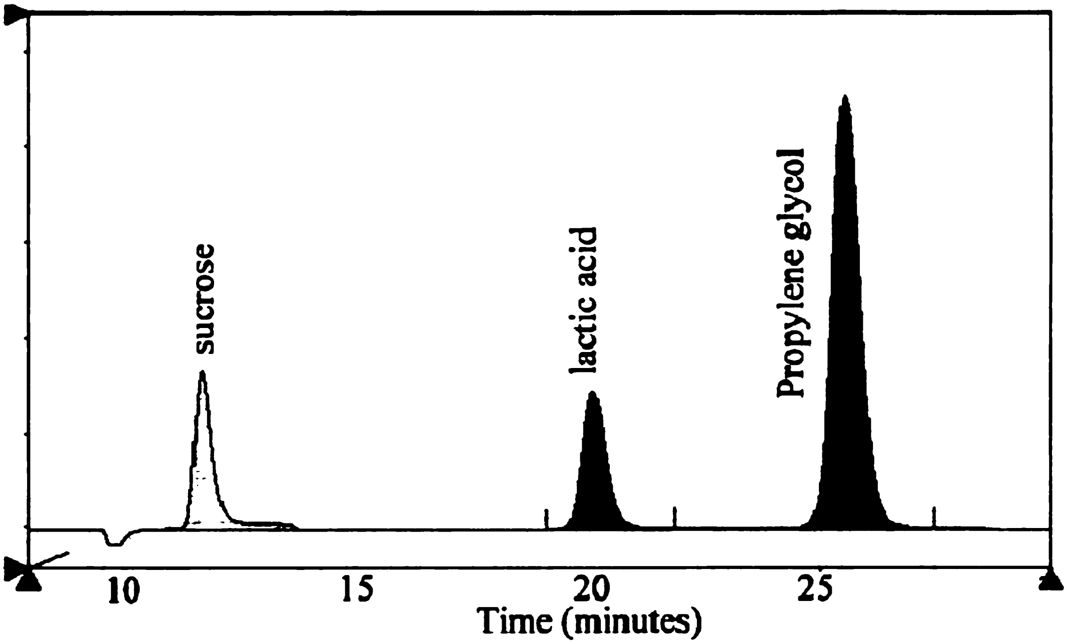

Figure 2-19. Typical HPLC chromatograph of liquid products

For peaks assignment of liquid by-products, the first step was to list some possible by-product compounds and get their peak positions (residence times, called "real") by injecting pure compounds to our HPLC. Then their peak positions in the technical reference of HPLC column (called "menu") were collected. The real/menu ratio, which is listed in Table 2-7, was obtained by comparing the real and menu positions for each compound. This table shows that the ratios are very close to a constant for LA, PG, EG, Acrylic and Propionic acid. Therefore, we can estimate the "real peak" position from "menu" with quite good approximation. Then real/menu ratio was used to convert unknown peak position in our chromatography to menu residence time, by which the compound can be initially assigned from the technical reference of HPLC column. Finally, pure compound was used to verify the assignment. The peak assignments for all possible liquid by-products are listed Table 2-8.

Table 2-7. Real peak position and menu value

Chemicals	Real	Menu	Real/menu
LA	20.5	16.7	1.23
1,2 PG	25.5	21.5	1.19
2-Propanol	33.0	28.5	1.16
EG	24.8	20.7	1.20
Acrylic	30.0	25.2	1.19
Propionic acid	28.4	24.0	1.19

Table 2-8. Peak assignment

Chemicals	Real	Menu	Convert to menu	Convert to real
LA	20.5	16.7		20.2
1,2 PG	25.5	21.5		26.0
1,3 PG		22.2		26.8
1-Propanol	39.0		32.5	
2-Propanol	33.0	28.5	27.3	
EG	24.8	20.7		24.8
Ethanol		27.0		32.4
Methanol		23.8		28.8
Acrylic	30.0	25.2	25.0	
Propionic	28.4	24.0	23.5	

2.5.3. Catalyst characterization

The BET surface and dispersion of catalyst were measured by Micromeretics Pulse Chemisorb 2700. Total surface area (BET) was measured by nitrogen adsorption at 77 K and analyzed with the BET method. Twenty to fifty milligrams of catalyst was loaded into a quartz sample tube which was sealed to the Chemisorb 2700 and heated to 423 K for 20 minutes to drive off any weakly adsorbed species, most of which was water. After calibration of nitrogen, a continuous flow of 5% nitrogen in helium was passed over the sample and the effluent gas composition was tested for nitrogen concentration. First a liquid nitrogen bath was used to cool the sample to 77K to get the adsorption profile, then liquid nitrogen bath was removed and the sample was heated to room temperature (by air) to get the desorption profile. The same procedure was followed for

10% nit

given c

surface

measur

measur

10% nitrogen and 18.75% nitrogen in helium. The volume of nitrogen adsorbed at a given composition along with pressure was used in BET analysis to determine catalyst surface areas down to the micro pore level. The metal dispersion on catalyst support was measured by hydrogen adsorption using same instrument using the method of BET measurement. These analyses were finished by Bryan Hogle.

Chapter 3. Lactic acid hydrogenation in autoclave

This first part of the research includes catalyst screening, experimental condition optimization, testing MSU catalysts, hydrogenation of lactate and development of carbon balance.

3.1. Commercial catalyst testing

The first thing for this project was to choose suitable catalysts. We know transition metal, supported metal and metal oxide have the potential to be good catalysts for carboxylic acid hydrogenation. Therefore, the first step was to obtain these kinds of catalyst samples from manufacturers.

3.1.1. Catalyst screening

In the first batch of experiments, we emphasized lactic acid conversion and looked for catalyst with the highest activity. These samples are commercial catalysts or industr

was co

ranged

to 200

loadin

are vis

conversi

supports

the supp

reaction.

carbon-su

industrially developed new catalysts, which were listed in Chapter 2. Catalyst screening was conducted in the Parr autoclave with a stirring speed of 1200 rpm. Reaction pressure ranged from 1000 to 2000psi (7.2~14.5MPa) and temperature was increased from 100°C to 200°C until a reasonable conversion was reached. For all experiments, the catalyst loading was 1gram (as received basis) in 100 gram 5 % lactic acid in water. The results are visualized in Figure 3-1.

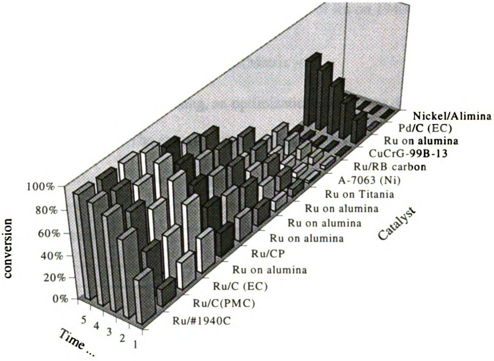

Figure 3-1. Five-hour conversion (temperature and pressure in parentheses)

The results clearly show that only supported ruthenium (Ru) can give reasonable conversion after 5 hours at such mild conditions. Ru on carbon and Ru on alumina supports showed almost the same performance. The problem with Ru on alumina is that the support degraded into very fine powder and formed an emulsion phase after 5 hours reaction. It is very difficult for the fine powder to precipitate. On the contrary, active carbon-supported ruthenium could survive under fast stirring and separated from the

3

c

ac

wa

Fo

30

12

see

product solution in a short time after reaction. So, if we use a powder catalyst in the stirred tank reactor for lactic acid hydrogenation, Ru/carbon is the best choice. From Figure 3-1, we also qualitatively know that the hydrogenation reaction rate increases with temperature and H_2 pressure for the same catalyst. High temperature leads to high conversion at the same reaction time (Ru/Alumina DC). For carbon supported ruthenium catalysts, different carbon supports have different activity. For example, the activity of Ru on RB carbon support (CCC) is much lower than that of Ru on 1940C (PMC).

3.1.2. Temperature and pressure optimization (Matrix –1)

On the base of catalyst screening, an optimization matrix was designed to identify optimal reaction conditions. The experiment conditions are given in Table 3-1.

Table 3-1. Optimization Matrix-1

Temperature	Pressure			
	500 Psig (3.4MPa)	1000 Psig (6.9MPa)	1500 Psig (10.3MPa)	2000 Psig (13.8MPa)
130°C	M14	M2	M12	M10
150°C	M1	M13	M11	M9
170°C	M8	M7	M6	M3

From catalyst screening, Ru/1940C from PMC, which was 5% ruthenium on active carbon with 63% H_2O) was the best catalyst. In this matrix, the catalyst loading was fixed at 1gram (as received basis) catalyst in 100 gram 5% Purac lactic acid in water. For all runs, the catalyst pre-reduction was conducted at 170°C and 300psi (2Mpa) H_2 for 30 minutes. The reaction time ranged from 5 to 9 hours. The stirring speed was fixed at 1200 rpm for all runs. The lactic acid conversions are visualized in Figure 3-2. It can be seen that the three highest 5-hour conversions come from the runs at 150°C. In addition, Figure 3-2 shows that the optimal reaction conditions for conversion should be located around 150°C. In the temperature range used, high pressure always favors the reaction rate.

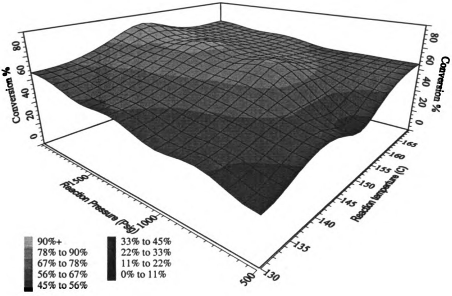

Figure 3-2. Lactic acid conversion vs. pressure & temperature after 5 hours

Experiment M8 (500psi and 170°C) was unusual. Although the 5-hour conversion was not as high as that in higher pressure at same reaction temperature, the initial reaction was very fast. Until 2 hours, the conversion was the highest in this matrix. The reasons are not clear yet, but it seems that something enhanced the initial catalyst activity. Methane, ethane and propane were found in the gas phase for all runs. At reaction temperature higher than 170°C, liquid by-products were detectable. The major liquid by-products are 1-propanol, ethanol and a trace amount of 2-propanol, which are shown in Figure 3-3.

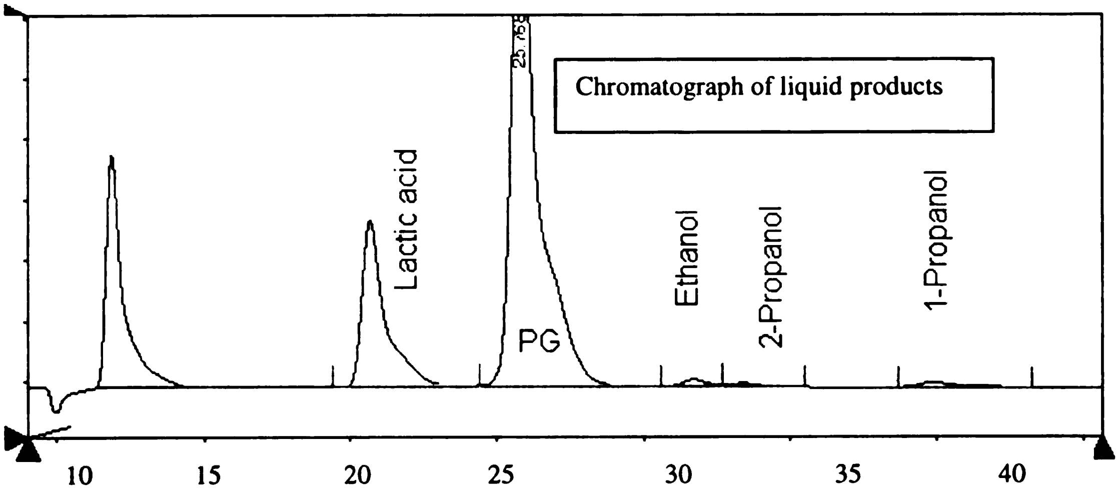

Figure 3-3. Liquid by-products distribution after 3 hours at 180°C and 2000psi

Table 3-2. Experiment numbers for Matrices 2 and 3

T=150°C	Matrix-2, Catalyst loading (50% moisture)		
Pressure	1	2	3
1000psi	99-9	99-7	99-8
1500psi	99-1(99-15)	99-2	99-3
2000psi	99-10	99-6	99-11
	Matrix 3, Catalyst loading (50% moisture)		
T=130°C	1	2	3
1000psi	99-16	99-18	99-19
1500psi	99-14	99-17	99-20
2000psi	99-12	99-13	99-22

3.1.3. Catalyst loading effects (Matrices 2 and 3)

To investigate the catalyst loading effects, two matrices were designed. The catalyst used was PMC 5% Ru/C with 50% water (new PMC). The catalyst pre-reduction

3.1.3. Catalyst loading effects (Matrices 2 and 3)

To investigate the catalyst loading effects, two matrices were designed. The catalyst used was PMC 5% Ru/C with 50% water (new PMC). The catalyst pre-reduction conditions were fixed at 500psi in hydrogen and 150°C for 12 hours. Reaction temperature was fixed at either 130°C or 150°C. Reaction pressure ranged from 1000 to 2000psi and catalyst loading was 1~4gram in 100 gram 10% J. T. Baker lactic acid water solution. Table 3-2 is the conditions of these two matrices.

The catalyst used in Matrix 2 and 3 was different from Matrix 1. The active metals are the same, but the active carbon support is different. So, we cannot compare these two Matrices with Matrix-1 directly. The results of Matrix 2 (150°C) are shown in Figure 3-5. For Matrix 3 (130°C), the results are shown in Figure 3-4. These data show that this Ru/C is also a good catalyst for hydrogenation of lactic acid. Over 90% selectivity and 97% conversion can be achieved at optimal reaction conditions. Once again high pressure increases the reaction rate and enhances the selectivity at the same catalyst loading.

As expected, lactic acid conversion linearly increased with loading at low temperature and low pressure because the conversion was low and reaction was controlled by the availability of catalyst surface (Figure 3-4). For high temperature and high pressure, it showed the similar trend in the first few hours because the lactic concentration was high and the reaction was still controlled by the availability of catalyst. But at high conversion, as the lactic acid concentration was getting lower and lower, lactic acid diffusion became more and more important, so the catalyst loading effect became less and less significant (Figure 3-5).

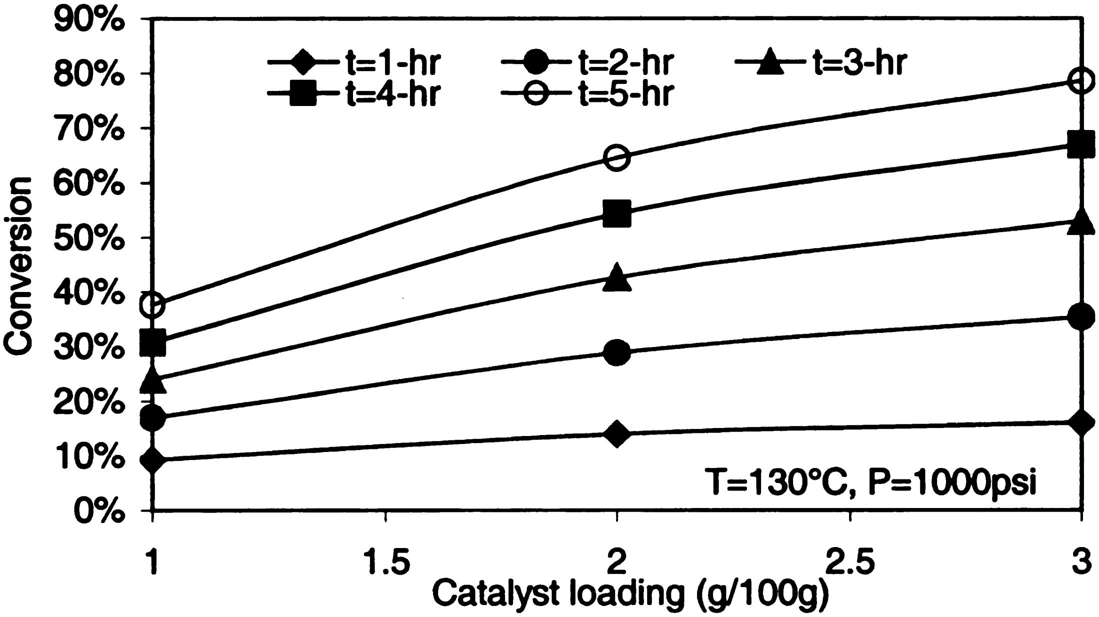

Figure 3-4. Catalyst loading effect at low temperature and pressure

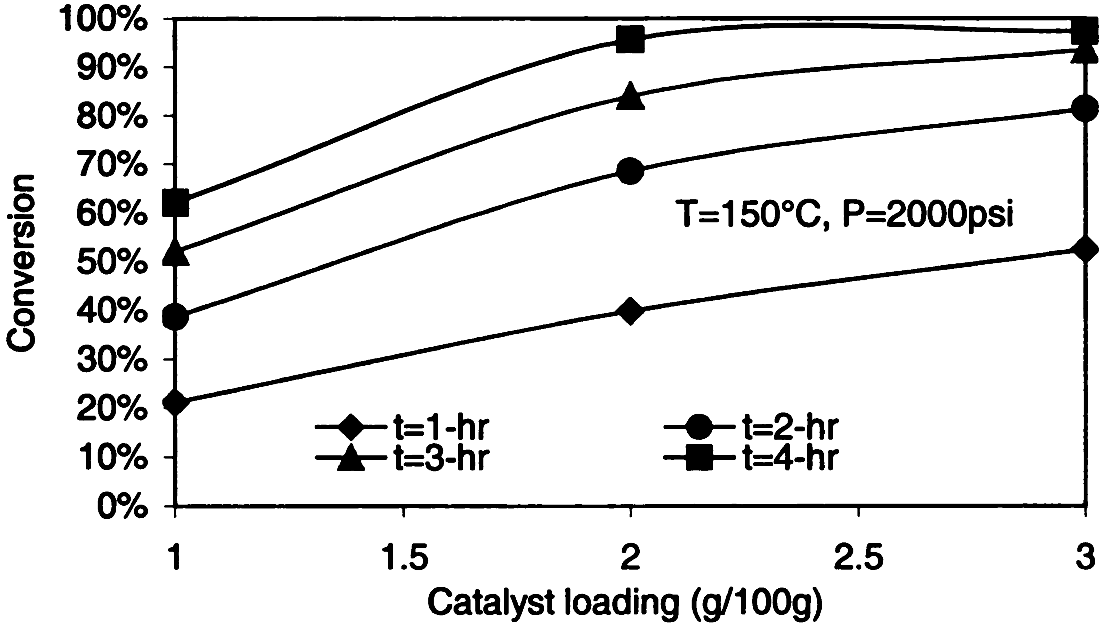

Figure 3-5. Catalyst loading effect at high temperature and pressure

The effect of catalyst loading on selectivity is much more complicated than conversion of lactic acid. It is an indication of how the catalyst loading affects the side reaction. For high temperature (150°C) hydrogenation, selectivity slightly decreased with catalyst loading at high pressure, which is shown in Figure 3-6. Although these decreases are within the analytical error, this trend was repeatedly shown at other reaction times. The decreasing trend in selectivity with catalyst loading is easily understood because the high loading favors side reactions. Here, we choose the 3-hr selectivity for comparison because the lactic acid and propylene glycol concentrations at this time are about half of the maximum, and so we can analyze the liquid sample with the highest reliability.

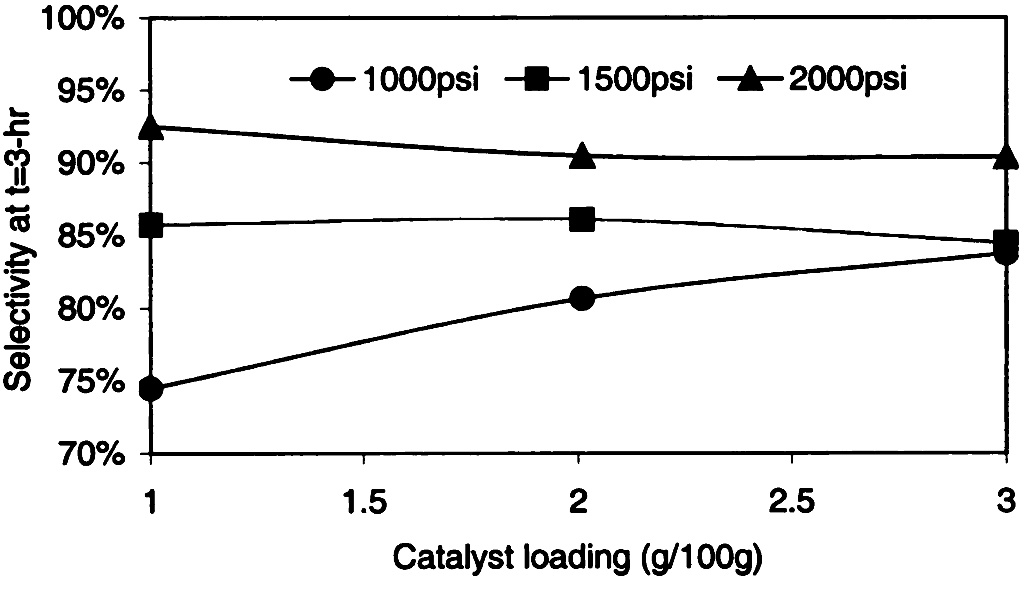

Figure 3-6. Selectivity changes with catalyst loading at 150°C

The most unusual thing is the selectivity trend at low pressure (1000psi). It almost linearly increases with catalyst loading. This is also related to the low selectivity at low pressure, from which we can get a clue about the reaction pathway. At low temperature (130°C), the conversion was low and the loading effect is much more predictable. When the loading changes from 1 to 2 gram/100g, the selectivity was maintained unchanged. But when the loading further was increased to 3 gram/100g solution, the catalyst favored extensively the side reaction and thus selectivity went down (Figure 3-7).

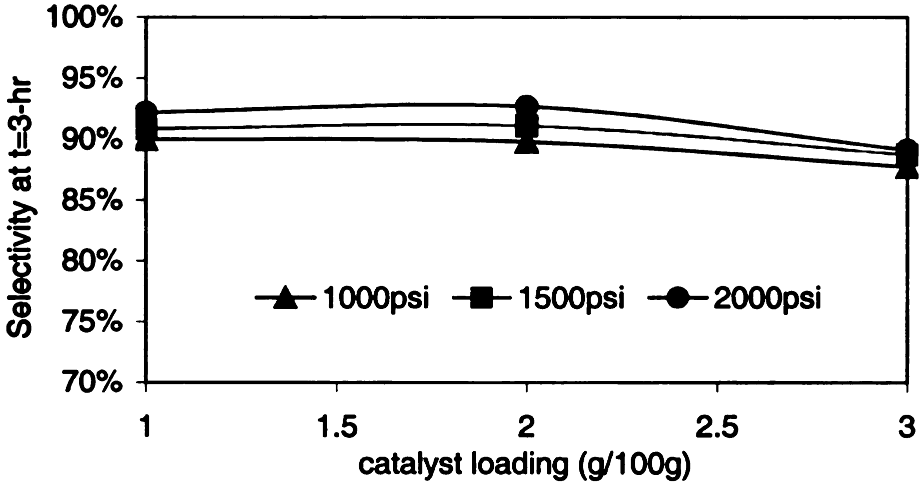

Figure 3-7. Selectivity change with catalyst loading at 130°C

3.1.4. Catalyst pre-reduction effect

The pretreatment of catalysts will affect the activity substantially. Figure 3-8 shows that 30 minutes pre-reduction doubles the initial reaction rate. Over a 20% difference in conversion still exists, even after 5 hour. That means that part of the active sites cannot catalyze this reaction if the catalyst is not reduced before the reaction.

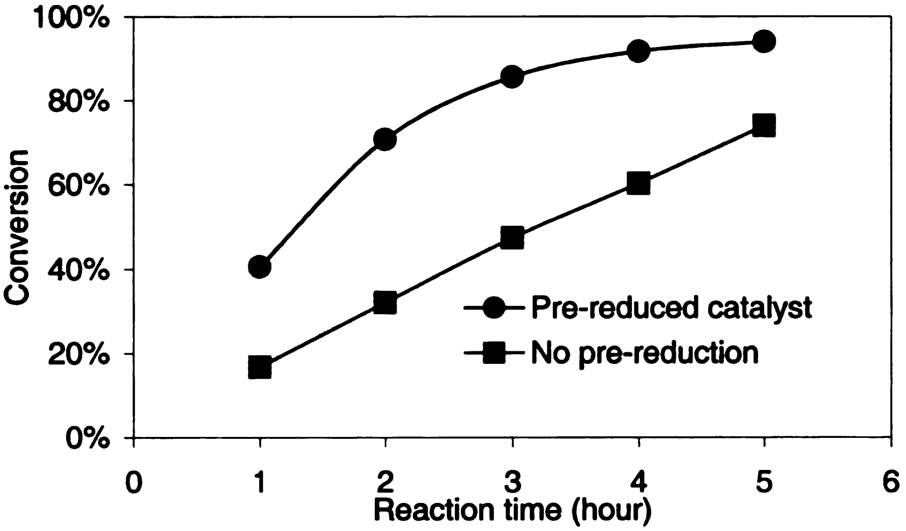

Figure 3-8. Pre-reduction effect

3.1.5. Lactic acid concentration effects

To investigate possible hydrogenation of high concentration lactic acid, 10% and 30% lactic acid were used in run M15 and M16. The catalyst loading was 1gram of 5% Ru/C per 100g solution. Standard temperature and pressure (150°C and 2000psi) were used. The comparison with 5% lactic acid is summarized in Figure 3-9. At the same catalyst loading, high lactic acid concentration will lead to lower conversion at the same reaction time. The actual reaction rate (mole lactic acid/hr.gcat) for high concentration lactic acid was higher than that of low concentration lactic acid, but the conversion vs. time curve was low. Therefore, this reaction is not a first order reaction because conversion vs. time curve depends on reactant concentration. When using 30% lactic acid, with long enough reaction time (13.5 hrs), we still could get 85% conversion. From the trend of conversion curve (M16), we also could say that the catalyst still had activity after 13.5 hour because the curve still went up. That means that catalyst activity can be maintained for a long period of reaction.

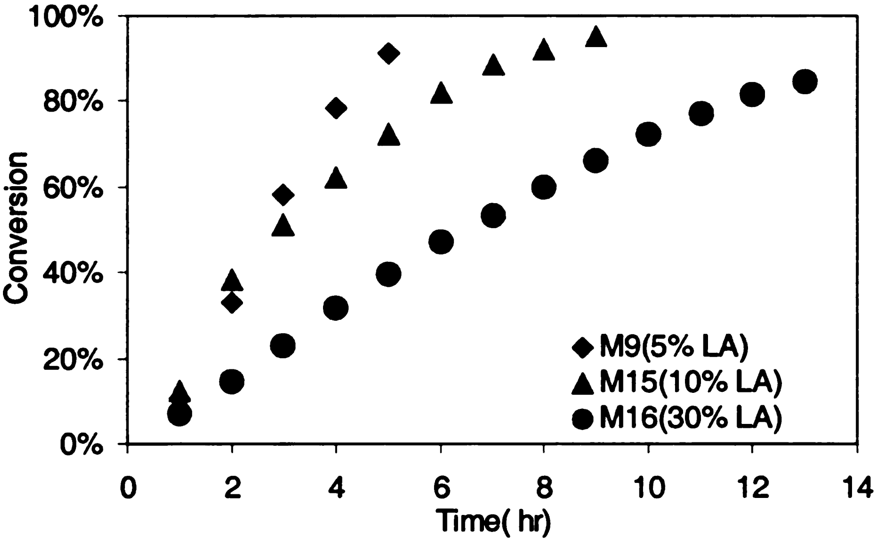

Figure 3-9. Reactions at different lactic acid concentration

3.1.6. Gas product evolution

The continuous gas phase monitoring in the autoclave (Figure 3-10 and Figure 3-11) shows that most gas products were formed in the first two hours of the hydrogenation reaction. One possible reason is that most by-product gas comes from the extremely active sites, which may exist in fresh catalyst and disappear after several hours of reaction. How these highly active sites deactivate is not yet clear. Metal leaching, poisoning from the products, and collapse of the support during the stirring all could contribute to the deactivation of extremely active sites.

The gas product composition strongly depends on the catalyst support. For Ru/Alumina, the dominant gas by-product was methane; for PMC Ru/1940C (♣) we got almost equal amounts of methane, ethane and propane at the same temperature and pressure (See Figure 3-10 and Figure 3-11). This indicates that support plays an

---

♣ We used two PMC catalyst samples, the first one is Ru/1940C and second one is Ru/C-new important role in this catalytic hydrogenation. Even for active carbon supports, different gas by-products may be produced for different active carbons. The gas product composition of PMC Ru/C-new was different from that of PMC Ru/1940C (see Table 3-6).

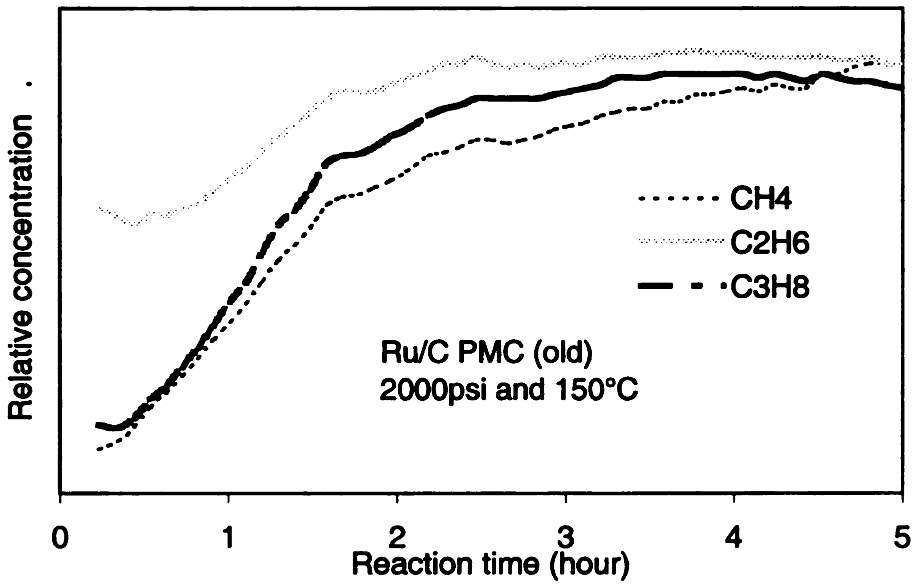

Figure 3-10. Gas product evolution for Ru/C (PMC)

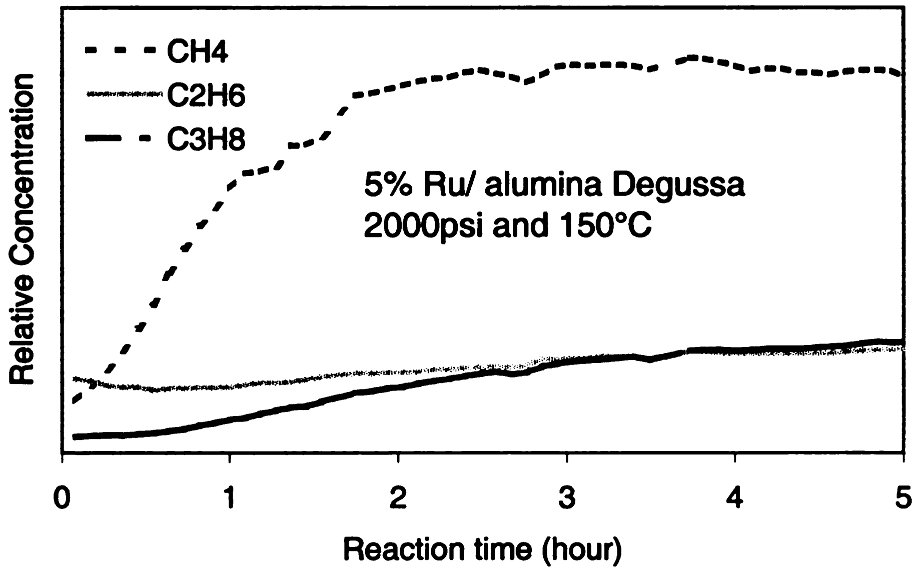

Figure 3-11. Gas product evolution for Ru/Alumina (Degussa)

3.2. Lactic acid conversion over laboratory prepared catalysts

This section focuses on hydrogenation over the catalysts prepared at MSU. These catalysts are supported ruthenium on active carbon, titania, or alumina. The precursors are ruthenium (III) chloride hydrate and Alfa ruthenium nitrosyl nitrate hydrate. Different reduction schemes, precursors, and supports led to different ruthenium loadings and dispersions. The specifications are shown in Chapter 2. The reaction conditions are given in Table 3-3.

Table 3-3. Details of MSU ruthenium catalysts and test conditions

No	Exp. No	Catalyst No	P(psi)	T(C)	Dispersion	Loading (Ru/catalyst)
1	M53	CG5P - G	2000	150	6 %	5.0%
2	M52	CG5P - H	2000	150	3 %	5.0%
3	M44	CG6M - F	2000	150	13%	5 %
4	M54	SA135-C	2000	150	14%	5.0%
5	M57	SG6 - D	2000	150	10%	4.4%
6	M56	CG5P-NO1-I	2000	150	38%	5.0%
7	M55	CG5P - A	2000	150	10%	5.4%
8	M58	TiP25-Cl9 - J	2000	150	N/A	5.0%
9	M59	ALg - E	2000	150	13.5%	4.7%
10	M60	AL100 - B	2000	150	0%	5%

The reactions were conducted with 100 gram 5% lactic acid in water with 1-gram catalyst (♥). The catalyst was pre-reduced at 400 psi H_2 and 150°C for 1 hour before adding solution. The final conversions and selectivity are given in Table 3-4. For run M60 (Table 3-3), only 5-hour data is shown in this table because the AL100 - B supported ruthenium has zero dispersion and the 5-hour conversion was less than 10%. These runs show those laboratories prepared catalysts are as good as commercial samples. Selectivity as high as 92% of the theoretical was observed with nearly complete lactic acid conversion. With twice the loading, the performance of these catalysts was

---

[♥] The MSU catalysts contain no water, which are different from commercial one (over 50% H_2O), close to the best commercial catalyst (Ru/C PMC). The interesting thing is the relationship between the performance and dispersion, which is shown in Figure 3-12. Low dispersion definitely is not good for this reaction (No1, 2, 10), but the highest dispersion does not mean the highest activity (No 6). A moderate dispersion (around 10~15%) is required for both good conversion and selectivity.

Table 3-4. Conversion and selectivity

No	Exp. No	Support		1-hr	2-hr	3-hr	4-hr	5-hr	6-hr	7-hr	8-hr	Dispersion
5	M57	SG6 - D	Con. %	29	61	80	90	96	100			10%
			Select. %	91	89	89	90	91	90			
6	M56	CG5P-NO1-I	Con. %	29	51	68	84	93				38 %
			Select. %	79	80	85	87	88				
7	M55	CG5P - A	Con. %	37	65	83	87	91	96	99		10%
			Select. %	73	69	73	79	82	84	87		
4	M54	SA135-C	Con. %	26	49	70	78	84	90		100	14%
			Select. %	92	90	93	96	94	92		91	
1	M53	CG5P - G	Con. %	18	29	41	47	65				6%
			Select. %	67	69	71	77	75				
2	M52	CG5P - H	Con. %	7	26	36	44	56				3%
			Select. %	86	81	86	86	89				
3	M44	CG6M - F	Con. %	35	74	90	96	99				13%
			Select. %	83	88	91	92	92				
8	M58	TiP25-C19 - J	Con. %	26	55	78	91	96				N/A
			Select. %	77	91	87	91	94				
9	M59	ALg - E	Con. %	9	37	63	79	91				13.5%
			Select. %	90	89	83	81	81				
10	M60	AL100 - B	Con. %					9				0%
			Select. %					78				

---

the metal loading actually is equal to 2 gram commercial catalyst

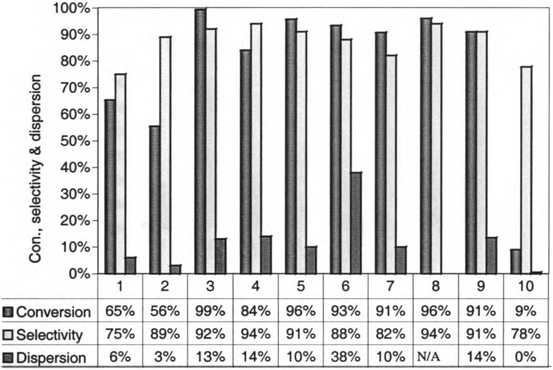

	1	2	3	4	5	6	7	8	9	10
■ Conversion	65%	56%	99%	84%	96%	93%	91%	96%	91%	9%
□ Selectivity	75%	89%	92%	94%	91%	88%	82%	94%	91%	78%
■ Dispersion	6%	3%	13%	14%	10%	38%	10%	N/A	14%	0%

Figure 3-12. Five-hour conversion and selectivity for MSU catalysts

The gas by-products depend on both the type of support and the dispersion of catalyst. No simple relationship between dispersion and gas phase composition can be found. Figure 3-13 shows gas by product distribution vs. dispersion for MSU laboratory prepared catalysts. Just like commercial Ru/C catalysts, no apparent liquid by-product was found since we only used low reaction temperature (150°C). The change of selectivity with time is an indication of how the side reactions occur over different catalysts. This issue will be further discussed in Chapter 6.

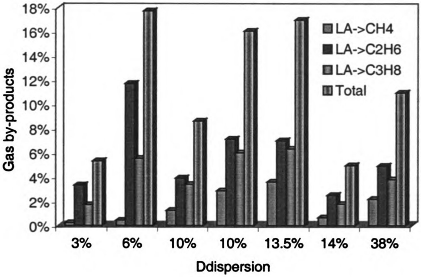

Figure 3-13. Gas by-product distribution after five-hour reaction

3.3. Lactate salt hydrogenation

As we know the direct hydrogenation of lactate salt in aqueous phase was not reported in literature and is not favorable thermodynamically. Our experiments have verified this unfavorability. Experiments conducted at 150~170°C and 2000psi over 5% Ru/C (PMC) for five hours showed that calcium and potassium lactate did not produce any detectable propylene glycol, and only ammonia lactate give a barely detectable peak in liquid HPLC chromatograph. The experiments in this section are summarized in Table 3-5.

Table 3-5. Summary of all experiments for lactate salt hydrogenation

No	T	P	Conversion % at hour							Reaction specification
	°C	Psig	1	2	3	4	5	6	7	
M3	170	2000	17	36	52	66	78			5% lactic hydrogenation at170°C
M4	170	2000	17	33	53	69	79			5 % LA, adding KOH to K^+/LA =0.02
M5	170	2000	17	31	45	56	63		75	5 % LA. adding KOH to K^+/LA =0.1
M9	150	2000	11	33	58	78	91			5% Lactic hydrogenation at 150°C
M17	150	2000	19	37	46	53	67			KLA, , add H_2SO_4 to H/LA=1 at 1 hr
M18	150	2000	12	30	42	52	63			LA +K_2SO_4, K^+/LA ratio =0.6
M19	150	2000	12	33	48	62	75			LA +K_2SO_4, K^+/LA ratio =0.3
M20	150	2000	0	0	14	29	44	60	74	CaLA, add H_2SO_4 to H/LA =1 at 2 hr
M21	~170	2000	No reaction							KLA+700 psi CO_2
M22	~170	2000	No reaction							CaLA+ 800 psi CO_2
M26	150	2000	21	41	58	76	92			CaSO4 saturated lactic acid

Note: KLA is potassium lactate. CaLA is calcium lactate. Their mole concentrations equal to 5% Lactic acid. LA is lactic acid. K^+/LA is potassium ion and lactic acid mole ratio. H/LA is free H^+ and lactic acid mole ratio

3.3.1. Potassium lactate hydrogenation

After the failure of direct hydrogenation of lactate, hydrogenating acidified salt (without purification) was the next step. First, a low concentration of potassium hydroxide (KOH) was added to the lactic acid to test the potassium ion effect. Figure 3-14 shows the reaction rate (conversion) decreases with the addition of potassium hydroxide. Addition of potassium hydroxide in an amount up to 2% of lactate present did not affect lactic acid hydrogenation up to 5-hour reaction. But higher KOH concentration [10 % mole of initial lactic acid present] slowed the hydrogenation noticeably after 2-hour reaction. The difference increases with time because the free acid concentration becomes lower and lower. These experiments show that K+ only slows the reaction and does not terminate it; with two more hours of reaction, almost the same conversion can be achieved. Adding KOH brings K+ into solution and decreases the free lactic acid concentration at the same time. To distinguish these two factors, potassium sulfate was added to lactic acid.

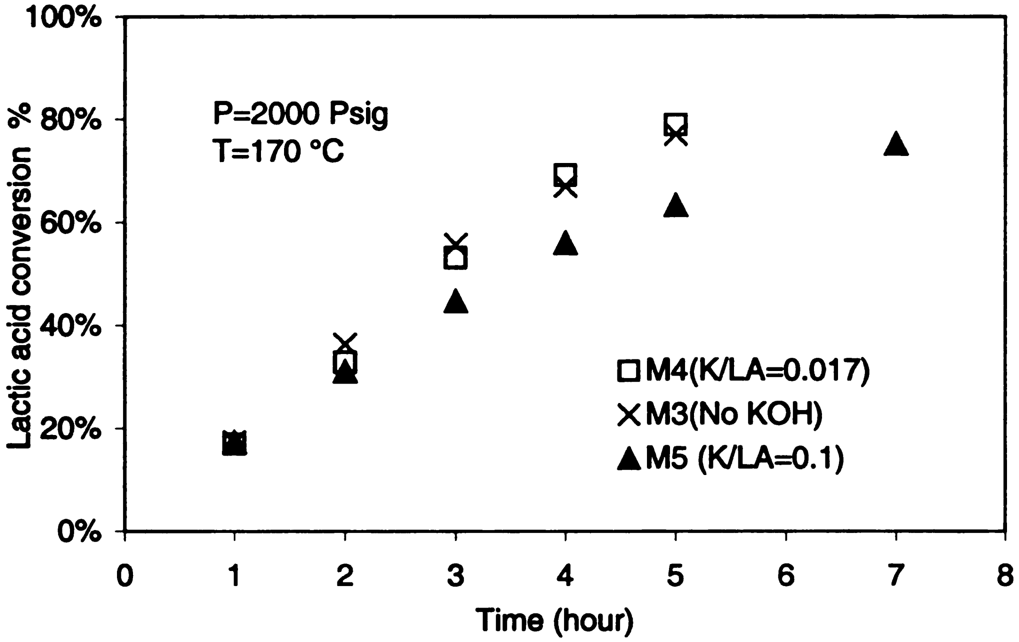

Figure 3-14. K$^+$ ion effect on lactic acid hydrogenation at 170°C

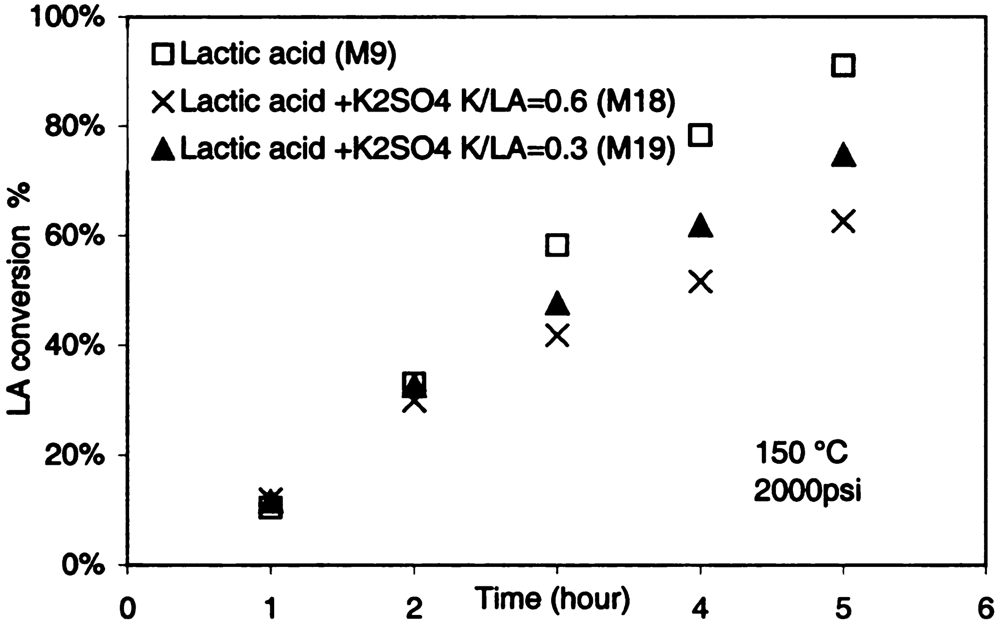

Figure 3-15. Adding potassium sulfate to lactic acid at 150°C

Figure 3-15 shows that potassium salt retards the hydrogenation reaction. When the potassium to free lactic acid molar ratio equals 0.3, the 5-hour conversion decreased about 15% compared to no salt addition. For the ratio increased to 0.6, the conversion decreased up to 30% at 5-hour. These runs clarify that potassium ions do affect the hydrogenation in the some way and that the effect increases with ion concentration. The mechanism is unclear yet. The second pK_a of sulfuric acid is 1.9 and is lower than that of lactic acid (pKa=2.9), therefore, the proton transfer cannot occur.

3.3.2. Calcium ion

Calcium lactate could not be hydrogenated to PG at our reaction conditions (the first two hours of M20, see Table 3-5 and Figure 3-16), even with 800psi CO_2 over the reaction mixture (♣) (M22, see Table 3-5). The purpose of addition of CO_2 was to acidify the lactate salt, but the first pK_{a1} (♣) of H_2CO_3 is 6.4, which is much larger than that of lactic acid (pKa=2.9). Therefore, it did not work. For hydrogenating acidified calcium lactate, the situation is a little different from that of potassium because the solubility of formed calcium sulfate is extremely low (0.2g/100water). That means that very limited concentration of Ca^+ exist in the liquid phase and most of the calcium will precipitate in the form of calcium sulfate. In run M20, the initial solution was calcium lactate equivalent to 5% lactic acid in molar concentration. After two hour, no detectable PG was formed. Then an equal molar quantity of H_2SO_4 was added to the reactor from the feed tank. The hydrogenation immediately began after the addition of acid, but the reaction rate (the slope in conversion profile) was lower than pure lactic acid hydrogenation because the precipitated $CaSO_4$ still stayed in the reactor. The solution became a slurry at the end of the experiment. The slurry might clog catalyst pores and increase resistance to lactic acid diffusion. In M26, lactic acid saturated with $CaSO_4$ was hydrogenated at 150°C. The results show that the trace amount of calcium ion does not affect the lactic acid hydrogenation at all. Therefore, if we can simply filter out precipitated $CaSO_4$ before hydrogenation, the calcium ions remaining in solution will not slow down the following hydrogenation reaction.

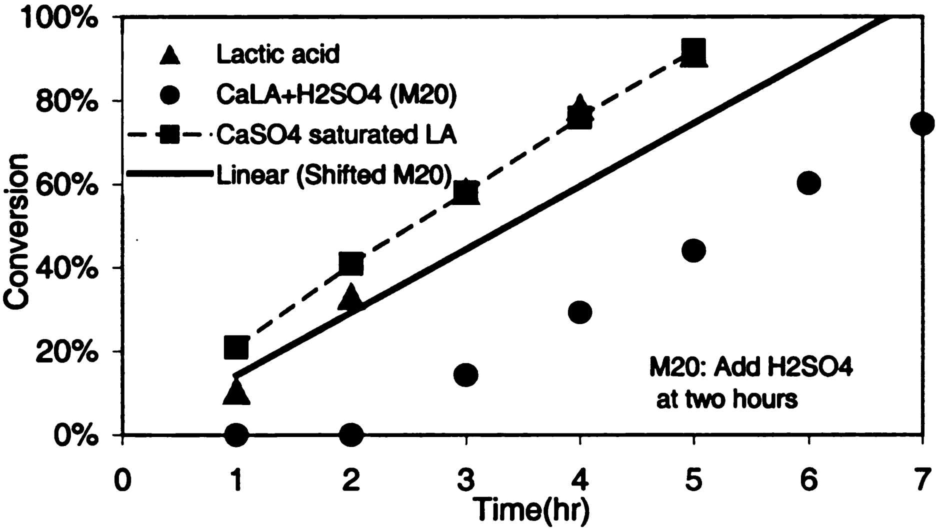

Figure 3-16. Calcium ion effect at 150°C

In summary, direct hydrogenation of lactate salts is impossible at our hydrogenation conditions and with our catalyst. The potassium and calcium metal ion in lactic acid solution will retard hydrogenation reaction. The effect depends on ion concentration. Low concentration (<2%) potassium and calcium ion do not poison the catalyst and slow down the reaction. For calcium lactate, after acidifying and simple filtration, the solution can be directly hydrogenated without the requirement of further purification.

♣ The idea here is to use CO_2 (H_2CO_3) as acid, the experiments showed it cannot free lactic acid

♣ pK_{a1} is at 25°C and atmosphere, high pressure and temperature may slightly change its value.

3.4. Carbon balance

To verify the reliability of analytical methods, we have calculated the carbon balance for the experiments of Matrices 2 and 3. We did this balance by combining gas phase analysis from the mass spectrometer with liquid phase HPLC analysis. This calculation needs the total gas phase volume, which includes the gas in the reactor after reaction and the gas removed during sampling. The total gas volume was measured by water displacement after reaction, and gas removed by sampling was estimated. In the sampling process, liquid and gas escaped the reactor together. For each sample, we took out about 1.2 ml liquid. The sample loop is about 2.5 ml, and we need to fill the sampling loop 3~4 times. That means that we lost about 50ml gas (at reaction pressure) for all sampling (5~7 samples).

Because the gas phase by-products change with reaction time and we only analyzed the gas phase after the reaction for most of experiments, this method will introduce a maximum error of 5% if we assume the by-products concentrations linearly increase with time. This is the biggest source of error in carbon balance. The carbon balance is defined as:

$$\frac{\text{Carbon lost from liquid (HPLC) - Carbon recovered in gas (mass spectrometer)}}{\text{Inital carbon in liquid}}$$

The data and calculation are summarized in Table 3-6. The overall carbon balance in these reactions closed to within ±4%, an indication that the experimental results are extremely reliable. Table 3-6 also includes a very low pressure run (330psi), which produced lot of gas methane, ethane and propane after 12 hour. The major gas product was methane for the runs at 150°C, and the catalyst loading seems only to increase methane formation (Figure 3-17).

Table 3-6. Summary of carbon balance

No		P_{RX}	Rx	Cat. g	Mass spectrometer peaks height			P_{H2O}	P_{H2}	V_{gas} At P_{RX}	By-products in gas Concentration %		
		psi	Hour	g	M15	M28	M29	psi	psi	psi	CH_4	C_2H_6	C_3H_8
9	T=150 °C	1000	8	1	3.3E-07	4.6E-08	1.2E-07	69	931	307	3.6	0.3	1.1
7		1000	4.2	2	3.5E-07	6.0E-08	1.6E-07	69	931	307	3.8	0.4	1.4
8		1000	4.5	3	4.0E-07	1.3E-07	1.3E-07	69	931	307	4.3	0.9	1.2
15		1500	6	1	4.3E-08	3.3E-08	3.3E-08	69	1431	307	0.5	0.2	0.3
5		1500	4.2	1.5	1.4E-07	6.0E-08	5.0E-08	69	1431	307	1.5	0.4	0.4
2		1500	9.8	2	2.1E-07	6.0E-08	5.0E-08	69	1431	307	2.3	0.4	0.4
3		1500	5.3	3	4.3E-07	3.2E-08	3.2E-08	69	1431	307	4.6	0.2	0.3
4		1500	3.8	4	5.1E-07	4.0E-08	4.0E-08	69	1431	307	5.5	0.3	0.4
10		2000	4.7	1	1.3E-07	1.2E-08	1.0E-08	69	1931	307	1.4	0.1	0.1
6		2000	4	2	1.2E-07	4.5E-08	4.0E-08	69	1931	307	1.3	0.3	0.4
11		2000	4	3	9.8E-08	6.0E-08	5.5E-08	69	1931	307	1.0	0.4	0.5
23		330	12	2	1.8E-06	1.2E-06	3.1E-07	69	261	307	18.9	7.9	2.8
16	T=130 °C	1000	8.3	1	8.0E-08	1.2E-07	7.1E-08	39	961	307	0.9	0.8	0.6
18		1000	5.1	2	7.5E-08	9.6E-08	4.5E-08	39	961	307	0.8	0.6	0.4
19		1000	5.1	3	9.1E-08	1.1E-07	6.6E-08	39	961	307	1.0	0.7	0.6
14		1500	7.4	1	2.2E-08	1.8E-08	1.8E-08	39	1461	307	0.2	0.1	0.2
17		1500	6.3	2	1.2E-08	2.4E-08	1.4E-08	39	1461	307	0.1	0.1	0.1
20		1500	5	3	3.7E-08	1.2E-07	5.0E-08	39	1461	307	0.4	0.8	0.4
12		2000	4	1	1.4E-08	8.0E-09	8.0E-09	39	1961	307	0.1	0.0	0.1
13		2000	6.1	2	5.6E-08	5.0E-08	8.0E-09	39	1961	307	0.6	0.3	0.1
22		2000	6.1	3	1.2E-07	1.1E-07	1.9E-08	39	1961	307	1.3	0.7	0.2

No		P_{RX}	Cat. g	total dry gas volume		Initial LA	carbon come from gas		final liquid phase		LA left Liquid		Recovered Carbon
		psi	g	mole	L(STD)	Mole	Mole	%LA	Con%	Sel%	%LA	Mole	%
9	T=150 °C	1000	1	0.56	12.5	0.12	0.0139	11.6	72	78	16.0	0.0192	96
7		1000	2	0.56	12.5	0.12	0.0165	13.8	85	82	15.3	0.0183	99
8		1000	3	0.56	12.5	0.12	0.0178	14.8	96	82	17.6	0.0211	97
15		1500	1	0.86	19.3	0.12	0.0050	4.2	71	92	6.0	0.0072	98
5		1500	1.5	0.86	19.3	0.12	0.0103	8.6	76	90	7.5	0.0090	101
2		1500	2	0.86	19.3	0.12	0.0127	10.6	98	92	8.4	0.0100	102
3		1500	3	0.86	19.3	0.12	0.0169	14.0	96	80	18.8	0.0226	95
4		1500	4	0.86	19.3	0.12	0.0203	16.9	99	79	21.0	0.0252	96
10		2000	1	1.16	26.0	0.12	0.0068	5.7	46	88	5.3	0.0064	101
6		2000	2	1.16	26.0	0.12	0.0114	9.5	95	86	13.5	0.0161	96
11		2000	3	1.16	26.0	0.12	0.0127	10.6	97	90	9.5	0.0115	101
23		330	2	0.16	3.5	0.12	0.0224	25.4	69	78	15.3	0.0183	103
16	T=130 °C	1000	1	0.61	13.6	0.12	0.0088	7.3	54	90	5.5	0.0066	102
18		1000	2	0.61	13.6	0.12	0.0066	5.5	65	93	4.4	0.0052	101
19		1000	3	0.61	13.6	0.12	0.0083	7.0	79	86	11.3	0.0136	96
14		1500	1	0.92	20.7	0.12	0.0028	2.3	53	97	1.6	0.0019	101
17		1500	2	0.92	20.7	0.12	0.0024	2.0	81	95	4.0	0.0047	98
20		1500	3	0.92	20.7	0.12	0.0100	8.4	84	90	8.0	0.0096	101
12		2000	1	1.24	27.7	0.12	0.0017	1.4	47	91	4.3	0.0052	97
13		2000	2	1.24	27.7	0.12	0.0059	7.6	87	95	4.3	0.0052	101
22		2000	3	1.24	27.7	0.12	0.0134	11.2	93	87	12.2	0.0146	1.0

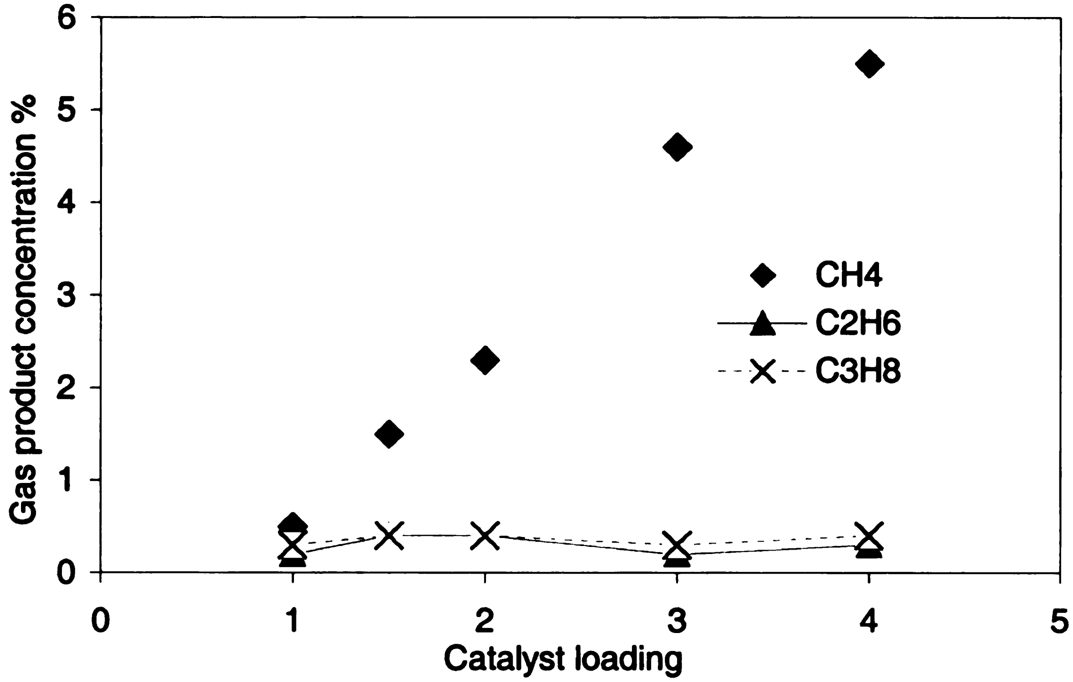

Figure 3-17. Catalyst loading effect on the gas products at1500psi and 150°C

3.5. Conclusion

Studies on batch hydrogenation of lactic acid in the autoclave indicate the following:

- Only supported ruthenium catalyst is active enough to give reasonable conversion in mild conditions.
- Lactic acid can be hydrogenated to propylene glycol at around 150°C and 1000~2000psi with carbon or alumina supported ruthenium catalyst.
- With Ru/C catalysts, selectivity over 90% at a conversion close to 100% can be achieved at optimal reaction conditions.
- Direct hydrogenation of lactate salt is impossible in aqueous phase for this catalyst system and at these reaction conditions. Acidified calcium lactate can be

hydrogenated to propylene glycol if the precipitated calcium sulfate is filtered before hydrogenation.

- The carbon balance shows that our analytic methods are reliable

Chapter 4. Conversion of Lactic Acid to Propylene Glycol in a Trickle Bed Reactor

After successfully converting lactic acid to propylene glycol (PG) in batch reactor, a laboratory scale trickle bed reactor was used to continuously hydrogenate lactic acid to PG. Racemic lactic acid, L+ lactic acid, and unrefined lactic acid were tested in this study. The granular catalysts used in this investigation were carbon-supported ruthenium prepared in our laboratories.

4.1. Control parameters and catalysts in trickle bed reactor

The upper limits of trickle-bed reactor system are 1280psi for pressure and 300°C for temperature. Catalysts were prepared by ruthenium salt and activated carbon. The details of trickle bed reactor system and catalyst preparation were shown in Chapter 2.

4.1.1. Control parameters

Before experiments in the trickle bed reactor, operating parameters, such as gas and liquid superficial velocity were calculated and compared with literature values to ensure our operation is in the range of typical operation of a trickle bed reactor.

4.1.1.1. Liquid superficial velocity

Superficial velocity is defined as the velocity in the trickle bed reactor tube without catalyst present. Liquid superficial velocity is calculated from liquid flow rate. The liquid flow rate used is 0.5~4 ml/min and the corresponding superficial velocity is 0.24~2.0cm/min. The equation used to calculate superficial velocity is

$$u_L = \frac{4F_L}{\pi d^2}(\text{cm/min}) \qquad \begin{cases} \text{d is tube diameter (1.57cm)} \\ \text{F}_\text{L} \text{ Liquid flow rate mL/min} \end{cases}$$

According to Ramachandran (64), the commonly used liquid superficial velocity is 0.6cm/min in pilot reactors and 6~12 cm/min in commercial reactors. Therefore, our trickle bed reactor was operated in the same liquid superficial velocity range as a pilot reactor.

4.1.1.2. Gas superficial velocity

Gas superficial velocity is defined as the gas velocity in column without catalyst. The gas flow rate used is 30~500 ml/min (STP) and the corresponding gas superficial velocity is 0.2~4 cm/min at 100°C and 1200psi, which is shown in the Table 4-1. This number is much smaller than that used in commercial reactor (15~300 cm/sec, according to Ramachandran), because of the high pressure used.

Table 4-1. Gas superficial velocity at 1200psi and 100°C

Gas flow ml (STD)	30	100	200	300	400	500
Superficial velocity (cm/s)	0.004	0.013	0.027	0.040	0.054	0.067
Superficial velocity (cm/min)	0.2	0.8	1.6	2.4	3.2	4.0

4.1.1.3. Flash vaporization

When dry hydrogen encounters the lactic acid water solution, part of the water will flash or vaporize. The maximum extent of flash vaporization depends on steam saturation pressure (temperature), liquid/gas flow rate ratio, and the pressure in the reactor. Figure 4-1 shows the water vapor pressure change with temperature and the extent of flash vaporization at different H_2/LA molar ratios and temperature. The maximum amount of water vaporized is less than 0.5% of that fed at our operating conditions (<120°C), so no steam saturator is needed.

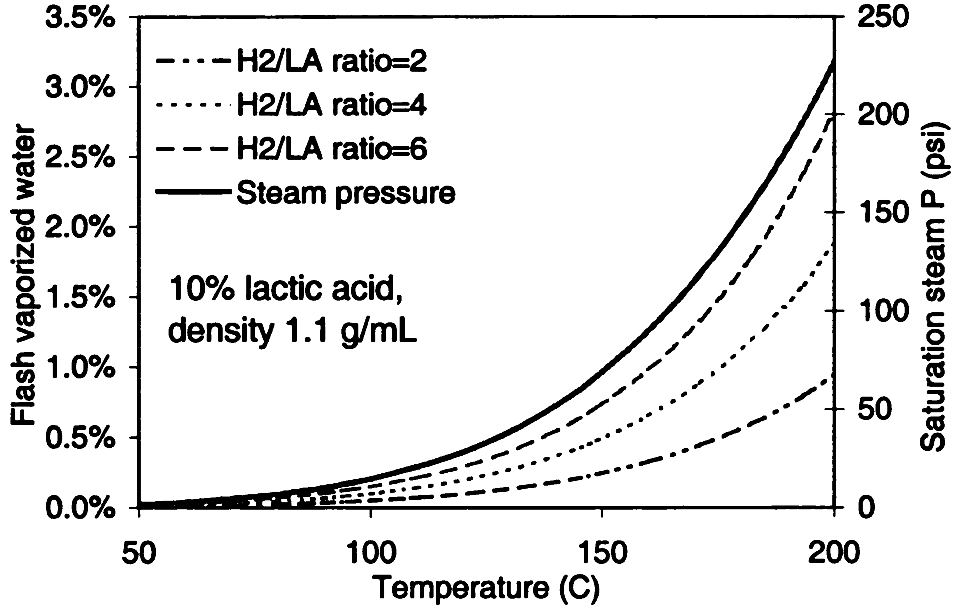

Figure 4-1. Flash vaporization and steam saturation pressure

4.1.1.4. Conditions of operation

All reactions in the trickle bed were carried out at temperatures of 70~150°C and pressures of 200~1200psi. Lactic acid was fed to the reactor in aqueous solutions of 5~17.2 w% lactic acid. The liquid flow rate ranged from 0.5~4.0 ml/min, giving a weight hourly space velocity (kg lactic acid/kg catalyst/hr) of 0.3~2. The hydrogen to lactic acid feed molar ratio varied from 2:1 to 10:1.

4.1.2. Catalysts

First, the prepared granular catalysts were characterized by physical and chemical adsorption, and then tested in the autoclave reactor. Only the ones with good performance in the batch reactor were used in the trickle bed reactor studies.

4.1.2.1. Catalyst characterization

Three granular active carbon supports were used to prepare catalysts for trickle bed uses. The procedure described in Chapter 2 was used to prepare 5% ruthenium on activated carbon catalysts. The BET surface areas of both carbon support and prepared catalyst were measured (Table 4-2). Chemisorption was used to measure active metal dispersion and the bond strength between metal and hydrogen. Dispersion is defined as the percentage of active metal accessed by hydrogen and is an indicator of how much metal is available for catalyzing the reaction. Intermediate temperature (the position of the first peak in the hydrogen desorption curve) during the hydrogen desorption is a reflection of how strong the metal-hydrogen bond is (Figure 4-1). The hydrogen desorption peak above 300 °C most likely comes from strong adsorbed hydrogen on ruthenium, which may not involve the hydrogenation reaction and cannot come from carbon support because the hydrogen adsorbed on carbon cannot desorb below 700°C (75).

Table 4-2. Catalyst supports specification

Support	Size	BET (m^2/g)	Maker or name
WV-B #1	14x35		Nuchar
CG5P #2	20x50	648	Cameron – Yakima
CG6M #3	12x40	728	Cameron – Yakima

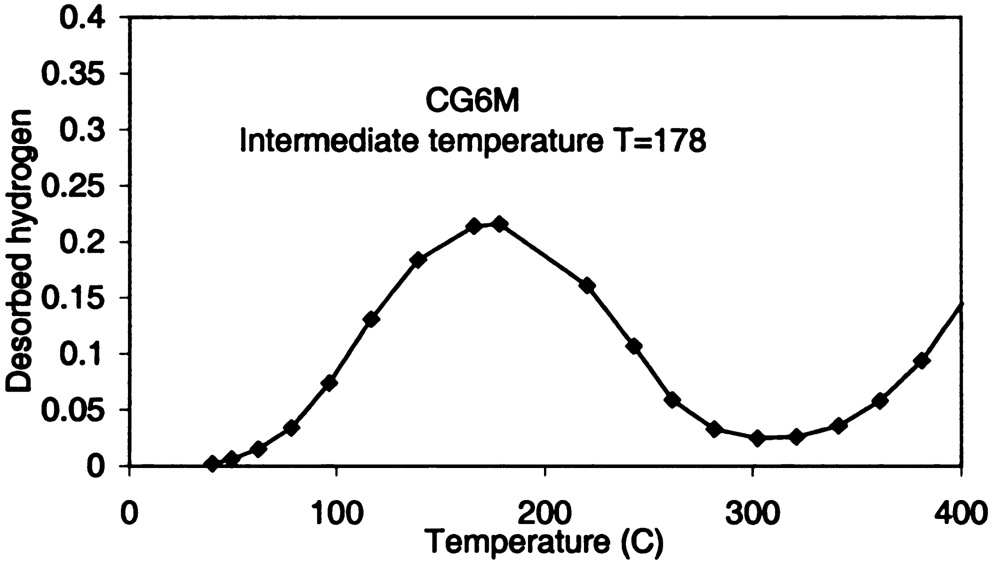

Figure 4-2. Hydrogen desorption profile during dispersion measurement

Table 4-3. Catalyst properties

No	Support	BET (m^2/g)	Dispersion	Intermediate temperature (°C)
A	WV-B	881	7.4%	245
B	CG5P	670	8.7%	220
C	CG6M	697	5.0%	178
D*	CG6M	N/A	5.0%	N/A

*Catalyst D is prepared by the same support and the same procedure as catalyst C

4.1.2.2. Initial autoclave test of granular catalysts

The three catalysts (A, B, C) described in Table 4-3 were first tested in the batch reactor at standard reaction conditions (2gram catalyst/100g 10% solution, 150°C and 2000psi). The conversion profiles for three catalysts are given in Figure 4-3, which shows that the activity of catalyst from WV-B is apparently lower than the other two. Therefore, only the catalysts prepared from CG5P and CG6M carbon supports were used in the trickle bed reactor. Compared to a powder catalyst (CG6M-F, 5% ruthenium on ground CG6M support, shown in Table 2-4), the conversions from granular catalysts are much lower (at same catalyst loading and reaction condition) than that of powder catalyst because of intra-particle mass transfer resistance.

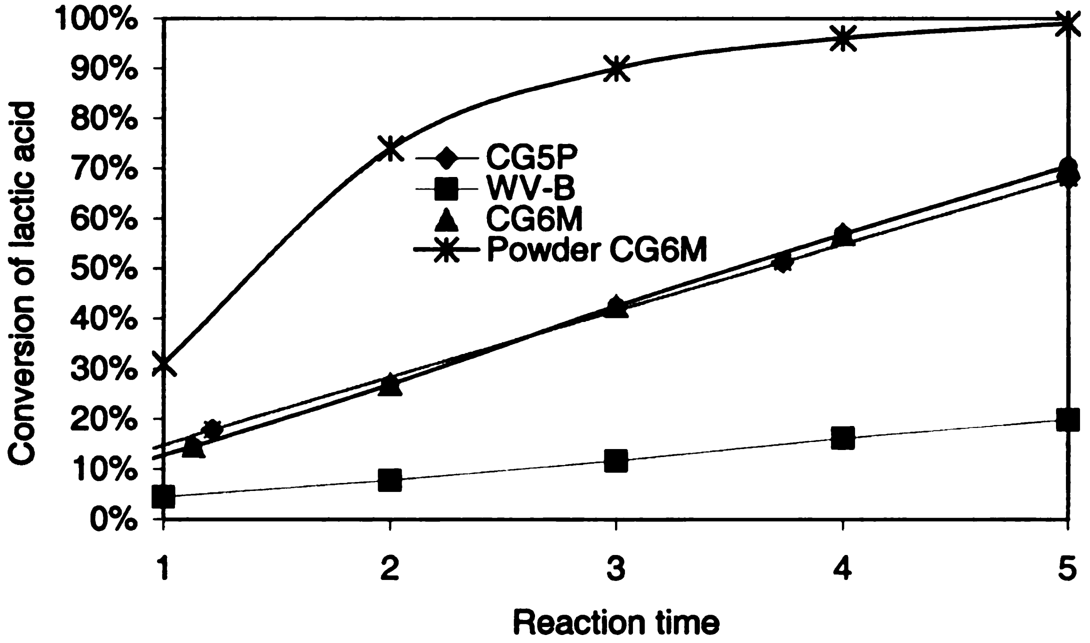

Figure 4-3. Granular catalysts performance in batch reactor

hyd

in h

per

disp

low

4.2.

sho

pre

wit

rea

The dispersion of CG5P is larger than that of CG6M (see Table 4-3), but the hydrogen-catalyst bond is stronger than CG6M as shown by the temperature of first peak in hydrogen desorption (T=178 and 220°C). Therefore, the two catalysts have similar performance in batch reactor. Although WV-B catalyst has the highest BET area and dispersion, the very strong hydrogen-catalyst bond (T=245°C) makes its reactivity very low as shown in Figure 4-3.

4.2. Trickle bed reaction (racemic lactic acid)

Three catalysts charges were prepared for trickle bed reactions. The details are shown in Table 4-4.

Table 4-4. Three catalyst charges used in trickle bed

	Charge 1	Charge 2	Charge 3
Catalyst	B	C	D
Support name	CG5P	CG6M	CG6M
Ruthenium loading	5%	5%	5%
Weight (gram)	30	27	48
Volume (ml)	71	64	118
Used for testing	Temperature Pressure H_2/LA ratio	Temperature Pressure H_2/LA ratio Adding sulfur	Temperature Pressure Unrefined sample

The first two catalyst Charges (1 and 2) were tested at different temperatures, pressures, H_2/LA ratios, and for rate enhancement by sulfur addition. Charge 3 fully filled with catalyst was used to investigate the temperature and pressure effects in trickle bed reactor.

4.2

is s

4.2

at 2

wa

30

hy

ex

lac

rea

ba

ca

C

re

n1

im

co

4.2.1. Results

The racemic lactic acid hydrogenation in the trickle bed reactor with three charges is shown in this section.

4.2.1.1. Charges 1 and 2

Before reaction, the catalyst was reduced at 150°C for 12 hours in pure hydrogen at 250psi. All feeding in this section was 10 % lactic acid (racemic) in water; flow rate was fixed at 1.0 ml/min unless specified. The hydrogen flow rate varied from 50 to 300ml/min to change the hydrogen to lactic acid molar ratio from 2:1 to 7.6:1. The hydrogen pressure was fixed at 1200psi and temperature ranged from 80~140 °C. The experimental results are summarized in Table 4-5. These data clearly demonstrate that lactic acid hydrogenation can be conducted in a continuous mode of operation. The reactivity of CG6M is higher than CG5P at all conditions, which is different from the batch reactor results. We cannot see any difference in autoclave reactions for these two catalysts (Section 4.1.2.2). The reason may be the particle size difference. Because CG6M is smaller than CG6P and the mass transfer is the major resistance in a trickle bed reactor, therefore the activity of CG6M is higher than that of CG5P. Experiment n9 and n10, both run at 120°C, show a selectivity of 86% with a conversion over 95%. The implication of these runs, of maintaining high selectivity at nearly complete lactic acid conversion, is that the downstream separation and purification of PG will be very simple.

CG5P (30 gram) (Charge 1)

4.2.1.2.

catalyst

support

pressure

4-6. The

temperat

effects o

Table 4-5. Trickle bed reaction summary (Charge 1 and Charge 2)

	No	Temperature (C)	H2/LA mole Ratio	Conversion %	Selectivity %
CG6M (27 gram)(Charge 2)	n1	80	2.5	35	77
	n7	100	2.5	67	87
	n8	120	2.5	82	88
	n2	80	5.1	31	79
	n6	100	5.1	66	88
	n9	120	5.1	95	87
	n4	80	7.6	36	81
	n5	100	7.6	62	90
	n10	120	7.6	98	85
CG5P (30 gram) (Charge 1)	13-n2	80	2	25	79
	14-n1	100	2	50	87
	14-n2	120	2	67	85
	13-n3	80	4	23	78
	13-n7	100	4	54	84
	14-n3	120	4	90	82
	14-n6	130	4	93	77
	14-n5	140	4	97	74
	13-n4	80	6	22	77
	13-n6	100	6	64	82
	14-n4	120	6	95	83

4.2.1.2. Charge 3

After the successful hydrogenation with Charges 1 and 2, a third charge of catalyst was prepared by filling the trickle bed tube to the top with catalyst D (CG6M support). Then a matrix of conditions was designed at three temperatures and six pressures at fixed H_2/LA ratio=4:1. The conversion and selectivity are shown in Table 4-6. The general trends are that conversion and selectivity are sensitive to reaction temperature, pressure, H_2/lactic acid molar ratio, catalyst type and catalyst loading. The effects of each parameter will be discussed in the following sections.

Table 4-6. Results of trickle bed with 48gram catalyst (Charge 3)

T°C		Catalyst D (CG6M) (48gram), H2:LA=4:1					
		Pressure (psi)					
		200	400	600	800	1000	1200
80	Conversion	21.0%	33.5%	43.3%	50.7%	58.0%	63.2%
	Selectivity	59.4%	70.5%	76.0%	77.7%	78.8%	78.6%
100	Conversion	52.0%	70.7%	81.5%	87.6%	91.1%	93.6%
	Selectivity	73.8%	76.5%	77.8%	79.6%	80.4%	80.7%
120	Conversion	77.4%	86.9%	94.3%	97.7%	98.7%	99.6%
	Selectivity	34.1%	42.1%	48.9%	56.2%	63.2%	68.6%

4.2.2. Temperature effect

Temperature effect was investigated in Charge 1(CG5P) and Charge 2 (CG6M). Lactic acid conversions increase almost linearly with temperature at 80~120 °C (Figure 4-4) for all hydrogen to lactic acid molar ratios.

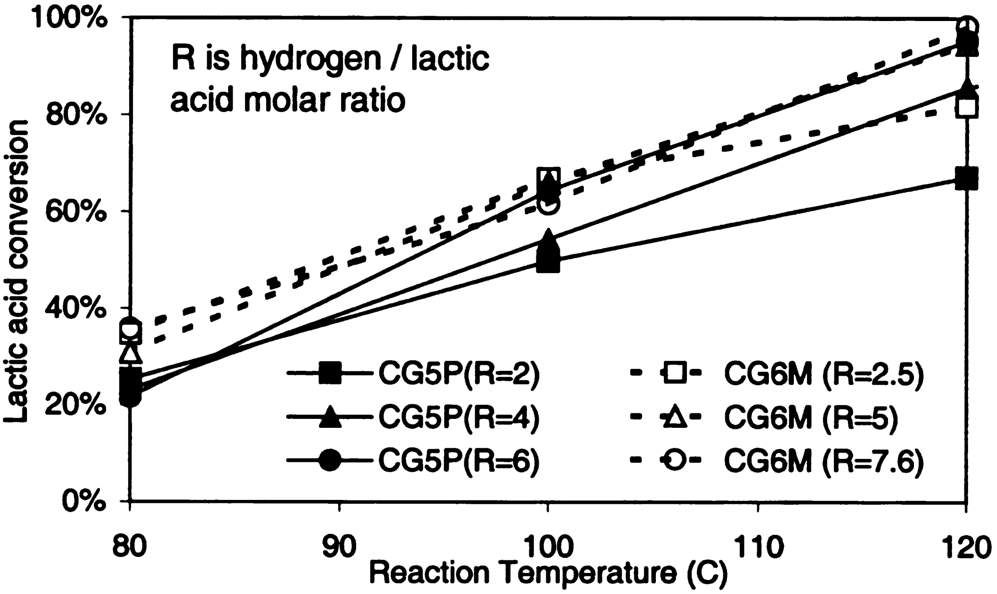

Figure 4-4. Lactic acid conversion vs. reaction temperature

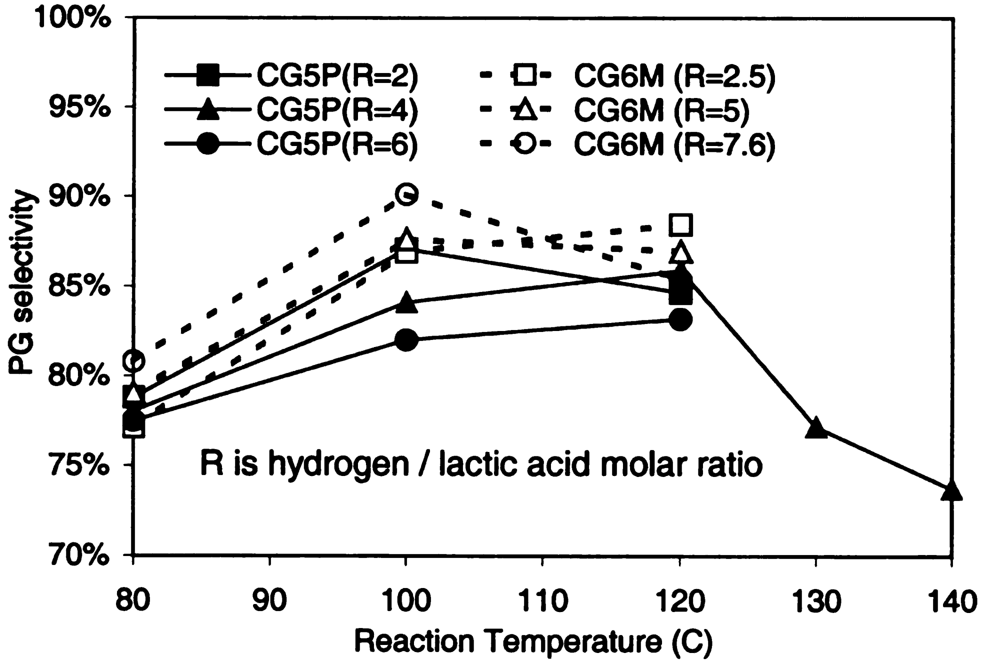

Figure 4-5. PG selectivity vs. reaction temperature

The selectivity change with temperature is very similar to that in the autoclave reactor, with maximum selectivity located around 100~120°C (Figure 4-5) for the trickle bed reactor instead of 150°C in the batch reactor. High temperature and low temperature are not good for selectivity. The existence of an optimal temperature for selectivity is for high and low temperatures both favor side reactions. No clear relation can be found between hydrogen and lactic acid molar ratio and the PG selectivity. High selectivity for CG6M catalyst presumably comes from its support properties.

4.2.3. Pressure effect (Charge 3, fully filled CG6M)

The pressure effect was investigated in Charge 3(48-g CG6M catalyst). Feed solution is 8.6% J. T. Baker lactic acid in water, hydrogen to lactic acid molar ratio was fixed at 4.7, and liquid flow rate was fixed at 2 ml/min. Three temperatures (80, 100 and 120°C) and six pressures (200, 400, 600, 800, 1000, 1200 psi) were used.

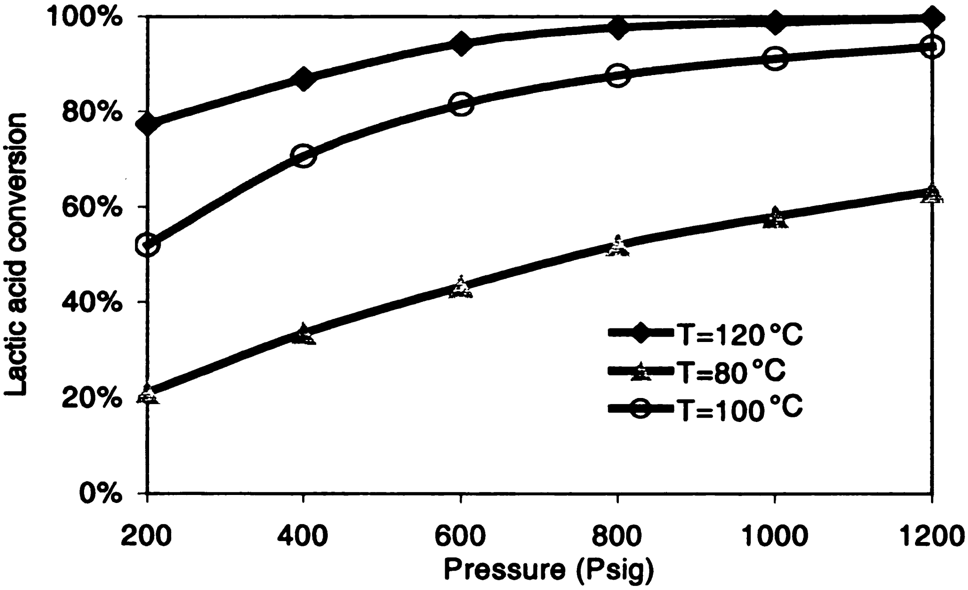

Figure 4-6. Conversion profile vs. temperature and pressure

in Fi

conv

(35%

high

100%

from

and 1

(>600

4.2.4.

selecti

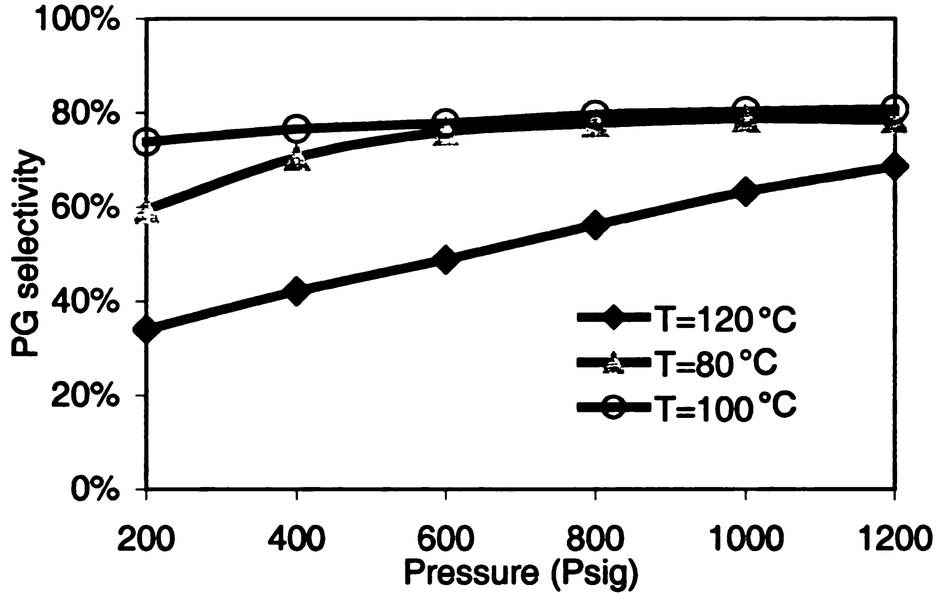

Figure 4-7. Selectivity profile vs. temperature and pressure

The selectivity and conversion change with pressure and temperature are shown in Figure 4-6 and Figure 4-7. At high temperature (120°C), even at 200psi, the conversion reaches 80%, but the selectivity at high temperature was extremely low (35%). At low temperature (80°C), the conversion increased with pressure linearly. At high temperature (120°C), the increase became slower because it was already close to 100% conversion and no difference can be seen for the reaction at 1000psi and 1200psi from the point of view of conversion. For selectivity, 100°C is apparent better than 80°C and 120°C, which is consistent with the reaction in Charge 1 and 2. At high pressure (>600psi), the selectivity difference for 100°C and 80°C almost disappears.

4.2.4. Hydrogen/lactic acid molar ratio

Hydrogen to lactic acid molar ratio only slightly affects the conversion and selectivity. Figure 4-8 shows conversion vs. hydrogen to lactic acid molar ratio for

Charge 1 and 2. At low temperature (80°C), the ratios did not change the lactic acid conversion at all because the lactic acid conversion was low and plenty of hydrogen was available. However, at high temperature (120°C), the rapid reaction (high conversion) made the reaction hydrogen limited at the catalyst surface and bulk liquid. Therefore, a high ratio always enhances hydrogen mass transfer and increases the lactic acid conversion. The selectivity vs. temperature and hydrogen/lactic acid ratio is shown in Figure 4-9. High hydrogen to lactic acid ratio lowers selectivity at high temperature because the extra hydrogen favors deep hydrogenation (side reactions). Like conversion, selectivity is not affected by hydrogen to lactic acid ratio at low temperature.

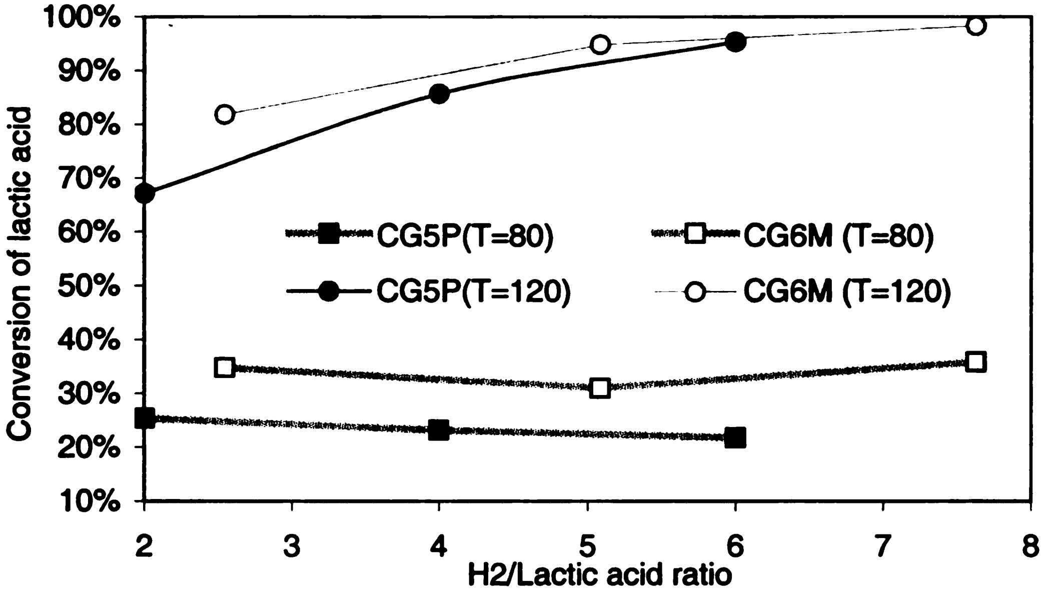

Figure 4-8. Effect of molar ratio on conversion

4.

mo

spa

liqu

line

sele

ml/

cata

incr

flat.

the c

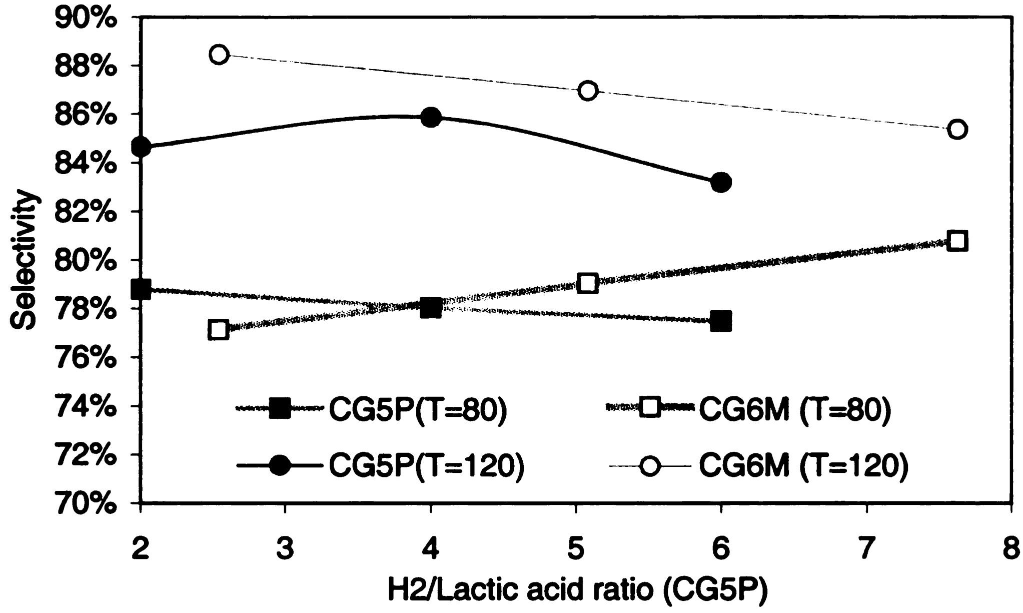

Figure 4-9. Effect of molar ratio on selectivity

4.2.5. The effect of changing liquid flow-rate

Figure 4-10 is the effect of liquid flow-rate (maintaining the hydrogen/lactic acid molar ratio=4:1) for Charge 1 at 100 °C and 1200psi. The X-axis is WHSV (weight hour space velocity), which is defined as lactic acid feed rate (g/hr) per gram catalyst. The liquid feed is 10 % lactic acid and the flow rate was 0.5~3 ml/min (WHSV=0.1~0.6). The linear decrease of lactic acid conversion with liquid flow rate is expected. However, the selectivity also decreases from 90% to 80% when the liquid flow rate changes from 0.5 ml/min to 3 ml/min. The reasonable explanation is excess hydrogen available on the catalyst surface, which enhances the side reactions (deep hydrogenation).

The PG output (g/min) vs. liquid flow rate is given in Figure 4-11. PG output increases quickly at the beginning (from 0.5 to 2 ml/min), and then the curve tends to be flat. When flow rate change from 2 to 3 ml/min, the PG output was unchanged because the conversion goes down quickly while selectivity changes little.

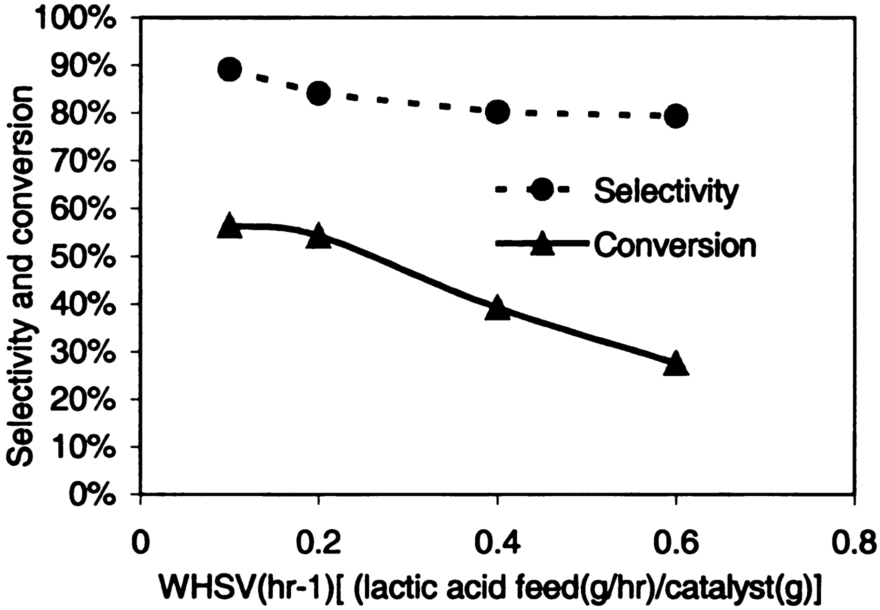

Figure 4-10. Conversion and selectivity vs. weight hour space velocity

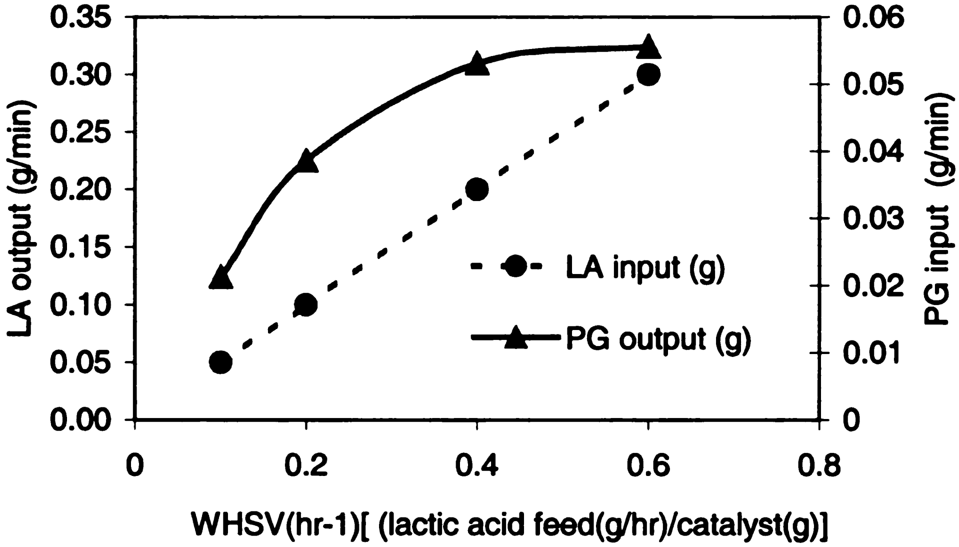

Figure 4-11. Effect of weight hour space velocity

4.2.6. Long time and low concentration lactic acid hydrogenation

This experiment used Charge 2 (27g CG6M) and 5.6% lactic acid feed at 100°C and 1200psi. Hydrogen/lactic acid molar ratio was maintained constant at 4:1; liquid flow rate was 1 ml/min for 27 hour and 0.3 ml/min for 67 hour. Total reaction time was 94 hours and the total lactic acid feed was about 3000ml. The selectivity almost was unchanged during this period, and low flow-rate led to high conversion (Figure 4-12). Catalyst deactivation is not a detectable in this extended time reaction.

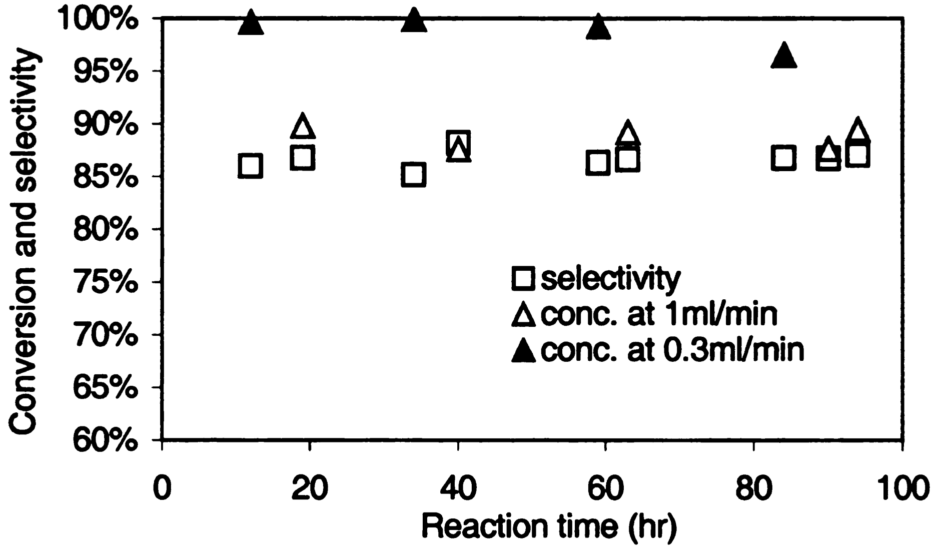

Figure 4-12. Conversion and selectivity of extended time reaction

4.2.7. High lactic acid concentration feed

Using high lactic acid feed concentration has the potential to improve productivity and reduce the quantity of water that has to be handled in this process. Nevertheless, the corrosion problems of higher lactic acid concentrations are always technical challenges in industry. Therefore, 17.2 % lactic acid was used to show the concentration effect. Reactions were conducted at 1200psi and 100°C with 1 ml/min liquid feed rate with Charge 1(30gram CG5P). The hydrogen to lactic acid molar ratio was 1.16~5.83:1. The results are shown in Table 4-7. The comparison with 10 % lactic acid feed at the same temperature and pressure is shown Figure 4-13. When lactic acid feed concentration changed from 10% to 17.2%, the conversion decreased about 10 % at different hydrogen to lactic acid molar ratios. The PG selectivity for 17.2% feed is only slightly lower than that of 10% lactic acid feed at low H_2/LA ratio.

The selectivity and conversion at high concentration are relatively unaffected by hydrogen to lactic acid molar ratio (Figure 4-13). One possible explanation is that G-L mass transfer does not control the reaction because the increase of hydrogen (ratio) does not affect the reactions.

Table 4-7. Results of 17.2% lactic acid feeding

H2/LA molar ratio	Conversion	Yield	Selectivity
1.16	45%	33%	73%
2.33	43%	33%	77%
3.5	43%	34%	79%
4.67	43%	34%	79%
5.83	43%	34%	79%

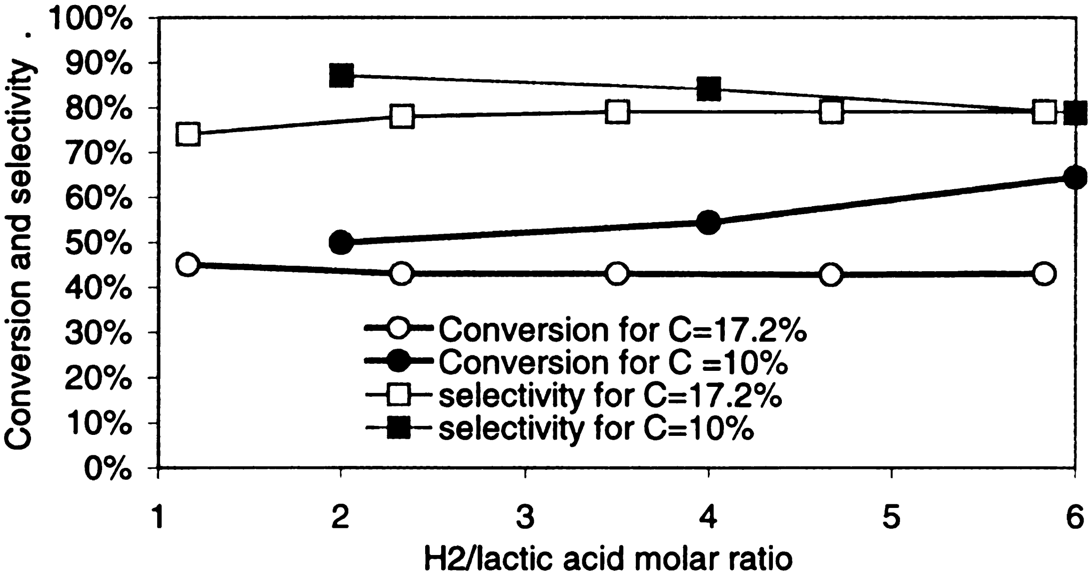

Figure 4-13. Selectivity and conversions for two lactic acid concentrations

4.2.8.

selecti
patent
poisor
format
may fa
hydrog
longer
from t

(27gra
Hydro
The su

4.2.8. Addition of sulfur to lactic acid feed

The idea to add sulfur to the liquid feed stream is to find a way to enhance the selectivity. In related work on sugar hydrogenolysis over ruthenium catalysts (U.S. patents 5,600,028 and 4,430,253), the addition of small quantities of sulfur partially poisons the ruthenium catalyst, which lowers conversion and essentially eliminates the formation of methane and ethane from the sugar feedstock. Applying the same principal may facilitate an increase in selectivity to PG by eliminating lactic acid deep hydrogenation to hydrocarbon by-products. Slightly higher reaction temperatures or longer space velocities may compensate for the decrease in catalyst activity stemming from the addition of sulfur.

The experiments were conducted at 100°C and 1200psi in Charge 2 (27gram CG6M). Sodium sulfide (Na_2S) solution was mixed with 10% lactic acid feed. Hydrogen to lactic acid molar ratio was fixed at 4:1 and liquid flow rate was 1 ml/min. The sulfur concentration in lactic acid was continuously increased (Table 4-8).

Table 4-8. Results of adding Sulfur

Conversion %	Yield %	Selectivity	ppm of $Na_2S.9H_2O$	Time (min)
68	59	88	0	120
63	55	87	100	120
60	51	85	100	130
57	49	87	300	120
56	49	88	300	60
56	48	86	300	70
53	45	84	600	120
52	45	85	600	60
47	41	88	600	60
33	27	84	600	100
Total sulfur (S) mole				0.0013

The addition of Na_2S in liquid feed slowly decreased the lactic acid conversion, and the selectivity was almost unchanged. That means that the deactivation by sulfur is not selective. A simple calculation is given in Table 4-9 to show the deactivation process. In this calculation, we assume that only surface ruthenium calculated from dispersion is active and that lactic acid conversion is proportional to the amount of active surface ruthenium. The calculation indicates that for every two sulfur atoms passing over the catalyst, one surface ruthenium atom will be deactivated (Table 4-9). This shows that sulfur deactivates ruthenium active sites with a very high efficiency.

Table 4-9. Calculation shows the deactivation is fast

Catalyst (CG6M)	Weight (g)	27
Total Ru (g)	G	1.36
Total Ru	Mole	0.013
Dispersion	%	5
Ru on Surface	Mole	0.00067
Total Na2S.9H2O addition	Gram	0.304
Total S	Mole	0.0013
Sulfur added /Surface Ru	Mole/mole	2
Lactic acid conversion (before)	%	68
Lactic acid conversion (after addition of sulfur)	%	33
Fraction of sites deactivated	%	49

cata

equ

add

at 1

4.3.

furth

resid

samp

acid)

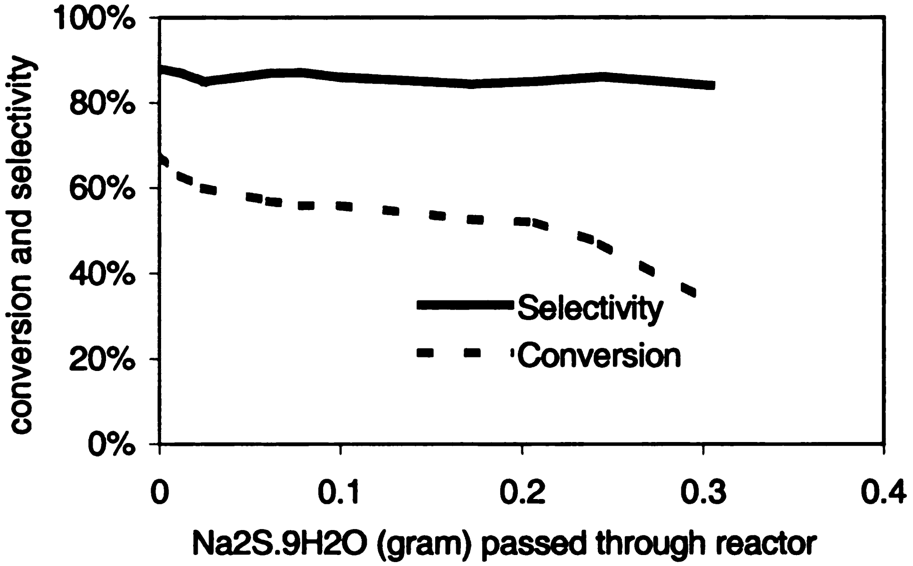

Figure 4-14. Conversion and selectivity change with addition of sulfur

Figure 4-14 visualizes the catalyst activity change with the addition of sulfur. The catalyst was continuously deactivated by adding sulfur-containng lactic acid solution. No equilibrium state was found; thus with enough sulfur, all active sites will disappear. In addition, the catalyst was deactivated permanently. With a 12-hour reduction in hydrogen at 150°C and 300psi, no reactivity could be recovered.

4.3. Conversion of unrefined lactic acid to PG in trickle bed reactor

The use of unrefined lactic acid to produce propylene glycol has the potential to further lower production costs. To investigate possible catalyst deactivation from the residual impurities from fermentation present in unrefined lactic acid, a raw lactic acid sample from Cargill was used as feed. The sample is unrefined lactic acid (L-(+)-lactic acid), which contains 50% lactic acid by weight and some amount of unknown impurities (*). By comparing its reactivity with refined DL-lactic acid (J. T. Baker, 85%) and Purac L-(+)-lactic acid (FCC grade, 88%), the effect of impurities in the Cargill sample on catalyst performance was investigated.

4.3.1. Reaction conditions

All experiments were conducted in the trickle bed reactor with Charge 3 described in Section 4.2.1. Reactions were carried out at temperatures from 80 - 120°C and pressures from 200 – 1200psi. Lactic acid was fed to the reactor in aqueous solutions of ~10% by weight. The liquid feed rate to the reactor was fixed at 2.0 ml/min, giving a weight hourly space velocity (kg lactic acid/kg catalyst/hr) of 1.3. The hydrogen to lactic acid feed molar ratio was fixed at 4:1, which is an optimal ratio from former experiments.

4.3.2. Results and discussion

4.3.2.1.Hydrogenation at different Pressure and Temperature

Conversion of unrefined and reagent grade lactic acids is shown in Figure 4-15, and the selectivity profile comparison is given in Figure 4-16 as a function of temperature and pressure.

---

[*] Impurities here refer to components other than lactic acid and water; HPLC analysis showed no other peaks, so we are confident there are minimal quantities of other organic acids present.

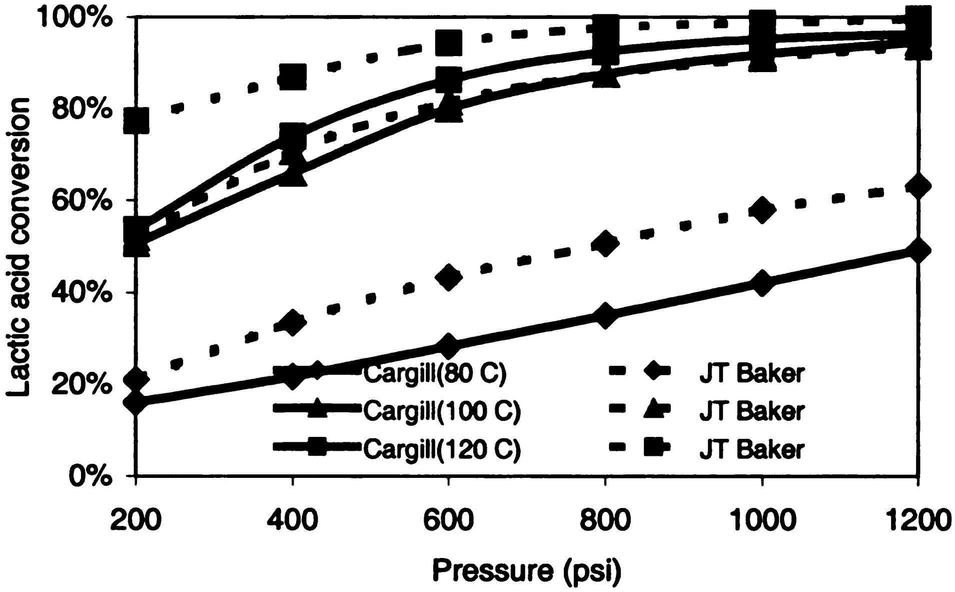

Figure 4-15. Conversion profile comparison of Cargill and pure lactic acid

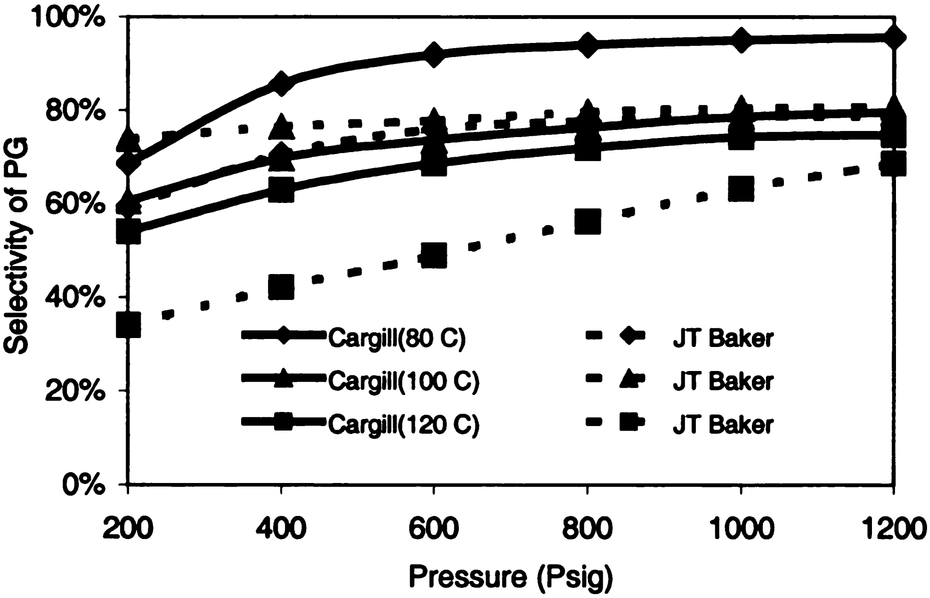

Figure 4-16. Selectivity profile comparison of Cargill lactic acid and regular lactic acid

J. T. Baker lactic acid hydrogenation was conducted first because we know from former experiments that it does not deactivate the catalyst. Following that Cargill lactic acid was used. The temperature order we used was 100, 80 and 120°C and the pressure order was 1200 to 200psi in 200psi increments.

Both refined lactic acid and Cargill lactic acid show a trend of increase in conversion with pressure and temperature. However, compared to refined lactic acid, the conversion of the Cargill lactic acid is lower at most reaction conditions. Apparently, either impurities or catalyst deactivation are responsible for the lower reactivity. The yield difference at 100°C and high pressure (1000 and 1200psi, these are the first two experiments with Cargill lactic acid) is barely distinguishable, but the difference increases as the experiments progress.

Results of the selectivity in Figure 4-16 are a little surprising because we failed to enhance the selectivity by adding sulfur (Na_2S) as shown in Section 4.2.8. At most reaction conditions, Cargill lactic acid has higher selectivity than refined lactic acid. The most exciting result is at 80 °C; the observed selectivity of 95% is the highest we have achieved in the trickle bed reactor. In addition, like conversion, the selectivity difference at 100 °C is much smaller than at the other temperatures, likely because of the catalyst selective deactivation over the course of the run.

4.3.2.2. Catalyst deactivation from impurities in Cargill lactic acid

The most crucial issue is catalyst deactivation from the impurities. After finishing the investigation of temperature and pressure, the catalyst Charge was treated (reduced) at 150 °C and 300 psi hydrogen for 12 hours. We typically conduct this treatment every 15~20 hours online to ensure that the catalyst is not oxidizing; in all cases the catalyst performance is the same or slightly better following the treatment. Then, a confirmation experiment was done to verify the change in catalyst activity. This experiment used standard reaction conditions (100 °C and 1200 psi); other parameters are same as the experiments in Section 4.3.2.1. The results are shown in Figure 4-17.

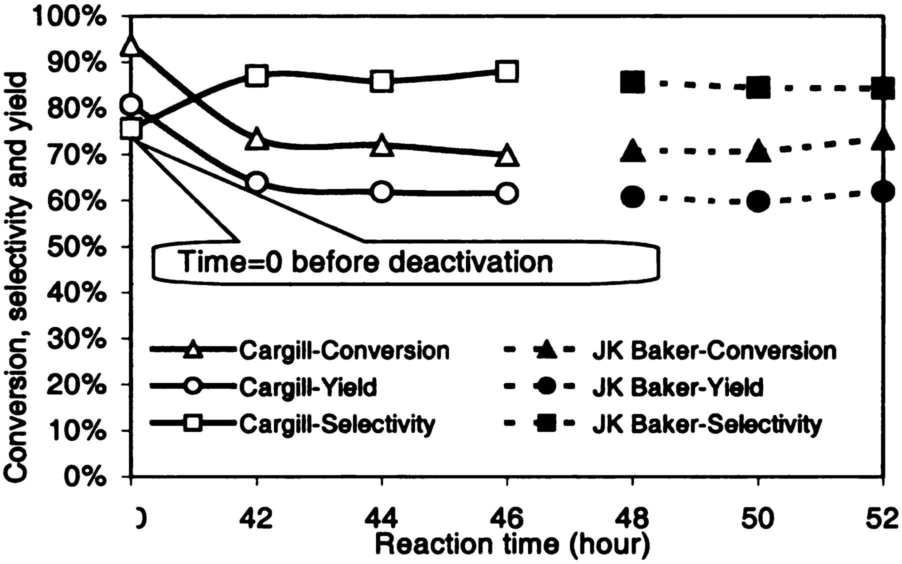

Figure 4-17. Catalyst deactivation (Switch from Cargill to pure lactic acid at 6 hr)

After comparing results at the start and after the temperature and pressure investigations, it is clear that the catalyst partially deactivates during the reaction. After 40-hour of reaction with Cargill lactic acid, which is equivalent to passing the entire 960-ml original Cargill sample (50%) over the catalyst, lactic acid conversion decreases from 95 to 70% and selectivity increases from 80% to about 90%. Apparently, this deactivation is selective, in that selectivity increases somewhat. Thus, by-products formation is reduced more rapidly than PG formation. From a process standpoint, deactivation would require progressively more recycle of lactic acid, but would result in overall higher yields.

4.3.

refir

Refi

two

chro

addi

other

acid

For e

after

show

4.3.2.3. The effect of lactic acid sources

The purpose of this experiment is to investigate the reactivity difference between refined lactic acid (J. T. Baker), Purac lactic acid and, Cargill unrefined lactic acid. Refined lactic acid comes from chemical synthesis with no optical activity and the other two are L (+) lactic acid. The impurities in the Cargill lactic acid do not appear in HPLC chromatography, so at least we know that no other organic acids are in the impurities. In addition, identical concentrations, temperature, and pressure were used to eliminate any other effects. The experiments were conducted at 100°C and 1200psi. Hydrogen to lactic acid molar ratio was fixed at 4:1 and all the lactic acids were diluted to 9.3% by weight. For each lactic acid, total reaction time was five hours, and the first sample was taken after two hours stabilization and analyzing product every hour after that. The results are shown in Figure 4-18.

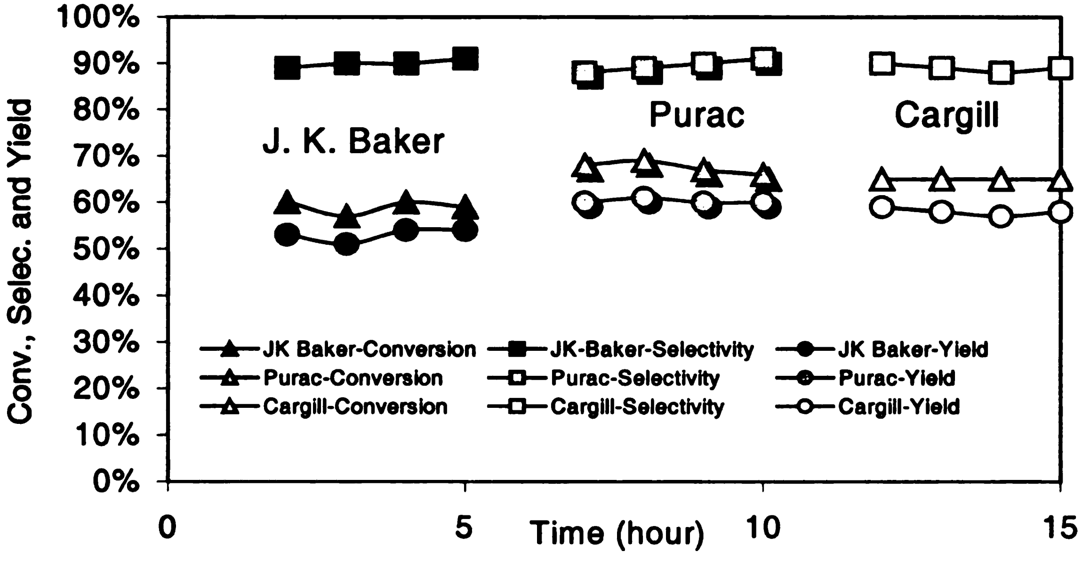

Figure 4-18. Conversion, selectivity and yield of three lactic acids

From these results, we notice that the reactivity of racemic lactic acid is slightly lower than L+ lactic acid, although we did not found any difference in batch reactor and the confirmation test (Figure 4-17). The reason is unclear yet; but the catalyst was left in reactor without pressure for a week before this run. Likely air leaked in the reactor and some oxidation happened. The Purac and Cargill lactic acid are very similar, but a 3% decrease in conversion and yield after five hours of feeding Cargill lactic acid is detected. That means that deactivation does happen during the five-hour reaction. This is consistent with the average decrease of 25% conversion over the 40-hour Cargill lactic acid feeding.

The gas phase composition is monitored by a mass spectrometer (Figure 4-19). As shown in Figure 4-18, the first five hours was racemic lactic acid feed, then five hours of Purac lactic acid, and finally five hours of Cargill lactic acid. It is apparent that the impurities affect the gas by-product composition. The most significant change is the relative amount of methane and ethane, although the total gas phase product yield are very close for Cargill and Purac lactic acid.

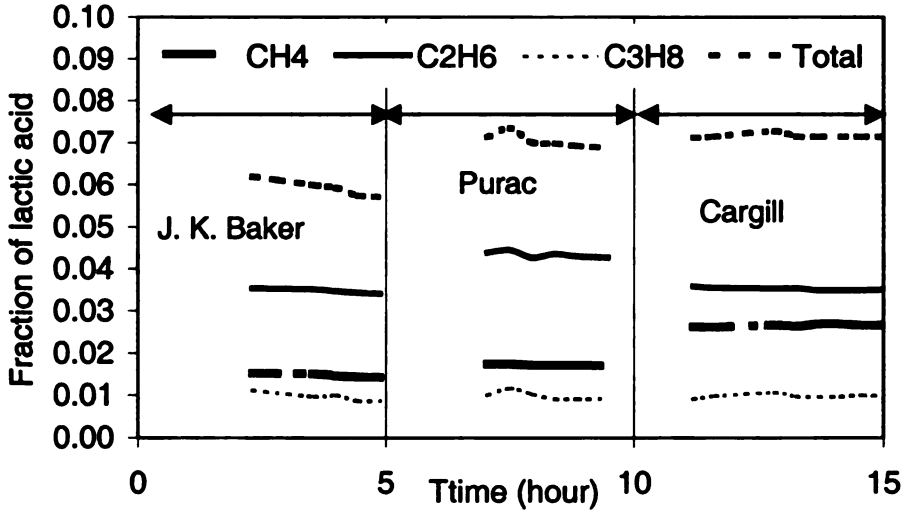

Figure 4-19. Gas phase composition changes with reaction time and feed

4.3.3. Summary

Identical concentration of Baker, Purac and Cargill lactic acids were hydrogenated at 80~120°C and 200~1200psi in a trickle bed reactor on 5% Ru/CG6M. The comparison of three lactic acids shows that the impurities in Cargill lactic acid slowly deactivate the catalyst. After passing 1000 ml of the unrefined Cargill sample, the conversion decreased by 25% and at the same time the selectivity increased from 80% to 90%. Therefore, the deactivation process is selective. In addition, reducing the catalyst in hydrogen at 150°C could not recover the activity. Purac and Cargill lactic acid have very similar liquid products, but the gas phase by-products are different.

4.4. Conclusion

Studies on catalytic hydrogenation of lactic acids at 80~120°C and 200~1200psi in a trickle bed reactor over granular activated carbon supported ruthenium catalysts indicate the following:

1. Lactic acids from variable sources can be continuously converted to propylene glycol in a trickle bed reactor.
2. CG6M is the best catalyst among those we made and as in batch reactor, high dispersion is not connected to high reactivity.
3. The stronger adsorption of hydrogen (as seen from the Intermediate temperature in Table 4-3) correlates with low activity in this hydrogenation
4. Lactic acid conversion increases with temperature at the same pressure and hydrogen to lactic acid ratio shows that intra-particle diffusion or surface reaction also controls the trickle bed hydrogenation beside gas-liquid mass transfer.

5. L+ or fermented lactic acid has slightly higher reactivity than racemic lactic acid in trickle bed hydrogenation.
6. The deactivation from sulfur (Na_2S) only decreases the lactic acid conversion and does not change the selectivity at all. Therefore, sulfur deactivates the catalyst without any preference for the favored reaction.
7. The impurities in Cargill unrefined lactic acid selectively deactivate the catalyst. After passing 1000-ml Cargill sample, the conversion decreased by 20% and at the same time the selectivity increased by 10%. Further reduction of the catalyst in hydrogen at 150°C cannot recover the activity.
8. These studies imply that there may exist two kinds of active sites on the catalyst surface and we may be able to selectively poison the catalyst to achieve higher propylene glycol selectivity, provided lower conversions can be accommodated.

Chapter 5. Mass transfer, kinetics and modeling

In three-phase hydrogenation, gas-liquid (G-L), liquid-solid (L-S) and intra-particle mass transfer will significantly influence the reaction rate. To investigate intrinsic kinetics, mass transfer effects must be eliminated by choosing suitable process parameters (catalyst particle size, stirring speed, catalyst loading, initial concentration, and reaction pressure and temperature).

5.1. H_2 solubility measurement

H_2 solubility or saturation concentration is a very important parameter in mass transfer analysis. However, no H_2 solubility data are available in the literature for high temperature and pressure. The measured solubility of H_2 at our reaction conditions will be reported in this section.

5.1.1. Apparatus

The equipment used for solubility measurement is shown in Figure 5-1. It consists of a high-pressure reactor with stirrer (Parr autoclave, 300 ml), a burette with two port caps (for gas out and mixture in), and a water-bath with a glass cylinder for measuring the gas volume by water displacement. A needle valve was used in the liquid outlet to control the saturated liquid fluid rate. Coiled steel tubing was used after the needle valve to cool down the saturated liquid to minimize flash vaporization.

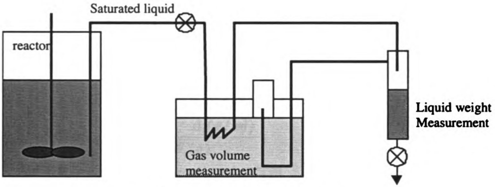

Figure 5-1. Apparatus for solubility measurement

5.1.2. Experimental steps

The first step was to fill the reactor with liquid (water or reactant solution) and seal it. Then the reactor was heated up to the desired temperature and pressurized to the desired pressure at the same time. High stirring speed (1200 rpm) was used to ensure the gas and liquid reached equilibration within 10 minutes. After stopping stirring, another 10 minutes was allowed to let the liquid and gas fully separate. The saturated liquid was then taken out from the dip tube to purge the liquid outlet line. A hydrogen source with constant pressure (pressure regulator and a high-pressure cylinder tank) was connected to the reactor to maintain a constant pressure in the reactor.

While the burette was empty and the glass cylinder was filled with water, the needle valve was carefully opened to let saturated liquid depressurize in the burette. The liquid was collected in the bottom and the gas displaced the water in the glass cylinder. When the liquid level in the burette reached about 20 ml or the gas volume in the glass cylinder was over 100 ml, the needle valve was closed and the liquid in the burette (weight and volume) and the gas volume in the cylinder were recorded.

5.1.3. Calculation and results

Hydrogen solubility can be calculated as:

$$S\,(\mathrm{ml/g}) = \frac{V_{gas}(ml) - \dfrac{W_l(g)}{d_l(g/ml)}}{W_l(g)}$$

V_{gas} is the total volume in mL (STP)

W_l is the liquid weight (g)

d_l is liquid density (g/mL)

Table 5-1. Solubility in HPLC water (ml (STP)/g)

T (°C)	136atm	102atm	68atm	34atm
	13.8Mpa	10.3Mpa	6.9Mpa	3.4Mpa
	2000psi	1500psi	1000psi	500psi
100	2.39	1.78	1.26	0.58
130	2.64	2.1	1.41	0.62
150	2.87	2.35	1.58	0.65
170	3.15	2.62	1.78	0.66

Table 5-1 is the hydrogen solubility in HPLC water. The solubility slightly increases with temperature at a given pressure. To verify the measurement, these data were compared to literature data (65) in Figure 5-2. The comparison shows that this measurement is reliable.

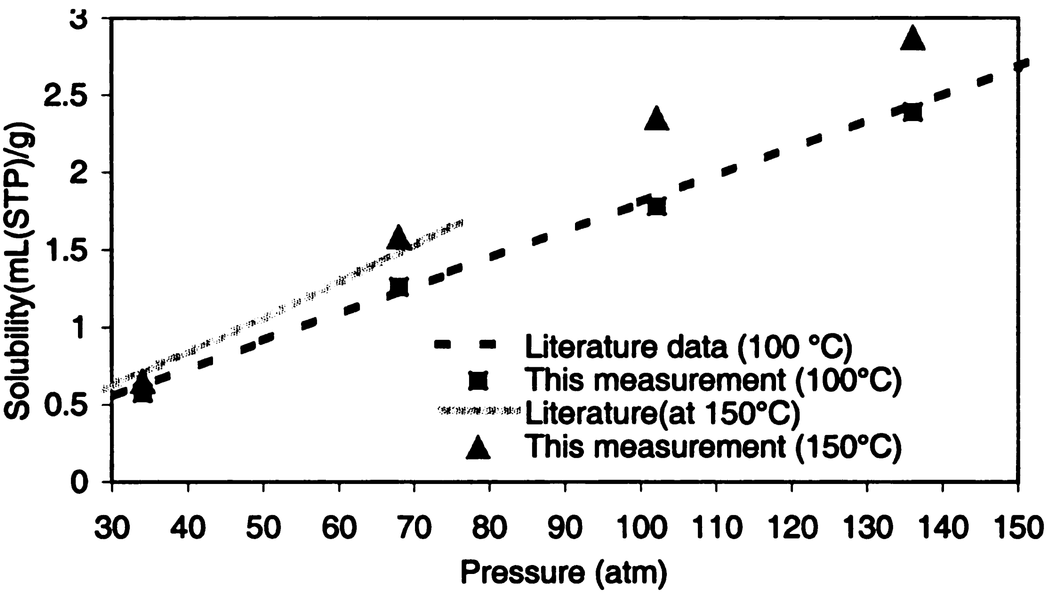

Figure 5-2. Comparison of measured solubility and literature data

5.1.4. Solubility of hydrogen in 10% lactic acid

In the same way, hydrogen solubility in 10% lactic acid water solution was measured. Table 5-2 shows that H_2 solubility in lactic acid has the same trend as in water, but the solubility in lactic acid solution is smaller than that in pure water at all our experiment conditions. The average difference is about 12%. At 100°C, the solubility linearly increases with pressure and can be represented by $S = 0.0012 * P - 0.165$. At 1200psi, solubility is 1.28 ml/g or $5.7\times10^{-5} mole/mL$.

Table 5-2. Solubility of hydrogen in 10% lactic acid (ml(STP)/g)

T (°C)	Pressure (psi)			
	500	1000	1500	2000
100	0.46	0.99	1.63	2.24
130	0.57	1.31	1.93	2.46
150	0.62	1.47	2.05	2.57
170	0.65	1.57	2.17	2.66

5.2. Characterization of mass transfer in the batch reactor (autoclave)

Understanding mass transfer in the batch reactor should be relative simple because the fast stirring rate most likely eliminates gas-liquid and liquid–solid mass transfer, and the powder catalyst also makes the intra-particle mass transfer unimportant. Experiments and calculations from literature correlations were used to investigate mass transfer effects in the autoclave reactor. From comparison of the reaction rate with mass transfer rate, one can figure out the influence of mass transfer on conversion of lactic acid to PG.

5.2.1. Suspension of catalyst

Catalyst suspension is not directly related to mass transfer, but the assumption for mass transfer study is that catalyst powder is evenly distributed in the liquid. Therefore, it is necessary to verify that the entire solid catalyst is suspended, or that no catalyst settles at the bottom of reactor. The minimum stirring speed requirement in the autoclave was given by Zwietering (66) (1959).

$$N_m = \frac{2(d_R / d_T)^{1.33} d_P^{0.2} \mu_L^{0.1} g^{0.45} (\rho_P - \rho_L)^{0.45} w^{0.13}}{\rho_L^{0.55} d_T^{0.85}}$$

where d_R and d_T are the reactor diameter and the stirrer diameter respectively and w is the catalyst loading (g/100g). N_m is the minimum speed needed to suspend all catalyst. Minimum speed requirement for different catalyst loadings is shown in Figure 5-3. It is clear that the stirring speeds we used (200~1200rpm) are much larger than the minimum suspension speed.

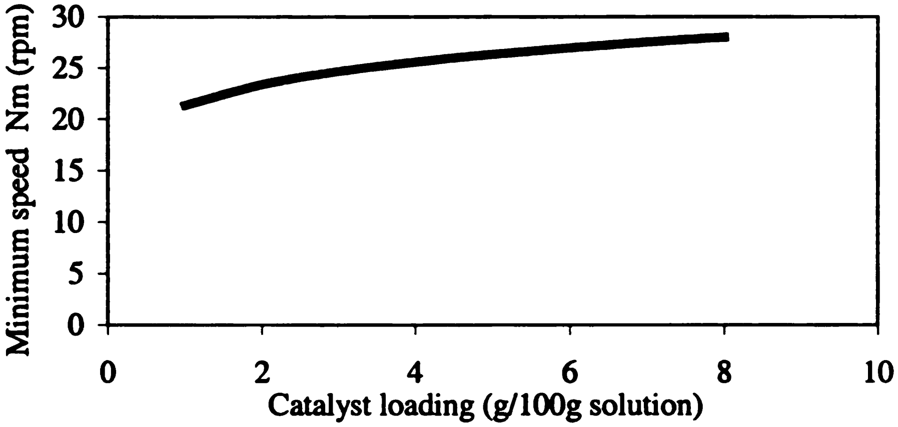

Figure 5-3. Minimum stirring speed for catalyst suspension

5.2.2. Maximum reaction rate and pseudo first order rate constant in batch reactor

The highest reaction rate is needed for investigating the mass transfer effects. Reaction rate is defined as converted lactic acid mole per weight of catalyst and time. The fastest reaction happens at high temperature and high pressure. Therefore, the reaction rates are calculated only for the reaction at 150°C and 2000psi (matrix 2, see Chapter 3). The initial reaction rate is the fastest because it is at the highest reactant concentration and with fresh catalyst. The maximum rate is about 0.081 mole/hr when the catalyst loading is 3g per 100g solution as shown in Table 5-1.

$$R_{LA}\left(\frac{mole}{hr\cdot g_{cat}}\right)=\frac{dC_{LA}}{w\rho_L dt}=C_{LA0}\frac{d(1-x)}{\rho_L w dt}=-\frac{C_{LA0}(mole/ml)}{w(g_{cat}/100g_{liuqid})\rho_L(g_{Liquid}/ml)}\frac{dx}{dt}$$

Table 5-3. Reaction rate for three catalysts loading at 150°C and 2000psi

Catalyst loading (g/100g)	1	2	3
C_{LA0} mole/ml	0.001	0.001	0.001
Solution density (g/ml) ρ_L	1.1	1.1	1.1
	Conversion %		
1 hr	21	40	53
2 hr	39	69	81
3 hr	52	84	94
4 hr	62	95	97
Max dx/dt (at t=0) (1/hr)	0.23	0.49	0.67
Max rate (mole/hr)	0.028	0.058	0.081
Max rate (mole/hr.g)	0.028	0.029	0.027

Table 5-4. Pseudo first order constant

<table>
<tr><td rowspan="10">P=2000psi T=150°C</td><td>Loading</td><td>Time (hr)</td><td>Con %</td><td>-ln(1-x)/wρ</td><td>k(1/hr)</td><td rowspan="10">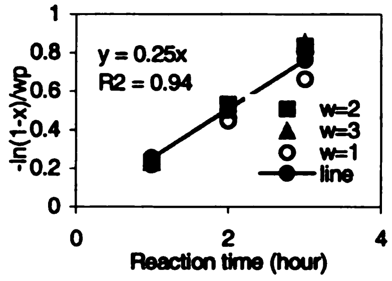 </td></tr>
<tr><td rowspan="3">1g/100g</td><td>1</td><td>21</td><td>0.22</td><td>0.22</td></tr>
<tr><td>2</td><td>39</td><td>0.45</td><td>0.22</td></tr>
<tr><td>3</td><td>52</td><td>0.66</td><td>0.22</td></tr>
<tr><td rowspan="3">2g/100g</td><td>1</td><td>40</td><td>0.23</td><td>0.23</td></tr>
<tr><td>2</td><td>69</td><td>0.53</td><td>0.27</td></tr>
<tr><td>3</td><td>84</td><td>0.83</td><td>0.28</td></tr>
<tr><td rowspan="3">3g/100g</td><td>1</td><td>53</td><td>0.23</td><td>0.23</td></tr>
<tr><td>2</td><td>81</td><td>0.50</td><td>0.25</td></tr>
<tr><td>3</td><td>94</td><td>0.85</td><td>0.28</td></tr>
<tr><td colspan="7">k=0.25 (1/hr) from fitting all data</td></tr>
</table>

If the reaction is assumed as first order for lactic acid, we can calculate the rate constant. The calculation is shown in Table 5-4. The data from all loadings fall on the same line. Therefore, the same rate constant is obtained for all loading.

$$-r_{LA} = -\frac{dC_{LA}}{\rho_L wdt} = kC_{LA} \Rightarrow -\frac{dC_{LA}}{C_{LA}} = \rho_L wkdt \Rightarrow \ln\left(\frac{C_{LA0}}{C_{LA}}\right) = \rho_L wkt \quad \Rightarrow \ln(1-x) = -\rho_L wkt$$

5.2.3. Gas-liquid mass transfer

A simple method was used to estimate the magnitude of the hydrogen–water mass transfer coefficient in batch reactor. The principle is to measure the pressure change in a sealed reactor after the beginning of stirring. From the pressure drop rate, the mass transfer coefficient can be calculated. Because the limit of the precision of pressure measurement and the speed of time recording, this method is only for the estimation of the magnitude of the mass transfer coefficient.

5.2.3.1. Principle and procedure

First, a certain amount of liquid (water) was charged into the sealed reactor; then the reactor was heated with stirring to specified temperature (25 or 100°C). When the temperature stabilized, the stirring motor was stopped. The reactor was pressurized carefully to a desired pressure with hydrogen. To minimize the mass transfer during the pressurization, the hydrogen was introduced from the gas phase (not from dip tube). The mass transfer during pressurizing is assumed small enough to be neglected; this was confirmed by the very slow pressure drop observed without stirring. The stirrer was then turned on; reactor pressure drop with time was recorded immediately after the beginning of stirring at specified speed.

5.2.3.2. Data analysis

Let S_0 be the hydrogen solubility at temperature T and pressure P, S (ml/g) the hydrogen concentration in the liquid at time t, and $k_L\alpha$ the gas (G) liquid (L) mass transfer coefficient. Then, the rate of change of hydrogen concentration will be:

$$\frac{dS}{dt} = (S_0 - S)k_L\alpha$$

Hydrogen solubility S_0 will change during the experimental process because the pressure P will change. In the low pressure range, we can estimated the change with Henry's law $S_0=H*P$ (at 150°C, H=0.0218 ml/g.atm, from the measurement in Section

5.1). From the hydrogen mass balance, the instant hydrogen concentration in liquid phase S can be calculated.

$$S = \frac{22400 * V_G (P_0 - P)}{R * T * W_L} \quad (\text{ml/g})$$

where W_L is the liquid weight in reactor, V_G is gas phase volume at room temperature, P_0 is the initial pressure in reactor, and P is the pressure at time t.

$$\text{Let } \beta = \frac{22400 * V_G}{R * T * W_L} \quad \text{then } S = \beta(P_0 - P)$$

$$\frac{dS}{dt} = \frac{-\beta dP}{dt} = k_L \alpha (S_0 - S)$$

$$\text{where } S_0 = H * P \text{ and } S = \beta(P_0 - P)$$

dS/dt is obtained by fitting S vs. t data to a fourth order polynomial and differentiating the polynomial. Plotting dS/dt vs. S_0-S and forcing a line to pass through the origin, the mass transfer coefficient $k_L\alpha$ can be calculated from the slope.

5.2.3.3. Results and comparison with literature

The measured mass transfer coefficients at different liquid loading in the reactor are given in Table 5-5. The regression coefficients R^2 in most of the regressions are 0.90~0.98, with the worst case of 0.8. That is reasonably good considering the very simple experimental equipment and method. It is seen that $k_L\alpha$ sharply increases after the stirring speed reaches 800rpm. Due to the limitation of equipment and experimental method, the reactor had to be filled to 73~87% of capacity to ensure measurable gas pressure drops. This leads to a very bad flow pattern in the reactor, because the stirrer blades are on the bottom of the reactor. Therefore, the coefficients we measured are the mass transfer coefficient at the worst conditions, and represent an estimate of the lower bound of gas-liquid mass transfer. Visual experiments were conducted to show the effects of stirring speed. Only the glass linear was used in visual experiments, so the gas liquid interaction can be seen from the wall of glass liner. The experiments showed that gas bubbles were formed when the stirring speed reaching 300rpm, and after 500rpm, no clear liquid phase could be seen. This partially explains the mass transfer coefficient change with stirring speed.

Table 5-5. Summary of mass transfer coefficient

Water=218g (25 °C)			Water=256 (25 °C)			Water=260 (100 °C)		
R(rpm)	$k_L\alpha(\mathrm{s}^{-1})$	$k_L\alpha(\mathrm{min}^{-1})$	R(rpm)	$k_L\alpha(\mathrm{s}^{-1})$	$k_L\alpha(\mathrm{min}^{-1})$	R (rpm)	$k_L\alpha(\mathrm{s}^{-1})$	$k_L\alpha(\mathrm{min}^{-1})$
347	0.0055	0.33	82	0.0034	0.2	216	0.0033	0.2
600	0.0096	0.58	600	0.013	0.75	615	0.01	0.61
805	0.02	1.19	734	0.018	1.1	891	0.03	1.78
847	0.023	1.4	869	0.025	1.5			
913	0.036	2.2	870	0.028	1.7			
1023	0.054	3.2	933	0.037	2.2			
1075	0.068	4.1	1186	0.098	5.9			
1280	0.14	8.2	1337	0.139	8.3			

The comparison with literature data (67) is shown in Figure 5-4. The literature data come from a large (2L) Parr autoclave and the mass transfer coefficient is measured for hydrogen in methanol. The density of methanol is close to water and the hydrogen solubility in methanol is 1.4 cc/g at measurement conditions, so it is very close to our system. The higher solubility of H_2 in water than in methanol and the bad flow pattern measurement are possibly canceled out. Therefore, the mass transfer coefficients are very close to our measurement at low stirring speeds. However, the liquid and gas contact pattern is much different in high stirring speed and fast mass transfer cannot be achieved with large liquid loading. This comparison verifies that this result is reasonably good.

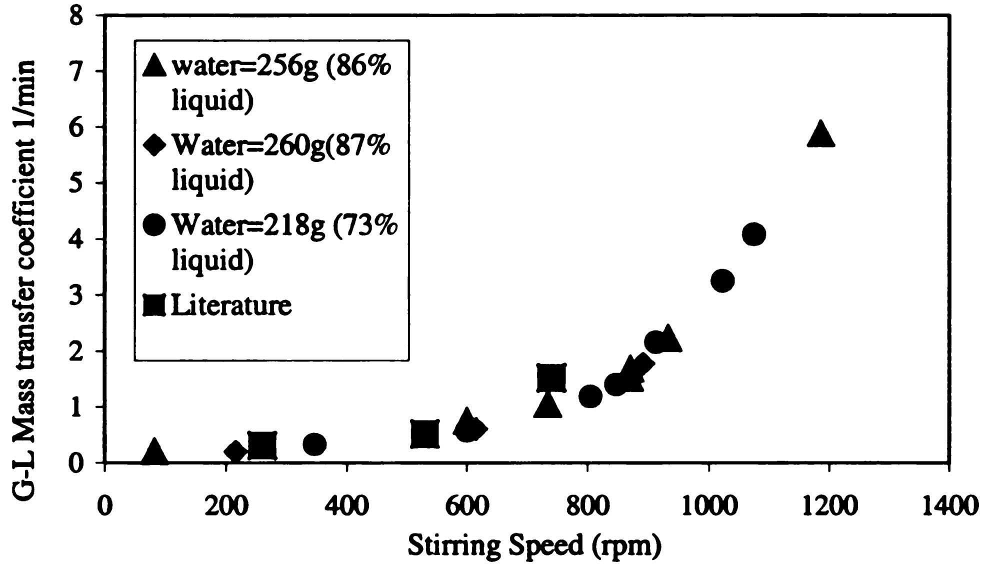

Figure 5-4. Hydrogen–water mass transfer coefficient in the autoclave

5.2.3.4. Comparing G-L mass transfer with reaction rate

At a stirring speed of 1000rpm, the G-L coefficient is about 3 (1/min), which is equal to 180 (1/hr). The solubility of hydrogen in 10% lactic acid at 2000psi and 150°C is 2.57cc/g (0.115 mole/L). Therefore, the maximum gas-liquid mass transfer rate (when hydrogen concentration in solution is zero) will be 2.1 mole/hr (100g solution→0.1L), which is much faster than the maximum observed reaction rate (0.081 mole/hr, see Section 5.2.2.). Therefore, G-L mass transfer in batch reactor is negligible. Alternatively, the hydrogen concentration in liquid can be estimated as

$$R_G(mole/hr) = K_L a(S_0 - S)*V_L \Rightarrow \frac{S}{S_0} = 1 - \frac{R_G}{K_L a V_L S_0} = 1 - \frac{0.081}{180 \cdot 0.1 \cdot 0.115} = 0.96 \text{ ->} 1$$

That means that the liquid hydrogen concentration is 96% of the solubility limit and gas liquid mass transfer will not control the autoclave hydrogenation of lactic acid to PG.

5.2.3.5. Comparing with literature correlation

Gas- liquid mass transfer in mechanically stirred tank reactors has been investigated by a number of workers. Ramachandran (64) (1983) has given an extensive review. Among these investigators, Bern *et al* (68) (1976) correlation is relatively reliable, for it used data from different size reactors (include commercial reactor).

$$k_L a = 1.099 \times 10^{-2} N^{1.16} d_I^{1.979} u_g^{0.32} V_L^{-0.521}$$

N is stirring speed (rpm)

d_I is the diameter of impeller (cm)

u_g is superficial gas velocity (cm/s) based on the reactor diameter

V_L is the liquid volume in reactor (ml)

With a fixed superficial gas velocity (0.001 cm/s), which was estimated from actual hydrogen consumption rate, the mass transfer coefficient was calculated at different stirring speeds. Compared to measurements in Section 5.2.1 (Figure 5-5), the predicted value is very close to the measured value at both low and high speeds. However, the deviation in medium stirring speed is significant. This calculation also shows the measurement is consistent with published data.

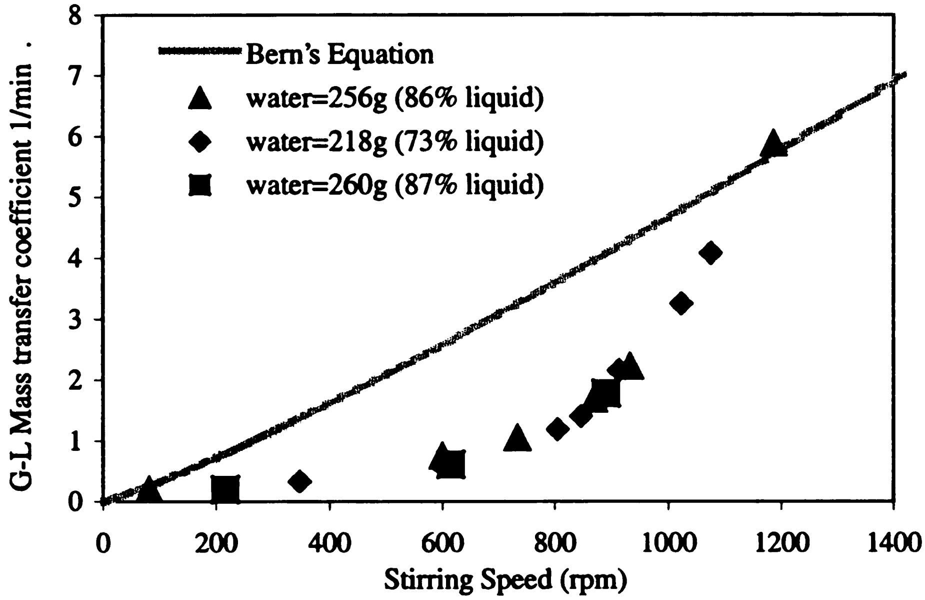

Figure 5-5. Comparison of Bern's correlation and measurement

5.2.3.6. Verification by investigating the stirring speed effect

As shown in Section 5.2.3.4 , the maximum rate for G-L mass transfer calculated using the measured coefficient is much larger than the maximum reaction rate, so we conclude that the G-L mass transfer resistance is negligible. This conclusion also is supported by the following lactic acid reactions at different stirring speeds.

These reactions were conducted at exactly the same temperature, pressure, catalyst loading and pre-reduction conditions [150°C, 2000psi, 1-gram 5% Ru/C powder (Moisture 52.6% Lot 325980 England), 30 minutes reduction at 150°C]. The experimental results are summarized in Table 5-6. Virtually no relationship can be seen between the conversion and stirring speeds. That means the mass transfer does not control this reaction even at a stirrer speed of 200. The maximum difference in conversion is about 10%; this deviation may come from the uneven catalyst reduction. The later experiments showed that one-half hour was not enough time to completely reduce powder catalyst, because the powder catalyst did not have good contact with hydrogen gas during the reduction process.

Table 5-6. Stirring speed effects

No	Speed	Conversion at hour				
		1	2	3	4	5
M36	200	28%	58%	81%	93%	98%
M33	400	26%	49%	67%	81%	91%
M35	600	15%	48%	81%	95%	99%
M29	800	10%	31%	57%	74%	89%
M28	1000	27%	54%	74%	90%	97%
M27	1200	25%	44%	63%	79%	93%

5.2.4. Liquid-solid mass transfer

It is well known that the coefficient of liquid-solid (L-S) mass transfer is very large compared to gas liquid mass transfer, so no actual measurement was conducted. Only a creditable correlation was used. The commonly used correlation is from Sano *et al.* (1974)(72).

$$\frac{k_s d_p}{DF_C} = 2 + 0.4\left(\frac{e d_p^4 \rho_L^3}{\mu_L^3}\right)^{1/4}\left(\frac{\mu_L}{\rho_L D}\right)^{1/3} \qquad e = \frac{P}{\rho_L V_L}$$

F_c is the shape factor of particles (=1)

$$a_p = \frac{6w(g)\rho_B(mL/g)}{100(ml)\cdot d_p(cm)}$$ external area of particles per unit volume of solution

ρ_L Liquid density (1.1 g/ml)

P power consumption (watt)

We do not know the exact power consumption P, but it should be around 20~300 watt. The particle size used is dp=0.05cm as an upper limit. The L-S mass transfer coefficient of hydrogen $k_S a_p$ was calculated and shown in Figure 5-6. The calculation shows that liquid-solid mass transfer is much faster than that at the gas-liquid interface. Therefore, its resistance also can be neglected.

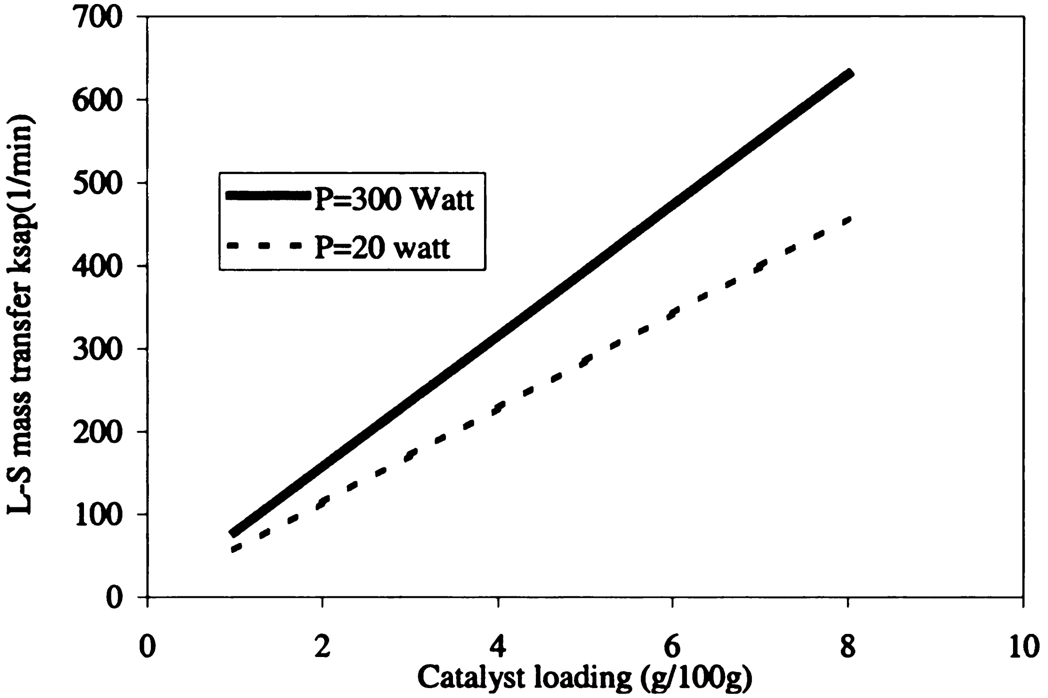

Figure 5-6. L-S mass transfer coefficient from Sano's correlation

Another recommended correlation is from Boon-long et al (73). Their equation does not need the power consumption, but it needs stirring speed. Figure 5-7 shows results from this correlation. Comparing with Sano's correlation, the stirring power consumption of our autoclave at 1200 rpm is around 20W.

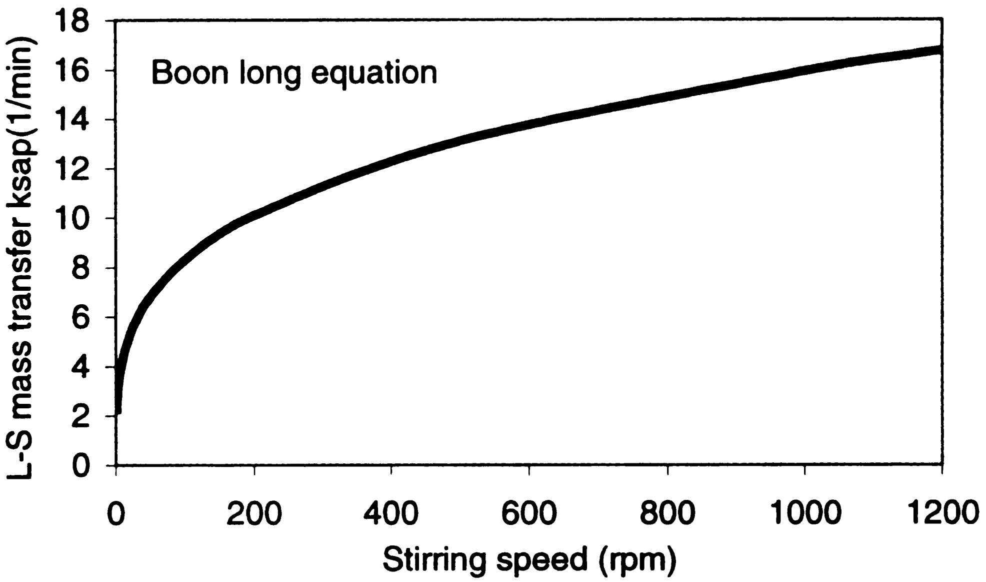

Figure 5-7. Mass transfer coefficient from Boon-long's equation

5.2.5. Intra-particle mass transfer

Because we do not known the reaction order, the observable modulus (Weisz – Prater criterion) was calculated to estimate the effect of intra-particle mass transfer.

$$\eta\phi^2 = \frac{(-R_G)L^2}{\rho \cdot C_A De}$$ where $(-R_G)$ is observed reaction rate (mole/gcat.sec)

The diffusivity of hydrogen and lactic acid are calculated from correlation (Appendix-1) and catalyst true density (ρ) is 0.8 g/ml forCG5P as measured in incipient wetness. Lactic acid consumption rate (mole/gcat.sec) was taken from Table 5-4. The modulus Characteristic length of catalyst is obtained by $L=D_P/6$, where D_P is the catalyst diameter. The effective diffusivity $D_e= \varepsilon_B^2 D$ is 3.3×10^{-5} cm^2/s at 100°C for hydrogen in water. Figure 5-8 shows that if the catalyst particle size is smaller than 0.02 mm, the observable modulus will be less that 0.1, and then mass transfer can be neglected.

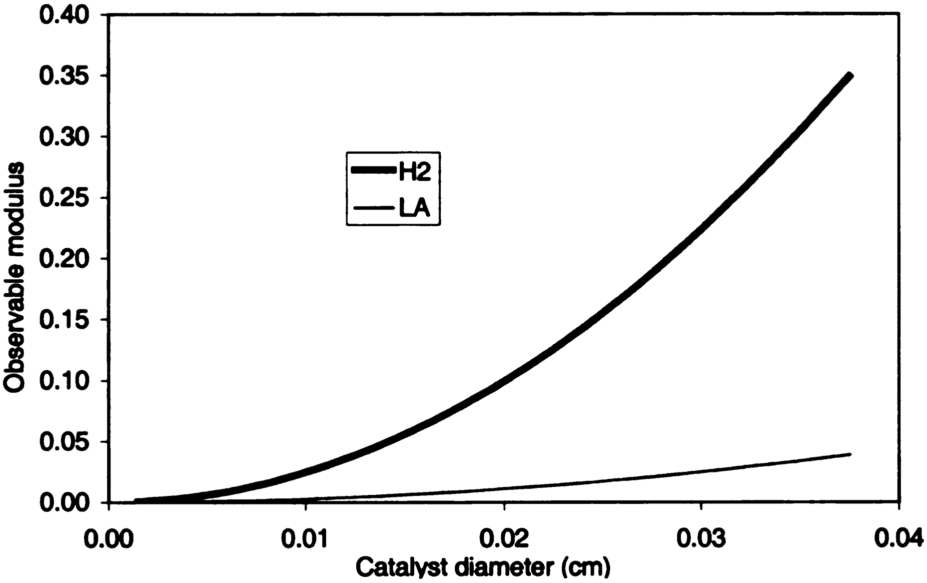

Figure 5-8. Observable modulus changes with catalyst diameter (10% lactic acid)

5.2.6. Summary of mass transfer in the batch reactor

The powder catalyst used in batch reactor is less than 0.01cm diameter; therefore, the intra-particle mass transfer is negligible. The slowest mass transfer is gas-liquid. The maximum G-L mass transfer is 50 times large than the maximum reaction rate. Therefore, the calculations and experiments show that mass transfer in autoclave is unimportant, and the intrinsic reaction kinetics can be determined.

5.2.7. Batch reactor macro kinetics

Since G-L, L-S and intra-particle mass transfer all can be neglected in batch reactor for lactic acid hydrogenation, then the observed rate in batch should be the intrinsic rate. The data used in the following analysis are from Matrix 2 and Matrix 3 as shown in Chapter 3. Two temperatures (130 and 150°C), three pressures (1000, 1500, 2000psi) and three different catalyst loading (1, 2 and 3 gram/100g solution) were the variable parameters. The same catalyst and pre-reduction conditions were used. To avoid complications from possible active metal leaching and deactivation, only initial rates will be considered here.

5.2.7.1. Initial reaction rate

The initial reaction rate was obtained by fitting the lactic acid concentration profile (C_{LA}~t) to a fourth order polynomial, differentiating the polynomial and setting the time to zero to get the initial reaction rate. This method is shown in Figure 5-9 and Figure 5-10 for experiment 99-15 (1 gram catalyst, 1500psi and 150°C). All initial rates are summarized in Figure 5-11.

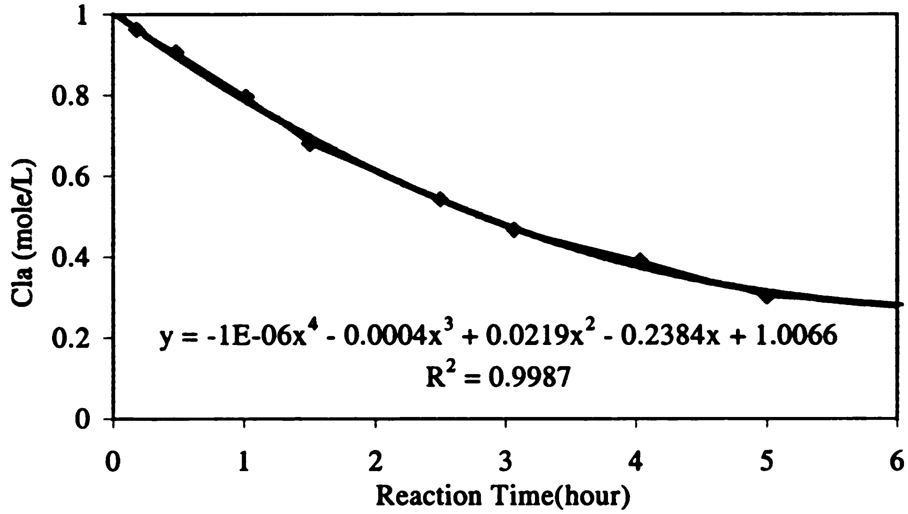

Figure 5-9. Fit concentration curve to 4th order polynomial

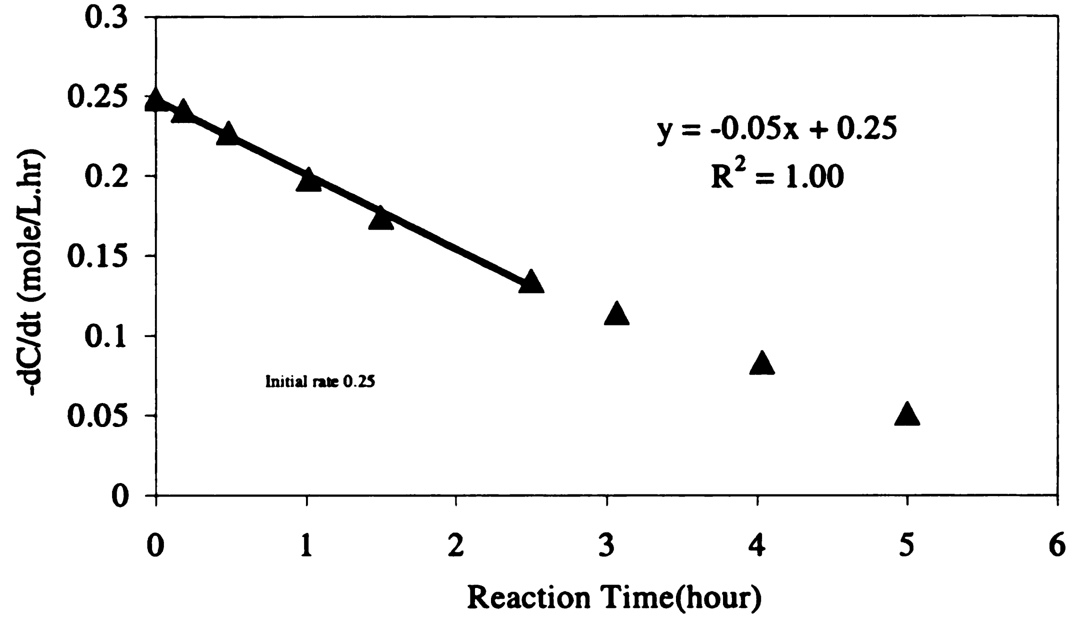

Figure 5-10. Get initial reaction rate from extrapolating the rate curve

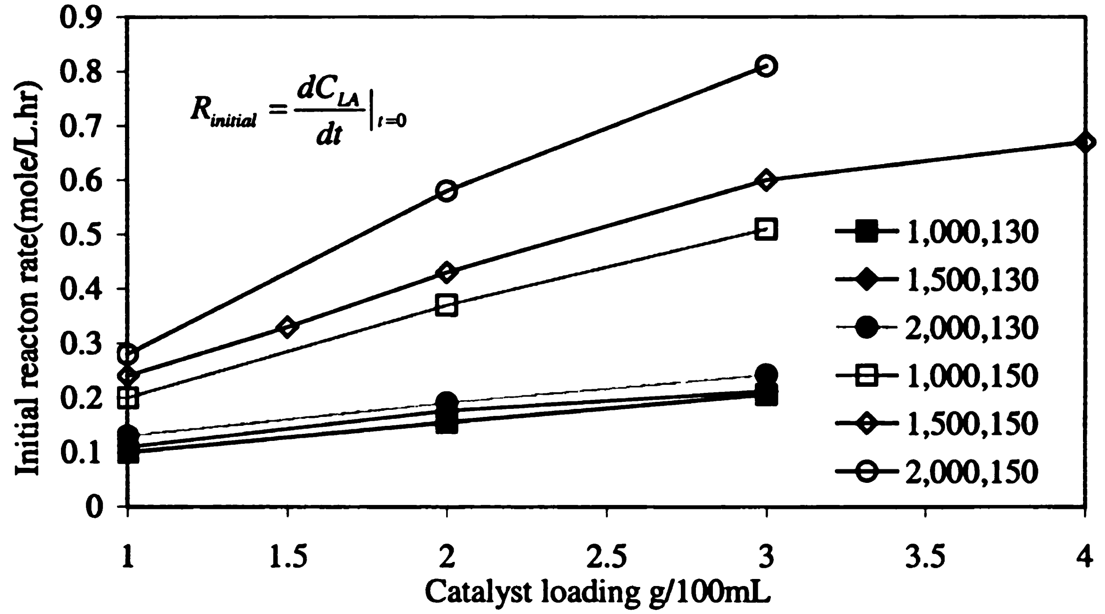

Figure 5-11. Initial reaction rates with catalyst loading

5.2.7.2. Activation energy

From regressing the initial reaction rate by

$$R_{initial} = k_0 \exp\left(\frac{-E}{RT}\right) w^m P_{H_2}^n$$

One can get the macro activation energy, catalyst loading effect "m" and hydrogen pressure effect "n". First, the equation was rewritten as

$$\ln R_{initial} = \ln k_0 - \frac{-E}{RT} + m \ln w + n \ln p_{H2}$$

Then the multiple variable regressions were used to get energy E and constants m and n.

The result is shown in Table 5-7. Then initial rate expression is

$$R_{initial} = 1.95 \times 10^{10} \exp\left(\frac{-96000}{RT}\right) w^{0.66} P_{H_2}^{0.3}$$

The activation energy (96kJ/mole) shows that this is a chemical reaction control process, which also verifies that the mass transfer is negligible in the batch reactor (consistent with mass transfer analysis in Section 5.2.6.). This regression shows hydrogen pressure only slightly affects the initial rate (m=0.3), which indicates that lactic acid hydrogenation is not a simple surface reaction. The comparison of initial rate and predicted initial rate by the regressed expression is given in Figure 5-12.

Table 5-7. Regression results

No	T	Ptotal (psi)	rate mole/L.hr)	PH$_2$(psi)	Cat (g/100g)	ln(rate)	Regression Statistics	
99-16	T=130°C	1000	0.103	961	1	-2.27	Multiple R	0.98
99-18		1000	0.11	961	2	-2.21	R Square	0.95
99-19		1000	0.12	961	3	-2.12	Adjusted R^2	0.94
99-14		1500	0.061	1461	1	-2.80	Standard Error	0.19
99-17		1500	0.089	1461	2	-2.42	Observations	20
99-20		1500	0.178	1461	3	-1.73	Coefficients	
99-12		2000	0.086	1961	1	-2.45	Intercept	23.7
99-13		2000	0.129	1961	2	-2.05	X Variable 1	0.30
99-22		2000	0.135	1961	3	-2.00	X Variable 2	0.66
99-9	T=150°C	1000	0.2	931	1	-1.61	X Variable 3	-11490
99-7		1000	0.37	931	2	-0.99	Results	
99-8		1000	0.51	931	3	-0.67	KO	1.95E+10
99-15		1000	0.24	931	1	-1.43	m	0.66
99-5		1000	0.33	931	1.5	-1.11	n	0.30
99-2		1500	0.43	1431	2	-0.84	E/R	11490
99-3		1500	0.6	1431	3	-0.51	E(KJ/mole)	96
99-4		1500	0.67	1431	4	-0.40		
99-10		2000	0.28	1931	1	-1.27		
99-6		2000	0.58	1931	2	-0.54		
99-11		2000	0.81	1931	3	-0.21		

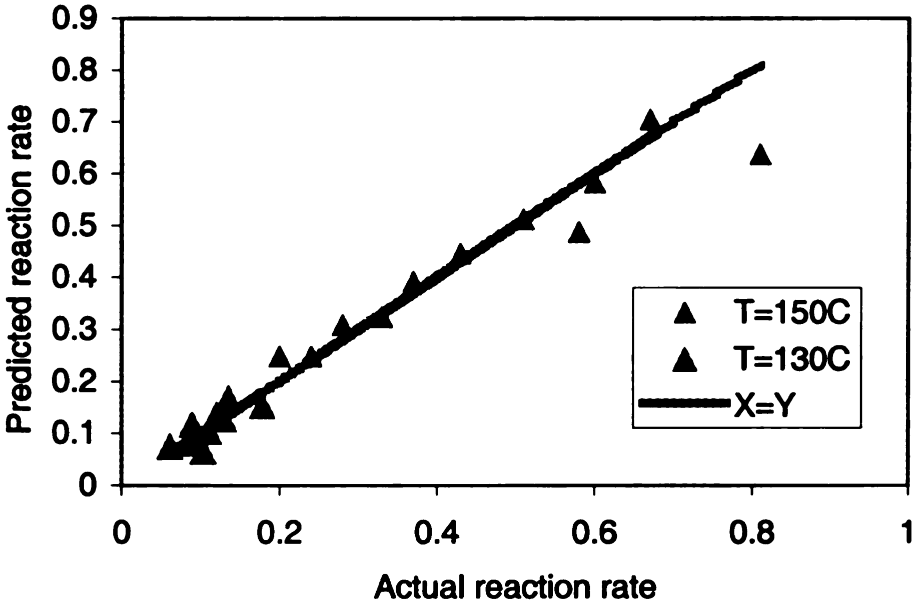

Figure 5-12. Comparison of experiment and predicted rates

5.2.8. Kinetics model

Even thought the main reaction is simple, without the knowledge of surface reaction, it is still very difficult to get a reasonable kinetic model. From Chapter 6, the main reaction path for PG formation is LA to propane-1,1,2-triol to propene-1,2-diol (or 2-Hydroxy-propionaldehyde) to propylene glycol. Based on the main reaction mechanism, a H-W model is derived and fit to the low temperature reaction data.

5.2.8.1. Model derivation

The Hougen-Watson (H-W) model will be used to get a workable reaction model. First, we assume that all species molecularly adsorb on to single sites. The reaction consists of six steps, hydrogen and lactic acid adsorption, formation and dehydration of propane-1,1,3-triol and the formation of PG. Hydrogen and lactic acid adsorption are not likely the controlling steps because fast adsorption is seen from the literature and our experiments. The other surface reactions are the possible control step. S is active site; K is equilibrium constant and k is rate constant. Cv is the vacant active site concentration and C_T is the total active site concentration.

$$\begin{array}{ccc} \text{LA(lactic acid)} & \Rightarrow & \text{Propane - 1,1,2 - triol (PT)} \\ & & \Downarrow \\ \text{Propylene glycol (PG)} \Leftarrow & & \left\{\begin{matrix}\text{2 - Hydroxy - propionaldehyde} \\ \text{Propene - 1,2 - diol}\end{matrix}\right\}(PD) \end{array}$$

1. $H_2 + S \xleftrightarrow{K_1} S \cdot H_2$	Hydrogen adsorption
2. $LA + S \xleftrightarrow{K_2} S \cdot LA$	Lactic acid adsorption
3. $S \cdot H_2 + S \cdot LA \xleftrightarrow{K_3} S \cdot PT + S$	Form propane-1,1,3-triol
4. $S \cdot PT \xleftrightarrow{K_4} S \cdot PD + H_2O$	Dehydration
5. $S \cdot PD + S \cdot H_2 \xleftrightarrow{K_5} S \cdot PG + S$	Form PG
6. $S \cdot PG \xleftrightarrow{K_6} PG + S$	PG desorption

We assume the first hydrogen addition (reaction 3) is the irreversible rate controling step and all other reactions are in equilibrium. Also we assume that total active site density is constant and neglect the water adsorption.

$$\mathrm{K}_1 = \frac{\mathrm{C}_{\mathrm{S\text{-}H_2}}}{P_{\mathrm{H_2}} C_v} \quad \rightarrow \quad \mathrm{C}_{\mathrm{S\text{-}H_2}} = \mathrm{K}_1 P_{\mathrm{H_2}} C_v$$

$$\mathrm{K}_2 = \frac{\mathrm{C}_{\mathrm{S\text{-}LA}}}{C_{LA} C_v} \quad \rightarrow \quad \mathrm{C}_{\mathrm{S\text{-}LA}} = \mathrm{K}_2 C_{LA} C_v$$

$$\mathrm{K}_4 = \frac{\mathrm{C}_{\mathrm{S.PD}}}{C_{\mathrm{S\text{-}PT}}} \quad \rightarrow \quad C_{\mathrm{S\text{-}PT}} = \mathrm{C}_{\mathrm{S.PD}} / K_4 = \frac{\mathrm{C}_{\mathrm{PG}} C_v}{\mathrm{K}_6 \mathrm{K}_1 K_4 P_{\mathrm{H_2}}}$$

$$K_6 = \frac{\mathrm{C}_{\mathrm{PG}} C_v}{C_{S\text{-}PG}} \quad \rightarrow \quad C_{S\text{-}PG} = \frac{\mathrm{C}_{\mathrm{PG}} C_v}{\mathrm{K}_6}$$

$$\mathrm{K}_5 = \frac{\mathrm{C}_{\mathrm{S.PG}} C_v}{C_{\mathrm{S\text{-}PD}} C_{S.H2}} \quad \rightarrow \quad \mathrm{C}_{\mathrm{S.PD}} = \frac{\mathrm{C}_{\mathrm{S.PG}} C_v}{C_{S.H2}} = \frac{\frac{\mathrm{C}_{\mathrm{PG}} C_v}{\mathrm{K}_6} C_v}{\mathrm{K}_1 P_{\mathrm{H_2}} C_v} = \frac{\mathrm{C}_{\mathrm{PG}} C_v}{\mathrm{K}_6 \mathrm{K}_1 P_{\mathrm{H_2}}}$$

$$\mathrm{R} = k_3 C_{S.H2} C_{LA}$$

$$C_T = C_v + \mathrm{C}_{\mathrm{S\text{-}H_2}} + \mathrm{C}_{\mathrm{S\text{-}LA}} + C_{S\text{-}PG} + C_{S\text{-}PT} + C_{S.PD} \qquad \mathrm{C_T} \text{ is total active site concentration}$$

$$= C_v + \mathrm{K}_1 P_{\mathrm{H_2}} C_v + \mathrm{K}_2 C_{LA} C_v + \frac{\mathrm{C}_{\mathrm{PG}} C_v}{\mathrm{K}_6} + \frac{\mathrm{C}_{\mathrm{PG}} C_v}{\mathrm{K}_6 \mathrm{K}_1 K_4 P_{\mathrm{H_2}}} + \frac{\mathrm{C}_{\mathrm{PG}} C_v}{\mathrm{K}_6 \mathrm{K}_1 P_{\mathrm{H_2}}}$$

$$C_v = \frac{C_T}{1 + \mathrm{K}_1 P_{\mathrm{H_2}} + \mathrm{K}_2 C_{LA} + \frac{\mathrm{C}_{\mathrm{PG}}}{\mathrm{K}_6} + \frac{\mathrm{C}_{\mathrm{PG}}}{\mathrm{K}_6 \mathrm{K}_1 K_4 P_{\mathrm{H_2}}} + \frac{\mathrm{C}_{\mathrm{PG}}}{\mathrm{K}_6 \mathrm{K}_1 P_{\mathrm{H_2}}}}$$

$$r = k_3 C_{S.H2} C_{S.LA} = \mathrm{K}_1 P_{\mathrm{H_2}} \mathrm{K}_2 C_{LA} \frac{{C_T}^2}{\left(1 + \mathrm{K}_1 P_{\mathrm{H_2}} + \mathrm{K}_2 C_{LA} + \frac{\mathrm{C}_{\mathrm{PG}}}{\mathrm{K}_6} + \frac{\mathrm{C}_{\mathrm{PG}}}{\mathrm{K}_6 \mathrm{K}_1 K_4 P_{\mathrm{H_2}}} + \frac{\mathrm{C}_{\mathrm{PG}}}{\mathrm{K}_6 \mathrm{K}_1 P_{\mathrm{H_2}}}\right)^2}$$

$$= \frac{a_0 C_{LA} P_{\mathrm{H_2}}}{\left(1 + a_1 P_{\mathrm{H_2}} + a_2 C_{LA} + a_3 \mathrm{C}_{\mathrm{PG}} + a_4 \frac{\mathrm{C}_{\mathrm{PG}}}{P_{\mathrm{H_2}}}\right)^2}$$

PG addition experiments (Section 6.1.4) showed the PG concentration only slightly affects the hydrogenation rate; therefore, the PG concentration term can be neglected for simplification (equal to very large K_6 or very low surface PG concentration). The simplified expression is:

$$R = a_0 C_{LA} P_{H_2} \Big/ \left(1 + a_1 P_{H_2} + a_2 C_{LA} + a_3 C_{PG} + a_4 \frac{C_{PG}}{P_{H_2}}\right)^2 = \frac{a_0 C_{LA} P_{H_2}}{\left(1 + a_1 P_{H_2} + a_2 C_{LA}\right)^2}$$

To fit the constants, rewrite the rate express as

$$1/\sqrt{R} = \frac{1}{\sqrt{a_0 C_{LA} P_{H_2}}} + \frac{a_1 \sqrt{P_{H_2}}}{\sqrt{a_0 C_{LA}}} + \frac{a_2 \sqrt{C_{LA}}}{\sqrt{a_0 P_{H_2}}}$$

5.2.8.2. Fitting the data of the reactions at 130°C

The data used for fitting the parameters are from Matrix 3 (see Chapter 3). We only use the data from low temperature reactions to fit the model because the reaction rates are low and mass transfer is negligible at these conditions and conversions. The catalyst loading is 1,2, or 3 gram and the pressure was 1000, 1500, or 2000psi. First, the conversion curve was fitted by third order polynomial and then the relation of rate and time was obtained by differentiating the polynomial. For each experiment, 12 points (30 minutes interval, 5 hours) were used. The total numbers of data points were 108. The fitted parameters are shown in Table 5-8 and the comparison of original data and model is given Figure 5-13.

Table 5-8. Regression results for 130°C in autoclave

a0	0.021	$R = \frac{0.021 C_{LA} P_{H_2}}{\left(1 + 0.0088 P_{H_2} + 10.3 C_{LA}\right)^2}$ P in psi and C_{LA} in mole/L
a1	0.0088	
a2	10.3	
Multiple R	0.85	

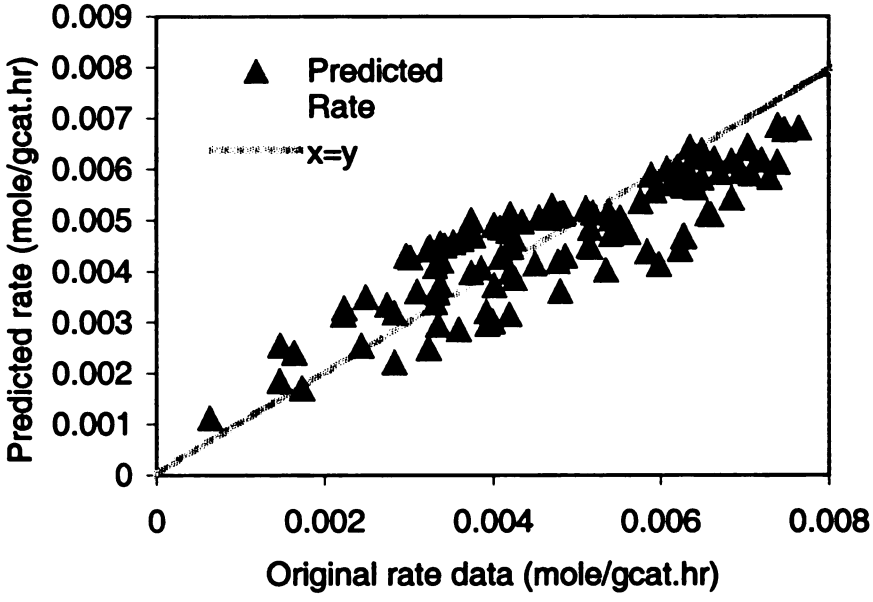

Figure 5-13. Comparison of model prediction (130°C)

In the point of view of mathematics, the regression result is not good, but this is the only model that gives all positive kinetic constants. Using only initial data to fit the model did not give any improvement in regression quality, which implies that no significant catalyst deactivation and leaching happen during the batch hydrogenation of lactic acid. Other possible models are dehydration control (reaction 4) and second hydrogen addition (reaction 5), but neither gives positive rate constants. Actually, modeling of this process only from the reaction data is very difficult and inaccurate because of the side reaction. The difficulty is that side reactions consume larger amounts of hydrogen than the main reaction. Two moles of hydrogen are needed for PG formation, but six moles will be consumed for methane formation for every mole of lactic acid. That means that 10% of lactic acid converted in the side reaction will use 30% of the hydrogen consumed. Therefore, the poor regression may come from side reactions and the first hydrogen addition (reaction 3) is most likely the rate-controlling step.

5

c

h

th

5.

pa

the

is

a r

me

hei

10

ope

bec

liqu

5.3. Continuous reactor (trickle bed)

In trickle bed reactor, the relative velocities of gas, liquid, and solid are very low compared to the stirred autoclave; therefore, mass transfer most likely controls the hydrogenation process. Experiments and literature correlation will be used to investigate the trickle bed kinetics.

5.3.1. Dynamic Liquid holdup

Liquid holdup (dynamic or free draining and static or residual) is a very important parameter in the trickle bed reactor. Static holdup is the fraction of liquid that remains in the catalyst pore after it has been completely wetted and drained. Dynamic liquid holdup is the fraction of liquid that is drained out after a sudden shut-off of liquid feeding and is a measurement of residence time in the trickle bed. The dynamic liquid holdup was measured in a trickle bed filled with 48 grams of CG6M Ru/carbon catalyst (61cm height) using HPLC water as liquid. Because the viscosity of water is 5% less than that of 10% lactic acid, the measured liquid holdup is a little smaller than that during actual operation. Figure 5-14 shows that the liquid holdups at 100 and 150°C are very close because the viscosity change with temperature is very slow. Liquid holdup increases with liquid flow at low flow rate, leveling out at higher liquid flow rate.

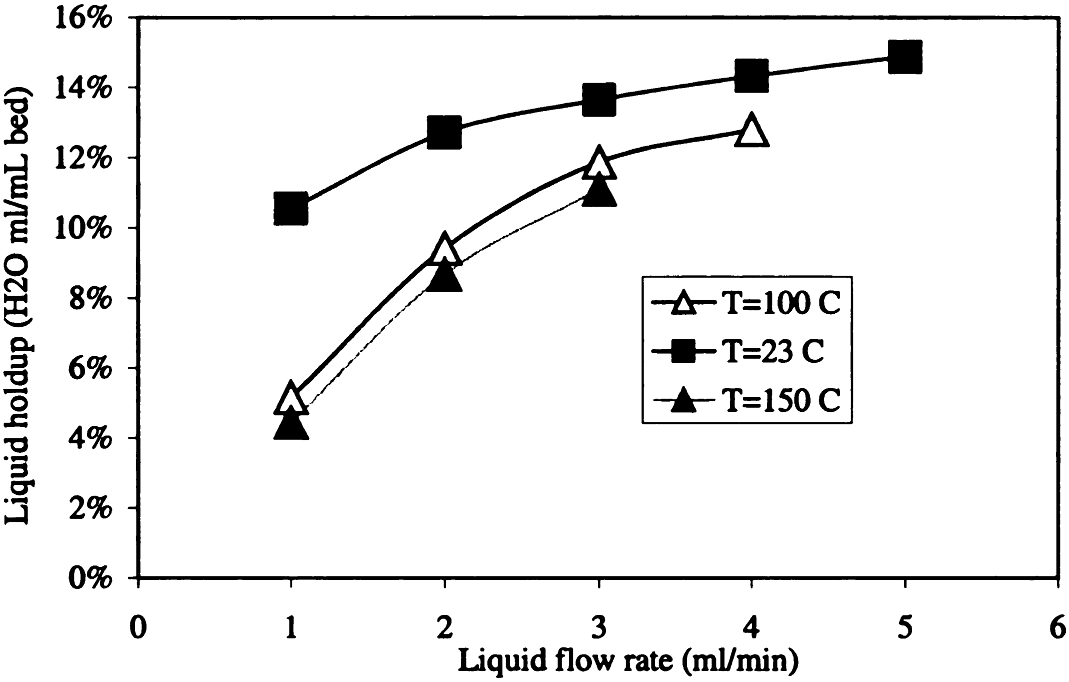

Figure 5-14. Liquid holdup at different liquid flow rates

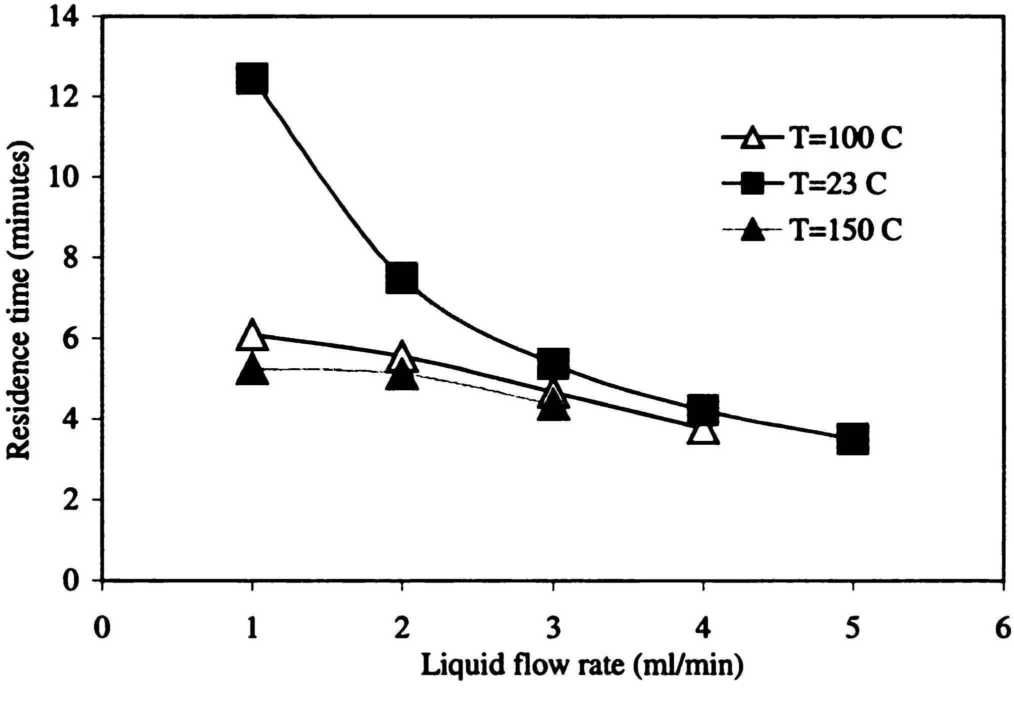

Figure 5-15. Liquid residence time in the trickle bed

The residence time, which is defined as the ratio of holdup volume to liquid flow rate, is given in Figure 5-15. Except for one point at 23°C, all other data form a slowly decreasing curve. That means that the residence times almost are independent of liquid flow rate and temperature. The average residence time is about 5 minutes when the liquid flow rate ranges from 1 to 3 ml/min.

5.3.2. Residence time distribution (species adsorption on catalyst)

The liquid residence time distribution is the reflection of trickle bed flow pattern and species adsorption on the catalyst. The experiment was done with a mixture of ethanol (3.3%), lactic acid (4.2%) and PG (2.3%) in water at room temperature (to ensure no reaction) with the reactor not pressurized. The liquid flow rate was fixed at 2 ml/min. According to the literature, gas flow rate does not affect the liquid flow very much, so it was fixed at 25 ml/min. After switching the liquid feed from pure water to the feed solution, the liquid composition in the outlet was monitored by HPLC. After the outlet concentration was fully stabilized after 2 hours, the desorption profile was recorded by switching back to pure water.

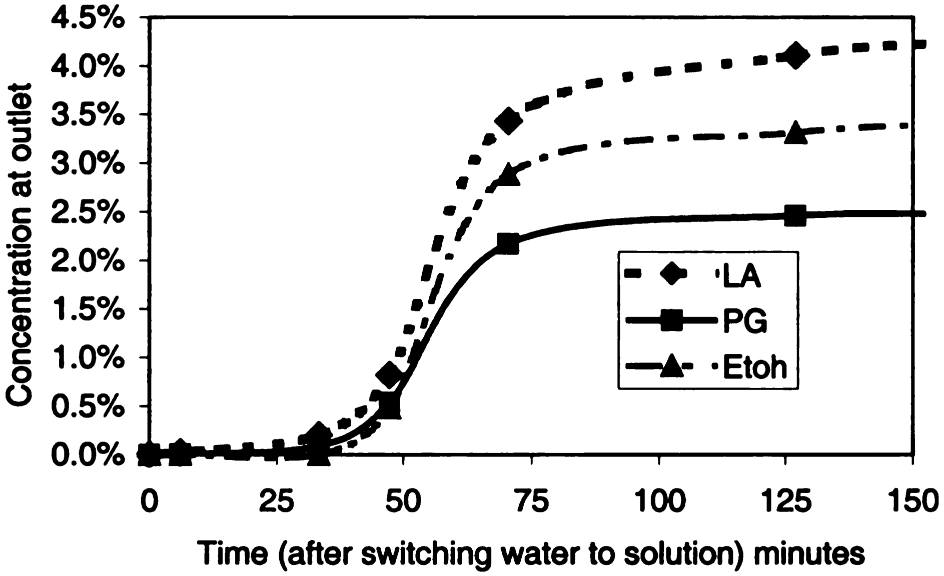

Figure 5-16. Outlet concentration change with time aftr switch to solution

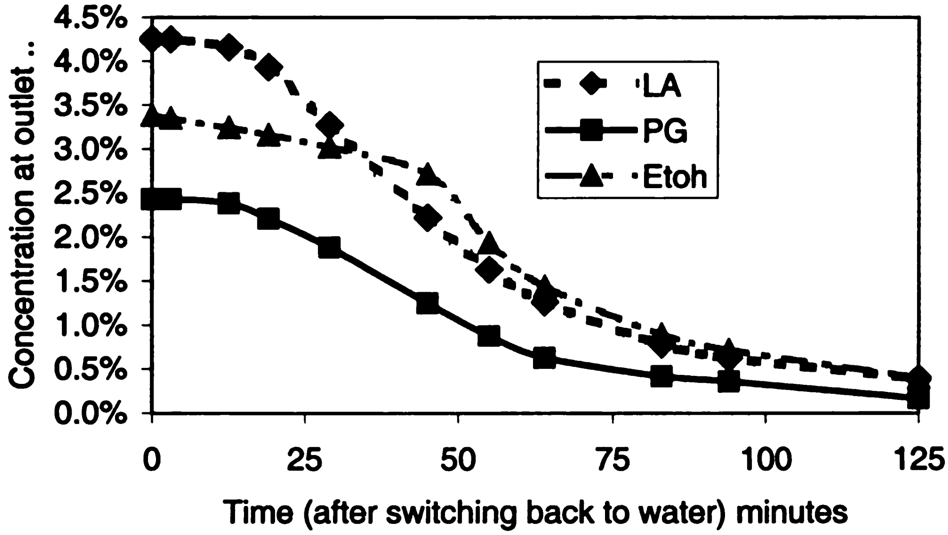

Figure 5-17. Outlet concentration change with time after switching back to water

Figure 5-16 and Figure 5-17 are the adsorption and desorption profiles. The "residence times" of all three species in this experiment are over 50 minutes, while actual residence time is only 5 minutes from Section 5.3.1. Therefore, the actual information shown here reflects species adsorption on the catalyst.

A simple calculation shows where these adsorbed species go (Table 5-9). First, the quantities of adsorbed species (collected from the water during desorption) are much larger than in the static holdup (calculated from the porosity of catalyst) and the dynamic holdup (measured from last section). If all adsorbed species adsorbed on ruthenium (10% dispersion), then each ruthenium atom would have to adsorb 53 lactic acid (or ethanol, or PG) molecules! Therefore, the carbon support is clearly the main adsorbent for the reactant and products. The desorption and adsorption curves measured are actually a characterization of the carbon support.

As seen from the adsorption and desorption curves, the liquid was well distributed, with no apparent liquid by-pass, and the carbon adsorbs all three species without apparent preference. Only the desorption of ethanol is slightly different from that of lactic acid and PG, as seen in desorption curves (Figure 5-17). The species balance of adsorption and desorption in Table 5-10 shows that water flow can strip off most adsorbed species.

Table 5-9. Residual species after switching to water

	Lactic acid	PG	Ethanol	Total
Species desorbed into water (g)	4.7	2.6	4.5	11.8
Maximum possible quantity in dynamic holdup* (g)	0.64	0.36	0.51	1.5
Maximum possible quantity in catalyst pore ** (g)	1.7	0.97	1.4	4.0
Excess adsorbed on catalyst (g)	2.3	1.3	2.7	6.3
Excess adsorbed on catalyst (mole)	0.026	0.017	0.058	0.1
Total Ruthenium (on surface)(mole)				0.0019
Species (mole)/Surface Ru (mole)				53

* Total dynamic holdup 15ml

** Total catalyst pore volume 40ml

Table 5-10. Balance of desorption and adsorption

	Lactic acid	PG	Ethanol	Total
Species adsorbed from solution (g)	5.4	2.9	4.4	12.7
Species desorbed into water (g)	4.8	2.6	4.5	11.9
Difference	0.6	0.3	-0.1	0.8

5.3.3. Reaction rate and pseudo first order constant in the trickle bed

To account for the effects of mass transfer, reaction rate has to be first calculated. For simple isothermal operation, a constant H_2 concentration in gas phase and constant overall effectiveness factor is assumed. The mass balance in control volume is:

$$\frac{dF_L C_{LA}}{dV_R} = -r_{obs}\rho$$

V_R is the bed volume, F_L is liquid feeding flow rate (ml/min). ρ is catalyst bulk density (g/ml). The observed reaction rate r_{obs} is defined as:

$r_{obs} = k^{'}C_{LA}$ $k^{'}$ is pseudo first order reaction constant.

$$\frac{dF_L}{dV_R} = \frac{dC_{LA}}{dV_R / F_L} = -k^{'}\rho C_{LA} \Rightarrow \frac{dC_{LA}}{C_{LA}} = -k^{'}\rho dV_R / F_L$$

After integration, we get the relation between conversion and "constant" $k^{'}$.

$$\ln\left(\frac{C_{LA}}{C^{0}_{LA}}\right) = k'\rho V_R/F_L \Rightarrow \ln(1-x) = -k'\rho V_R/F_L \Rightarrow k' = \frac{-F_L \ln(1-x)}{V_R \rho}$$

$$\rho = 0.42\ \mathrm{g/mL\ and}\ F_L = 2mL/\min \quad V_R = 118mL$$

Table 5-11 gives two sets of data from two catalysts. The hydrogen to lactic acid mole ratio is 4:1. Feed lactic acid concentration is 10 W%. The maximum rate constant is calculated to be 0.12, which come from the CG6M catalyst.

Table 5-11. Pseudo first order reaction constants in trickle bed

	F_L flow rate	P(psi)	Con%	k (ml/g_{cat}.min)	Rate(R (mole/kg.hr)
48gram CG6M catalyst (118ml)					
80°C	2.0	200	16%	0.0067	0.045
	2.0	400	22%	0.0096	0.064
	2.0	600	28%	0.013	0.08
	2.0	800	35%	0.017	0.11
	2.0	1000	42%	0.021	0.14
	2.0	1200	49%	0.026	0.17
100°C	2.0	200	51%	0.027	0.18
	2.0	400	66%	0.042	0.28
	2.0	600	80%	0.062	0.41
	2.0	800	88%	0.082	0.54
	2.0	1000	92%	0.097	0.65
	2.0	1200	95%	0.12	0.77
120°C	2.0	200	54%	0.030	0.20
	2.0	400	74%	0.052	0.35
	2.0	600	86%	0.076	0.50
	2.0	800	92%	0.097	0.65
	2.0	1000	95%	0.12	0.77
	2.0	1200	96%	0.12	0.83
30gram (71ml) CG5P catalyst					
100°C	0.5	1200	57%	0.054	0.36
	1	1200	54%	0.050	0.33
	2.0	1200	39%	0.032	0.21
	3.0	1200	28%	0.021	0.14

5.3.4. Mass transfer coefficients in the trickle bed

Hydrogen needs three steps (from gas to liquid, liquid to catalyst and diffusion in the catalyst pore) to reach the active sites. In this section, gas to liquid (G-L) and liquid to solid (L-S) mass transfer coefficients will be calculated by credible literature correlations and the intra-particle mass transfer will be investigated by both calculation and experiment.

For the coefficients of G-L and L-S mass transfer, which are weak function of gas flow rate (69), Goto & Smith (70) recommend two dimensionless correlations. The G-L mass transfer coefficient at 100°C vs. liquid flow rate is calculated in Figure 5-18.

$$\frac{K_L a}{D} = \alpha_L \left(\frac{G_L}{\mu}\right)^{n_L} \left(\frac{\mu}{\rho D}\right)^{1/2}$$

$K_L a$ Gas-liquid mass transfer coefficient (1/sec)

D Diffusivity (cm^2/sec)

G_L Liquid mass flow rate (g/cm^2.sec)

ρ Liquid density (g/ml)

μ Liquid viscosity (cp)

For catalyst CuO.ZuO (0.54mm), α_L=7.8 and n_L=0.39.

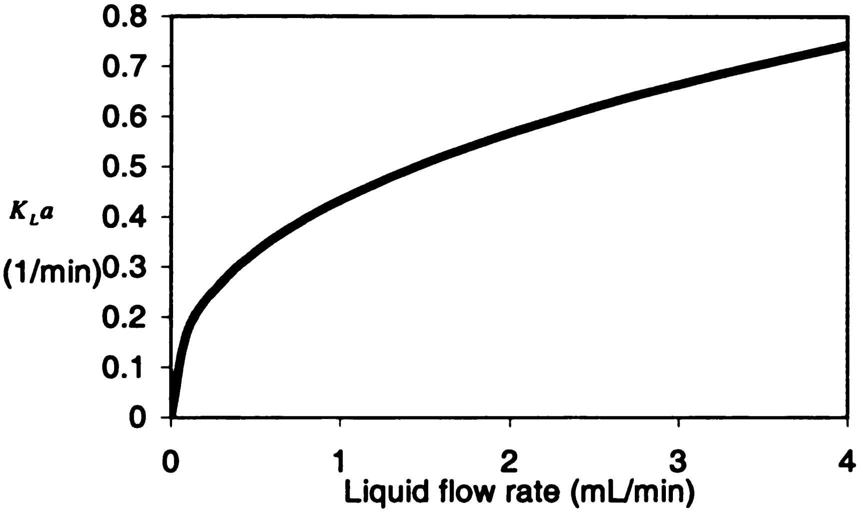

Figure 5-18. G-L mass transfer coefficient vs. flow rate

By comparing the maximum G-L mass transfer rate with average lactic acid consumption rate $^{(*)}r_{obs}$, we can estimate the importance of G-L mass transfer. To make the comparison possible, we need to know the liquid holdup h_d as measured in Section 5.3.1. The units of observed reaction rate are mol/kgcat.hr. The maximum mass transfer rate calculated from $k_L a C^*_{H_2}$ is in mole/hr.L, which needs to be transformed to the same units by using dynamic liquid holdup and catalyst bulk density.

$$R_{G\text{-}L} = k_L a C^*_{H_2} h_d / \rho \qquad \rho = 0.42\,\mathrm{g/cm^3}$$

The maximum H_2 concentration is its solubility. Ten typical reaction rates were picked from Table 5-11 and the comparison of G-L mass transfer rate with average lactic acid consumption rate is given in Table 5-12. For all ten runs, the maximum mass-transfer rate of hydrogen and average lactic acid consumption rate are of the same order of magnitude. The ratio of maximum hydrogen G-L mass transfer rate and maximum lactic acid consumption rate is less than two (the stoichiometry) for most of the trickle bed runs. Therefore, gas-liquid mass transfer of hydrogen limits the trickle bed reaction.

For H_2 L-S mass transfer, Goto & Smith correlation is

$$k_s a_P = 1.48 u_L \left(\frac{d_P G_L}{\mu}\right)^{-0.52} \left(\frac{\mu}{\rho D}\right)^{-2/3} 6(1-\varepsilon)/d_P \qquad \varepsilon = 0.41$$

$k_S a_P$ is liquid-solid mass transfer coefficient (1/sec) and dp is catalyst particle size. The mass transfer coefficient calculated for hydrogen and lactic acid at 100°C are shown in Figure 5-19. Like batch reactor, L-S mass transfer coefficient is an order of magnitude larger than that of the G-L mass transfer. The maximum mass transfer rate can be calculated as

$$R_{L\text{-}S} = k_s a C^*_{H_2} h_d / \rho$$

The maximum L-S mass-transfer rates are calculated and shown in Table 5-12. The maximum L-S mass-transfer rate is a magnitude larger than lactic acid consumption rate; therefore, resistance of Liquid-solid mass-transfer is almost negligible. However, the actually hydrogen concentration in liquid is much less than its solubility because the G-L mass transfer limitation, therefore, L-S may be part of H_2 mass transfer resistance at some conditions. For lactic acid L-S mass transfer, the lactic acid concentration is much larger than that of hydrogen, so L-S mass transfer will not a problem unless the conversion is very high.

[♣] Calculated from liquid flow rate, lactic acid conversion X and the total catalyst weight by $F_L C_{LA0} X / W_{cat}$

Table 5-12. Comparisons of H_2 G-L mass transfer and observed reaction rate

	F_L(ml/min)	k_La (1/min)	P(psi)	Con%	Observed rate* (mole/kg.hr)	$R_{G\text{-}L}$ (G-L) (mole/kg.hr)	$R_{L\text{-}S}$ (mole/kg.hr)
			48gram CG6M catalyst (118ml)				
100C	2.0	0.57	200	51%	0.18	0.07	3
	2.0	0.57	400	66%	0.28	0.14	6
	2.0	0.57	600	80%	0.41	0.21	10
	2.0	0.57	800	88%	0.54	0.28	13
	2.0	0.57	1000	92%	0.65	0.34	16
	2.0	0.57	1200	95%	0.77	0.41	19
			30gram (71ml) CG5P catalyst				
100C	0.5	0.33	1200	57%	0.36	0.24	10
	1	0.43	1200	54%	0.33	0.31	14
	2.0	0.57	1200	39%	0.21	0.41	19
	3.0	0.66	1200	28%	0.14	0.48	23

* Average lactic acid consumption rate over entire trickle bed reactor

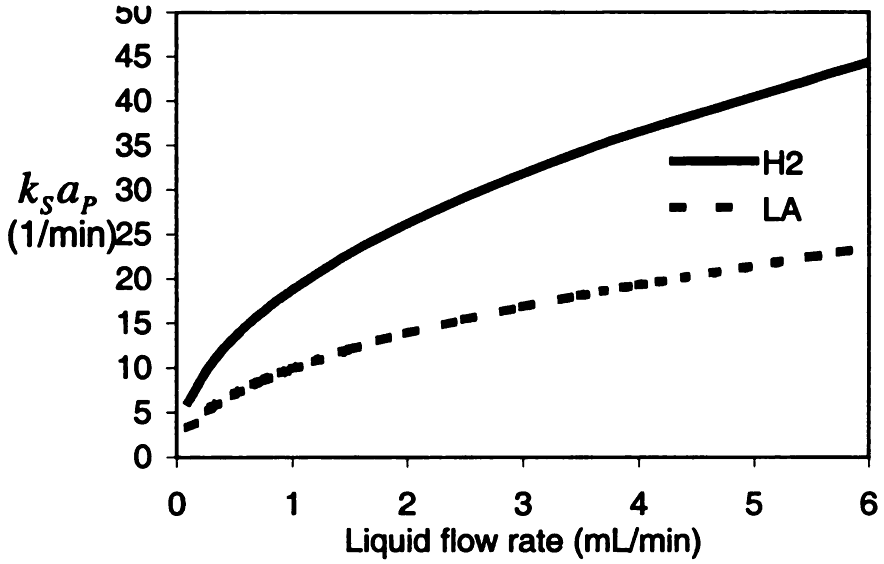

Figure 5-19. L-S mass transfer coefficient vs. liquid flow rate

5.3.5. Intra-particle mass transfer in the trickle bed

Intra-particle mass transfer in trickle bed reactor can be estimated by the observable modulus (Weisz –Prater criterion).

$$\eta\phi^2 = \frac{(-R_G)L^2}{\rho \cdot C_A D_e}$$ where (-R_G) is obsered reaction rate (mole/gcat.sec)

The diffusivity of hydrogen and lactic acid are calculated from correlation (Appendix-1) and catalyst true density is 0.8 g/ml as measured in incipient wetness. Maximum lactic acid consumption rate (0.77 mole/kg.hr) was taken from Table 5-12. The modulus for hydrogen and lactic acid vs. catalyst particle size (Figure 5-20) shows that hydrogen intra-particle is a control factor in trickle bed because the catalyst diameter we used is 0.05cm and $\eta\phi^2$ larger than 0.1.

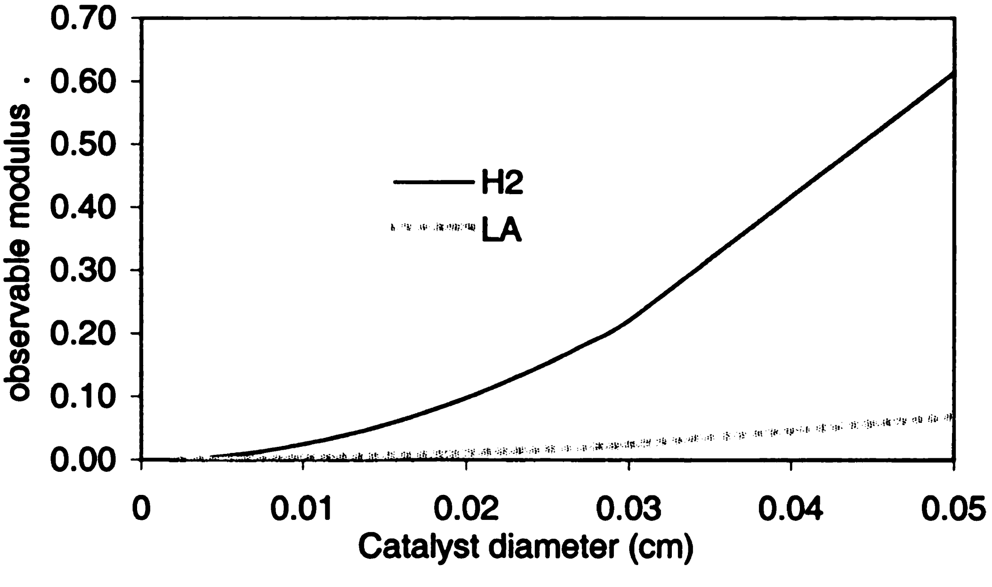

Figure 5-20. Observable modulus in trickle bed (100°C and 1200psi)

5.3.6. Trickle bed kinetics

The trickle bed experiments analyzed in this section are from the trickle bed reactor with 48-g (118-ml) CG6M catalyst. Liquid feed was fixed at 2 ml/min of 10% lactic acid, and H_2 to lactic acid molar ratio was fixed at 4:1. These reactions were conducted at three different temperatures and six different pressures.

5.3.6.1. Macro kinetics in trickle bed

In Section 5.3.3, the pressure effect was lumped into rate constant for simplification and comparison with mass transfer. In this section, reaction was assumed as first order with respect to both hydrogen pressure and lactic acid concentration. The rate expression used in Section 5.2.7.2 is not used here for the simplified case. From the mass (mole) balance of a differential volume across the reactor, one can relate the rate constant with outlet concentration by a differential equation. After integrating the differential equation, lactic acid conversion can be related to reaction hydrogen pressure.

$$F_L dC_{LA}\,(\text{disappearance}) = -R\rho_B dV_R\,(\text{reacted lactic acid})$$

$$R = k_v P_{H2} C_{LA} \qquad \text{R : mole/(g.cat)} \cdot \text{min}, F_L : \mathit{ml/}\text{min}, C_{LA} : \mathit{mole/mL}$$

$$F_L dC_{LA} = -k_v \rho_B P_{H2} C_{LA} dV_R$$

$$\ln\frac{C_{out}}{C_{in}} = -\frac{V_R}{F_L}\rho_B k_v P_{H2} \Rightarrow \ln(1-x) = -\frac{V_R}{F_L}\rho_B k_v P_{H2}$$

Plotting $-\ln(1-x)$ vs. P_{H2}, and forcing the line to pass through the origin (set intercept to zero), then the pseudo first order constant k_v in trickle bed can be obtained from the slope of the line. The calculations at three temperatures given in Table 5-13 show that the linear relationship is reasonable good. With k_v at three different temperatures, The Arrhenius plot (Figure 5-21) gives macro activation (slope = $-E_a/R$) energy of Ea=48kJ/mole. Therefore, it is not a chemical reaction controlled process. As a comparison, in batch reactor, the macro activation energy is 96kJ/mole, a typical number for chemical reaction. From here, we can preliminarily conclude that in the trickle bed, lactic acid hydrogenation is a mass transfer controlled process.

Table 5-13. Pseudo first order constant at different temperature

Temp(C)	P (psi)	Con %	$-\ln(C_{out}/C_{in})$	S1*	k_v (ml/psi.sec.gcat)
80	200	21.0	0.24	8.75E-04	2.43E-05
	400	33.5	0.41	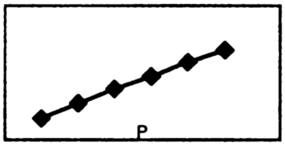	
	600	43.3	0.57		
	800	50.7	0.71		
	1000	58.0	0.87		
	1200	63.2	1.00		
100	200	52.0	0.73	2.49E-03	6.92E-05
	400	70.7	1.23	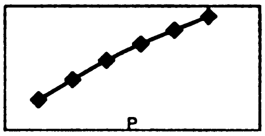	
	600	81.5	1.69		
	800	87.6	2.09		
	1000	91.1	2.42		
	1200	93.6	2.75		
120	200	77.4	1.49	4.65E-03	1.29E-04
	400	86.9	2.03	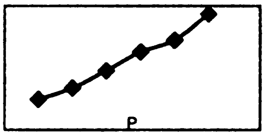	
	600	94.3	2.86		
	800	97.7	3.77		
	1000	98.7	4.34		
	1200	99.6	5.62		

* S1=$V_R \rho_B k_v / F_L$

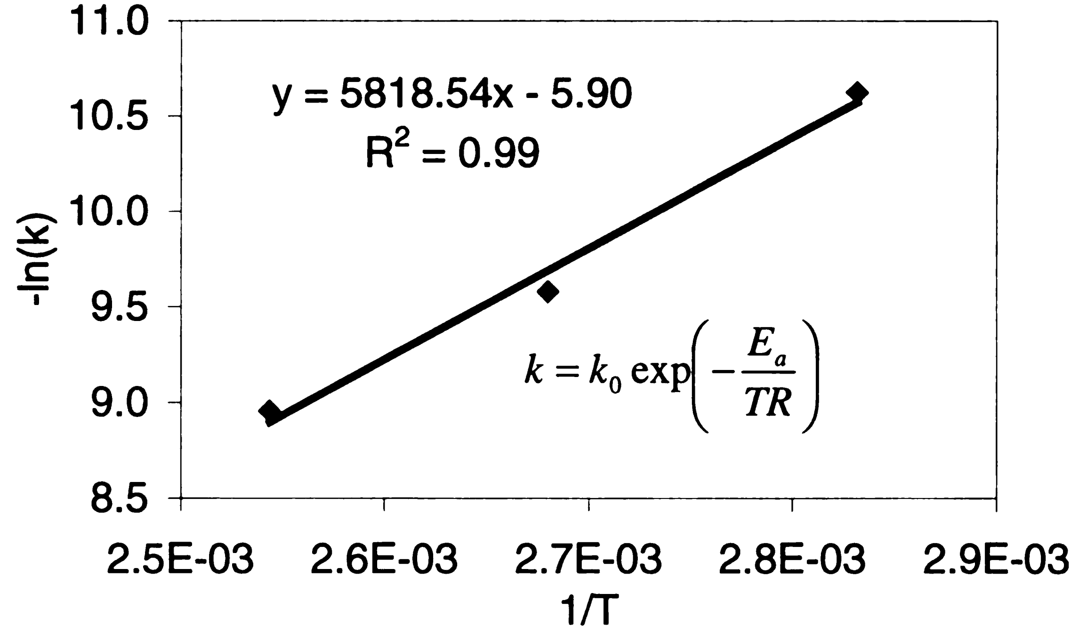

Figure 5-21. Arrhenius plot for pseudo first order reaction

5.3.6.2. The limiting reactant in liquid phase

The above sections show that gas-liquid mass transfer plays an important role, but it can not be the solely controlling factor because the G-L mass transfer limits the hydrogen liquid concentration, which also limits the L-S mass transfer rate. Therefor, L-S mass transfer may also limit the process at some conditions and locations in the trickle bed.

The limiting reactants in the liquid can be identified by calculating the D*C term (diffusivity and concentration) of hydrogen and lactic acid. From their ratio in the range of operating conditions of interest (Doraisewamy and Sharma (71)), we can see the limiting reactant.

$$\gamma = \frac{D_{LA}C_{LA}}{0.42D_{H2}C_{H2}} \qquad \mathrm{H}_2 + 0.42LA \longrightarrow PG + H_2O \text{ (♥)}$$

The ratio is indicative of the relative availability of the species at the reaction site. Thus, a value γ>>1 implies a gaseous reactant limitation, while γ<<1 indicates liquid reactant limitation. If the conversion of lactic acid is 99% (for 10% lactic acid feed), the concentration is 1.1 mole/L at inlet and 0.01 at outlet. The hydrogen concentration in liquid phase is unknown yet. However, from hydrogen solubility, we know the maximum possible concentration at 100°C is 0.23~1.4 ml/g (0.01~0.063mole/L)(p=200~1200psi).

$$\gamma > \frac{D_{LA}C_{LA}}{0.42D_{H2}C_{H2}} = \frac{5\times10^{-5} * (1.1 \sim 0.01)}{0.42 * 1.3\times10^{-4} * (0.23 \sim 1.3)/22.4} \geq 0.1 \sim 80$$

Therefore, in the inlet region of trickle bed reactor, hydrogen is the limiting reactant, but close to the outlet, the limiting reactant may switch to lactic acid.

[♥] The stoichiometry comes from considering main reaction and side reactions see Appendix-A

In conclusion, G-L, L-S mass transfer and chemical reaction will play a role at some conditions and at some positions of the trickle bed reactor. In the next section, we give a mathematical model for all these resistances and give concentration profiles along the trickle bed.

5.4. Trickle bed modeling

Modeling all details of the three-phase trickle bed flow and reaction is impossible at this stage, however for our reactor radial diffusion can be neglected. The trickle bed can thus be seen as a plug flow or one-dimensional reactor.

5.4.1. Model equations and boundary conditions

From a steady mass balance for hydrogen (A) and lactic acid (B) in liquid, we can relate bulk and catalyst surface concentrations of hydrogen and lactic acid (A_L, B_L, A_S, B_S) to the kinetic parameters and reaction conditions. In a control volume (a slice of cylinder), the mass balance for hydrogen (A) is:

$$\begin{pmatrix} \text{H}_2 \text{ from Axial Diffusion} \\ + \text{H}_2 \text{ from Liquid flow} \\ + \text{H}_2 \text{ diffuse from gas to liquid} \end{pmatrix} = \begin{pmatrix} \text{H}_2 \text{ transfer from bulk} \\ \text{liquid to catalyst surface} \end{pmatrix} = \begin{pmatrix} \text{reaction} \\ \text{consumption of H}_2 \end{pmatrix}$$

Dynamic liquid hold up (h_d) is used to relate catalyst volume to liquid phase volume. Reaction rate (lactic acid mole/gcat.min) is defined as $\text{R} = \text{k}_1 A_S^m B_S^n$. Intra-particle diffusion effects were combined into the reaction rate constant k_1. Therefore, it is actually not a real constant and will change with reaction conditions.

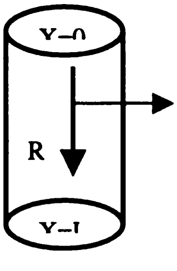

The mathematical expression for the hydrogen mass balance is

$$D_A \frac{d^2 A_L}{dx^2} - u_L \frac{dA_L}{dx} + K_L a(A^* - A_L) = k_s a_{PH}(A_L - A_S) = 2R\rho / h_d$$

The boundary conditions are

$$-D_A \frac{dA_L}{dx} = u_L(A_{Li} - A_L) \quad at\, x = 0 \qquad\qquad \frac{dA_L}{dx} = 0 \quad at \quad x = L$$

For B (lactic acid), the mass balance is similar to hydrogen, but no gas to liquid mass-transfer term.

$$\begin{pmatrix}\text{LA from Axial Diffusion}\\ \text{LA from Liquid flow}\end{pmatrix} = \begin{pmatrix}\text{LA diffuse from bulk liquid}\\ \text{to catalyst surface}\end{pmatrix} = \begin{pmatrix}\text{reaction}\\ \text{consumption of LA}\end{pmatrix}$$

$$D_B \frac{d^2 B_L}{dx^2} - u_L \frac{dB_L}{dx} = k_s a_{PLA}(B_L - B_S) = 2R\rho / h_d \quad \text{For B (lactic acid)}$$

The boundary conditions are

$$-D_B \frac{dB_L}{dx} = u_L(B_{Li} - B_L) \quad at\, x = 0 \qquad\qquad \frac{dB_L}{dx} = 0 \quad at \quad x = L$$

D_A , D_B Hydrogen and lactic acid diffusivity (m^2/s)

A_L , B_L Hydrogen and lactic acid concentration in bulk liquid (mole/m^3)

A_{Li}, B_{Li} Hydrogen and lactic acid concentration in liquid in inlet (at x=0) (mole/m^3)

A_S, B_S Surface concentration of hydrogen and lactic acid at catalyst surface (mole/m^3)

A^* Saturation concentration (hydrogen solubility) (mole/m^3)

K_L Overall gas to liquid mass transfer coefficient (m/s)

u_L Liquid flow velocity (m/s)

a, a_s Gas liquid interfacial area per unit volume of reactor (m2/m3)

m, n Reaction order respecting to A and B

ρ Catalyst bulk density (0.44 g/ml)

5.4.2. Analysis of the model

Table 5-14. Model equations and boundary conditions for trickle bed reactor

$D_A\frac{d^2A_L}{dx^2}-u_L\frac{dA_L}{dx}+K_La(A^*-A_L)=$ $k_sa_{PH}(A_L-A_S)=2\rho k_1A_S^mB_S^n/h_d$	$D_B\frac{d^2B_L}{dx^2}-u_L\frac{dB_L}{dx}=$ $k_sa_{PLA}(B_L-B_S)=\rho k_1A_S^mB_S^n/h_d$
$-D_A\frac{dA_L}{dx}=u_L(A_{Li}-A_L)\quad at\,x=0$ $\frac{dA_L}{dx}=0\quad at\quad x=L$	$-D_B\frac{dB_L}{dx}=u_L(B_{Li}-B_L)\quad at\,x=0$ $\frac{dB_L}{dx}=0\quad at\quad x=L$

The four-coupled equations (two differential and two algebraic) are summarized in Table 5-14. Bulk hydrogen concentration A_L, liquid lactic acid concentration B_L, and surface concentrations of hydrogen and lactic acid (A_S *and* B_S) change along reactor length (x-axis). This is a standard two-point boundary value problem in mathematics and is very difficult to solve, even with numerical methods.

Only if the surface reaction is pseudo zero order in either A or B and first order for the other, the two differential equations are de-coupled and can be solved analytically. For example, if lactic acid surface concentration is constant and the reaction is first order with respect to hydrogen, then reaction rate can be simplified as $R=k_1A_S(mole/gcat.\mathrm{min})$. The de-coupled equations (for hydrogen) can be simplified as

$$D_A\frac{d^2A_L}{dx^2}-u_L\frac{dA_L}{dx}+K_La(A^*-A_L)=k_sa_{PH}(A_L-A_S)=2\rho k_1A_S/h_d$$

$$-D_A\frac{dA_L}{dx}=u_L(A_{Li}-A_L)\quad at\,x=0\qquad \frac{dA_L}{dx}=0\quad at\quad x=L$$

With introduction of dimensionless variables,

$z=\frac{x}{L}$ Dimensionless distance

$C_L = \frac{A_L}{A^*}$ Dimensionless concentration

$C_S = \frac{A_S}{A^*}$ Dimensionless surface concentration

$C_U = \frac{A_U}{A^*}$ Dimensionless inlet concentration

$\alpha_{GL} = \frac{K_L a_B L}{u_L}$ Dimensionless gas –liquid mass transfer coefficient

$\alpha_{LS} = \frac{k_S a_P L}{u_L}$ Dimensionless liquid solid mass transfer coefficient

$\alpha_R = \frac{\rho k_1 L}{u_L h_d}$ Dimensionless reaction rate constant

$Pe_A = \frac{u_L L}{D_A}$, $Pe_B = \frac{u_L L}{D_B}$ Dimensionless liquid phase peclet number for H_2 and LA

The dimensionless form is

$$\frac{1}{Pe_A}\frac{d^2C_L}{dz^2} - \frac{dC_L}{dz} + \alpha_{GL}(1 - C_L) = \alpha_{LS}(C_L - C_S) = 2\alpha_r C_S$$

$$\frac{1}{Pe_A}\frac{dC_L}{dz} = C_L - C_U \quad at\ z = 0 \qquad \frac{dC_L}{dz} = 0 \quad at \quad z = 1$$

The surface concentration Cs from the algebraic equation is found

$$\alpha_{LS}(C_L - C_S) = 2\alpha_r C_S \Rightarrow C_S = \frac{\alpha_{LS} C_L}{\alpha_{LS} + 2\alpha_r} = \beta_S C_L$$

Then the differential equation is simplified as

$$\frac{1}{Pe_A}\frac{d^2C_L}{dz^2} - \frac{dC_L}{dz} - (\alpha_{GL} + \beta_S)C_L = -\alpha_{GL}$$

$$\frac{dC_L}{dz} = 0\ at\ z = 1, \frac{dC_L}{dz} = Pe(C_L - C_U)$$

With given numerical values of $\alpha_{GL}, \beta_S, Pe\ and\ C_U$, this equation can be solved in Mathematica. For example when $\alpha_{GL} = 1, \beta_S = 1, Pe_A = 2\ and\ C_U = 1$, the solution is

$$C_L = \frac{1}{2}\left(1 + \frac{2(3+\sqrt{5})\exp(2\sqrt{5} + (1-\sqrt{5})z)}{2 - 2\sqrt{5} + 4(2+\sqrt{5})\exp(2\sqrt{5})} + \frac{(\sqrt{5}-1)\exp(1+\sqrt{5})z)}{\sqrt{5} - 3 + (3+\sqrt{5})\exp(2\sqrt{5})}\right)$$

If $Pe_A -> \infty$ or neglecting the diffusion term, then it become a plug flow, the differential equation is simplified as:

$$\frac{dC_L}{dz} + (\alpha_{GL} + \beta_S)C_L = \alpha_{GL} \quad \text{with at } z = 0, C_L = C_U),$$

The analytical solution is

$$C_L = \frac{\exp(-z(\alpha_{gL}+\beta_{Ls}))(C_{Li}-1+\exp(z(\alpha_{gL}+\beta_{Ls}))\alpha_{gL}+C_{Li}\beta_{Ls}}{\alpha_{gL}+\beta_{Ls}}$$

For $Pe_A = 200$, $Pe_A = 0.01$ and $Pe_A = 1$, the hydrogen concentration profile is shown in Figure 5-22, which shows that it is almost a plug flow at $Pe_A = 200$. In our trickle bed reactor, $Pe_A = \frac{u_L L}{D_A} = \frac{0.02cm/s \times 61cm}{1.3\times10^{-3}cm^2/s} = 9384$ for hydrogen at 100°C; therefore our system is almost a true plug flow. In the same way, we can verify this is true for lactic acid (lactic acid diffusivity is smaller than that of hydrogen). In the following treatment, axial dispersion (diffusion) terms will be neglected.

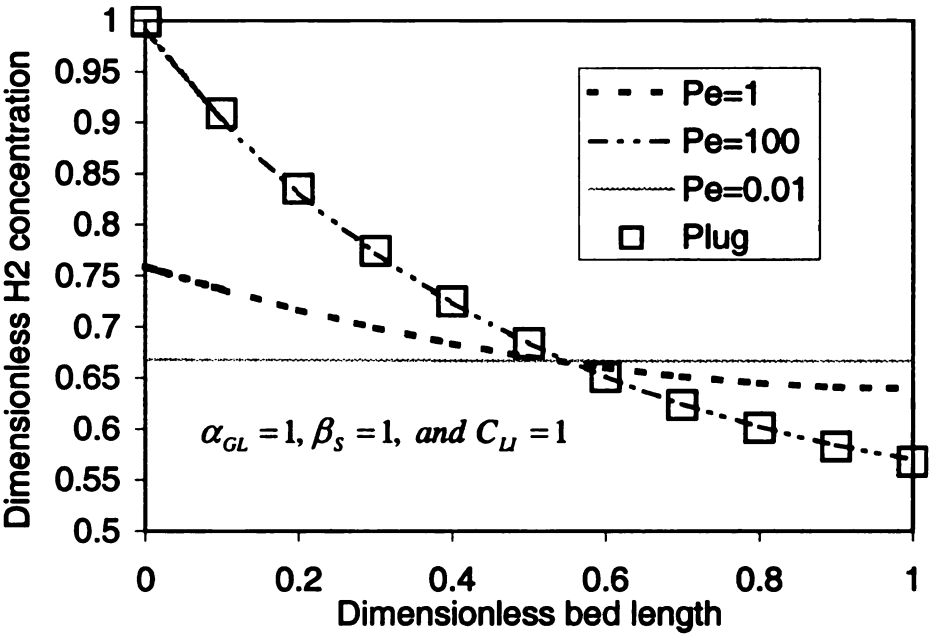

Figure 5-22. H_2 in bulk liquid with constant liquid reactant concentration

5.4.3. Modeling of trickle bed

After neglecting diffusion terms, the reaction order for both hydrogen and lactic acid surface concentrations was set to one. This is the only form we can solve at this stage, and then the trickle bed system will be simplified as the following.

$$\boxed{\begin{aligned}&-u_L\frac{dA}{dx}+K_La(A^{*}-A)=k_Sa_{PH}(A-A_S)=2k_1\rho A_SB_S/h_d\\&A=A_{LI}\quad at\,x=0\\&-u_L\frac{dB}{dx}=k_Sa_{PLA}(B-B_S)=k_1\rho A_SB_S/h_d\\&B=B_{LI}\quad at\,x=0\end{aligned}}$$

A_s and B_s were obtained by solving the algebraic equation in the term of A_L and B_L in Mathematica (neglecting the negative roots).

Then A_s and B_s were plugged into the two differential equations, which were then solved in Mathematica.

5.4.4. Model parameters

The parameters needed for this model are listed in Table 5-15. G-L and L-S coefficients were calculated from correlation as listed in Table 5-16.

Table 5-15. Model parameters at 100°C

Symbol	Name	Unit	Source	Value
u_L	Superficial liquid flow rate	Cm/min	Calculation	1.03
K_La	Gas-liquid mass transfer (H2)	1/min	Correlation	0.57
K_sa_{PH}	Liquid - solid mass transfer (H2)	1/min	Correlation	9.0
K_sa_{PLA}	Liquid - solid mass transfer (LA)	1/min	Correlation	4.8
B_{LI}	LA concentration in inlet	Mole/ml	Measurement	0.0011
A_{LI}	H2 concentration in inlet	Mole/ml	Saturation	Solubility
k_1	Surface reaction constant	L^2/mole.gcat.sec	The unknown	
ρ	Catalyst bulk density	g/ml	Measurement	0.44
h_d	Dynamics holdup	ML/ml	Measurement	0.1

Table 5-16. L-S mass transfer coefficients for hydrogen and lactic acid

$K_s a_{pH}$ (1/sec) for hydrogen			
FL(ml/min)	T=80 (KS-2)	T=100 (KS-2)	T=120 (KS-2)
1	4.2	6	6.6
2	7.2	9	10.2
3	9	12	13.2
4	10.8	14.4	16.2
$K_s a_{pLA}$ (1/sec) (lactic acid)			
	T=80 (KS-2)	T=100 (KS-2)	T=120 (KS-2)
1	2.9	3.5	3.7
2	4	4.8	5.2
3	4.9	5.9	6.3
4	5.5	6.8	7.2

Table 5-17. Simulation results for k_1

	P(psi)	Conversion	A* mole/ml	k_1	$K_L a$	$k_S a$ (LA)	$k_S a$ (H_2)
100°C	200	52.0%	1.0E-05	N/A	0.57	9	4.8
	400	70.7%	2.0E-05	171	0.57	9	4.8
	600	81.5%	3.0E-05	57	0.57	9	4.8
	800	87.6%	4.0E-05	39	0.57	9	4.8
	1000	91.1%	5.0E-05	31	0.57	9	4.8
	1200	93.6%	5.9E-05	25.5	0.57	9	4.8

5.4.5. Simulation results at 100°C

The principle of this simulation is to match lactic acid conversion by choosing a suitable k_1. The results are shown in Table 5-17, which shows that k_1 increases with pressure decreasing. At p=200psi, the maximum conversion is 21% (set $k_1=\infty$), that is the maximum mass transfer rate and so this model fails at this condition. The bulk and surface concentration profiles are shown in Figure 5-23.

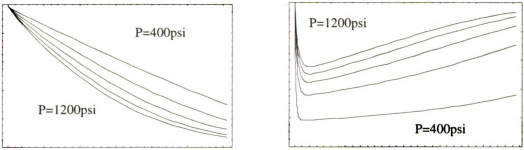

C(surface LA)/Bin~ Reactor length C(Bulk H2)/A*~Reactor length

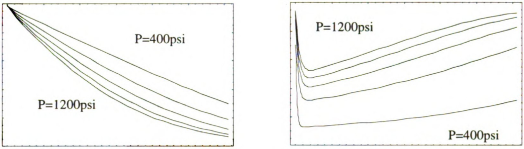

Reactor length Reactor length

Figure 5-23. Simulation results at 100°C and 400~1200psi

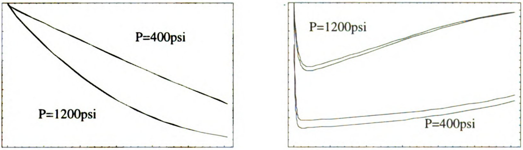

C_{LA}/Bin ~Reactor length C_{H2}/Bin~reactor length

Figure 5-24. Comparison of bulk liquid and surface concentration

With only one adjustable parameter, all concentration profiles along the trickle bed can be calculated. The results are consistent with the kinetic analysis. Figure 5-24 shows that lactic acid bulk concentration and surface concentration are almost identical (at P=1200 and P=400psi). However, for hydrogen the catalyst surface concentration is always lower than bulk concentration, which indicates the L-S mass transfer also limits the process.

The decrease in k_1 with increasing reaction pressure can be explained by the partially wetted catalyst. At low hydrogen pressure, G-L mass transfer is very slow, and most hydrogen directly comes from gas phase and the model does not include this part. At high pressure, the main path for hydrogen mass transfer is gas-liquid, which is what this model is based on. Therefore, to match the conversion, k_1 has to become larger and larger to deplete the bulk hydrogen to reach high mass transfer rates with pressure decreases. As in all trickle bed modeling, the partially wetted catalyst is always a problem.

5.5. Summary

Hydrogen solubility, a very important parameter in kinetics investigation, is measured at our reaction conditions. The comparison with literature shows our measurement is very reliable. The investigation of residence time distribution in the trickle bed shows that the carbon support strongly adsorbs both reactant and product, which makes the hydrogenation process even more complicated. Trickle bed dynamic liquid holdup is another very important parameter and is a bridge between liquid volume and catalyst volume in trickle bed modeling. Most trickle bed modeling in literature has missed this issue.

The calculation with creditable literature correlations and experiments shows that G-L, L-S and intra-particle mass transfer can be neglected in the batch reactor at our reaction conditions. The intrinsic kinetics is analyzed and the activation energy is 96kJ/mole. The initial reaction rate for 10% lactic acid hydrogen with Ru/C powder catalyst is well represented by:

$$R_{initial} = 1.95\times10^{10}\exp\left(\frac{-96000}{RT}\right)w^{0.66}P_{H_2}^{0.3}$$

At 130°C, an H-W model was derived and the parameter fitting is reasonably good considering the existence of side reactions. This is the only H-W that gives all positive constants. Therefore, the first hydrogen addition to lactic acid is most likely the rate controlling step.

$$R = \frac{0.021C_{LA}P_{\mathrm{H}_2}}{\left(1+0.0088P_{\mathrm{H}_2}+10.3C_{LA}\right)^2}$$

Calculations and experiments have verified that G-L mass transfer is the major resistance in trickle bed reactor. Macro kinetic analysis shows that the activation energy is only 48kJ/mole in trickle bed, which indicates that mass-transfer is the rate controlling step. That further confirms the mass transfer calculations.

Finally, a one-dimensional trickle bed model is derived. This model consists of two differential and two algebraic equations. In this model, dynamic liquid holdup was used to relate catalyst and liquid volume. Mathematically, it is a typical two-point boundary value problem and is very difficult to solve. With reasonable simplification (surface reaction is first order with respect to hydrogen and lactic acid), the model was solved in Mathematica. Bulk hydrogen and lactic acid, surface hydrogen and lactic acid concentration profiles are plotted.

Chapter 6. Mechanistic insight

The focus of this chapter is to investigate the mechanism of lactic acid hydrogenation, which is helpful to further enhance the performance of the lactic acid to PG. By combining product distribution under data from different reaction conditions with different catalysts, specially designed control reactions (propionic acid, propylene glycol, ethanol and methanol hydrogenation), and the knowledge of organic chemistry, it should be possible to propose reasonable pathways for propylene glycol formation and side reactions.

6.1. Control experiments for mechanism elucidation

Several hydrogenation reactions of substrates other than lactic were studied to probe the possible reaction pathways. These substrates chosen represent possible intermediates or by-products and were subjected to the conditions as for lactic acid hydrogenation.

6.1.1. PG hydrogenation (M47, M48)

Propylene glycol (PG) is the desired product. PG hydrogenation is used to investigate the possible deep hydrogenation or further reaction of PG at reaction conditions. Two runs were conducted, one at the standard condition (150°C and 2000psi) and another at higher temperature (170°C). The first one was used to identify the source of gas by-products and the second one was for the liquid by-products identification. In run M48 (1 gram Ru/C new PMC at 150°C and 2000psi), a 10% propylene glycol water solution was hydrogenated for 6.2 hours. 6.4% of the PG was converted and no detectable liquid products were detected. The final gas phase analysis (Figure 6-1) shows methane and very limited amount of ethane are the products from PG hydrogenation. For lactic acid hydrogenation at the same conditions and catalyst loading (See Chapter 3, carbon balance), 4.5% of the lactic acid was converted to gas and 40% was converted to PG after 4.7 hours hydrogenation. The results from lactic acid and PG hydrogenation at the same conditions show PG deep hydrogenation is the major side reaction at standard reaction conditions because about the same quality of gas is formed . As seen in Figure 6-1, the ethane peaks are very small compared with the methane peaks at both temperatures[♦]. Therefore, PG deep hydrogenation could not be the major source of ethane formation.

[♦] The response factors of methane, ethane, propane, CO and CO_2 are in the same magnitude

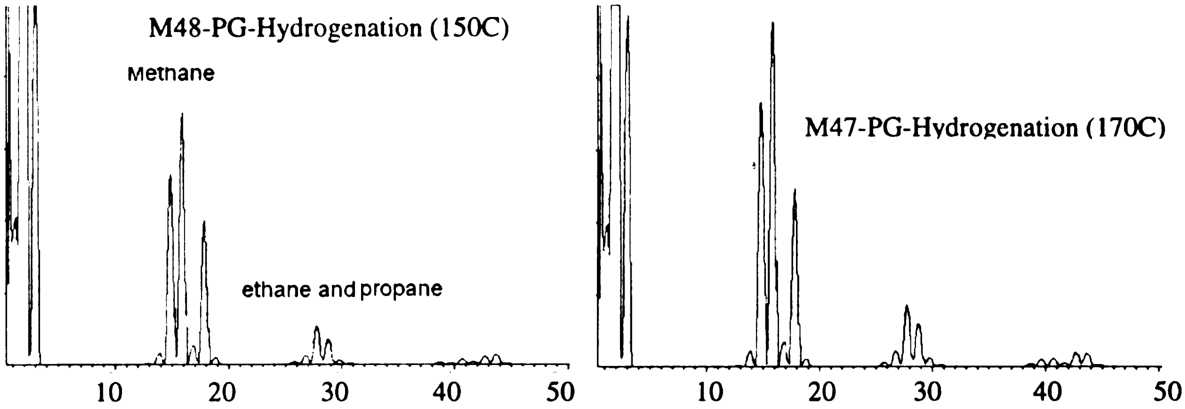

Figure 6-1. Gas products from propylene glycol hydrogenation at 150 and 170°C

Table 6-1. Product distribution for PG hydrogenation at 170°C

		Liquid (mole)			Gas (mole)		Sum
		PG	Ethanol	2-propanol	CH_4	C_2H_6	
Before		0.066	0	0	0	0	0.066
After	Mole	0.055	0.0015	0.001	0.007	0.0014	0.065
	% of initial PG	83.3	2.3	1.5	10.6	2.1	99.85

In experiment M47, increasing the temperature to 170°C and fixing the other reaction conditions as in M48, shows that 17% PG was consumed after 6.2 hours. PG was converted to methane, ethane, 2-propanol and ethanol. The gas and liquid analyses were summarized in Table 6-1; as in run M48, the major by-product gas was methane. The liquid analysis (Figure 6-2) shows that only 2-propanol and ethanol comes from PG hydrogenolysis. These two runs also imply that the majority of ethane, 1-propanol, methanol and propane must directly arise from the lactic acid hydrogenation and not from PG deep reactions, or that they are quickly further converted to other by-products if they are formed.

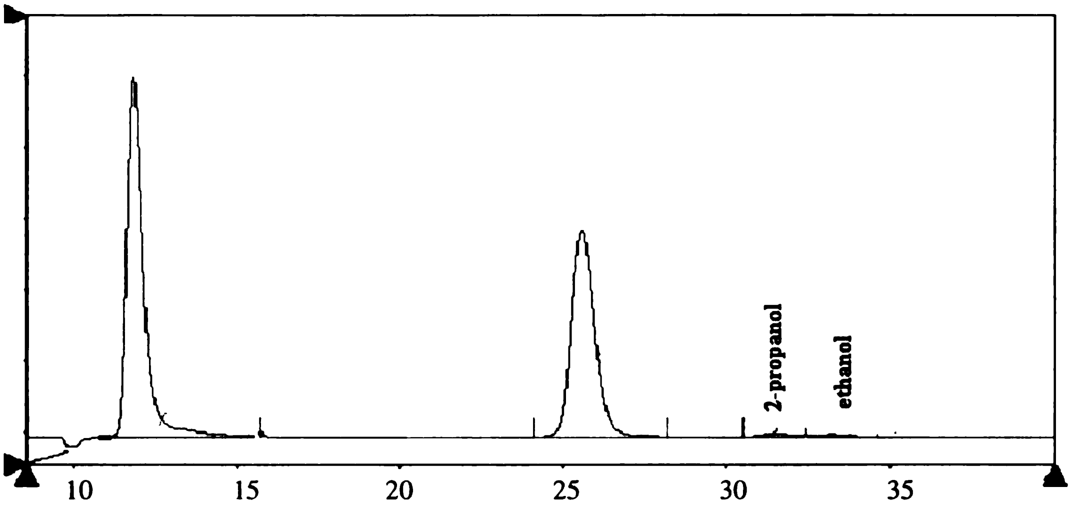

Figure 6-2. Liquid products from PG hydrogenation at 170°C

6.1.2. Ethanol and methanol hydrogenation on Ru/C catalyst (M49)

Because ethanol and methanol were found in high temperature lactic acid hydrogenation, it is reasonable to assume that they are intermediate. The idea is thus to investigate their survivability at standard reaction conditions. In this experiment, a mixture of 6.4% ethanol and 5.5% methanol in water solution was hydrogenated under the same conditions as standard lactic acid hydrogenation (1% PMC Ru/C catalysts, 150°C and 2000psi). After 4 hours of reaction, 24% methanol and 28% ethanol were converted (Figure 6-3) and no liquid by-products were found. In gas products, ethane is barely detectable and methane is almost the only product from hydrogenation of methanol and ethanol (Figure 6-4).

This experiment shows that ethanol and methanol can be converted to methane and the reaction rate is much faster than that of PG at the same conditions. Therefore, ethanol, methanol and PG (from last section) are possible intermediates for methane formation. This run also implies that ethane does not come from ethanol hydrogenation.

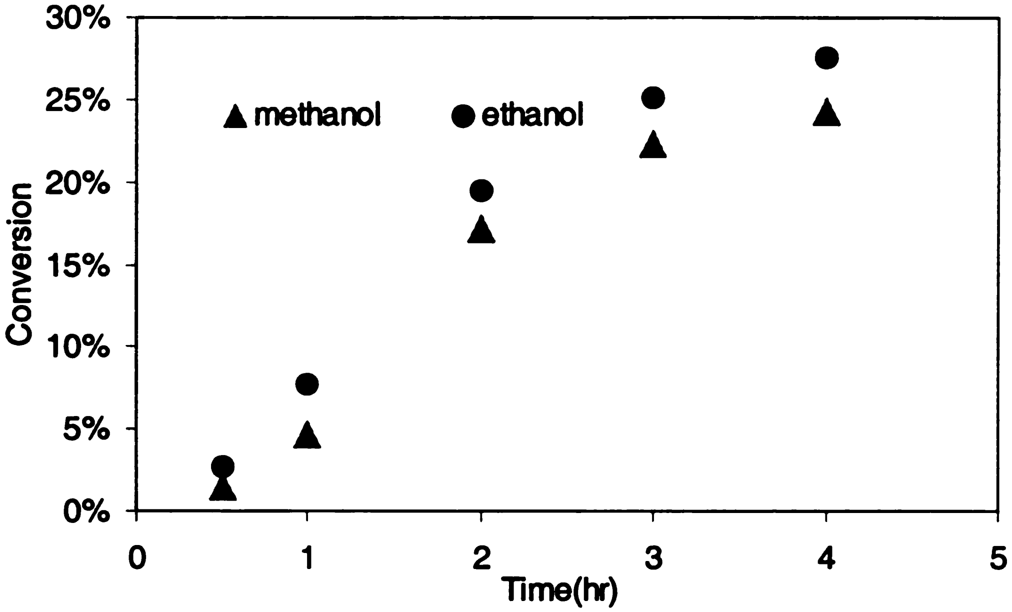

Figure 6-3. Conversion of methanol and ethanol hydrogenation at 150°C

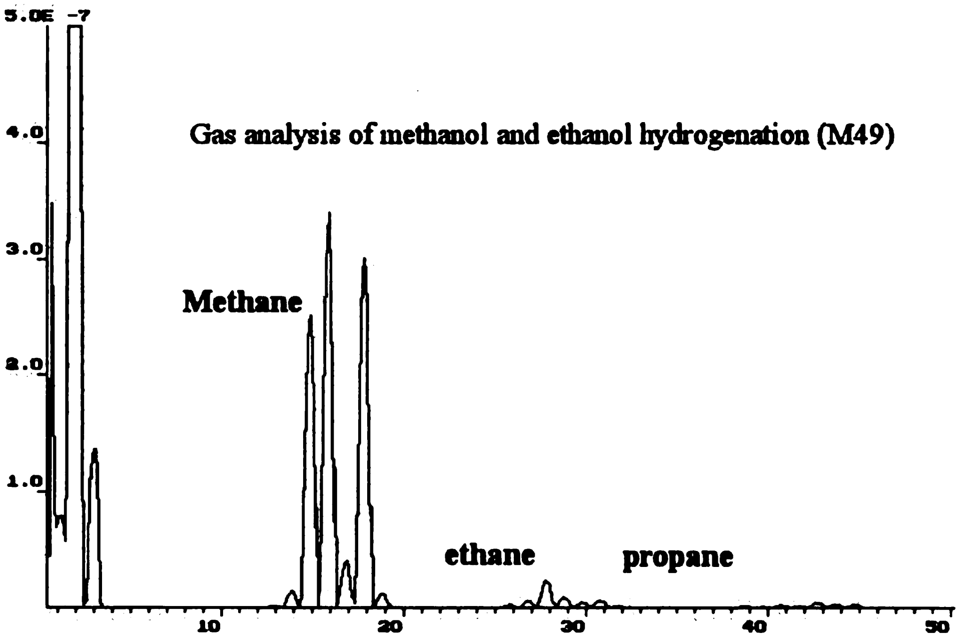

Figure 6-4. Gas phase analysis of methanol and ethanol hydrogenation at 150°C

6.1.3. Propanoic acid hydrogenation

Propanoic acid was not found in the liquid by-products of lactic acid hydrogenation. The purpose of studying propanoic acid was simply to compare its reactivity with that of lactic acid. A 10% propanoic acid solution in water was hydrogenated with 2 gram Ru/C PMC (3310, the third batch catalyst from PMC) at 2000psi and 150~320°C in the Parr autoclave. At the standard reaction temperature (150°C), propanoic acid hydrogenation is much slower than that of lactic acid (Figure 6-5). For propanoic acid hydrogenation, no detectable 1-propanol was found in the liquid products after 6 hours at 150~320°C. All reacted propanoic acid was converted to methane and ethane. Only a trace amount of propane was formed.

It needs to be pointed out here that propanoic acid hydrogenation needs much higher temperature (almost 300°C) to achieve the same rate as lactic acid hydrogenation and the primary ending product is gases (methane and ethane) rather than 1-propanol. From this experiment, we can conclude that propanoic acid is not an intermediate product in the lactic acid hydrogenation because of its high stability in the lactic acid hydrogenation environment.

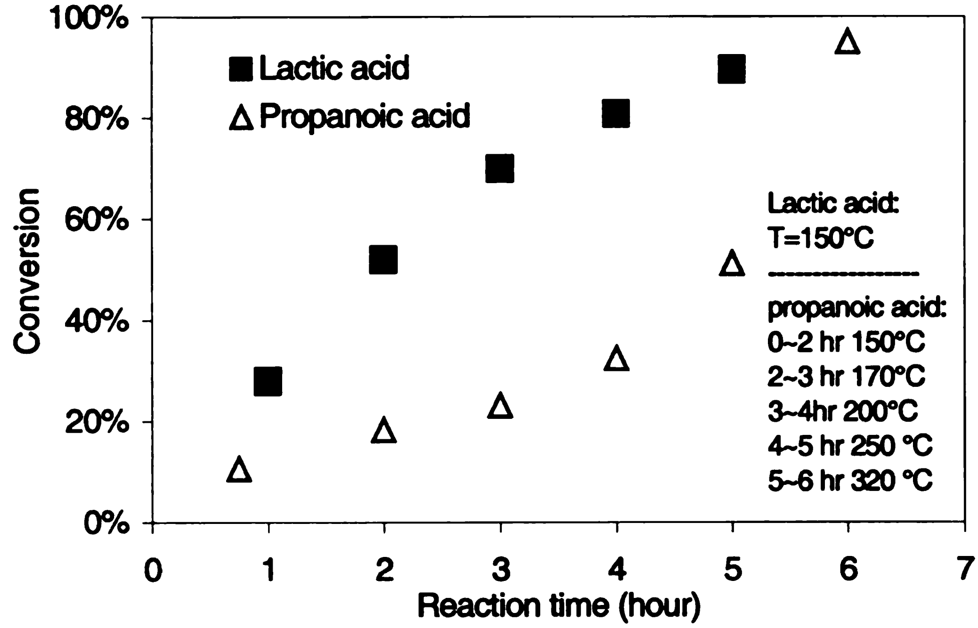

Figure 6-5. Comparison of lactic acid and propanoic acid hydrogenation

6.1.4. Adding PG in lactic acid hydrogenation

Four experiments were designed to investigate the product (PG) effect on lactic acid hydrogenation. The initial solutions were 10% lactic acid and 0~20% PG. All of these reactions were conducted at 150°C and 1500psi with 2-gram Ru/C new PMC catalyst. The conversion profiles are shown in Figure 6-6. These results show that with the high concentration of PG, lactic acid still can be converted in a rate close to pure lactic acid hydrogenation. Therefore, the lactic acid hydrogenation is not reversible, in agreement with thermodynamic calculation. It is also clear that lactic acid and PG are not competing for the same reactive sites. The slight decrease in reaction rates with increasing PG concentration may come from the slower desorption of the PG product from the catalyst surface because of the high PG concentration in solution.

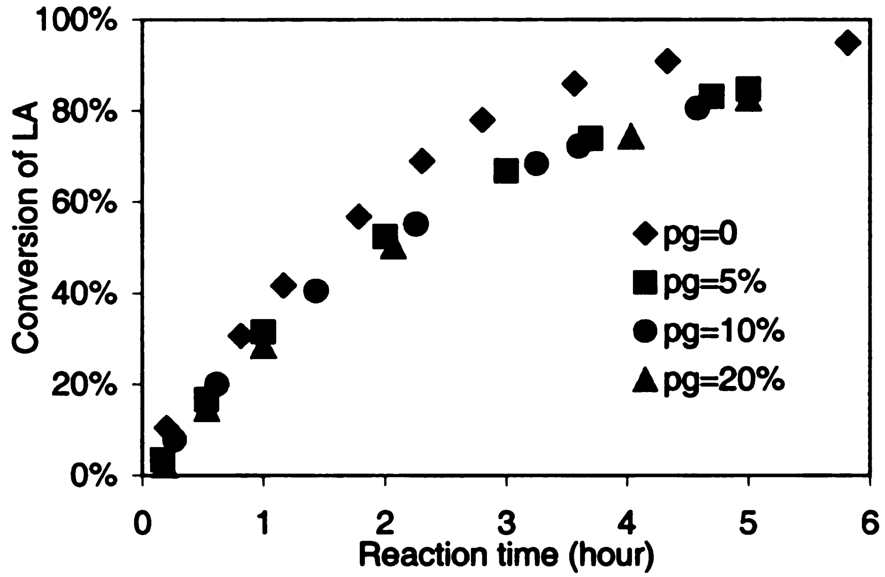

Figure 6-6. Conversion profiles for adding different PG concentration

Figure 6-7 shows the conversion and "macro" selectivity (♣) after 4 hours hydrogenation. Because of the PG hydrogenolysis, the "macro" selectivity became worse and worse as the PG concentration increased. One explanation is that PG does not disturb lactic acid hydrogenation and the PG deep reactions lower the macro selectivity. From these runs, it is reasonable to assume that two kinds of active sites exist on the catalyst. One is good for lactic acid and another is good for PG deep hydrogenation.

[♣] In here macro selectivity is defined as the molar ratio of PG increased to converted lactic acid. So, this selectivity is not the real selectivity of lactic acid hydrogenation because of PG deep hydrogenation.

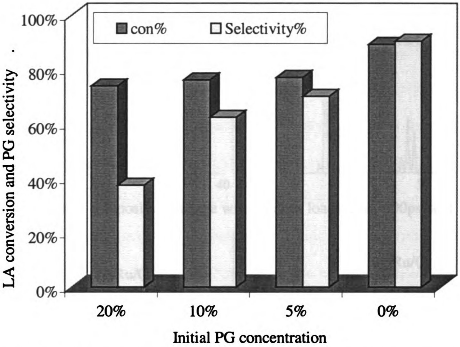

Figure 6-7. PG addition effect lactic acid hydrogenation at 150°C and 1500psi

6.2. Gas by-product information at different reaction conditions

The change of product gas composition with reaction conditions may give some clues about the side reactions. Catalyst loading, pressure and temperature effects will be shown in this section. Figure 6-8 to Figure 6-10 are gas analyses for Matrices 2 and 3 (see Chapter 3). As shown in Chapter 2, the Mass 15 and Mass 16 peaks are for methane, the Mass 28 peak is ethane, and Mass 29 & the peaks around Mass 40 come from propane. Because these spectra are final gas analyses and the reaction times are not exactly same, only a qualitative analysis will be given here.

At a given temperature and pressure, increased catalyst loading increases both methane and ethane formation. Low temperature and low pressure tend to favor ethane and propane formation. One reasonable explanation is that the severe reaction conditions (high T and P) quickly cleave the formed ethane and propane to methane before they leave the catalyst surface.

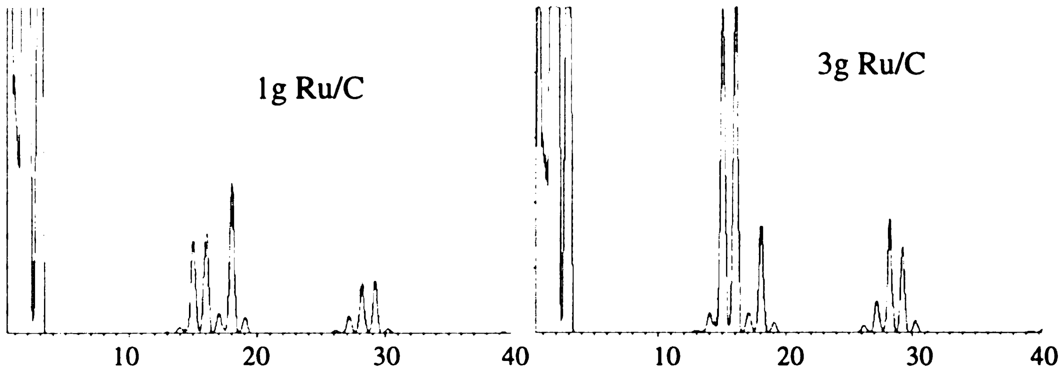

Figure 6-8. Gas product composition change with catalyst loading at 1000psi and 150°C

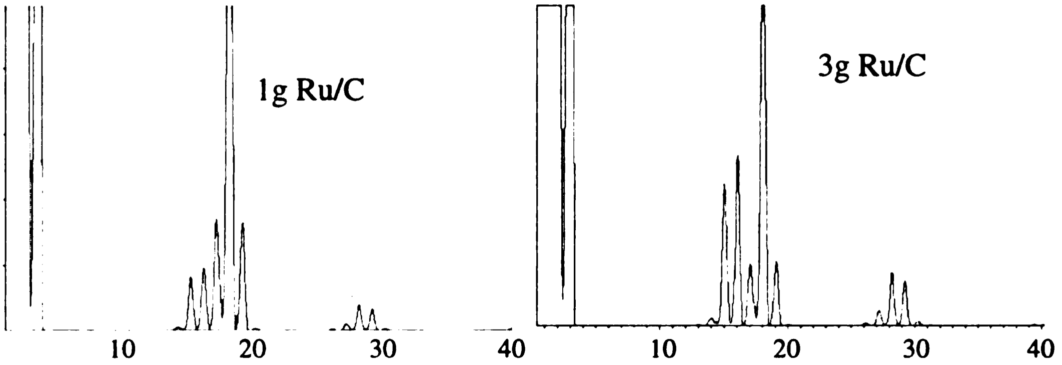

Figure 6-9. Gas product composition change with catalyst loading at 2000psi and 150°C

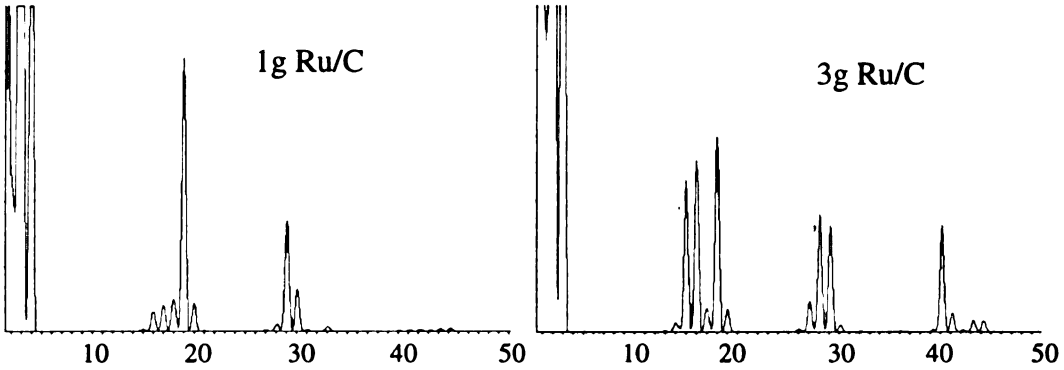

Figure 6-10. Gas product composition change with catalyst loading at 1000psi and 130°C

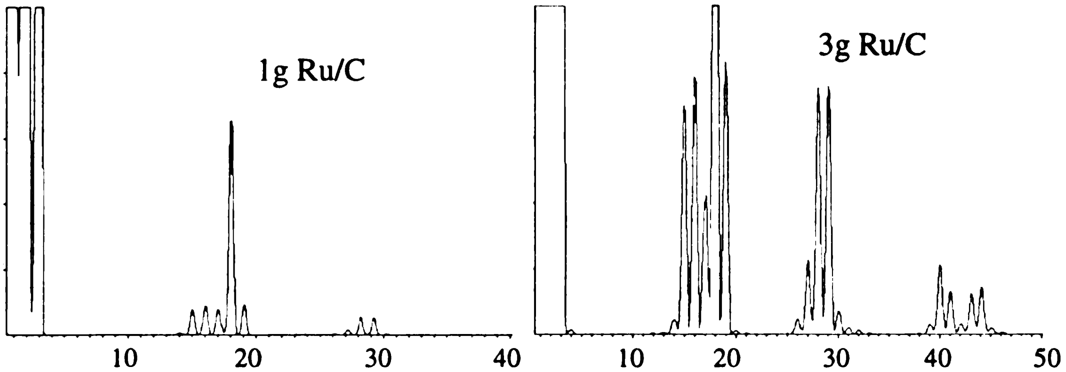

Figure 6-11. Gas product composition change with catalyst loading at 2000psi and 130°C

6.2.1. Gas composition for low pressure hydrogenation (330psi)

The gas phase analysis of products from low-pressure hydrogenation of lactic acid in the autoclave is shown in Figure 6-12. Low hydrogen pressure presumably leads to low hydrogen concentration on the catalyst surface, which is not favorable for deep hydrogenation (we assume that high surface hydrogen concentration will lead to more deep hydrogenation). Therefore, the ethane and propane concentrations have the same magnitude as methane in the gas phase. The selectivity is lower than seen at high pressure, but the difference is only 10%. That means that the reaction mechanism does not change dramatically at such a low pressure.

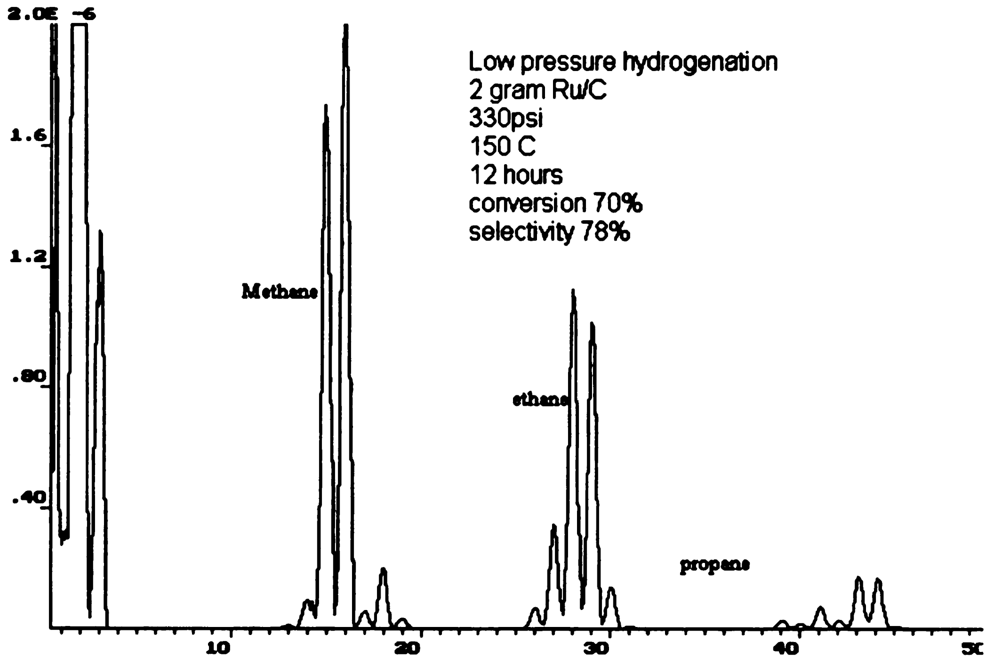

Figure 6-12. Gas phase spectrum after 12 hours at 330psi and 150°C

6.2.2. Gas product distribution in trickle bed reactor

Because different catalysts were used in the trickle bed and autoclave reactors, it is not appropriate to compare them directly. For two catalysts (CG5P and CG6M), the slightly different carbon supports gave very similar gas product distributions (Figure 6-13 and Figure 6-14). In the autoclave, propane was the major gaseous product instead of methane as in the autoclave. If we assume these two catalysts are similar to the powder Ru/C (PMC) catalyst used in autoclave reactor, then the different gas product distribution may come from the difference in mass transfer between trickle bed and autoclave reactors. In the trickle bed reactor, hydrogen availability to catalyst is limited due to slow diffusion. In addition, low reaction temperature should not favor deep hydrogenation because propane has more chance to leave the catalyst rather than being hydrogenated to methane. Therefore, propane is the dominant by-product. However, the deficit of hydrogen on the catalyst surface in the trickle bed reactor only inhibits the methane formation but not propane formation, and the selectivity in the trickle bed reactor is not as high as in the obtained in autoclave runs.

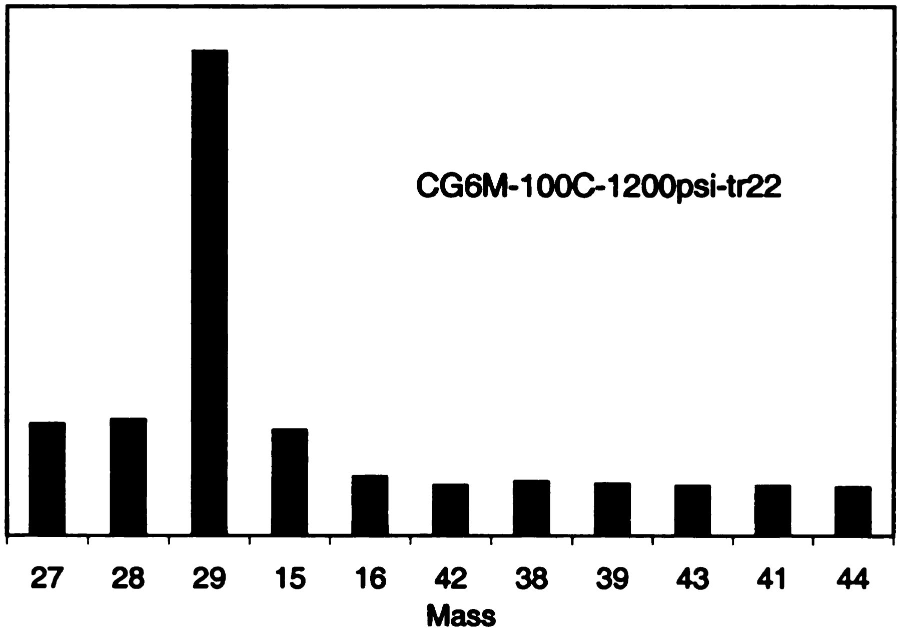

Figure 6-13. Gas phase analysis for CG6M catalyst in trickle bed

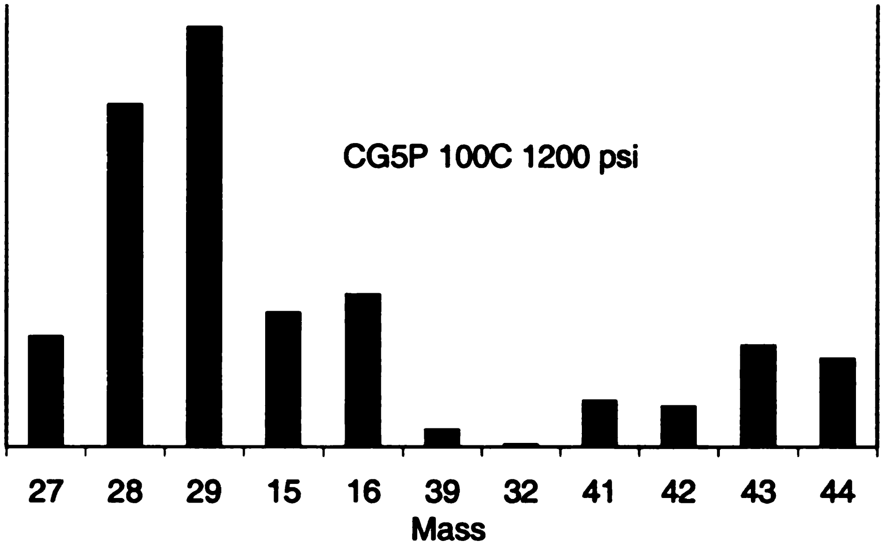

Figure 6-14. Gas phase analysis for CG5P catalyst in trickle bed

6.2.3. Catalyst deactivation by unrefined Cargill lactic acid samples

H_2 adsorption was used to investigate the change in active site density after catalyst use. After passing 4000ml of 10% Cargill lactic acid over the CG6M catalyst, the conversion decreased from 95 to 70% and the selectivity increased from 80% to 90%. Therefore, deactivation by impurities in the Cargill lactic acid is a selective process. The double peaks in fresh catalyst desorption support the idea that two kinds of active sites must exist on the catalyst surface. After deactivation, the second sharp peak (higher temperature) obviously was reduced. Therefore, it is highly possible that this peak represents the active sites used for PG deep hydrogenation.

6.3. Rationalization of the reaction paths

For rationalizing the reaction paths, AB initio energies for related molecules were calculated (Table 6-3) and some related bond energy, which is the energy need to break the bond, is also listed in Table 6-2. Combining the information from above sections and molecules calculation, the main reaction and side reaction pathways will be discussed in this section.

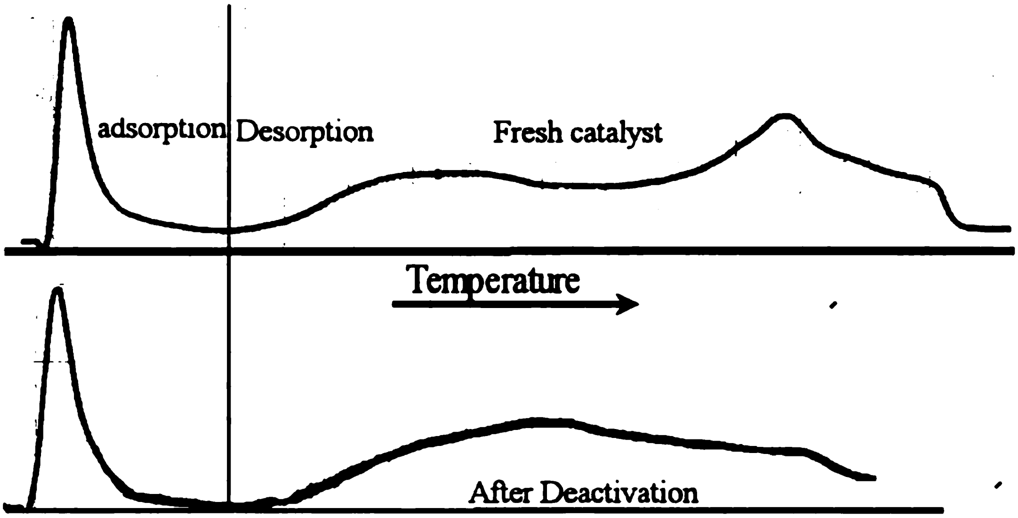

Figure 6-15. H_2 adsorption and desorption profiles change after deactivation

Table 6-2. Average bond energy

Bond	C—C	C—O	C=C	C=O
Average energy (KJ/mole)	348	358	614	799

Table 6-3. AB initio energy (Kcal/mole) for different structures (*)

Structure	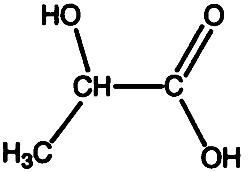	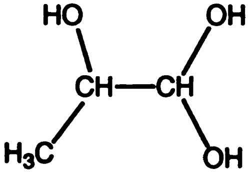	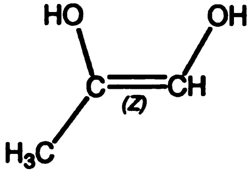
Name	Lactic acid	Propane-1,1,2-triol	Propene-1,2-diol
Energy	-211905	-212345	-165246
Structure	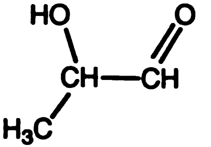	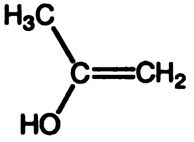	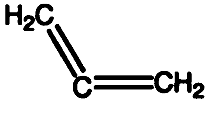
Name	2-Hydroxy-propionaldehyde	Propen-2-ol	Propa-1,2-diene
Energy	-165252	-118914	-71706
Structure	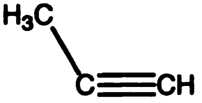	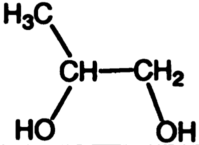	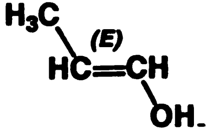
Name	Propyne	Propylene glycol (PG)	Propen-1-ol
Energy	-71816	-166002	-118910
Structure	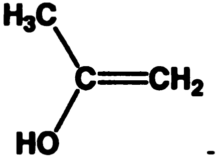	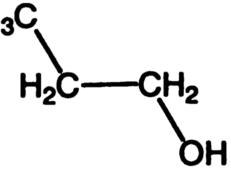	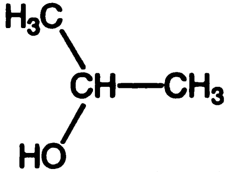
Name	Propen-2-ol	1-propanol	2-propanol
Energy	-118914	-119669	-119673
Structure	H_2O	CH_4	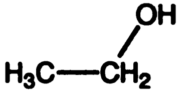
Name	H2O	Methane	Ethanol
Energy	-47039.96	-24928.7	-95463.2
Structure	$H_3C—OH$	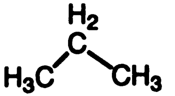	$H_3C—CH_3$
Name	Methanol	Propane	Ethane
Energy	-71215.4	-73346.6	-49137.4
Structure	$H_2C═CH_2$	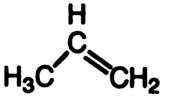	H2
Name	Ethene	Propene	H2
Energy	-48362.9	-72575.3	0

* Calculated by SPARTAN, product of Wavefunction Inc, with HF-STO-3G single point energy

The first step of lactic acid hydrogenation should be the formation of propane-1, 1,2-triol by the addition of H_2 because no propanoic acid is formed during hydrogenation and the AB initio energy of propane-1, 1,2-triol is less than that of lactic acid. "No propanoic" implies that the first step of lactic acid hydrogenation does not take off hydroxyl group. The second step is the dehydration of propane-1, 1,2-triol. Two possible products are propene-1,2-diol and 2-hydroxy-propionaldehyde (Table 6-3), both products have higher energy than that of propane-1, 1,2-triol (Table 6-4).

Table 6-4. AB initio energy change during reaction

Compound	Energy KJ/mole
Lactic acid	-211905
Propane-1, 1,2-triol	-212345
2-Hydroxy-propionaldehyde+H2O	-212292
Propene-1,2-diol+H2O	-212286
PG+H2O	-213042

The AB initio energy of propene-1,2-diol is a little higher than that of 2-hydroxy-propionaldehyde, but the difference is so small (6 KJ/mole) that we can not exclude anyone to be the intermediate for PG formation. At low temperature, propene-1, 2-diol may be dominant intermediate because propene-1,2-diolcan can be further hydrogenated to PG with syn stereochemistry (Both hydrogen add to the double bond from the same face). This assumption is supported by the optically active product at low temperature from lactic acid hydrogenation reported by Antons (63). Either propene-1,2-diol or 2-hydroxy-propionaldehyde can be hydrogenated to PG because the low energy of PG and the favorable hydrogenation environment (ruthenium catalyst and hydrogen) for C=O and C=C bonds (Figure 6-16).

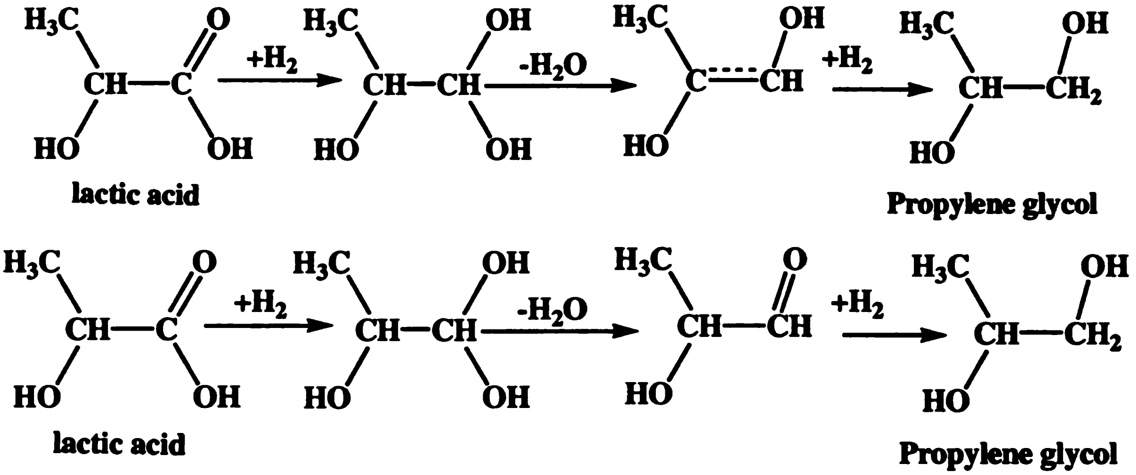

Figure 6-16. PG formation path

6.3.1. Side reaction 1(methane formation)

In PG, ethanol, and methanol hydrogenation, the major gas product is methane and only a trace of ethane was produced. So the most likely the first step of PG deep hydrogenation will be the cleavage of the C2-C3 bond to form ethanol and methanol, which will be further converted to methane quickly as partially verified in Section 6.1.2. Although this path is not supported by AB initio calculation (the energy of methanol plus ethanol is higher than PG), this analysis is supported by the high temperature hydrogenation of PG (170°C, a trace amount of ethanol was found in the liquid, Section 6.1.1) and no CO was found in gas phase at any reaction condition. The comparison of the conversion of PG hydrogenation (6.4% after 6.2 hour) at 150°and 2000psi and the lactic acid hydrogenation at same conditions shows that most methane comes from PG hydrogenolysis. The mechanism of methane formation from PG is shown in Figure 6-17.

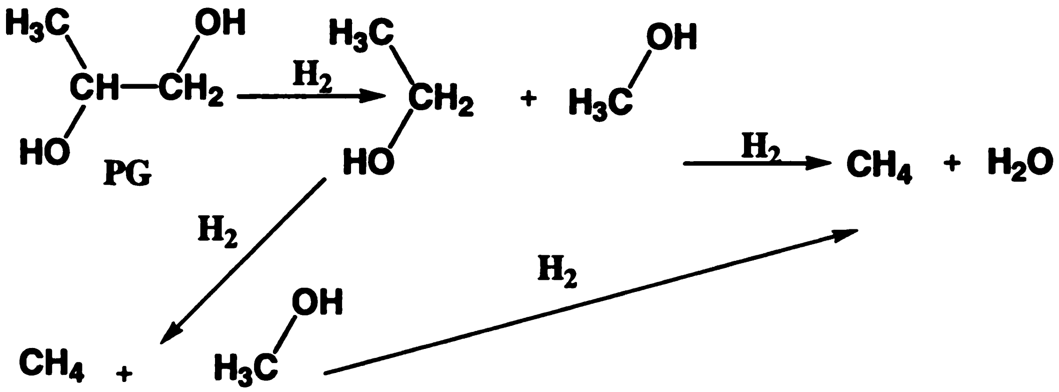

Figure 6-17. Scheme of PG hydrolysis

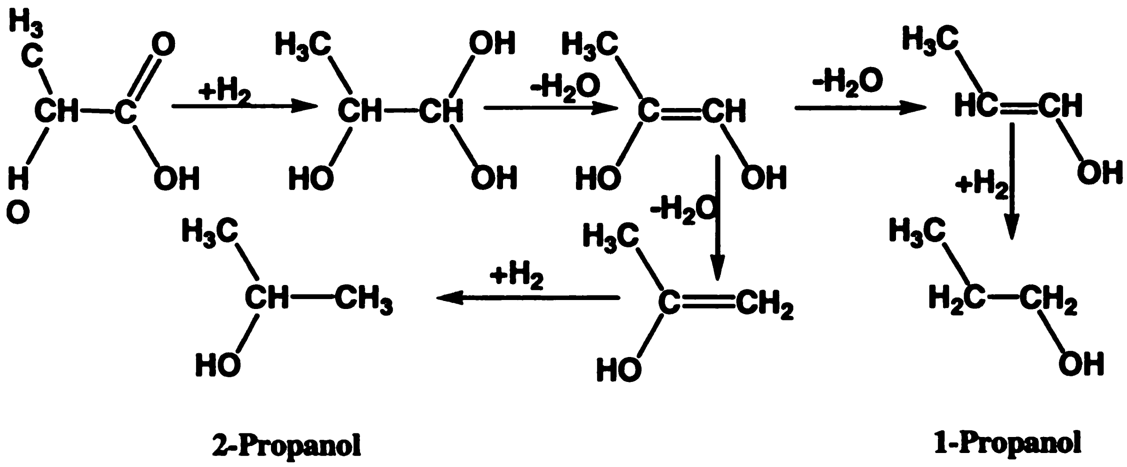

Figure 6-18. Propanol formation scheme

6.3.2. Side reaction 2 (propanol formation)

2-Propanol was detected in high temperature PG hydrogenation (Figure 6-2), so part of 2-propanol may come from PG hydrogenation. However, 1-propanol comes directly from lactic acid hydrogenation. The following scheme is derived from by-product information, bond energies, and common chemistry knowledge. The key point here is that propene-1,2-diol dehydrates to propen-1-ol or propen-2-ol when hydrogen is not available for hydrogenation. In addition, adding hydrogen to a C=C double bond is easier than adding H_2 across a C-OH bond. Figure 6-18 shows the 1-propanol and 2-propanol formation scheme from lactic acid hydrogenation.

6.3.3. Side reaction 3 (propane formation)

Propane may be the product of hydrogenation of 1-propanol and 2-propanol, but it does not come from PG hydrogenation. at most reaction conditions, propane formation is very limited in autoclave, so the formation of propanol is not favorable. Figure 6-19 is the propane formation scheme. In trickle bed reactions, the gas product almost is exclusively propane. The reason could be that the intermediate propene-1,2-diol (Figure 6-18) tends to further dehydrate into propen-2-ol and propen-1-ol because the low pressure and mass transfer effect lead to low surface hydrogen concentration.

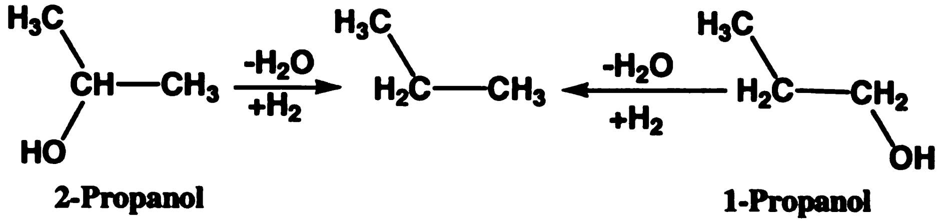
H3C
CH—CH3
HO
2-Propanol
-H2O
+H2
H3C
H2C—CH3
-H2O
+H2
H3C
H2C—CH2
OH
1-Propanol

Figure 6-19. Propane formation scheme

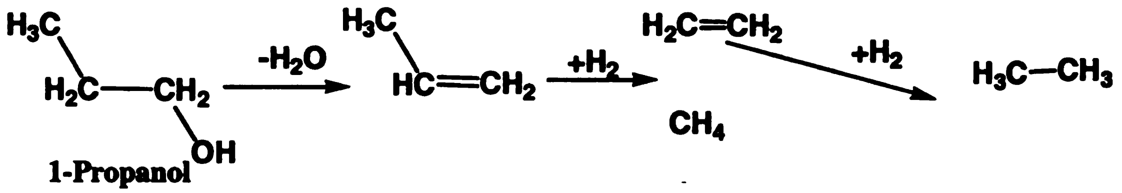
H3C
H2C—CH2
OH
1-Propanol
-H2O
H3C
HC═CH2
+H2
H2C═CH2
CH4
+H2
H3C—CH3

Figure 6-20. Ethane formation scheme

6.3.4. Side reaction 4 (ethane formation)

The only clue about ethane formation is that it always comes out with propane. That means it comes from the same path as propane. We already know the ethanol can not be converted to ethane. Therefore, the only possible path is propanol hydrogenation. Figure 6-20 is the possible scheme for ethane formation.

6.4. Summary

The following conclusions can be obtained from the above analyses:

- The first step of lactic acid hydrogenation is the formation of propane-1,1,2-triol, which dehydrates to propene-1,2-diol or 2-hydroxy-propionaldehyde, which will be hydrogenated to PG when enough hydrogen is available propene-1,2-diol. This is the main reaction.
- If the reaction pressure is low or mass transfer limits the catalyst surface hydrogen concentration, propene-1,2-diol may be further dehydrated to propen-1-ol and propen-2-ol, which are the precursors of 1-propanol and 2-propanol.
- Forming ethanol and methanol from breaking of the C-C bond is the pathway of PG deep hydrogenolysis. Ethanol and methanol can quickly undergo further hydrogenated into methane.
- Ethane and propane both arise via the 1-propanol or 2-propanol hydrogenation, which is formed when the hydrogen supply is limited on catalyst surface at high temperature and low pressure.

With this knowledge, one has the potential to suppress the side reactions and enhance the selectivity for PG. For example, modifying the catalyst surface to decrease the highly active sites may decrease PG deep hydrogenolysis and thus enhance the selectivity.

Chapter 7. Summary and Recommendations

Important conclusions from above chapters will be summarized in this chapter and some recommendations for the further research also is outlined.

7.1. Summary

Lactic acid obtained from fermentation was converted to propylene glycol in a stirred tank reactor (autoclave) and a continuous trickle bed reactor with supported ruthenium catalyst at mild reaction conditions.

7.1.1. Hydrogenation of lactic acid in autoclave

Lactic acid water solution (5%~30%) was hydrogenated to propylene glycol in a stirred tank reactor with powder catalyst. Only supported ruthenium was active enough to give reasonable conversion at our conditions. The carbon-supported catalyst is good in separating catalyst and liquid. When reaction temperature is below 170°C, the only liquid product is propylene glycol; therefore, the product purification is very simple. The major by-products are methane, ethane and propane; the relative amount of gas by-products depends on reaction conditions. As high as 90% PG yields and over 95% lactic acid conversion were achieved at optimal conditions. The optimal temperature is around 150°C. Higher pressures are always good for reaction rate and propylene glycol yield, but 1500~2000psi is sufficient; these are very mild reaction conditions compared to prior carboxylic acid hydrogenation studies in the literature.

The calculations and experiments show that gas-liquid, liquid-solid and intra-particle mass transfer are negligible in the autoclave at our reaction conditions. The intrinsic kinetics has been analyzed and the activation energy is 96KJ/mole. The initial reaction rate for 10% lactic acid hydrogen with Ru/C powder catalyst is well represented by:

$$R_{initial} = 1.95\times10^{10}\exp\left(\frac{-96000}{RT}\right)w^{0.66}P_{H_2}^{0.3}$$

This equation indicates that initial reaction is very sensitive to reaction temperature and catalyst loading but less so to hydrogen pressure.

Direct hydrogenation of lactate salts was impossible in aqueous phase for our catalyst and reaction conditions. Low metal ion (K or Ca) concentration does not affect the lactic acid hydrogenation reaction. Acidified calcium lactate can be hydrogenated to propylene glycol at the same rate as pure lactic acid if the precipitated calcium sulfate is filtered before hydrogenation.

An H-W model was given and the kinetic parameters were fit by using the data at 130°C. The fitting results were reasonably good considering the existence of side reactions. This is the only model that gives all positive constants. Therefore, the first addition of H_2 to lactic acid to form Propane-1,1,2-triol is most likely the rate controlling step.

7.1.2. Hydrogenation reaction in trickle bed reactor

A trickle bed reactor with laboratory prepared 5% Ru on active carbon catalysts was used to continuously convert lactic acid to propylene glycol at even mild reaction conditions with conversion over 90% and selectivity over 95%. The reaction temperature can be as low as 100 °C and pressure can be as low as 800psi without significant sacrifice of the PG yield.

Experiments and calculation show that gas-liquid, liquid-solid and intra-particle mass transfers and surface chemical reaction together control the lactic acid hydrogenation reaction in trickle bed reactor. Gas to liquid mass transfer is the major resistance. Lactic acid conversion increases with temperature at the same pressure and hydrogen to lactic acid molar ratio. Like the reaction in autoclave, propylene glycol selectivity increases with hydrogen pressure.

7.1.3. Catalyst characterization and deactivation

The catalysts prepared from different carbon supports have different hydrogen desorption profiles. Stronger hydrogen adsorption on the catalyst relates to the lower reactivity toward lactic acid hydrogenation. Two kinds of active sites may exist on supported ruthenium catalyst: both sites for lactic acid hydrogenation and only one kind of sites for PG deep hydrogenolysis. Carbon support adsorbs both reactant and product.

Pure lactic acid did not deactivate the catalyst over a 100-hour reaction. The impurities in unrefined sample slowly deactivated the catalyst. The deactivation is selective because with the lactic acid conversion decreasing from 95% to 70% yet the PG yield increasing from 80% to 90% after 4000ml of sample was reacted. However, addition of sulfur (Na_2S) to pure lactic acid deactivates the catalyst without any enhancement in selectivity, only decreasing the lactic acid conversion. The loss in activity could not be recovered by high temperature hydrogen reduction.

7.1.4. Kinetic parameter measurement and trickle bed modeling

Hydrogen solubility was measured at our reaction conditions. The comparison with literature shows our measurement is very reliable. Trickle bed dynamic liquid holdup, which is a bridge between liquid volume and catalyst volume in trickle bed, was measured in our trickle bed reactor. Gas-liquid mass transfer coefficient was measured in the autoclave and the results are consistent with published data and correlation.

A one-dimensional trickle bed model was derived. This model consists of two differential and two algebraic, equations and forms a typical two-point boundary value problem. With simplification, the model was solved in Mathematica. Bulk hydrogen and lactic acid, surface hydrogen and lactic acid concentration profiles were plotted. The results give us more information about the role of gas-liquid and liquid-solid mass transfers.

7.1.5. Reaction pathway

A simple surface reaction scheme was given. The first step of lactic acid hydrogenation is the formation of propane-1, 1, 2-triol, which dehydrates to 2-hydroxy-propionaldehyde or propene-1,2-diol, which will be hydrogenated to PG when enough hydrogen is available. This is the main reaction path. If the reaction pressure is low or mass transfer limits the catalyst surface hydrogen concentration, propene-1, 2-diol may be further dehydrated to propen-1-ol and propen-2-ol, which are the precursors of 1-propanol and 2-propanol. Forming ethanol and methanol from breaking the C-C bond is the pathway of PG deep hydrogenolysis. Ethanol and methanol can be quickly further hydrogenated into methane. Ethane and propane all come from the 1(2)-propanol hydrogenation, which is formed when hydrogen supply is limited on catalyst surface at high temperature and low pressure. This scheme is supported by specially designed reactions and theoretical analysis.

7.2. Recommendations

The conversion and yield achieved is unbelievable good without the knowledge of reaction pathway and catalytic mechanism. To further enhance the performance, surface reaction pathways, the role of catalyst support and the changes in optical property of product with reaction conditions need to be extensively investigated.

7.2.1. Surface reaction pathway investigation

Although a simple surface reaction pathway was given, it is mostly from inference and deduction. We did not do anything to verify and apply our theory. It is very important to verify and correct this scheme by advanced surface analysis techniques and specially designed reactions.

Another important aspect for this process is the role of catalyst support. Activated carbon support strongly adsorbs both reactant and product, and different carbon supports show different reactivity. Therefore, the carbon support must play a very important role in lactic acid hydrogenation. This can be done by systematically investigating the catalyst activity for different carbon supports; the variable parameters of the carbon support may include the source of carbon (coal, wood...) and its physical properties (BET are, pore size distribution).

7.2.2. Selective deactivation of the catalyst and yield enhancement

Another way to enhance the propylene glycol yield is via selective deactivation of the catalyst. The possibility comes from the reaction of Cargill unrefined sample in trickle bed reactor, although we do not know the composition of the impurities. We are sure there exist some compounds that can deactivate the high activity sites to suppress the propylene glycol deep hydrogenolysis. Searching for this type of compound may provide another way to enhance the propylene glycol yield.

7.2.3. Production of optically active propylene glycol

Combining the results of this work and the patent of Antons (63), lactic acid from fermentation (L+) can be continuously converted to optically active propylene glycol in a trickle bed reactor. The very mild reaction temperature (<100°C) ensures very high ee efficiency. This process provides an economical process to produce optically active propylene glycol because the pressure used in our process is much lower than that shown in the patent. The change in ee efficiency of this reaction with catalyst and reaction conditions may be studied to find the optimal conditions.

Appendix A. Parameters calculation and physical data

A.1. Lactic acid consumption rate and hydrogen consumption rate

Two moles hydrogen is needed to hydrogenate one mole lactic acid to PG, but six moles will be consumed for methane formation for every mole of lactic acid. If we assume 10% lactic acid is converted to methane then side reaction will use 30% hydrogen.

$$C_3H_6O_3 + 2H_2 \longleftrightarrow C_3H_8O_2 + H_2O$$
$$C_3H_6O_3 + 6H_2 \longleftrightarrow 3CH_4 + 3H_2O$$

$$C_3H_6O_3 + 0.9\times 2H_2 + 0.1\times 6H_2 \longleftrightarrow 0.9C_3H_8O_2 + 0.1\times 3CH_4 + (0.9 + 0.1\times 3)H_2O$$
$$C_3H_6O_3 + 2.4H_2 \longleftrightarrow 0.9C_3H_8O_2 + 0.3CH_4 + 1.2H_2O$$

Therefore, the hydrogen consumption rate (mole/hr) is 2.4 time of the rate of lactic acid consumption if side reactions are included.

A.2. Bulk density of catalyst

For CG6M, the trickle bed height (H) is 61 cm; the reactor diameter (d) is 1.57 cm, the thermocouple diameter (d_0) is 0.125 cm and total catalyst weight is 48 gram. Therefore the catalyst bulk density is:

$$\rho = \frac{W}{H\pi(d^2 - d_0^2)/4} = \frac{48}{61\pi(1.57^2 - 0.125^2)/4} = 0.42 g/cm^3$$

For CG6P, the bulk density is 0.47g/ml.

A.3. External porosity

For both CG5P and CG6M, the average particle diameter (dp) is about 0.05cm, and the ratio of dp to trickle bed diameter is 0.03. From the figure 5-68 in Perry's handbook (74), we find the external porosity ε_e is 0.41.

A.4. Internal porosity and catalyst density

Combining catalyst bulk density and the incipient wetness measurement, one can calculate the internal porosity by

$$\varepsilon_i = \frac{v}{w/\rho} = \frac{5ml}{4.4g/0.47g/ml} = 0.48 \quad \text{for CG5P}$$

Catalyst density can be calculated as

$$\rho_t = \frac{\rho}{1-\varepsilon_e} = \frac{0.42}{1-0.41} = 0.79g/ml \quad \text{for CG6M.}$$

Table A-1. Catalyst density and porosity

Catalyst	Bulk density g/ml	Catalyst (g)	Add water (ml)	Internal porosity	Catalyst density g/ml
CG5P	0.42	4.4	5	0.48	0.80
CG6M	0.47	6.3	9.7	0.65	0.71

A.5. Diffusion coefficients

H_2 and lactic acid diffusion coefficients were calculated from the equation Eq139 in Perry's Handbook (74). That also is called Wilke and Chang (1955) equation.

$$D = \frac{7.4\times10^{-8}T(\theta M_w)^{0.5}}{\mu_L v_M^{0.6}}$$

where the mole volume of H_2 at normal boiling point, v_M, is 14.3 cm^3/mole;

θ is a constant, for water solution it is 2.6;

The viscosity of water at 100 °C is 0.28 Ns/m^2

From this data we can calculate the hydrogen diffusion coefficient is 1.3E-4 cm^2/sec. For lactic acid diffusion in water, the molar volume is calculated from its density at its normal boiling temperature, which comes from extrapolating the data at 0~80 °C and 0~88% lactic acid water solution. The mole volume of lactic acid is 70 $cm^3/mole$. The diffusion coefficients are summarized in Table A-2.

Table A-2. Diffusivity (cm^2/sec)

	80°C	100 °C	120 °C	140 °C	160 °C
H_2	1.02E-4	1.29E-4	1.3E-4	1.07E-4	8.02E-5
Lactic acid	3.96E-5	5.01E-5	5.05E-5	4.15E-5	3.11E-5

A.6. Basic physical data used in kinetic calculation

Table A-3. Thermodynamic properties for LA and PG

Name	Lactic acid	PG	Name	Lactic acid	PG
Molecular	$C_3H_6O_3$	$C_3H_8O_2$	Molecular	$C_3H_6O_3$	$C_3H_8O_2$
GAS No	598-82-3	57-55-6	Molecular W	90	76
Formation heat KJ/mol	-682.0	-485.7	Tai (auto-ignition point)	N/A	371 °C
Combustion heat	-1356.0	-1838.2	Bp (°C)	190	188
Cp J/mol.k	210.5	190.8	Tc (°C)	254	255
Flash point		99	Pc (atm)	50	60
Melt point (°C)	16.8	-60			

A.6.1. Lactic acid

Lactic acid is, when pure and anhydrous, actually a white crystalline solid with a low melting point. However, because of the physical properties and the difficulties in the preparation of the pure and anhydrous acid this material is rare. Lactic acid appears generally in the form of more or less concentrated aqueous solutions. Lactic acid undergoes intermolecular esterification spontaneously, resulting in the formation of lactoyllactic acid and chain polyesters containing more lactic acid units in the molecule. All data come from the book "Lactic Acid" (Holten, C.H, 1971) unless specified.

A.6.1.1.Density of aqueous solution of lactic acid

Table A-4. Densities of aqueous solutions of lactic acid

LA W%	Temperature °C								
	20	25	30	35	40	50	60	70	80
0.00	0.998	0.997	0.996	0.994	0.992	0.988	0.983	0.978	0.972
6.29		1.012		1.008					
9.16	1.020	1.018	1.016		1.011	1.007	1.001	0.995	0.989
12.19		1.025		1.022					
24.35	1.057	1.054	1.052		1.047	1.041	1.035	1.030	1.023
25.02		1.057		1.053					
37.30		1.086		1.081					
45.48	1.110	1.105	1.102		1.094	1.087	1.079	1.072	1.064
54.94		1.130		1.124					
64.89	1.155	1.152	1.147		1.140	1.132	1.124	1.115	1.108
75.33	1.179	1.175	1.170		1.161	1.153	1.143	1.134	1.125
85.32	1.199	1.195	1.190		1.181	1.172	1.163	1.153	1.144
88.60		1.201		1.192					

A.6.1.2.Viscosity of aqueous solution of lactic acid

Table A-5. Viscosities as a function of concentration and temperature (cp)

Lactic Acid W %	Temperature °C							
	25	30	35	40	50	60	70	80
0	0.8937	0.801	0.7225	0.656	0.5494	0.4688	0.4061	0.3165
6.29	1.042		0.838					
9.16	1.15	1.03		0.809	0.671	0.571	0.473	0.416
12.19	1.21		0.961					
24.35	1.67	1.46		1.13	0.918	0.746	0.632	0.532
25.02	1.725		1.328					
37.3	2.45		1.857					
45.48	3.09	2.74		2.03	1.59	1.26	1.02	0.843
54.94	4.68		3.38					
64.89	6.96	6.01		4.22	3.12	2.38	1.85	1.47
75.33	13.03	10.55		7.08	4.98	3.57	2.73	2.08
85.32	28.5	22.6		13.91	9.4	6.4	4.59	3.4

A.6.2. **Saturation pressures of lactic acid and propylene glycol**

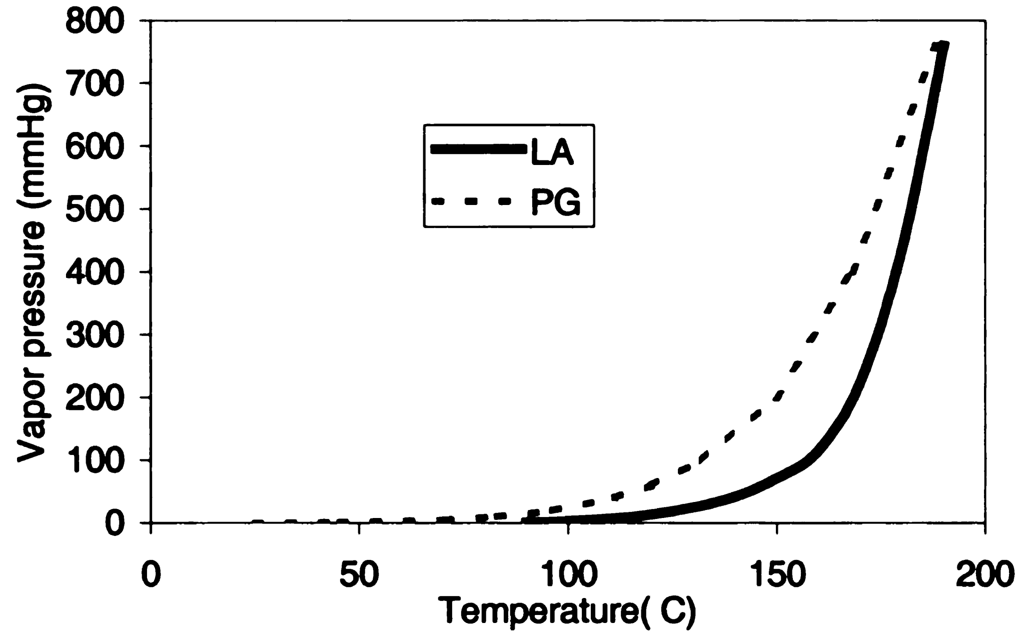

Figure A-1. Saturation pressures of lactic acid and propylene glycol

A.6.3. **Equilibrium of lactic acid hydrogenation to PG**

The Gibbs free energies and reaction heats (Kcal/mol) of lactic acid and, propylene glycol, water and hydrogen are listed in following.

Compound	Formation heat (kcal/mole)	Gibbs free energy (kcal/mole)
LA	-148	-123.1
PG	-100.6	-72.6
Water	-57.7	-54.6
H2	0	0
Reaction heat ΔH(kcal/mole)	-10.3	
Δ G (kcal/mole)	-4.1	

$$K_{298} = \exp(\frac{\Delta G}{RT}) = \exp(-\frac{4100}{1.987 * 298}) = 1017$$

$$\ln\frac{K_T}{K_{298}} = \frac{-\Delta Hr}{R}(\frac{1}{T} - \frac{1}{298}) = \frac{10300}{1.987}(\frac{1}{T} - \frac{1}{298}) = \frac{5184}{T - 17.4}$$

$$\ln(K_T) = \ln(1016.6) + \frac{5184}{T} - 17.4 = -10.47 + \frac{5184}{T}$$

$$K_T = \frac{C_{PG}}{C_{LA}P_{H2}} = \frac{C_{LA0} - C_{LA}}{C_{LA}P_{H2}} \qquad \frac{C_{LA}}{C_{LA0}} = \frac{1}{K_T P_{H2} + 1}$$

$$\text{Lactic acid conversion}\ \frac{C_{LA0} - C_{LA}}{C_{LA0}} = \frac{K_T P_{H2}}{1 + K_T P_{H2}}$$

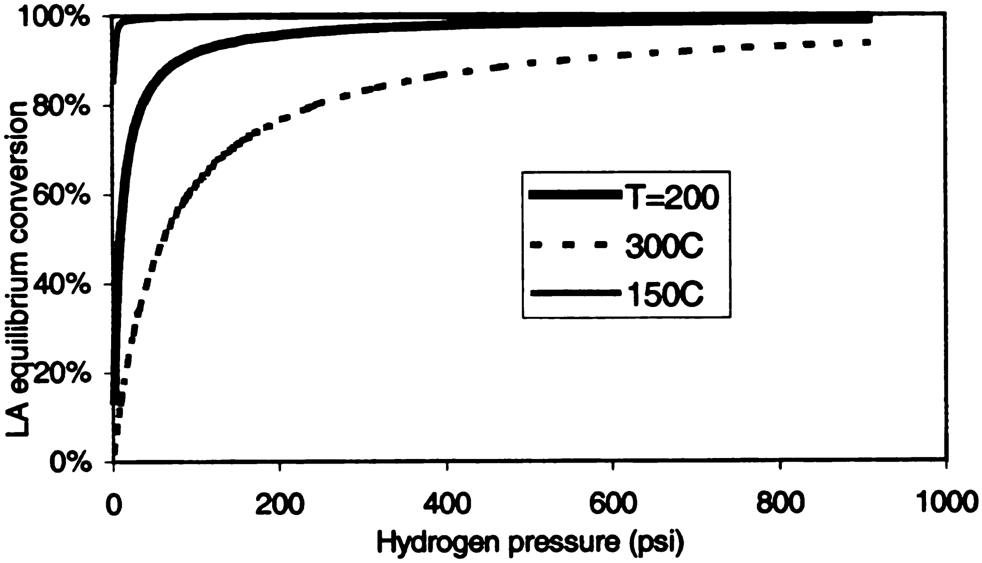

Figure A-2. LA equilibrium conversion

REFERENCE

1. Bennina, H "A histroy of lactic acid making", Kluwer Academic Publishers, (1990)
2. Holten, C.H, "Lactic Acid", p3, 1971
3. Chemical Market Reporter - 01-Mar-1999
4. Kroschwitz, J. I., M. Encyclopedia of Chemical Technology 4th ed., 13, 1043, John Wiley & Sons, 1992
5. Levy, N and Scaife, C. W., J. Chem. Soc., 1946,1100.
6. British Patent 1,123,147,1968
7. Kirk, R. E., et al Encyclopedia of Chemical Technology 2nd ed., 8, 167, Inter science Encyclopedia, 1952
8. Monteaguo, J. M., L. Rodriguez, J. Rincon, J. Fuertes, J. Chem. Tech. and Biotech, 68, p271, 1997
9. Urbas, B., U. S. Patent # 4,444,881, 1984
10. Giorno, L., P. Spicka, E. Drioli, Separation Sci. Tech., 31, p2159, 1996
11. Rincon, J., J. et al, Solvent Extraction and Ion Exchange, 15, p329, 1997
12. Boniardi, N., R. Rota, G. Nano, B. Mazza, J. Appl. Electrochemistry, 27, p125, 1997
13. Chemical Market Reporter - June 26, 1991
14. Walkup, P. C., C. A. Rohrmann, R. T. Hallen, D. E. Eakin, U. S. Patent # 5,071,754, 1991
15. Baniel et al, United States Patent, 5510526, 1996
16. McCoy, M., Ed., Chemical Market Reporter - July 14, 1997

17. Paparizos, C., S. R. Dolkyj, W. G. Shaw, U. S. Patent # 4,786,756, 1988

18. Ghose, T. K., Ed., Bioprocess Engineering - The First Generation, 367, Ellis Horwood Limited, 1989

19. Chemical Market Reporter - December 13, 1999

20. Chemical Market Reporter - July 20, 1998

21. Chemical Market Reporter - 08-May-00

22. Man, T. M Dissertation, Michigan state University,1998

23. Broadbent, H S, et al. J. Org.Chem. 24, p1847-1854,1959

24. Stefan Antons, Leverkusen, US patent 5731479,Mar,24,1998

25. Kida, K., S. Morimura, Y. Sonoda, Journal Fermentation and Bioengineering, 75, p213, 1993

26. Hiltunen, K. J. V. Seppala, M. Harkonen, Macromolecules, 30, p373, 1997

27. Lipinsky, E. S., R. G. Sinclair, Chem. Engr. Prog., 82, p26. 1986

28. Hiljanen-Vainio, M., J. Kylma, K. Hiltunen, J. V., Seppala, J. Appl. Poly. Sci., 63, p1335, 1997

29. Gruber; Patrick Richard, US patent #05981694,Nov. 9,1999

30. Sawicki, R. A., U. S. Patent # 4,729,978, 1988

31. Mok, W. S., M. J. Antal, Jr., M. Jones, Jr., J. Org. Chem., 54, p4597, 1989

32. Lira, C. T., P. J. McCrackin, Ind. Eng. Chem. Res., 32, 2608, 1993

33. Gunter, G. C., Ph.D. Dissertation Michigan State University, 1994

34. Gunter, G. C., J. E. Jackson, D. J. Miller, J. Catal., 148, 252, 1994

35. James, B. R. Homogeneous hydrogenation, John Wiley &sons, 1973

36. Mcquillin, F. J. Homogeneous hydrogenation in organic chemistry, D. Reidel publishing company, 1976

37. Everett Brown and H. Adkins, et al., J. Am. Chem. Soc., vol. 56, pp. p3689-691, 1934

38. Adkins, H. et al., J. Am. Chem. Soc., vol. 69, p3039-3041, 1947.

39. Carnahan, J.E. et al, J. Am. Chem. Soc., vol. 77, p3766-3768, 1955.

40. Ford, T. A. U.S Patents 2607807, Aug. 1952

41. Novotny; Miroslav, patent, US4273947: Hydrogenation of fluorine-containing carboxylic acids, 1981

42. Velenyi, L. J., S. R. Dolhyj, U. S. Patent # 4,663,479, 1987

43. Paul N, Rylander, hydrogenation methods, 1985, p78

44. Harada, K., Chem., Commum., p1071, 1970

45. Calvin, M., Trans. Faraday Soc., 34,p1181, 1938

46. Iguchi, M.,J. Chem. Soc. Jap., 60, p1287. 1939

47. Halpern, J., J. Am., Chem. Soc., 83, p753, 1961

48. Halpern, J., J. Am., Chem. Soc., 88, p5150,1966

49. M,Ando, and S.Emoto, Bull, chem. Soc. Jpn,47, p501, 1974

50. Adams, P. T.,R. E. Selff, and B. M. Tolbert, J. Am. Chem.Soc, 74, p2416, 1952

51. Richardson, A. S. and J. E. Taylor, U.S Patents 2340344,2340687 to 2340691, 1959

52. Stephen, H. and T. Stephen "the solubility of inorganic and organic compounds", The Macmillan company, New York, 1963.

53. Hofmann,H. P., chem. Eng. Tech., 47 , p823-868, 1975

54. Yuanxin Wu, et al., Ind. Eng. Chem. Res., 35, p397-405, 1996

55. Henry, H. C. and J. B. Gilbert, Ind. Eng. Chem. Proc. Des. Dev. 12,328,1973

56. Sato, Y. et al. "Flow pattern and pulsation properties of co-current downflow inn packed beds, J. Chem. Eng. Japan 6,315, 1973

57. Kim et al , J. Chem, Eng. Jpn,14,p311, 1981

58. Shigeo goto and J. M. Smith, AIChE Journal (vol. 21,No4), p706-720, 1975

59. Shigeo goto, et al, The Canadian Journal of Chemical Engineering Vol. 54, p551-555, 1976

60. Dick stegeman, et al, Ind. Eng. Chem. Res. 35, P378-385, 1996

61. Wammes, W. J. A. et al. AIChE Journal (vol. 37,No12), p1849-1862, 1991

62. Both hydrogen add to the double bond from the same face

63. Antons Stefan, US patent 5731479, March 24, 1998

64. Ramachandran, P. A., and R. V. Chaudhai, "Three-phase catalytic reactors", Gordon and Breach science

65. Stephen H and Stephen T., "Solubility of inorganic and organic compounds", Volume 1, The Macmillan Company, New York, 1963

66. Zwietering, T. N. "Suspending of solid particles in liquid by agitators. Chemical Engineering Science 8, 244,1958

67. Vasant R, et al Ind. Eng. Chem. Res. **1998**, 37, 3879-3887

68. Bern, L., Lidefelt, J. O. and Shoon, N. H., J. Am, Oil Chem. Soc. 53, 463(1976)

69. Sherwood, T, K and F A L Holloway, "performance of packed towers", Chem. Eng.Sci.,28,559(1973)

70. Shigeo Goto and J. M. Smith, AIChE J. (Vol, 21) N0 4,1975,p706

71. Doraisewamy, L. K. Heterogeneous Reactions; John Wiley and Sons; New York, 1984;Vol.I

72. Sano, Y. et al. Mass transfer from suspended particles in agitated vessels. J. Chem. Eng. Japan, 255 (1974)

73. Boon-long, S., et al. "Mass transfer from suspended solids to a liquid in agitated vessels". Chem. Eng. Sci, 33, 813 (1978)

74. Perry's Chemical Engineering Handbook, 6th ed

75. Zhang Z., "Reactive Properties of Hydrogen Adsorbed on Carbon Surfaces" Thesis, Michigan state University, 1998